BIOLOGICALLY-ACTIVE, ANTI-THROMBOTIC COATINGS FOR VASCULAR BIOMATERIALS

By

Jeremy John Glynn
B.S., University of Wisconsin – Madison, 2011

A DISSERTATION

Presented to the Department of Biomedical Engineering
of the Oregon Health & Science University
School of Medicine
in partial fulfillment of
the requirements for the degree of

Doctor of Philosophy
in Biomedical Engineering

December 2015

Department of Biomedical Engineering
School of Medicine
Oregon Health & Science University

CERTIFICATE OF APPROVAL

This is to certify that the Ph.D. dissertation of

Jeremy John Glynn

has been approved

Monica T. Hinds, Ph.D., Thesis Advisor
Assistant Professor, Biomedical Engineering

András S. Gruber, M.D., Committee Chair
Associate Professor, Biomedical Engineering

Owen J.T. McCarty, Ph.D.
Associate Professor, Biomedical Engineering
Associate Professor, Cell & Developmental Biology

Wohaib E. Hasan, Ph.D.
Assistant Professor, Knight Cardiovascular Institute

Kenton W. Gregory, M.D.
Associate Professor, Biomedical Engineering
Director, OHSU Center for Regenerative Medicine

To my parents, Lloyd and Sue. Thank you for your love, support, and encouragement – the “successful graduate student’s triad”

Acknowledgements

I am extremely thankful for the many people that guided and supported me during the course of this work. First and foremost, I would like to thank Dr. Monica Hinds for mentoring me through this process. She has been an incredible advisor to me throughout my graduate studies, and has been instrumental in my growth as a scientist. I cannot thank you enough.

I have also been fortunate to receive guidance from a number of other members of OHSU faculty, and especially from the BME department. In particular, I have learned a considerable amount from Dr. Owen McCarty on technical writing, career development and gym etiquette. I would also like to thank Dr. András Gruber for his guidance on my work, always delivered wisely and with humor. Much of my work was built upon the many years of research by Dr. Dusan Pavčnik, and I appreciate him supporting my research and providing helpful insight. On a day-to-day basis, I was fortunate to conduct my research in a great working environment that results from working with great lab mates: Dr. Casey Jones, Dr. Devon Scott-Dreschel, Taylor Lawson, Matt Hagen, and especially to Dr. Deirdre Anderson who has been a helpful and supportive co-worker my entire time at OHSU. Additionally, thank you to Dr. Wohaib Hasan and Dr. Kenton Gregory for being part of my dissertation committee and for the insightful feedback on my work.

There are numerous members of my class in the PMCB cohort that I would like to thank for letting me pretend to be one of their own and for being my friends in the pursuit of a PhD. Of these people, I would especially like to acknowledge Tyler Hulett, who shared a residence with me for the majority of this time, and even allowed my

Wisconsin gear to be displayed. I would like to thank Elizabeth Polsin who let me stumble through being her mentor and decided to come back for a second summer of lab work with me. I also owe Jennifer Johnson a huge thank you for providing critical assistance with all of the baboon studies.

My interest in science was established at a young age and has been fostered extensively by my parents, Lloyd and Sue. Though I'm sure pursuing a PhD at a research institute 2,000 miles from home was not their favorite decision of mine, they have been entirely supportive of this phase in my career, and to them I owe a considerable amount. While at UW-Madison, I was fortunate enough to work with Cheston Hsiao as he was completing his PhD work, and I learned many keys to being a successful PhD student from him.

Table of Contents

Acknowledgements....iv
Table of Contents....vi
List of Figures x
List of Tables....xiii
List of Abbreviations....xiv
Abstract....xvii
CHAPTER I: Introduction.... 1
1.1 Background 1
1.2 Thesis Summary.... 1
CHAPTER II: Background.... 4
2.1 Vascular Biology.... 4
2.1.1 Endothelial Cell Physiology.... 5
2.2 Hemostasis and Thrombosis 6
2.2.1 Platelets in Hemostasis and Thrombosis 7
2.2.2 Blood Plasma Coagulation.... 8
2.2.3 Blood Flow 11
2.3 Endothelial Regulation of Thrombosis 13
2.3.1 Endothelial Regulation of Platelet Activation.... 13
2.3.2 Endothelial Regulation of Plasma Coagulation 14
2.3.3 Endothelial Regulation of Fibrinolysis 15
2.3.4 The Thrombomodulin-protein C Pathway.... 15
2.4 Endothelial Progenitor Cells 23
2.5 Summary: Vascular Biology.... 25
2.6 Biomaterials.... 25
2.6.1 Biomaterial Thrombogenesis.... 26
2.7 Cardiovascular devices.... 30
2.7.1 Vascular Grafts 31
2.7.2 Artificial Venous Valves.... 36
2.8 Summary: Vascular Biomaterials and Devices 37
2.9 Endothelial Outgrowth Cells: Function and Performance in Vascular Grafts 39
2.9.1 Abstract.... 39
2.9.2 Introduction 40

2.9.3 Endothelial Outgrowth Cells 42
2.9.4 Performance Criteria for EOCs in Vascular Grafts 45
2.9.5 Vascular Tissue Engineering Applications using EOCs 54
2.9.6 Future Research Topics 60
2.9.7 Conclusion 61
CHAPTER III: Endothelial outgrowth cells regulate coagulation, platelet accumulation, and respond to tumor necrosis factor similar to carotid endothelial cells. 63
3.1 Abstract 63
3.2 Introduction 65
3.3 Materials and Methods 68
3.3.1 EC Isolation 68
3.3.2 EOC Isolation 68
3.3.3 Cell Culture and TNFα Treatment 68
3.3.4 Flow Cytometry 69
3.3.5 Reverse Transcription and Quantitative Polymerase Chain Reaction (qPCR) 70
3.3.6 Coagulation Factor Activation 70
3.3.7 Animal Care 71
3.3.8 Ex Vivo *Arteriovenous Shunt* 72
3.3.9 Statistical Analyses 73
3.4 Results 73
3.4.1 Morphology and Surface Marker Expression 73
3.4.2 Thrombus Formation and Inflammation: Gene Expression 76
3.4.3 Coagulation Factor Activation 77
3.4.4 Platelet Accumulation on Cell-seeded Vascular Grafts 79
3.5 Discussion 80
3.6 Conclusion 84
CHAPTER IV: *In vivo* assessment of two endothelialization approaches on bioprosthetic valves for the treatment of chronic deep venous insufficiency 88
4.1 Abstract 88
4.2 Introduction 90
4.3 Materials and Methods 93
4.3.1 EOC capture on antibody-modified SIS 93
4.3.2 EOC pre-seeded SIS valves 100

4.4 Results 102
4.4.1 Sheep EOC Characterization 102
4.4.2 Antibody Orientation 103
4.4.3 In vivo *EOC Capture Using Anti-KDR Antibody* 105
4.4.4 In vivo A*ssessment of EOC-pre-seeded SIS Valves* 106
4.5 Discussion 109
4.6 Conclusion 115
CHAPTER V: Crosslinking decreases the hemocompatibility of decellularized, porcine small intestinal submucosa 116
5.1 Abstract 116
5.2 Introduction 118
5.3 Materials and Methods 120
5.3.1 SIS Preparation 120
5.3.2 Extrinsic Pathway Activity 121
5.3.3 Platelet-poor Plasma Coagulation 121
5.3.4 Glycosaminoglycan Digestion 123
5.3.5 Thrombus Formation in a Whole Blood Arteriovenous Shunt 124
5.3.6 Statistics 125
5.4. Theory 125
5.5. Results 126
5.5.1 SIS Tissue Factor Activity 126
5.5.2 Platelet-poor Plasma Coagulation 127
5.5.3 Platelet Accumulation and Fibrinogen Deposition 131
5.5.4 Glycosaminoglycan Digestion 132
5.6 Discussion 133
5.7 Conclusion 140
CHAPTER VI: Thrombomodulin-modified decellularized small intestinal submucosa 144
6.1 Abstract 144
6.2 Introduction 145
6.3 Materials and Methods 147
6.3.1 Reagents 147
6.3.2 Thrombomodulin Modification 148
6.3.3 APC Generation 148
6.3.4 In Vitro *Stability* 149

6.3.5 Coagulation Assays 149
6.3.6 Baboon Ex Vivo Arteriovenous Shunt 151
6.3.7 Statistics 152
6.4 Results 152
6.4.1 Thrombomodulin-modified SIS Generates APC 152
6.4.2 In Vitro *Stability* 153
6.4.3 Coagulation Assays 154
6.4.4 Baboon Arteriovenous Shunt 156
6.5 Discussion 157
CHAPTER VII: Summary 161
CHAPTER VIII: Future Directions 166
8.1 Heparin and Thrombomodulin-modified SIS 166
8.1.1 Heparin-modified SIS Prolongs Plasma Coagulation 167
8.1.2 Dual-modified SIS Retains Full Thrombomodulin and Heparin Activities 168
8.1.3 Dual-modified SIS Reduces Platelet Accumulation 169
8.1.4 Summary: Heparin and Thrombomodulin-modified SIS 169
8.2 APC Signaling on ECs 170
8.3 Stability of Biologically-active Coatings In Vivo 172
References 173
Biographical Sketch 208

List of Figures

Figure 2.1: The blood coagulation cascade 9

Figure 2.2: Endothelial regulation of hemostasis and thrombosis 3

Figure 2.3: Structure of thrombomodulin 18

Figure 2.4: The interaction between inflammation and hemostasis in biomaterial thrombosis 27

Figure 2.5: Strategies to enhance *in situ* endothelialization of vascular grafts. 34

Figure 3.1: Morphology of endothelial and endothelial outgrowth cells 74

Figure 3.2: Representative flow cytometry histograms of ECs and EOCs treated with TNFα 75

Figure 3.3: Median fluorescence of ICAM-1 by ECs and EOCs measured via flow cytometry 75

Figure 3.4: Gene expression of ECs and EOCs in the presence and absence of TNFα treatment 77

Figure 3.5: Coagulation factor activation by untreated and TNFα-treated ECs and EOCs 78

Figure 3.6: Coagulation factor activation on cell-seeded vascular grafts in the presence and absence of TNFα treatment 79

Figure 3.7: Thrombus formation on cell-seeded vascular grafts in a baboon arteriovenous shunt 80

Figure S3.1: A cell-seeded ePTFE vascular graft connected to the baboon arteriovenous shunt loop 86

Figure S3.2: ICAM-1 expression of TNFα-treated ECs and EOCs measured by flow cytometry 86

Figure S3.3: APC generation of TNFα-treated ECs and EOCs normalized to untreated cells 87

Figure 4.1: SIS Device Construction and Deployment 97

Figure 4.2: Flow cytometry characterization of sheep EOCs. 103

Figure 4.3: Biotinylation of anti-KDR antibody 104

Figure 4.4: Confirmation of SIS modification 105

Figure 4.5: Thickness of suspended SIS devices post-implantation 106

Figure 4.6: Representative angiography of EOC-seeded SIS devices in sheep jugular veins and of a valve post-explantation 107

Figure 4.7: Thickness of explanted SIS valves post-implantation 108

Figure 4.8: Immunohistochemical staining of SIS valves 109

Figure 5.1: Tissue factor activity of SIS and clotting times of plasma treated with corn trypsin inhibitor 127

Figure 5.2: Prothrombin time (PT) and activated partial thromboplastin time (APTT) of plasma and plasma with SIS or cSIS 128

Figure 5.3: Coagulation times of plasma with SIS and cSIS 130

Figure 5.4: Mixed plasma clotting times 131

Figure 5.5: Platelet accumulation and fibrin deposition on SIS and cSIS devices 132

Figure 5.6: Plasma clotting time following enzymatic removal of GAGs 133

Figure S5.1: *Ex vivo* baboon arteriovenous shunt loop 141

Figure S5.2: Simplified diagram of plasma coagulation and coagulation assay reagents 142

Figure S5.3: Rate of platelet accumulation on SIS and cSIS 143

Figure S5.4: Residual anticoagulant activity of SIS 143

Figure 6.1: Role of thrombin, thrombomodulin and APC thrombosis 147

Figure 6.2: APC Generation of TM-SIS 153

Figure 6.3: Activity of TM-SIS following incubation in plasma 154

Figure 6.4: Prothrombin Time (PT) and Activated Partial Thromboplastin Time (APTT) of SIS and TM-SIS 155

Figure 6.5: Surface-initiated, tissue factor and contact activated coagulation times 156

Figure 6.6: Platelet accumulation and fibrinogen deposition on SIS and TM-SIS 157

Figure S6.1: Surface-initiated coagulation times of SIS modified with non-specific proteins 160

Figure S6.2: Plasma coagulation times initiated in solution 160

Figure 8.1: Coagulation times of plasma incubated with Hep-SIS 167

Figure 8.2: APC generation and plasma coagulation times for dual-modified SIS 168

Figure 8.3: Platelet accumulation on SIS and Hep-TM-SIS devices 169

Figure 8.4: APC enhances barrier integrity of ECs 171

Figure 8.5: Barrier function of ECs treated with APC and TNFα 172

List of Tables

Table 2.1: Common cardiovascular devices and blood-contacting materials with estimated usage worldwide 31

Table 2.9.1: Defining properties of EOCs 44

Table 2.9.2 : A summary of studies characterizing how fluid shear stress affects EOC function and response to TNFα treatment 53-54

Table S3.1. Primer sequences used for qPCR gene expression analysis and the size of the amplified cDNA in base pairs (bp) 84

Supplementary Table S3.2. Gene expression of ECs and EOCs in the presence and absence of TNFα treatment 85

Table S5.1: Reaction conditions for enzymatic digestion of glycosaminoglycans (GAGs) 140

List of Abbreviations

acLDL	Acetylated low density lipoprotein
ADP	Adenosine triphosphate
ANOVA	Analysis of variance
APC	Activated protein C
APTT	Activated partial thromboplastin time
BSA	Bovine serum albumin
CAG	Cysteine-alanine-glycine
CD	Cluster of differentiation
CDVI	Chronic deep venous insufficiency
cSIS	Crosslinked SIS
DMSO	Dimethyl sulfoxide
DNA	Deoxyribonucleic acid
EC	Endothelial cell
ECM	Extracellular matrix
ECMO	Extracorporeal membrane oxygenation
EDTA	Ethylenediaminetetraacetic acid
EOC	Endothelial outgrowth cell
eNOS	Endothelial nitric oxide synthase
EPC	Endothelial progenitor cell
EPCR	Endothelial protein C receptor
ePTFE	Expanded polytetrafluoroethylene
F	Factor (ex. FX)

FBS	Fetal bovine serum
Fc	Fragment crystallizable
FMO	Fluorescence minus one
GAG	Glycosaminoglycan
GAPDH	Glyceraldehyde 3-phosphate dehydrogenase
GP	Glycoprotein
GPCR	G-protein coupled receptor
HBSS	Hanks balanced salt solution
HMWK	High molecular weight kininogen
ICAM-1	Intercellular adhesion molecule-1
IgG	Immunoglobulin G
KDR	Kinase domain repeat
MCAM	Melanoma cell adhesion molecule
NHS	*N*-hydroxysuccinimide
NO	Nitric oxide
PAI-1	Plasminogen activator inhibitor-1
PAR	Protease activated receptor
PBS	Phosphate buffered saline
PECAM	Platelet endothelial cell adhesion molecule
PGI_2	Prostacyclin
PK	Prekallikrein
PT	Prothrombin time
qPCR	Quantitative polymerase chain reaction

RGD	Arginine-glycine-aspartate
rh	Recombinant human
RNA	Ribonucleic acid
SELEX	Systematic evolution of ligands by exponential enrichment
SIS	Small intestinal submucosa
t-PA	Tissue-type plasminogen activator
TBS	Tris-buffered saline
TF	Tissue factor
TFPI	Tissue factor pathway inhibitor
TM	Thrombomodulin
TNFα	Tumor necrosis factor α
VCAM-1	Vascular cell adhesion molecule-1
VEGF	Vascular endothelial growth factor
VEGFR	Vascular endothelial growth factor receptor
vWF	von Willebrand factor

Abstract

Biologically-active, Anti-thrombotic Coatings for Vascular Biomaterials

Jeremy J. Glynn

Department of Biomedical Engineering
School of Medicine
Oregon Health & Science University

October 2015
Thesis Advisor: Monica T. Hinds, PhD

Cardiovascular disease is the leading cause of death in most developed countries and imparts a massive clinical burden. Numerous devices have been developed to treat cardiovascular conditions, and millions of blood-contacting devices are used worldwide every year. However, unacceptably high rates of thrombosis have precluded the clinical use of numerous devices, such as a small diameter vascular graft or an artificial venous valve. Inspired by the function of the endothelium, the natural lining of blood vessels, this work utilized multiple strategies to incorporate biologically-active modifications onto vascular biomaterials to interact with blood cells and proteins in an attempt to reduce material-induced thrombosis. Work in this thesis characterizes the cellular phenotype of a novel progenitor-derived endothelial-like cell, two *in vivo* assessments of bioprosthetic venous valve endothelialization, the hemocompatibility consequences of crosslinking a decellularized matrix, and a novel modification of decellularized matrix for protein C activation. This dissertation describes novel biomaterials designed for vascular applications for the advancement of cardiovascular medicine.

CHAPTER I: Introduction

1.1 Background

Biomedical engineering strives to address current unmet clinical needs by utilizing an engineering skillset in partnership with knowledge of physiology and cell biology. Within biomedical engineering is the field of biomaterials, which seeks to develop materials that integrate with cells and tissues to regulate biological processes. A shifting paradigm in biomaterials research has been in the definition of "biocompatibility" to reflect not just a tolerance of the material by the body, but instead to consider the capacity of the material to promote a pro-healing response and integration into the surrounding tissue. A similar focus can be applied to hemocompatibility. Instead of developing materials that are simply tolerated with regard to activation of coagulation, biomaterials can be developed that actively produce factors that reduce thrombogenesis. Thus, the hypothesis of this research was that biologically-active modifications with anti-thrombotic activity would reduce biomaterial-initiated thrombus formation.

1.2 Thesis Summary

The development of biomaterials for vascular applications has traditionally focused on materials that are considered biocompatible based on minimal immune or inflammatory response, and do not promote blood coagulation or platelet activity. These selection criteria have resulted in the current types of materials typically used in vascular devices today: polyurethanes, Dacron (polyethylene terephthalate), and ePTFE are used predominantly in vascular grafts and prostheses, while metals such as stainless steel and nitinol are commonly used in stents. These materials have facilitated

numerous beneficial therapeutic interventions, including bypass grafting of the peripheral vasculature and post-angioplasty stenting of arteries to treat atherosclerotic plaques. However, there are considerable limitations with the applications that these materials can be used for. For instance, there is currently no clinically-accepted commercial vascular graft less than 5 mm in diameter; similarly, there is no artificial venous valve that can be used to treat chronic venous insufficiency. Both of these devices are limited due to unacceptably high rates of thrombosis.

Recognizing that endothelial cells (ECs) are the key regulators of these detrimental processes, there is great interest instilling the functionality of ECs into these materials. Considerable research by Zilla, *et al*. and others has investigated seeding patients' own ECs onto clinical graft materials such as ePTFE. However, the processes of harvesting ECs from a patient's vessel and culturing sufficient cell numbers to seed such grafts were both challenging and expensive. Novel endothelialization strategies, or applying endothelial-like functions to acellular materials, are alternate approaches to reduce biomaterial-mediated thrombosis without requiring the harvest and expansion of mature ECs.

The goal of this research was to develop and apply biologically-active, anti-thrombotic modifications to vascular biomaterials in an attempt to reduce material-induced thrombosis. Inspired by the function of the endothelium, the natural lining of blood vessels, this work utilized multiple strategies to incorporate endothelial cell function in vascular biomaterials. First, this work characterizes a unique population of endothelial-like cells, known as "endothelial outgrowth cells," or EOCs, with regard to regulation of thrombotic and inflammatory processes. EOCs are derived from progenitor

cells found circulating in peripheral blood and can be rapidly expanded in culture, addressing some major limitations of using mature vein ECs for seeding vascular materials. We provide the first comparison of baboon EOCs and carotid ECs isolated from the same donors to characterize EOC regulation of key endothelial processes.

Following this work, we describe two methods to accelerate the endothelialization of a decellularized matrix biomaterial by either seeding with EOCs pre-implantation, or by binding circulating progenitor cells *in situ* using a specific capture antibody. This decellularized matrix, derived from porcine small intestinal submucosa (SIS), has been used in the construction of a bioprosthetic venous valve. We performed an *in vivo* assessment of these two endothelialization techniques to determine how they affect the detrimental remodeling of SIS that previously limited the function of the valve.

Seeding materials with ECs prior to implantation is limited by *in vitro* culture of cells and increasing the complexity of the surgical implantations. Therefore, we identified biomaterial modifications that are acellular to provide off-the-shelf functionality. As carbodiimides are commonly used to crosslink decellular matrices and to immobilize biomolecules, the effect of crosslinking on the hemocompatibility of SIS was first characterized. Additionally, this work determined the anti-thrombotic activity of SIS modified with thrombomodulin, a protein found on the endothelium that is responsible for catalyzing activation of protein C, an anticoagulant and anti-inflammatory molecule.

The results from this work provide insight into the development of biologically-active, anti-thrombotic modifications to vascular biomaterials to address current limitations in cardiovascular therapies.

CHAPTER II: Background

2.1 Vascular Biology

The cardiovascular system of large, multicellular organisms evolved to overcome the restrictions of diffusion-limited transport of molecules needed to support cellular metabolism. Blood, composed of cells suspended in a nutrient-rich plasma, is the fluid medium in which molecules and various cells are transported and also plays critical roles in temperature control, pH regulation and metabolic waste removal. In humans, a four-chambered heart provides the primary pressure to drive blood through a system of blood vessels that perfuse all the tissues in the body. Arteries and arterioles carry blood to tissues and are lined with vascular smooth muscle cells that contract and relax to regulate vessel diameter in response to a number of factors, most notably nitric oxide released by the local endothelium [1]. Blood vessel resistance and the corresponding blood flow through the vessel are highly dependent on changes to vessel diameter. If blood flowing through a vessel is considered analogous to water flowing through a cylindrical pipe, for a given vessel length the resistance of the vessel is inversely proportional to the 4^{th} power of the vessel radius, highlighting the significance of vessel dilation and contraction in regulating blood flow. Blood flow is typically unidirectional and laminar; however, vascular branching, atherosclerotic plaques, or vascular interventions such as stents can result in local flow disruption and recirculation.

2.1.1 Endothelial Cell Physiology[1]

The luminal surface of blood vessels is lined with a confluent monolayer of endothelial cells (ECs). As the interface between the blood and other organs, ECs integrate multiple physical and biochemical cues to regulate platelet adhesion and activation, leukocyte adhesion and transmigration, vascular permeability, vascular tone, and angiogenesis [2,3]. ECs locally mediate these processes through both membrane-bound factors, such as tissue factor, thrombomodulin, and E-selectin, as well as secreted factors, such as nitric oxide and prostacyclin [4]. A major determinant of the EC phenotype is the local hemodynamic environment. Wall shear stress resulting from blood flow through the vessel initiates EC cytoskeletal remodeling and causes cellular elongation and alignment in the direction of flow [5]. ECs respond to unidirectional, laminar flow by producing numerous factors which inhibit blood platelet recruitment and activation, intimal proliferation and leukocyte adhesion. Conversely, disturbed flow conditions which yield a low average wall shear stress promote EC dysfunction and facilitate the early stages of atherogenesis including leukocyte adhesion and transmigration into the sub-endothelial space [6]. Tools that measure blood flow and characterize regions of disturbed flow can be used to identify vascular locations prone to atherosclerosis, as the connection between atherosclerotic plaque localization and regions of disturbed blood flow has been repeatedly demonstrated.

[1] Section 2.1.1 was originally published in *Cellular and Molecular Bioengineering.* Jones CM, Baker-Groberg SM, Cianchetti FA, Glynn JJ, Healy LD, Lam WY, et al. Measurement science in the circulatory system. *Cell Mol Bioeng*. 2014;7:1–14.

2.2 Hemostasis and Thrombosis

In the event of injury that results in bleeding, it is necessary for the body to have a natural means of halting blood loss. This essential process, hemostasis, is required to prevent death from excessive bleeding. The necessity of this system is evident by the variety of natural toxins as well as commercial poisons that target hemostasis [7,8]. Conversely, the aberrant amplification of hemostasis can result in the occlusion of blood vessels, i.e. thrombosis. Thus, a careful balance of pro- and anti-thrombotic factors is necessary to maintain hemostasis without initiating pathogenic thrombosis. The factors that tip the balance in favor of a pro-thrombotic environment are generally organized into a three categories, known as “Virchow’s Triad” after the German physician Rudolf Virchow and his study of venous thrombosis. This triad is composed of 1) blood hypercoagulability, 2) blood stasis, and 3) endothelial dysfunction [9]. Blood hypercoagulability refers to a systemic condition of heightened pro-coagulant activity that can be due to a number of environmental and genetic factors [10]. Examples include genetic mutations such as Factor V Leiden [11], as well as oral contraceptive use [12], chemotherapy treatment [13], and systemic inflammation such as in sepsis [14]. A more detailed description of blood coagulation, as well as specific abnormalities that result in hyper- and hypo-coagulable states will be discussed in section 2.2.2. Blood stasis is a local perturbation in blood flow that results in an accumulation of activated coagulation factors. Without careful design and operation, blood stasis can occur in medical devices including artificial heart valves [15] and central venous catheters [16]. Blood stasis can also occur absent of a device in the left atrium during atrial fibrillation [17], or in the cusp of venous valves, especially in the elderly [18]. Endothelial cell

phenotype is dependent on the local hemodynamic environment; thus, endothelial dysfunction is closely related to abnormal (non-laminar) blood flow [19]. At a molecular level, endothelial dysfunction refers to a shift in the expression or secretion of molecules to favor pro-thrombotic and pro-inflammatory factors rather than anti-thrombotic molecules [20]. In instances where the vessel wall is damaged, such as angioplasty and stent deployment, the endothelial layer may actually be removed from the vessel wall, exposing the underlying pro-coagulant basement membrane proteins, secreted von Willebrand factor (vWF), and tissue factor (TF).

2.2.1 Platelets in Hemostasis and Thrombosis

Platelets are small, anuclear cells produced from megakaryocytes in the bone marrow. Although platelets lack DNA, they possess megakaryocyte-derived mRNA and cellular machinery necessary for protein synthesis. Platelets are primarily responsible for preventing hemorrhage by first forming a platelet-rich aggregate at the site of bleeding (the “platelet plug”) and also by facilitating plasma coagulation by catalyzing coagulation factor activation reactions on their activated membranes [21].

Platelet adhesion is initially mediated by the receptor complex glycoprotein Ib/V/IX. The interaction between vWF, generally deposited by ECs and exposed by vascular injury, and glycoprotein Ib is the major tethering mechanism. The collagen receptors glycoprotein VI and glycoprotein Ia also mediate tethering to exposed basement membrane [22]. Following the initial platelet adhesion, local agonists including adenosine (ADP), thrombin, and thromboxane A_2 activate platelets, typically through G-protein coupled receptors (GPCRs). Activated platelets then express

activated glycoprotein IIb/IIIa (integrin αIIb/β3) that enables binding to fibrinogen and platelet aggreagation.

2.2.2 Blood Plasma Coagulation

Coagulation reactions have historically been divided into the intrinsic, extrinsic and common pathways [23–25]. The intrinsic and extrinsic pathways provide two unique means to activate Factor (F)X and, by nature of the numerous enzymatic reactions that occur in each pathway, enable multiple points of regulation and feedback (Figure 2.1). The common pathway encompasses the terminal steps in plasma coagulation that results in a fibrin mesh that is the major protein component of a thrombus.

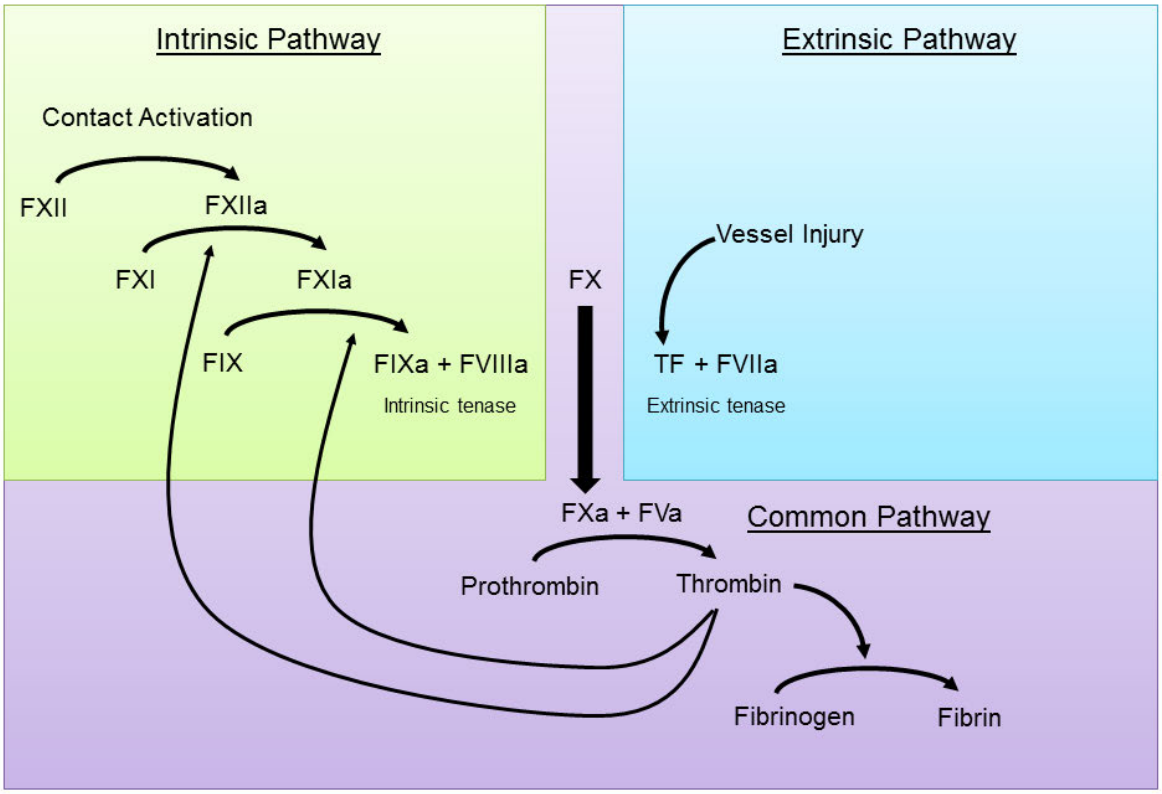

Figure 2.1: The blood coagulation cascade. The intrinsic and extrinsic pathways provide two mechanisms to activate FX. The common pathway results in the cleavage of fibrinogen to form fibrin, the major protein component of a thrombus. Thrombin feedback on the intrinsic pathway is central to thrombus propagation. Coagulation factors are indicated by 'F' followed by roman numerals; activated factors are designated with 'a'. "TF", tissue factor.

The extrinsic pathway is initiated when tissue factor becomes exposed on a damaged blood vessel. Small amounts of circulating FVIIa bind the exposed tissue factor and form the extrinsic "tenase", an enzyme complex capable of activating FX. The exposure of tissue factor is one of the main initiators of hemostasis and is critical for stopping hemorrhage [26,27].

Alternatively, the intrinsic pathway is initiated by contact with artificial or negatively-charged surfaces. The wide variety of substrates that initiate the intrinsic pathway include natural molecules such as polyphosphates on bacterial surfaces and

extracellular DNA released by neutrophils, as well as all synthetic materials and especially those with strong negative charges such as glass [28–30]. On these materials, FXII adsorbs and autoactivates; concurrently, high molecular weight kininogen (HMWK) also binds to the surface. FXIIa cleaves HMWK, releasing bradykinin which feeds back to activate additional FXII, as well as acting as a strong pro-inflammatory stimulus. After this initial activation of FXII and HMWK, FXIIa proceeds to activate FXI. Activated FXI then activates FIX which subsequently activates FVIII. FIXa and FVIIIa form the intrinsic tenase. Activated FX and FVa form the prothrombinase complex that catalyzes the conversion of the zymogen prothrombin to the enzymatically-active thrombin. Thrombin is the central protease in plasma coagulation and cleaves fibrinogen to initiate the polymerization of fibrin, the main protein constituent of a blood clot. Additionally, thrombin acts in positive feedback pathways to activate platelets, thrombin activatable fibrinolysis inhibitor (TAFI), protease activated receptor 1 on endothelial cells, and other targets to perpetuate thrombus formation.

An important feedback system between the intrinsic and extrinsic coagulation cascades results from activation of FXI by thrombin [31]. In normal hemostasis, once a small amount of thrombin is generated by the extrinsic pathway, thrombin activation of FXI and the proceeding intrinsic cascade becomes the dominant pathway for FX activation [25]. Thus in coagulation *in vivo*, FXI acts more as a positive feedback mechanism to initiate FIX and the intrinsic tenase complex rather than as the downstream target of contact-activated FXIIa. The introduction of a foreign biomaterial

surface may increase the relevance of contact activation and FXIIa-mediated activation of FXI [32].

The clinical phenotypes of patients that are deficient in one of the coagulation factors provide insight into the roles of these factors in hemostasis and thrombosis. Deficiencies in FVIII or FIX, both components of the intrinsic tenase complex, result in hemophilias A and B, respectively, which are characterized by prolonged bleeding times following injury and occasional bleeding including into joints [33]. A deficiency in FXI results in a mild bleeding phenotype with bleeding at sites of high fibrinolytic activity [34], while deficiency of FXII does not cause any significant detriment to the hemostatic system. However, deficiencies in either FXI or FXII result in diminished thrombotic response [35] and were protected from stroke [36] in mouse models. In contrast to the above factors, deficiencies in TF [26], FVII [37], FX [38], and FV [39] are embryonic or neonatal lethal in mice and, other than rare FV-deficient patients that possess residual FV activity, these phenotypes have not been observed clinically.

2.2.3 Blood Flow

In vivo, thrombotic reactions are highly-dependent on blood flow mechanics. Blood flow determines the transport of cells and coagulation factors to and away from the developing thrombus, as well as shear-dependent reactions such as platelet-vWF binding [40–42]. Shear rates range from <100 s^{-1} in large veins to 1000-1500 s^{-1} in arteries [43]. The influence of flow on thrombogenesis is evident in the difference in composition of thrombi in different vascular location. Arterial, “platelet-rich” thrombi that develop in vessels with high flow rates and are dominated by platelet accumulation due to flow-mediated depletion of coagulation factors and shear-activated platelet adhesion;

in contrast, the low flow environment of venous, “fibrin-rich” thrombi enables more extensive fibrin polymerization and red blood cell entrapment [44]. The role of blood flow in the development of venous thrombosis was known long ago as demonstrated by Virchow’s inclusion of blood stasis as one of his three major factors contributing to thrombosis.

A number of both *in vitro* and *ex vivo* models have been developed to study biomaterial hemocompatibility using flowing blood. *In vitro* models that use a parallel plate or a rotating loop of tubing are useful for simulating acute thrombosis as the circulation times in these devices are typically only a few minutes [43,45]. The measurement variable for these assays is generally the time required for blood clot formation to occur in the tubing, and anticoagulant drugs are used during the blood collection process. In contrast, *ex vivo* models that utilize a shunt loop allow for blood to flow directly from an animal’s blood vessel into tubing that connects to the device of interest before flowing back into the animal’s vascular system. Blood flow can be controlled either by an external pump or, if there is sufficient blood pressure to drive blood flow through the shunt loop, a clamp can be placed distal to the device to control the resistance and thus the flow rate [43,46,47]. In these systems, platelets and/or fibrinogen can be radiolabeled for the real-time measurement of thrombus accumulation on the biomaterial using a gamma camera. These models have been used to discern the effects of inhibiting different shear-dependent platelet adhesion proteins [48], anti-thrombotic effects of APC infusion and thrombin-mediated protein C activation [47,49], and the roles of intrinsic pathway coagulation factors XI and XII in graft thrombosis [50,51].

2.3 Endothelial Regulation of Thrombosis

In the design of vascular biomaterials, the endothelium is the model “material” that our bodies naturally use to cover the entire vascular system. The importance of the endothelium in regulating thrombogenesis has been demonstrated by multiple studies where the endothelium was mechanically disrupted by a balloon angioplasty, resulting in widespread thrombus deposition and luminal narrowing in the treated arteries [52–54]. The mechanisms by which the endothelium regulates hemostasis and thrombosis, summarized in Figure 2.2, generally affect three interconnected processes: platelet activation, plasma coagulation and fibrinolysis [55].

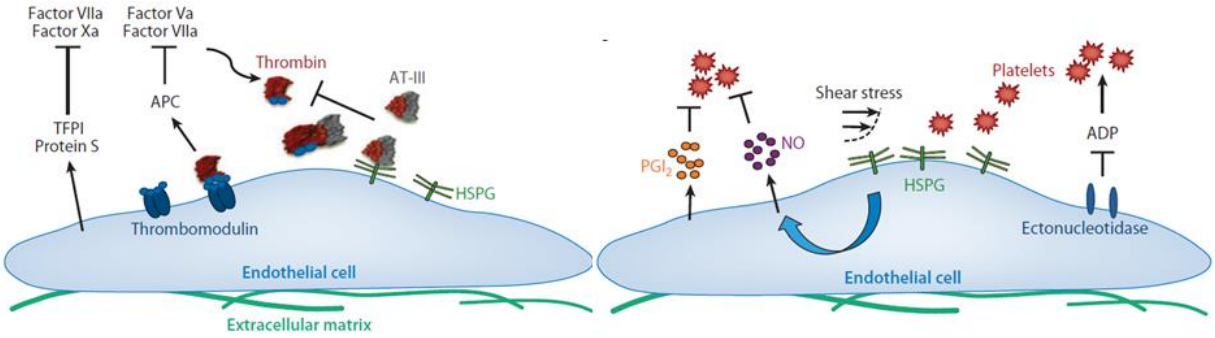

Figure 2.2: Endothelial regulation of hemostasis and thrombosis. ECs locally mediate blood coagulation and platelet adhesion through both membrane-bound factors such thrombomodulin and heparan sulfate proteoglycan (HSPG), as well as secreted factors, such as nitric oxide and prostacyclin (PGI_2). “TFPI”, tissue factor pathway inhibitor; “AT-III”, antithrombin III; “ADP”, adenosine diphosphate. Reprinted from Li and Henry, 2011 [55].

2.3.1 Endothelial Regulation of Platelet Activation

ECs secrete NO, which along with being a vasodilator is a potent inhibitor of platelet activation [56,57]. Prostacyclin (PGI_2) is also secreted by endothelial cells, and similarly inhibits platelet activation. The synthesis and secretion of NO and PGI_2 can both be modulated by fluid shear stress. In addition to secreted factors, ECs express membrane-bound proteins that directly inhibit platelet activation and adhesion to the

vessel wall. The EC surface has a layer of glycosaminoglycans (GAGs) known as the glycocalyx. The negative charge of these GAGs maintains a hydrated surface that also aids in repelling platelets and leukocytes [58]. Some of the prominent GAGs include heparan sulfate and dermatan sulfate, both of which can help mediate serpin-dependent inhibition of coagulation enzymes. Disruption of the glycocalyx partially inhibits endothelial mechanotransduction of fluid shear stress, thereby reducing the expression of anti-coagulant molecules such as NO [59].

2.3.2 Endothelial Regulation of Plasma Coagulation

Activation of coagulation zymogens to their active forms is often accelerated in the presence of activated platelets by the catalytic properties of the platelet membrane. As such, endothelial regulation of platelet activation and adhesion is tightly related to the regulation of plasma coagulation. However, some proteins expressed by ECs directly influence coagulation factor activity in the absence of platelets. Thrombomodulin is an endothelial membrane protein that, by binding thrombin, is responsible for the physiologic production of activated protein C (APC) as well as blocking the exosite on thrombin necessary for binding pro-coagulant molecules such as fibrinogen. APC directly inhibits coagulation by proteolytically inactivating FVIIIa and FVa, and also acts to reduce EC apoptosis in inflammatory conditions to sustain EC-dependent regulation of thrombosis [60]. Protein S, also secreted by ECs, is a cofactor that accelerates APC-dependent inhibition of FVa and FVIIIa. In addition to thrombomodulin, ECs express both TF and tissue factor pathway inhibitor (TFPI). Although ECs can be stimulated by tumor necrosis factor α (TNFα) or thrombin to express TF and initiate the extrinsic coagulation cascade, a healthy endothelium absent of these conditions will secrete

TFPI, which binds the TF-FVIIa complex to block extrinsic tenase activity. ECs also express the ectonucleotidase cluster of differentiation (CD)39 that degrades ADP, a platelet agonist.

2.3.3 Endothelial Regulation of Fibrinolysis

ECs secrete molecules that both promote and inhibit fibrinolysis, the breakdown of fibrin strands. The process of fibrinolysis requires circulating plasminogen to be activated into plasmin, the central enzyme responsible for fibrin breakdown. To accelerate plasmin activation and thus fibrinolysis, ECs secrete tissue-type plasminogen activator (t-PA), and urokinase under certain inflammatory conditions. A recombinant form of t-PA, Alteplase, is a common drug used in the acute treatment of stroke. Fibrinolytic activity can also be limited by ECs with the secretion of plasminogen activator inhibitor-1 (PAI-1).

2.3.4 The Thrombomodulin-protein C Pathway

The identification of thrombomodulin and its role in regulating coagulation was discovered by the collaborative research of Charles Esmon and Whyte Owen in the late 1970s and early 1980s [61]. The endothelial membrane protein thrombomodulin plays two distinct roles in regulating coagulation, both of which require binding to thrombin. First, thrombomodulin-bound thrombin has a much lower affinity for fibrinogen and platelets, reducing its pro-coagulant activity. Second, the thrombin-thrombomodulin complex is responsible for catalyzing the formation of APC, a potent anticoagulant and anti-inflammatory enzyme. The significance of APC activity is underscored by a significant increase in deep vein thrombosis among adults with heterozygous deficiency,

and severe thrombosis resulting in ischemic necrosis in homozygous deficient newborns [62].

In addition to thrombomodulin, EPCR accelerates protein C activation by thrombin by 10-20 fold [63]. The endothelium of large blood vessels, such as the portal vein and hepatic artery, is rich in EPCR, while capillary ECs have little to no EPCR expression [64]. Additionally, EPCR modulates endothelial signaling pathways. Most notably, endothelial PAR-1 can be activated by both thrombin and APC, though EPCR is necessary for APC-mediated PAR-1 signaling at physiologic concentrations of these proteases [65,66]. Thus, EPCR reduces thrombotic processes both directly by accelerating APC generation as well as enabling APC-mediated protection of endothelial cell functions [67]. Thrombotic complications have been observed in both basic and clinical studies that reduce EPCR activity. Blocking protein C binding to EPCR decreases survival of baboons challenged with sub-lethal doses of *E. coli*, and the animals showed both thrombotic and inflammatory pathologies that contributed to their mortality [68]. Similarly, humans with autoantibodies against EPCR have approximately two-fold greater risk of deep vein thrombosis.

As one of the most dominant natural anticoagulant mechanisms utilized by endothelial cells, the thrombomodulin-protein C pathway will be described in more detail.

Structure of thrombomodulin

Structural studies of thrombomodulin have identified a number of specific functional domains (Figure 2.3) [69,70]. At the N-terminus, the most distal extracellular region of the protein, is a C-type lectin domain. This domain comprises nearly 40% of

the mass of thrombomodulin and is somewhat unique in that it lacks a calcium binding domain. Functionally, the C-type lectin does not play a major role in thrombin binding or protein C activation, and instead has its most potent affects as an anti-inflammatory molecule as demonstrated by reduced survival of mice lacking this domain of thrombomodulin following endotoxin exposure and increased leukocyte accumulation in the lungs [71]. The mechanisms for this anti-inflammatory effect are that it binds to and sequesters the pro-inflammatory molecule high mobility group box B1 protein [71] as well as the Lewis Y antigen to suppress LPS-induced inflammatory responses [72].

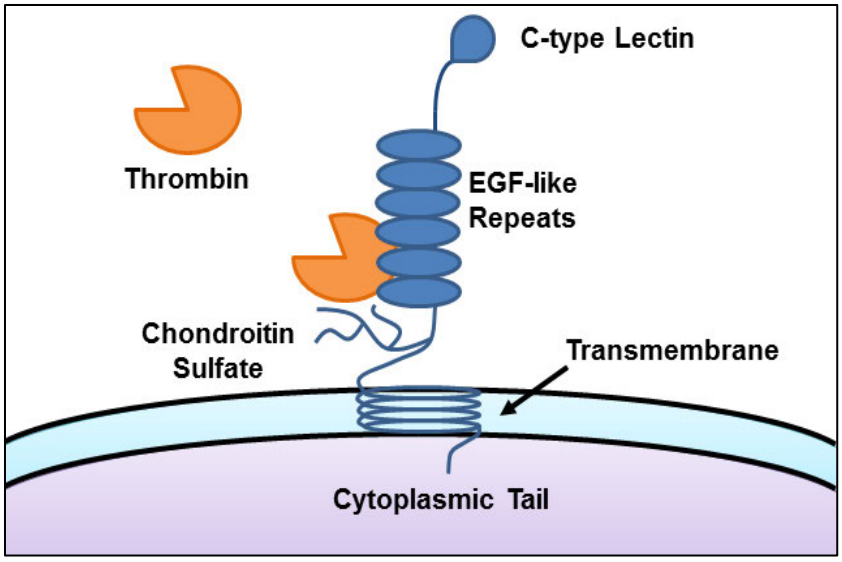

Figure 2.3: Structure of thrombomodulin. EGF repeats 4-6 facilitate thrombin binding and catalysis of protein C activation. Based on the illustration by Conway, 2012 [70]

Perhaps the most-studied domain of thrombomodulin is the grouping of 6 epidermal growth factor (EGF)-like repeats (EGF1-6), numbered from N- to C-terminal. The minimal domain required for binding thrombin consists of EGF5-6; however, EGF4 is also required to catalyze protein C activation [73,74]. Crystallography of the thrombin-thrombomodulin complex identified that the Met388 residue in repeat 4 is critical for properly orienting EGF5 [75], which is consistent with the numerous studies demonstrating that oxidation or disruption of this residue blocks protein C activation [76–78]. Interestingly, mutating this methionine to leucine (M388L) produces a thrombomodulin mutant that not only retains cofactor activity following treatment with oxidants, but also has approximately a 2-fold greater baseline catalytic rate than wild-type thrombomodulin [77,79]. In addition to facilitating protein C activation, EGF repeats 3-6 increase the catalytic rate of thrombin activatable fibrinolysis inhibitor (TAFI), which aids in clot stabilization.

The domain immediately extracellular to the transmembrane domain of thrombomodulin is serine-threonine-rich and presents sites for O-linked glycosylation [80,81]. Glycosylation with chondroitin sulfate affects many of thrombomodulin's activities including increasing affinity for thrombin and accelerating thrombin inhibition by protein C inhibitor, ATIII and heparin cofactor II [70,82,83].

The transmembrane domain of thrombomodulin contains 23 hydrophobic amino acids and is highly-conserved across species [69]. Notably, a mutation at Cys537 in the transmembrane domain results in a premature stop codon and causes shedding of the protein from the endothelium, resulting in ~180-fold higher concentrations of thrombomodulin in plasma [84]. A patient with this mutation did not have a history of bleeding incidents and yielded a normal pre-surgical coagulation assessment. However, surgery resulted in bleeding not responsive to red blood cell transfusions, fresh frozen plasma, desmopressin, or tranexamic acid. Thrombomodulin also contains a short cytoplasmic C-terminal tail containing phosphorylation sites that may regulate endocytosis and degradation of the protein [85,86].

Pleiotropic effects of APC

In humans, protein C is a 62 kDa protein synthesized in the liver that circulates at 4-5 µg/ml. Cleavage by APC exerts anticoagulant and anti-inflammatory effects through proteolytic activity in blood as well as signaling through protease activates receptors (PARs) on EC membranes. PARs are G-protein coupled receptors (GPCRs) that require the proteolytic removal of a small peptide from their extracellular N-terminus. Following the release of this peptide, the newly exposed N-terminus acts as a "tethered ligand" resulting in activation of the receptor complex [87]. The predominant

anticoagulant activity of APC is the inactivation of FVa. The significance of this anticoagulant activity is reflected in the fact that a mutation in FV at the APC cleavage site (Arg506Gln, “factor V Leiden”) is the most common hereditary risk factor for venous thrombosis in the Caucasian population [88,89]. APC also cleaves FVIIIa, a necessary component of the intrinsic tenase complex. Inactivaiton of both FVa and FVIIIa is accelerated by the cofactor protein S. The half-life of APC in plasma is approximately 20 min and is regulated through inactivation by serine protease inhibitors (serpins) [90]. Serpin activity is accelerated by GAGs, such as pharmacologically administered heparin as well as chondroitin sulfate on thrombomodulin, via a bridging mechanism.

In addition to the anticoagulant activities of APC resulting from the inactivation of plasma coagulation factors, APC signals via PARs on EC membranes. PAR1 is known as a major thrombin receptor on endothelial cells, and thrombin-mediated activation of PAR1 results in expression of surface ligands that facilitate rolling adhesion of platelets and leukocytes, inflammatory leakage of plasma proteins into tissues, and the production of platelet-activating factor, IL-6 and IL-8 [87]. In contrast to the pro-inflammatory effects of thrombin-mediated signaling, APC activation of PAR1 downregulates leukocyte adhesion ligands, inhibits apoptosis, and sustains endothelial barrier function in the presence of inflammatory stimuli. The disparate actions of APC and thrombin that result from activation of the same receptor seem to be dependent onn the binding of EPCR to APC and the co-localization of EPCR and PAR1 during APC-mediated activation. EPCR also plays a role in enhancing APC-mediated PAR1 signaling, as PAR1 has a much higher affinity for thrombin than APC, yet both are physiologically relevant PAR1 activators [63,91]. The dual-action of APC as both a

potent anticoagulant and anti-inflammatory has supported a number of *in vivo* studies in animals where APC has improved outcomes in septic infections, pulmonary inflammation, stroke and wound healing [65].

APC and thrombomodulin as therapeutics

Based on favorable animal studies, there have been a number of attempts to develop both APC and thrombomodulin into therapeutics for a variety of diseases [92,93]. The most well-known example was the development of APC into a therapeutic for sepsis, a blood-borne infection that causes disseminated intravascular coagulopathy and widespread inflammation. After promising preclinical studies in baboons where infusion of exogenous protein C rescued coagulopathies associated with *Escherichia coli* infection [94], a clinical trial was launched where recombinant activated protein C (Drotrecogin alfa) was used in a double-blind trial to treat patients with systemic inflammation and organ failure due to infection [95]. The trial demonstrated a reduction in mortality with only a slight increase in bleeding with APC treatment. The success of this trial led to the commercialization of APC by Eli Lilly and Company in 2001 under tha brand name Xigris®. On October 25, 2011, Xigris® was withdrawn from the market due to the preliminary results of a large, multi-center clinical trial that demonstrated a lack of efficacy compared to placebo as well as an increased risk of bleeding [96]. One reason for the discrepancy between the initial clinical data and the PROWESS-SHOCK trial has been attributed to the reduced sepsis mortality due to better standards of care as well as poor inclusion selection by physicians. Still, systemic infusion of APC as a treatment for sepsis is no longer considered a clinically beneficial treatment strategy.

Rather than abandoning the protein C pathway as a viable treatment strategy for sepsis, efforts have been ongoing to isolate specific effects of APC as well as to localize those effects for improved clinical outcomes [97]. Specifically, an APC variant where the FV binding site was mutated was developed. This variant possesses normal EPCR/PAR-1 signaling to preserve anti-inflammatory signaling on ECs but is unable to bind FV and thus has dramatically reduced anticoagulant function [98]. As such, this variant is expected to have a reduced risk of bleeding compared to wild-type APC and may provide a safer alternative to Drotrecogin alfa. As an alternative to delivering APC systemically, thrombomodulin has also been explored as a therapeutic. This strategy would have the advantage that APC would only be generated in the presence of thrombin, theoretically localizing APC generation to pro-thrombotic regions. ART-123 (Recomodulin) is a recombinant TM fraction containing EGF4-6 to facilitate protein C activation and was approved in 2008 in Japan for the treatment of disseminated intravascular coagulopathy and sepsis [99,100]. Additionally, a recombinant TM fraction containing EGF4-6, along with specific mutations to reduce sensitivity to oxidation and to prolong circulation times, has been introduced (Solulin), and is currently undergoing preclinical trials for the treatment of stroke [101,102].

In summary, the thrombomodulin-protein C pathway plays an important regulatory role in coagulation and inflammation as evidenced by the clinical manifestations of genetic abnormalities in this pathway and the commercial interest in harnessing this pathway as a therapeutic.

2.4 Endothelial Progenitor Cells

In adults, vascular repair and angiogenesis were thought to be due to the proliferation and migration of adjacent endothelial cells. The presence of a circulating progenitor cell with the capacity to differentiate into a mature endothelial cell was not widely accepted prior to the isolation of putative endothelial progenitor cells (EPCs) from adult blood by Asahara, et al. [103]. Following this seminal study, there has been an explosion of research on EPCs as the capacity for a blood borne cell to become an EC has many implications for human health, disease and therapeutic development. The number of cardiovascular disease risk factors a person possesses has been shown to correlate inversely with the quantity of circulating EPCs [104], while moderate exercise training has been shown to increase this quantity [105]. EPCs are recruited to hypoxic tissues such as developing tumors [106], ischemic tissues [107], as well as areas of endothelial damage such as denuded arteries [108].

In addition to the physiologic roles of EPCs, there has been considerable interest in the vascular biomaterials and tissue engineering community to utilize EPCs as a source for autologous ECs for various applications. The advantages of using EPC-derived cells rather than mature ECs in these applications include less-invasive harvest procedure (surgical removal for ECs vs. blood draw for EOCs), as well as the greater replicative potential of EPC-derived cells [109].

In contrast to the stem-like EPCs, mature circulating ECs (CECs) also circulate in the blood at low concentrations. Whereas EPCs are typically associated with vascular repair and vasculogenesis, CECs have been recognized as a marker of endothelial dysfunction or damage. Indeed, studies of various diseases have shown correlations

with endothelial dysfunction, measured by flow-mediated dilation or elevated plasma vWF, and the concentration of CECs [110,111]. Increased CECs are indicative of detachment of ECs from the blood vessel wall that can be due to multiple causes including mechanical injury, for instance following venipuncture or acute plaque rupture [112]. Alternatively, prolonged exposure to inflammatory cytokines and tissue proteases can disrupt endothelial adhesion to the basement membrane [113]. Conditions associated with CECs include acute coronary syndromes [111,113], congestive heart failure [110], septic shock [114], systemic lupus erythematosus [115], and multiple types of cancer [116–119]. Elevated CECs in blood is generally considered to result from these pathological conditions rather than being a causative factor.

There is general consensus that multiple markers are required to distinguish between circulating EPCs and mature CECs, which is accomplished by incorporating markers for both mature (ex. CD146 and CD31) and progenitor cells (ex. CD133 and CD34) in screening panels [120–123]. As such, the enumeration of CECs distinct from EPCs paralleled the development of multicolor flow cytometry which allowed for simultaneous detection of multiple endothelial-specific markers. A protocol devised by the Jain group at Massachusetts General Hospital utilizes multicolor flow cytometry to distinguish CECs (defined as $CD31^{bright}CD34^{+}CD45^{-}CD133^{-}$ cells) from EPCs (identified as $CD31^{+}CD34^{bright}CD45^{dim}CD133^{+}$ cells) [123]. This protocol has been used to quantify CECs and EPCs in patients with cancer, including a study demonstrating that the VEGF-specific antibody bevacizumab lowers both CECs and EPCs in patients with rectal cancer [124]. Additionally, differentiating between CECs and EPCs using multi-color flow cytometry has demonstrated that in breast cancer patients,

chemotherapy treatment decreased CECs but mobilized and increased circulating EPCs [116]. Although the identification and measurement of CECs may provide important metric for diagnosing and monitoring disease, cultures of CECs have very limited proliferation [125], and as such are not ideal for endothelializing vascular biomaterials *in vitro*. Furthermore, cultures of cells derived from peripheral blood that begin with a mixture of CECs and EPCs will become predominantly EPC-derived cells due to the significantly greater replicative potential of EPC-derived cells [126].

2.5 Summary: Vascular Biology

Residing at the interface of blood and the surrounding tissue, ECs are key regulators of hemostasis and thrombosis. Endothelial cells express a number of molecules, both membrane-bound and secreted, that regulate thrombosis through interactions with platelets, plasma coagulation factors, and the fibrinolytic system. Of these molecules, the endothelial cell membrane protein thrombomodulin plays a central role by binding thrombin and catalyzing the formation of APC. Endothelial progenitor cells can differentiate into EC-like cells both *in vitro* and *in vivo*, and an active area of research is the utilization of EPC-derived cells as an autologous source of an endothelial covering of vascular devices.

2.6 Biomaterials

The field of biomaterials is an interdisciplinary study using knowledge from materials science, physiology, cell biology, engineering, chemistry and more to design materials that elicit a desired biological response. Biomaterials research strives to develop materials-based treatments for specific medical needs through an informed design process that takes into consideration the biological requirements as well as

physical property requirements. Biomaterials are thus defined more by application than composition, and therefore the term encompasses a wide range of naturally-derived and synthetic materials, including (but not limited to) ceramics, metals, polymers, hydrogels, and a wide variety of naturally-derived compounds including collagens, glycosaminoglycans, decellularized tissues and many more [127]. Central to the study of biomaterials is the concept of *biocompatibility*, that is, “the ability of a materials to perform with an appropriate host response in a specific application” [128]. The host response is the encompassing term for all of the biological responses to a material once it is in contact with a biological system. This response includes mild inflammation surrounding sutures, fibrous encapsulation of an implant, calcification of an artificial heart valve, and thrombus formation at a vascular graft anastomosis. Although many of these host responses are typically framed negatively, these processes are part of the natural healing response; rather, it is only when one of these processes (ex. inflammation) persists to become a chronic reaction that the process is detrimental to the biomaterial integrity and ultimately patient health [129]. Because biomaterial-initiated thrombogenesis is a central concept of this work, the processes involved will be further discussed below.

2.6.1 Biomaterial Thrombogenesis

The hemostatic system is responsible for the necessary function of sealing leaks in the vascular system (i.e. stopping bleeding) to prevent death from hemorrhage. Alterations in the vessel wall such as those caused by atherosclerosis can initiate a detrimental upregulation of hemostatic activity that can result in detrimental thrombogenesis. Similarly, the foreign surface of a biomaterial can act as a trigger that

initiates thrombus formation that, unless regulated naturally or pharmacologically, can result in thrombosis and failure of the device. The clinical burden of device-initiated thrombosis is notable. Central venous catheter-related thrombosis affects approximately 5-15% of patients, and this number is significantly higher for cancer patients [130]. Furthermore, between 10 and 25% of vein grafts used for coronary artery bypass fail due to thrombosis [131]. Even low rates of stent thrombosis, ranging from 0.2 - 0.5% per year, results in tens of thousands of hospitalizations due to the vast number of stent procedures performed each year [132]. Specific mechanisms that contribute to biomaterial-mediated thrombosis will be discussed below. Although this discussion is divided into distinct processes for clarity, there is significant interaction between these systems (Figure 2.4).

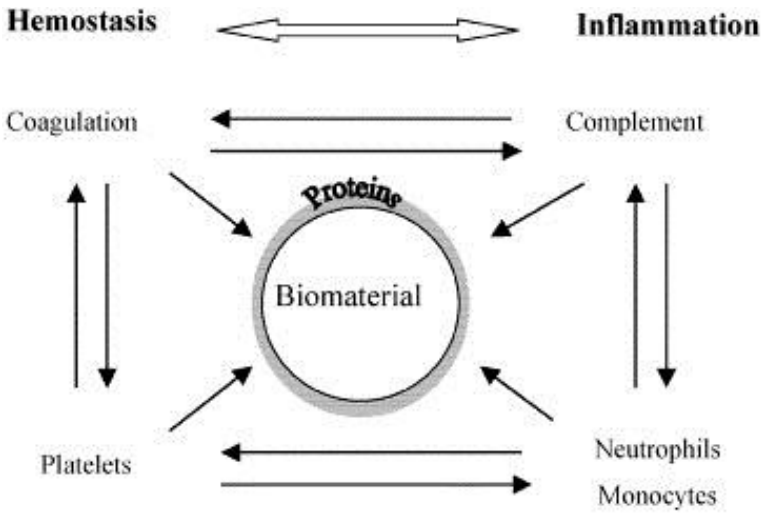

Figure 2.4: The interaction between inflammation and hemostasis in biomaterial thrombosis. The progression of biomaterial thrombosis is resultant from the combination of coagulation and complement systems as well as the signaling of platelets, neutrophils and monocytes. Reprinted from Gorbet and Sefton, 2004 [32].

Protein adsorption

Immediately upon contact with blood, plasma proteins adsorb to the biomaterials surface. The specific composition and quantity of protein adsorption is highly dependent

on materials surface properties including hydrophilicity and surface charge, as well as the blood flow characteristics such as wall shear rate [133]. Importantly, the composition of proteins adsorbed onto a material will change over time such that proteins with greater affinity for the material will displace those with less energetically-favorable interactions. This process is known as the “Vroman effect,” named after Dutch-American hemoatologist Leo Vroman. The composition of the proteins adsorbed to the biomaterial is important as some blood proteins, such as FXII and HMWK, will initiate pro-thrombotic reactions while other proteins, such as albumin, do not appreciably promote thrombogenesis. Furthermore, proteins such a fibrinogen can passively contribute to biomaterial thrombogenesis by adsorbing on biomaterials and providing attachment ligands for platelets.

Strategies to reduce protein adsorption on biomaterials typically involve altering the surface properties of a material. For instance, increasing surface hydrophilicity by conjugating hydrophilic polymers such as poly(ethylene glycol) (PEG) or poly(ethylene oxide) to the surface has been explored [134,135]. These polymers reduce protein adsorption on materials both through their hydrophilic nature, resulting in proteins having to displace water to adsorb, a thermodynamically unfavorable reaction, as well as through their long polymer structure that sterically inhibits proteins from binding the material surface [136,137]. Despite considerable advances in resisting adsorption of proteins to materials *in vitro*, these materials are limited *in vivo* as the polymer coatings are often eventually degraded following implantation.

Platelet adhesion

Circulating at a concentration of ~250,000 per µl, platelets are abundant and highly sensitive to a variety of stimuli to initiate activation and adhesion. With regard to biomaterials, activation of platelets can be accomplished by damaged endothelium from the surgical procedure, turbulent flow caused by anastomoses between a blood vessel and a graft, or external tubing and other foreign surfaces such as in extracorporeal membrane oxygenation (ECMO) devices. Activated platelets express a variety of receptors that enable their binding to proteins adsorbed onto the biomaterial surface. Bound platelets contribute to thrombogenesis by catalyzing coagulation reactions on their membranes, most notably FX and thrombin activation, and also by releasing granules containing ADP and thromboxane A_2 that recruit and activate additional platelets. As traditional synthetic biomaterials lack the inhibitory mechanisms of ECs to regulate platelet activation, platelets contribute significantly to biomaterial thrombosis. Even in high flow conditions, where activated coagulation factors can be rapidly removed from the material, platelets possess receptors and mechanisms to accumulate and contribute to device thrombosis.

Plasma coagulation

A traditional view of blood coagulation describes two main sources of activation: tissue factor and contact activation. The introduction of a foreign surface to blood is the best-described source of contact activation, and thus a great deal of study has been devoted to biomaterial-induced activation of the contact pathway. The contact pathway initiates with the adsorption and auto-activation of FXII to FXIIa. These adsorption and auto-activation reactions have traditionally been thought to occur at greater rates on

negatively-charged, hydrophilic surfaces such as glass. This observation provided the foundation for using reagents such as silica and kaolin as initiators for diagnostic assays of the contact pathway such as the activated partial thromboplastin time (APTT). The binding of FXII to a material surface initiates the formation of a contact activation complex with HMWK, prekallikrein (PK), and FXI. By reciprocal activation between FXII and kallekerin, sufficient amounts of FXIIa are produced to activate FXI to FXIa, and the coagulation cascade proceeds as discussed in Section 2.2.2. Biomaterials do not express TF like activated ECs; however, the pathway may contribute to biomaterial-initiated thrombosis by facilitating the binding and activation of leukocytes that express TF [138].

2.7 Cardiovascular devices

In response to the burden of cardiovascular disease on health throughout the world, a great number of vascular devices have been developed to correct or reduce the cardiovascular defect (Table 2.1). These devices range from pacemakers, where small leads are inserted into the heart muscle tissue and the rest of the device resides in the chest or abdomen, to vascular grafts used in bypass surgery, to extracorporeal devices used to re-oxygenate blood. Thrombo-embolic complications following device implantation are major causes of morbidity and mortality associated with device implantation. Although all of cardiovascular devices are present some risk for thromboembolic complications, the two devices focused on in this research currently do not have a clinically-viable option specifically due to high rates of thrombosis: a small diameter vascular graft, and an artificial venous valve. Therefore, strategies to apply

biologically-active, anti-thrombotic coatings to materials used in these devices is a potential method to advance the progress of these devices into the clinic.

Blood contacting device	Blood contacting material	No. per year
Catheters	Silicone, polyurethane, PVC, teflon	200,000,000
Guidewires	Stainless steel, nitinol	Millions
Pacemakers	Silicone, polyurethane, platinum	300,000
Vascular grafts	Dacron, ePTFE	200,000
Heart valves	Pyrolytic carbon, dacron, fixed natural tissue	200,000
Stents	Stainless steel, styrene-isobutyl polymer	4,000,000
Extracorporeal oxygenators	Silicone rubber	20,000
Artificial kidneys	Polyacrylnitrile, polysulfone, cellulose	1,200,000
Left ventricular assist devices	Polyurethane	1000

Table 2.1: Common cardiovascular devices and blood-contacting materials with estimated usage worldwide. Reprinted from Ratner, 2007 [139].

2.7.1 Vascular Grafts

When essential arteries become occluded, vascular grafts are used to restore blood flow. The three most common uses for vascular grafts are coronary artery bypass, peripheral artery grafting, and hemodialysis access [140]. Autologous vein grafts, typically harvested from the saphenous vein, can be used for coronary bypass grafting; however, approximately 15% of patients need alternative, synthetic grafts [141].The inferior patency rates of synthetic grafts, most commonly ePTFE, compared to autologous vein grafts (59% vs. 86% at 1 year) has resulted in synthetic grafts used only as a last option [142]. In peripheral arteries, which have larger diameters of 7-9

mm, ePTFE and Dacron (woven poly(ethylene terephthalate)) have both been used successfully with patency rates up to 80% for femoro-popliteal bypass grafts [140]. The discrepancy in patency rates between coronary and peripheral bypass grafts is primarily attributed to the increased diameter of peripheral grafts, which allows greater blood flow and requires a larger thrombus to form before occlusion.

Endothelial cell pre-seeded vascular grafts

Unlike in many animals, humans cannot spontaneously endothelialized a vascular graft more than 1-2 cm away from the implant site [143]. As ECs inhibit thrombogenesis and neotintimal hyperplasia, which are the primary causes of synthetic vascular graft occlusion [144], groups have investigated seeding endothelial cells (ECs) onto the grafts prior to implant. ECs can be harvested from a sample of vein and expanded *in vitro* to provide sufficient numbers to seed onto the graft [145]. The longest-running effort to utilize endothelialized vascular grafts clinically has come from Dr. Peter Zilla's work in femoro-popliteal bypass grafting. In these studies, ECs were isolated from a 4- to 5-cm long segment of either external jugular vein or cephalic vein. Cells were expanded until approximately 16 x 10^6 cells were obtained. Although cells were typically cultured in media supplemented with autologous serum, the group found that high serum concentrations of lipoprotein A correlated with low cell proliferation; therefore, a pooled "rescue" serum was created from donors with low lipoprotein A concentrations and used in cases where the EC cultures grew slowly [146]. Following *in vitro* expansion, ECs were seeded (~7-8 x 10^5 EC/ml) onto 6 mm ePTFE grafts 70 cm long that had been pre-coated with fibrinolytically-inhibited fibrin glue [147]. Immediately post-seeding, the grafts were cultured in a rotating bioreactor where grafts rotated at 6

rotations per hour at 37 °C for 3 hr in an incubator for full circumferential EC coverage, then cultured for approximately 10 more days. Overall, the endothelialization of grafts took 36.9 +/- 12.9 days from vein excision to implantation. Over approximately 9 years, 100 patients who did not have a suitable saphenous vein available for the bypass procedure received 113 of these *in vitro* endothelialized ePTFE grafts (13 patients received bilateral implantations) [148]. A follow-up phase 2 study added 76 patients who received 86 endothelialized ePTFE grafts. Overall, endothelialized grafts showed a primary patency rate of 62.8% after 7 years for all infrainguinal reconstructions; specifically, grafts implanted above-the-knee had a patency rate of 60% (SE = 0.12), while below-the-knee graft patency was 70.8% (SE = 0.06) [149]. These rates are similar to patency rates of vein grafts (66-68%) and much higher than non-endothelialized ePTFE rates (33-47%) [150–152].

Alternative endothelialization techniques

From these results, endothelialized ePTFE grafts seem to be a suitable option for patients in which a suitable saphenous vein is not available for grafting; however, the time, cost, specialized equipment and donor-site morbidity associated with EC harvest and expansion from veins has limited this technique from becoming clinically widespread. These issues have motivated alternate endothelialization techniques. Strategies to facilitate vascular graft endothelialization have either attempted to encourage rapid *in situ* endothelialization of the graft post-implantation, or have utilized alternate sources of endothelial cells that are more proliferative and more easily obtained, which are often derived from circulating endothelial progenitor cells (EPCs) [153]. A review of EPC-derived cells in vascular grafts is covered in section 2.9.

Investigations of accelerated *in* situ endothelialization of an “off-the-shelf” vascular graft material have typically sought to either facilitate capture of circulating EPCs, or to improve trans-anastamotic migration of vessel ECs onto the graft material (Figure 2.5). Delivery of growth factors to encourage migration of ECs onto the graft as well as increase the quantity of circulating EPCs have investigated the use of VEGF, stromal cell-derived factor-1 (SFD-1) and granulocyte-colony stimulating factor (G-CSF) treatment [154–156]. Molecules used for the capture of circulating EPCs include antibodies, aptamers and short peptides.

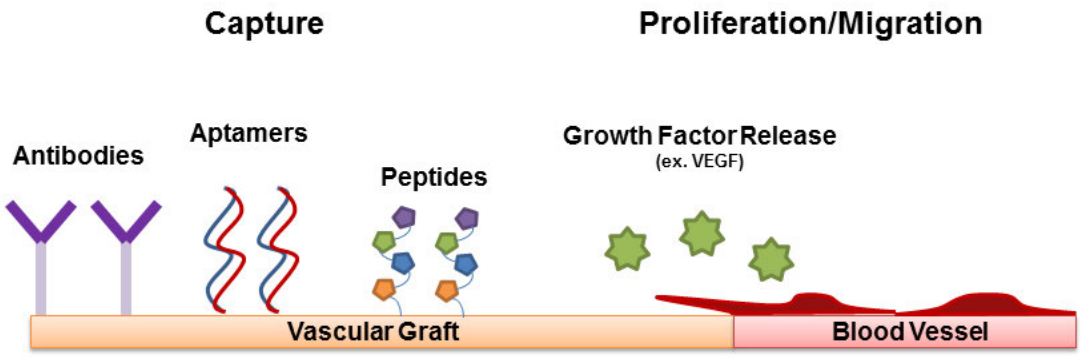

Figure 2.5: Strategies to enhance *in situ* endothelialization of vascular grafts. Capture molecules, including antibodies, aptamers and short peptides, are used to capture circulating endothelial progenitor cells. Alternative, biological molecules are released from the material to encourage the proliferation and migration of adjacent vessel wall ECs onto the vascular graft material. Figure elements not shown to scale. Based on Figure 1 from Melchiorri et al., 2013 [153].

Antibodies are widely used for highly-selective binding to defined molecular targets. Antibodies investigated for the capture of EPCs have been targeted towards kinase domain repeat (KDR, also known as VEGF receptor 2), as well as CD34 [157,158]. Of these two, CD34 is less specific for promoting endothelialization as it is

expressed on progenitor cells that can differentiate into cells other than ECs [159]. The immobilization techniques used to bind the antibodies to the vascular graft material has important consequences on capture efficacy, as antibodies oriented such that the epitope binding region is directed outward form the material facilitates greater EPC capture [158]. Aptamers are short sequences of DNA or RNA that form a globular structure and have the capacity to bind to epitopes of interest. Starting with a large library of potential sequences, the specific aptamers that demonstrate ideal binding properties can be isolated by “systematic evolution of ligands by exponential enrichment”, i.e. SELEX [160]. Aptamers selected for binding to ECs have been immobilized onto vascular graft materials [161]; however, the efficacy of these molecules as capture strategy *in vivo* is uncertain and may be limited through degradation by nucleolytic enzymes in blood [162]. Short peptides that facilitate cellular adhesion have also been used to accelerate endothelialization. The laminin-derived sequence arginine-glycine-aspartate (RGD) is a widely-recognized cellular adhesion sequence that has been applied to vascular grafts to encourage endothelialization [163]. Similarly, the elastin-like peptide sequence cysteine-alanine-glycine (CAG) has been incorporated into biomaterials [164]. CAG promotes EC adhesion to a greater extent than vascular smooth muscle cells, making it an attractive sequence to selectively encourage endothelialization of a graft material. However, the general lack of specificity of adhesion peptides may reduce the efficacy of peptide-based accelerated endothelialization. In summary, multiple strategies exist to modify biomaterials with capture molecules to bind circulating EPCs; of these, properly-oriented antibodies against KDR seem to demonstrate the best combination of stability in plasma and

endothelial specificity.

2.7.2 Artificial Venous Valves

Blood flow through a healthy venous system is driven by the contraction of adjacent skeletal muscle. One-way flow from the extremities to the heart is maintained by a series of bi-leaflet venous valves that prevent blood reflux. Chronic venous insufficiency is characterized by incompetent venous valves that are unable to close and prevent reflux. This disease currently affects over 2.5 million Americans and approximately 20% of patients develop skin ulceration [165–167]. Venous ulcers resulting from chronic venous insufficiency cause an estimated loss of 2 million workdays per year in the U.S. [166,167].

The current standard of care for chronic venous insufficiency is compression therapy; however, ulcer recurrence develops in approximately 20% of patients despite ongoing compression therapy [168,169]. Open surgical treatment options that involve augmenting the failing valve, valve transplantation, or ligating functional veins to diseased veins have been developed with varying success rates [170]. However, these techniques are limited to patients that are good candidates for open surgery, and there is a high failure rate for patients with post-thrombotic valve incompetence, which is the most common form of deep venous insufficiency [171]. The inability of current therapies to correct the valve dysfunction underlying venous insufficiency has motivated the development of novel strategies to restore venous valve function.

Early attempts in transplanting venous valves sought to use glutaraldehyde-fixed or cryopreserved venous valves as prosthetics [172]. These valves could be deployed via an open surgical procedure where the prosthetic valve was placed at the location of

a natural, potentially non-functioning, valve. Gluteraldehyde-preserved valves were attempted in many animal studies; however, the patency rates have been so poor that these valves never progressed to clinical trials. In contrast, cryopreserved valves implanted into dogs demonstrated 100% patency rates at 2 months as well as near-complete endothelialization of the luminal surface. However, cryopreserved valves implanted in a phase I feasibility study demonstrated only a 27% 2-year patency rate [172], and the authors deemed they were clinically unsuitable due to high occlusion rates and morbidity.

2.8 Summary: Vascular Biomaterials and Devices

Traditional cardiovascular biomaterials have been selected due to an inert activity, and commercial devices "continue to be manufactured on the basis of material choices, mechanical strength, regulatory compliance and surgical preferences rather than with a view towards biological integration and functional tissue regeneration" [144]. These selection criteria have resulted in limitations on cardiovascular device development due to biomaterial-initiated thrombosis. In particular, a small diameter vascular graft and an artificial venous valve are two applications without a clinically-accepted device due to unacceptably high rates of device thrombosis. Unfortunately, the lack of suitable biomaterials that can be used in vascular devices without causing thrombosis has necessitated pharmacological intervention to prevent device thrombosis. Systemic anticoagulation therapies unsurprisingly increase the risk of adverse bleeding events. Thus, there is a need for novel biomaterials with local anti-thrombotic activity to advance cardiovascular medicine.

The lack of a small diameter vascular graft for patients lacking a suitable vein for grafting remains one of the greatest challenges in cardiovascular medicine. Considerable progress has been made in the area of endothelialized ePTFE vascular grafts using a patient's own endothelial cells isolated from a section of vein. However, the technique is limited by injury caused by vessel isolation as well as the limited proliferation by the isolated mature endothelial cells. Recognizing these two challenges, there has been considerable interest in using cells derived from circulating endothelial progenitor cells to produce an autologous endothelial lining on vascular grafts. The progress in utilizing one type of endothelial progenitor-derived cell, endothelial outgrowth cells, is reviewed in the next section.

2.9 Endothelial Outgrowth Cells: Function and Performance in Vascular Grafts[2]

2.9.1 Abstract

The clinical need for vascular grafts continues to grow. Tissue engineering strategies have been employed to develop vascular grafts for patients lacking sufficient autologous vessels for grafting. Restoring a functional endothelium on the graft lumen has been shown to greatly improve the long-term patency of small diameter grafts. However, obtaining an autologous source of endothelial cells for *in vitro* endothelialization is invasive and often not a viable option. Endothelial outgrowth cells (EOCs), derived from circulating progenitor cells in peripheral blood, provide an alternative cell source for engineering an autologous endothelium. This review aims to highlight the role of EOCs in the regulation of processes central to vascular graft performance. To characterize EOC performance in vascular grafts, this review identifies the characteristics of EOCs, defines functional performance criteria for EOCs in vascular grafts, and summarizes the existing work in developing vascular grafts with EOCs.

[2] This review was originally published in *Tissue Engineering Part B: Reviews*. Glynn JJ, Hinds MT. Endothelial outgrowth cells: function and performance in vascular grafts. *Tissue Eng Part B Rev.* 2014;20:294–303.

2.9.2 Introduction

Cardiovascular disease is a major health burden worldwide. With over 7.5 million cardiovascular operations performed in the U.S. in 2010, there is high demand for novel solutions to treat vascular disease [173]. A key limitation in the field is the inability of the current materials, such as expanded polytetrafluoroethylene (ePTFE) and Dacron® (polyethylene terephthalate fibers), to achieve long-term patency in vascular grafts <5 mm in diameter [150,174,175]. Current vascular grafts predominantly fail by either thrombus formation or intimal hyperplasia leading to occlusion [55,176]. Treatment options for vascular disease would be significantly improved with the development of functional, small-diameter blood vessels to replace diseased tissue.

In vivo, endothelial cells (ECs) line the luminal surface of blood vessels and are responsible for regulating numerous processes including hemostasis and thrombosis, the transport of blood constituents into tissues, smooth muscle cell proliferation and vascular tone [4]. Recognizing the capacity for ECs to properly coordinate these processes *in vivo*, much effort has been placed into developing vascular grafts with an endothelialized lumen that can dynamically interact with the local environment [148,177–180]. In patients lacking a suitable saphenous vein to use as a bypass graft, endothelialized ePTFE grafts demonstrated improved patency rates at a 9-year follow-up [148]. A review of EC isolation and graft seeding techniques highlighted the utility of vein ECs in maintaining vascular graft patency, though isolations from veins typically have low yields and are invasive [181]. Thus, despite promising results in clinical trials, the limited availability of autologous ECs and the donor site morbidity resulting from EC harvest have limited the clinical potential of EC-seeded vascular grafts.

The discovery of circulating endothelial progenitor cells (EPCs) that could be isolated from peripheral blood and differentiated to an endothelial-like phenotype provided a promising new autologous cell source for endothelialization [103]. Since this discovery, research has sought to characterize the various subtypes of cells that differentiate from circulating progenitors [182–185], develop protocols for EPC characterization and quantification [120,121,186,187], and establish the clinical relevance of EPC count [188,189]. Among the phenotypically and functionally diverse progeny of EPCs, a population termed endothelial outgrowth cells (EOCs; also known as late outgrowth, blood outgrowth endothelial, or endothelial colony-forming cells) are particularly promising for vascular tissue engineering applications [126]. The features of EOCs that make them well-suited for tissue engineering include 1) robust proliferation rate, 2) high expansion potential, and 3) simple sourcing via venipuncture [126,183,190,191]. The high proliferation rate and expansion potential of EOCs allows very few colonies to be quickly expanded to the high cell number required for tissue engineering applications, and venipuncture is considerably less invasive than harvesting ECs from excised tissue.

In this review, the isolation and validation procedures for EOCs will be briefly described, followed by physiological methods to characterize EOCs performance in vascular grafts, and concluding with current vascular tissue engineering strategies utilizing EOCs. Although cellular adhesion and proliferation have been used to characterize the performance of EOCs on vascular grafts [153], this review aims to define EOCs' ability to regulate the biological processes required of a vascular endothelium. As the improper regulation of thrombosis, intimal proliferation, and

inflammation typically underlies vascular graft failure [55], these processes will be presented as performance criteria for a successful vascular graft. This review summarizes the results of multiple studies of EOCs regarding these processes to provide a broad report on EOC function with the understanding that subtle inter-lab variations in culturing conditions may produce individual variations in findings. Other derivatives of EPCs, as well as therapies utilizing undifferentiated EPCs, will not be discussed here; however, the authors direct interested readers to other reviews [109,182,192] for discussion on other EPC-derived cell types.

2.9.3 Endothelial Outgrowth Cells

As first demonstrated by Asahara et al., EC-like cells can be derived by culturing adherent, $CD34^+$ fraction of mononuclear cells from a peripheral blood draw in a pro-EC growth medium [103]. These cells differentiate 3-7 days post-plating, express numerous EC genes and surface antigens, and enhance angiogenesis in a mouse hind limb ischemia model. However, subsequent studies with these cells indicated the cells were unable to achieve a cobblestone-like EC morphology or form capillary-like tubes in Matrigel, and the cells expressed monocytic surface antigens [122,193]. In parallel with these developments, Lin et al. cultured peripheral blood mononuclear cells and noted occasional colonies of cells with cobblestone morphology and a high expansion capacity that appeared to originate from bone marrow [126]. The cells in these colonies became known as EOCs, and in contrast to the cells characterized by Asahara et al., these cells appeared after >7 days in culture, expressed CD146 (MCAM, clone P1H12), had angiogenic behavior in Matrigel, and lacked CD14 expression. Due to a lack of a unique marker defining either the progenitor population giving rise to EOCs or EOCs

themselves, a combination of surface antigen expression and functional assessment is currently required to distinguish the EOC population from other EPC-derived cell types [182]. A summary of defining properties exhibited by EOCs is listed in Table 2.9.1.

The multi-faceted and still-evolving definition of EPCs and their derivatives has consequently led to significant inter-lab variability in the terminology of endothelial progenitor and outgrowth cells. However, multiple groups have shown definitively that the highly-proliferative, non-monocytic, cobblestone cells discussed henceforth in this review are derived (in humans) from a rare $CD34^{+}CD133^{-}CD146^{+}$ circulating progenitor [120,194,195]. The scarcity of these progenitors in peripheral blood has been the greatest challenge in their characterization. From a translational standpoint, the low frequency in blood reduces the probability of successful outgrowth from any given blood draw. Fortunately, the procedure of drawing blood is minimally invasive and could be repeated for patients if the initial attempt is unsuccessful.

Properties of EOCs	
Morphology	Cobblestone under static conditions, will elongate with unidirectional fluid shear stress[190,196–199]
Surface marker expression	CD31+, vWF+, CD146+, CD309+, CD34+, CD133-, CD14-, CD45-[120,126,184,190,194]
Functional verification	Bind UEA-1 lectin and uptake AcLDL, angiogenic behavior in Matrigel™ [126,184,190]
Source	Progenitor isolated from peripheral blood, colonies appear after >7 days in culture[126]
Population doubling time	1-3 days[185,190,194,200]
Expansion potential	$>10^9$ cells[126,185,190,191]
Extracellular matrix production	Robust production of collagen IV and fibronectin[2]

Table 2.9.1: Defining properties of EOCs. Verification of a number of these properties can be performed to validate true EOC phenotype. Abbreviations: vWF – von Willebrand factor, UEA – ulex europaeus agglutinin, Ac-LDL – acetylated low density lipoprotein.

Additionally, multiple cell characterization methods must be utilized to confirm the presence of EC markers (CD31, VEGFR-2, CD34, CD146, von Willebrand factor), the absence of leukocyte markers (CD14, CD45), *in vitro* tube formation in Matrigel™, and AcLDL uptake. Thorough cell characterization is necessary to confirm the EOC phenotype due to the multiple cell types that may be generated using the current standard derivation protocols [120,182,183,200,201]. Furthermore, our group and others have noted that colonies of outgrowth cells occasionally assume a large, irregular shape with slow proliferation and limited expansion potential [194,200,202]. In the absence of any definitive markers that distinguish these various EPC-derived

populations, screening each colony is currently necessary to validate the EOC phenotype.

2.9.4 Performance Criteria for EOCs in Vascular Grafts

There are two general strategies for engineering vascular grafts using EOCs: covering existing clinically-used synthetic materials with EOCs to limit blood-material contact and improve patency, or incorporating vascular cell types in addition to EOCs (ex. smooth muscle cells) with a biodegradable or naturally-derived scaffold to recreate native blood vessel structure and function. For both approaches, EOCs should function as a healthy, native endothelium to facilitate long-term graft success. Chiefly, these functions include 1) serving as an anti-thrombotic interface with the blood 2) limiting leukocyte invasion and other inflammatory processes, and 3) inhibiting intimal hyperplasia, particularly at the graft anastomoses. These biological processes, methods to characterize them, and recent research elucidating EOCs' performance in them, will be further described individually.

Thromboprotection

Native ECs possess a variety of surface-bound and secreted molecules that influence the local hemostatic environment [203]. Thrombomodulin and the endothelial Protein C receptor, expressed on the EC surface, work in conjunction to activate Protein C, which in turn inactivates the coagulation Factors Va (FVa) and VIIIa (FVIIIa) to limit coagulation. Prostacyclin and nitric oxide (NO) secreted by ECs locally inhibit platelet adhesion and activation. EC secretion of tissue plasminogen activator (tPA) catalyzes the production of plasmin, which breaks down fibrin clots. Conversely, upregulation of tissue factor expression on the surface of ECs following vascular injury facilitates the

activation of FX to FXa, which then converts the zymogen prothrombin to the active enzyme thrombin to generate a fibrin thrombus. ECs also facilitate coagulation by releasing von Willebrand factor and P-selectin from Weibel-Palade bodies to initiate platelet aggregation and activation. In addition, ECs basally deposit von Willebrand factor to promote platelet aggregation in the event that ECs are detached from their underlying matrix. Platelet aggregation and activation initiates the coagulation cascade and the production of a fibrin thrombus. Developing a luminal surface that can actively regulate and respond to thrombotic pathways is a significant motivation for endothelializing vascular grafts.

The thrombogenicity of EOCs on vascular grafts can be characterized by a number of systems of varying complexity that are reviewed by McGuigan & Sefton in an in-depth discussion of evaluating biomaterial thrombogenicity [204]. Purified systems that measure the activity of a limited number of players in coagulation (ex. FX and Protein C activation, NO production) provide quick and straightforward information on cell thrombogenicity and are highly useful for studying individual signaling pathways. However, these results may not translate to *in vivo* performance due to the highly interconnected thrombotic regulatory mechanisms. Methods that study graft performance using whole blood, particularly at physiological flow rates, provide the best indication to *in vivo* thrombogenicity, though these systems can confound the roles of individual pathways [205,206].

EOCs express the fundamental proteins used by ECs to regulate thrombosis, including tissue factor, thrombomodulin, endothelial Protein C receptor, tissue plasminogen activator and von Willebrand factor [190,191,196,200,201,207–212].

Regulation of thrombus formation by EOCs has been suggested *in vitro* by studies demonstrating reduced platelet adhesion on EOC-lined materials and the generation of the anticoagulant activated Protein C [196,210,212]. Additionally, in response to pro-thrombotic stimuli, EOCs increase their expression of tissue factor, decrease plasma clotting time, and increase tissue plasminogen activator expression [201].

A number of strategies have been used in an attempt to improve EOCs' thromboprotective function prior to graft implantation. Similar to ECs, the most common method to reduce EOCs' thrombogenicity is to precondition the cells with fluid shear stress (described below). Instead of promoting the anti-thrombotic behavior of cells through external stimulation, EOCs can also be genetically modified for improved performance [108,208,211,213]. Thrombomodulin-overexpressing EOCs have demonstrated increased Protein C activation, decreased platelet adhesion under static conditions, and prolonged clotting times compared to native EOCs [211]. Additionally, EOCs overexpressing prostacyclin had similar proliferation, decreased apoptosis following H_2O_2 treatment, and increased angiogenic properties compared to native EOCs [214]. Together, these studies have shown that EOCs have the potential to regulate thrombosis by similar mechanisms as ECs and can provide a thromboresistant lining on graft materials.

Inflammatory response

Inflammation is characterized by an increase in vascular endothelial permeability, fluid and leukocyte transit across the endothelium into the tissue, leukocyte degradation of foreign objects and cytokine secretion [215]. While acute inflammation is beneficial to the healing process, chronic inflammation can result in detrimental remodeling by

processes such as fibrosis and calcification, which alter the local mechanical properties and reduce graft functionality [129]. When activated by injury or inflammatory cytokines, ECs facilitate inflammation by 1) releasing chemotactic factors to attract circulating leukocytes, 2) expressing selectins to allow leukocyte rolling adhesion along the vessel wall, 3) loosening intercellular junctions with adjacent endothelial cells, and 4) expressing integrin ligands to permit leukocyte diapedesis into the tissue. Although this review will highlight the role of only a few endothelial inflammatory markers, more thorough reviews of leukocyte adhesion [216], transmigration [217], and atherogenesis [218] have been previously published. Circulating leukocytes can be transiently bound by E- and P-selectins on cytokine-stimulated ECs to facilitate rolling adhesion along the vessel wall. Slowing the leukocytes permits the formation of stronger intercellular bonds to the endothelium via ICAM-1 (CD54) and VCAM-1 (CD106). Leukocyte diapedesis across the endothelium is facilitated by PECAM (CD31) and ICAM-1 [219].

The typical *in vitro* characterization of ECs' response to inflammatory cytokines is the measurement of surface expression of ICAM-1, VCAM-1, or E- and P-selectin. As with native ECs, EOCs significantly upregulate these adhesion proteins compared to their basal state in response to inflammatory cytokines or aberrant flow conditions. The inflammatory response of EOCs can be induced by treating the cells with the cytokine tumor necrosis factor-α (TNFα) which results in an increase in both ICAM-1 expression [220] and prothrombotic tissue factor expression [221]. Additionally, oscillatory fluid shear has a pro-inflammatory effect on EOCs resulting in increased monocyte adhesion [198]. The processes of inflammation and thrombosis are highly interdependent; in both ECs and EOCs, there is an increase in thrombogenicity following inflammatory cytokine

stimulation. TNFα stimulation of EOCs results in tissue factor protein upregulation similar to ECs and shortens the time to tissue factor/FVII-dependent thrombin generation and plasma clotting [201,221]. In summary, EOCs demonstrate an inflammatory response *in vitro* to TNFα and oscillatory shear stress similar to ECs.

Inhibiting intimal hyperplasia

In vivo, ECs limit vascular smooth muscle cell migration and proliferation predominantly through the release of NO generated by endothelial nitric oxide synthase (eNOS). Commonly, eNOS gene or protein expression levels are used as an indicator of NO production. Alternatively, NO can be measured in an *in vitro* assay quantifying NO metabolites [220,222], a fluorescent NO indicator probe [184], or a function-based NO assay that measures smooth muscle cell relaxation following controlled activation of eNOS [191]. The majority of groups have shown EOCs to have a lower expression of eNOS than mature ECs [184,190,196,200,220], though some groups have found no difference between cell types [201]. However, eNOS expression does not directly correlate with NO production, as evidenced by studies demonstrating that EOCs have lower eNOS expression but similar NO production as aortic ECs when stimulated by calcium [184] or fluid flow [220].

Intimal hyperplasia following vascular injury can also be reduced by activated Protein C [223,224]. Activated Protein C acts to inhibit inflammation-induced EC apoptosis and permeability, thereby maintaining functional EC regulation of underlying smooth muscle cells [65]. Similar to ECs, EOCs can activate Protein C [196,225]. To enhance Protein C activation, EOCs were engineered to overexpress thrombomodulin via adenoviral transfection. Although *in vitro* Protein C activation was increased [211],

thrombomodulin overexpression by EOCs seeded onto an ePTFE graft did not significantly reduce intimal hyperplasia or thrombus formation compared to non-transfected EOCs in a rat model [226]. The lack of improvement may be due to the reduced activity of human thrombomodulin with rat Protein C, the limited duration of thrombomodulin overexpression, or suppression of transcription factors downstream of thrombomodulin due to disturbed blood flow at the proximal anastomosis which dampened thrombomodulin-mediated effects.

The capacity of EOCs to limit intimal hyperplasia has been demonstrated in multiple animal models. EOCs transplanted in a balloon-injured rabbit carotid artery reduced injury-induced intimal hyperplasia; this reduction was enhanced by transplanting EOCs that overexpressed eNOS [213]. In a canine interpositional carotid implant model, EOC-seeded decellularized arteries reduced intimal thickness 3 month post-implantation throughout the length of the graft compared to grafts without EOCs [227]. Grafts wrapped with EOC-seeded scaffolds showed significantly reduced intima to media ratio at 14 days post-implant, suggesting the EOCs released paracrine factors, such as NO, to inhibit intimal proliferation [228]. Together, these studies show the potential for EOC-seeded vascular devices to limit intimal hyperplasia via NO release and Protein C activation.

Response to fluid shear stress

For vascular graft applications, EOCs need to remain adherent to the graft under physiologic shear stresses, averaging 15-20 dyn/cm^2 in arteries to 1-6 dyn/cm^2 in veins [229]. The EC response to fluid shear stress is well-established. As reviewed in [229,230], ECs subjected to arterial levels of fluid shear stress align in the direction of

flow, increase production of NO, decrease expression of inflammatory adhesion molecules, and increase thrombomodulin expression.

As fluid shear stress has a significant effect on EC phenotype, characterizing EOCs' response to fluid shear stress has been an area of active study. When subjected to fluid shear stresses of 10-15 dyn/cm^2, EOCs elongate in the direction of flow [190,202]. EC and EOC alignment, independent of fluid shear stress, alters immunogenicity and matrix protein deposition [2,3,5]. EOCs and aortic ECs both exhibited decreased VCAM-1 mRNA expression when subjected to fluid shear of 25 dyn/cm^2[231]. There are conflicting results on the relative gene expression of von Willebrand factor following fluid shear, as one group found no difference in von Willebrand factor gene expression at fluid shears of 5 or 25 dyn/cm^2 [231], but another group found that 15 dyn/cm^2 increased von Willebrand factor gene expression. factor between EOCs and ECs under static conditions or following fluid shear stimulation [196]. Compared to ECs, EOCs have an increased production of thrombomodulin and corresponding Protein C activation, but do not increase tissue factor expression following steady fluid shear stress, indicating a superior thromboprotective phenotype in arterial flow conditions [196,198]. Steady shear causes EOCs to increase eNOS gene expression [198,202,207] and NO production, suggesting an improved capacity to limit intimal hyperplasia [197,202,220,222]. Models that incorporate both fluid shear stress and inflammatory cytokines enable a better characterization of how these factors interact to influence EOC behavior. Following 24 hr of 6 dyn/cm^2 shear stress preconditioning, TNFα-induced tissue factor activity of EOCs was reduced compared to non-preconditioned EOCs [232]. Fluid shear stress preconditioning shows promise for

improving vascular graft performance. However, the additional time and equipment necessary for such treatment may not be practical for some applications.

In vivo, vascular branch points and bifurcations can result in disturbed blood flow conditions.[230] ECs exposed to disturbed flow exhibit a dysfunctional phenotype with increased expression of tissue factor, von Willebrand factor, ICAM-1, VCAM-1, E-selectin and reduced NO secretion [229]. This altered expression profile results in local susceptibility to thrombosis and atherosclerotic plaques [19,229]. Bidirectional fluid flow with peak shear stresses of ±0.3 dyn/cm^2 was used to simulate regions of disturbed flow and induced a similar upregulation of tissue factor gene expression in EOCs as in ECs, indicating a similar prothrombotic response to oscillatory shear stresses [199]. Additionally, oscillatory shear stress (0±10 dyn/cm^2, 1Hz) significantly increased monocyte adhesion on EOCs relative to EOCs under steady shear [198]. As vascular regions with disturbed and oscillatory blood flow are prone to EC dysfunction, there is motivation to develop a better understanding of EOC phenotype under similar disturbed flow conditions. A summary of the existing research characterizing EOCs' response to fluid shear stress is presented in Table 2.9.2.

Flow Conditions	Flow System	Substrate	Shear Stress	TNFα Treatment	Results (descr bed as flow treated EOCs compared to static unless stated otherwise)	Reference
Steady flow	Parallel plate	Fibronectin-coated Teflon A films spun-cast on glass	15 dyn/cm^2 for 24 or 28 hr	N/A	Increased eNOS, TM, ICAM-1 gene expression No significant difference in VCAM-1 or E-selectin gene expression	[220]
		Fibrin-based scaffold	15 dyn/cm^2 for 24 hr	10 U/mL for 24 hr	Increased NO production Decreased platelet adhesion Attenuated TNFα-induced upregulation of VCAM-1 and ICAM-1	[212]
		Gelatin-coated plastic	5 or 25 dyn/cm^2 for 5 hr	N/A	Decrease in VCAM-1 gene expression at 25 dyn/cm^2 No difference in vWF gene expression with either shear stress	[231]
		Collagen I-coated glass	15 dyn/cm^2 for 24 hr	N/A	Increased TM, eNOS, TFPI gene expression Increased TM protein Increased APC activity No differences in TF gene or protein	[196]
	Orbital rotator	Collagen-coated TCPS	6.0 dyn/cm^2 for 6 or 24 hr	110 U/mL for 2 hr	Decreased TF and eNOS gene expression at 6 and 24 hr Increased eNOS gene expression at 6 and 24 hr following TNFα treatment Attenuated TN-α induced TF activity at 6 and 24 hr	[232]
Steady and oscillatory flow	Cone and plate	Collagen I-coated TCPS	24 hr treatment with steady shear of 10 dyn/cm^2, or oscillatory shear of 0 ± 10 dyn/cm^2	N/A	Oscillatory shear reduced eNOS and P-selectin genes vs. steady shear Steady shear decreased monocyte adhesion vs. oscillatory Steady shear increased TM, ePCR and CD39 genes vs. oscillatory shear No significant difference in the gene or protein expression of E-selectin or VCAM-1 in oscillatory shear vs. steady shear	[198]

Steady, pulsatile, and oscillatory flow	Perfusion bioreactor	Fibronectin-coated Sylgard tubes	24 hr treatment with either low unidirectional shear of .3 ± 0.1, pulsatile shear of 6 ± 3 dyn/cm^2; or oscillatory shear of 0.3 ± 3 dyn/cm^2	N/A	Unidirectional increased TF gene expression Pulsatile decreased tPA gene expression Bidirectional increased TF, decreased tPA gene expression No condition had an effect on VCAM-1 or E-selectin gene expression	[199]

Table 2.9.2 : A summary of studies characterizing how fluid shear stress affects EOC function and response to TNFα treatment. Abbreviations: TNFα – tumor necrosis factor α, eNOS – endothelial nitric oxide synthase, TM – thrombomodulin, VCAM-1 – vascular cell adhesion molecule 1, ICAM-1 – intercellular adhesion molecule 1, TF – tissue factor, vWF – von Willebrand factor, TFPI – tissue factor pathway inhibitor TCPS – tissue culture polystyrene.

2.9.5 Vascular Tissue Engineering Applications using EOCs

Vascular tissue engineering strategies have typically sought to use EOCs either to cover current synthetic graft materials, or to integrate EOCs into a natural or biodegradable synthetic scaffold, potentially with other cell types, to mimic native vessel structure and protein composition. To ensure complete coverage of the tubular graft lumen, seeding is generally performed using multiple inoculations with manual or automated rotation, or by perfusing a cell suspension through the graft wall [200,201,207,226,233–235].

Synthetic scaffolding

Current clinical vascular grafts are constructed of synthetic materials, most commonly ePTFE and Dacron®. As these are both hydrophobic materials lacking natural adhesion peptides, surface modification of these materials is required prior to lining the lumen with EOCs. Additionally, a period of cell culture following seeding is

required to ensure EOC adhesion, spreading, and complete coverage of the luminal surface. This culture period also allows for in vitro pre-conditioning of the graft, for example by fluid shear stress or growth factors. Thus, when developing EOC-seeded synthetic grafts, there are in general 3 variables: 1) synthetic scaffold material, 2) biofunctional coating, and 3) culture time and conditioning.

As the current standard material for large diameter vascular grafts is ePTFE, a few groups have sought to modify this material for improved cell adhesion and use it as a scaffold for EOCs. ePTFE modified with the biodegradable, polyester elastomer poly(1,8-octanediol-*co*-citrate) and coated with fibronectin facilitated the adhesion of EOCs through 24 hours of 10 dyn/cm^2 shear stress [201]. Studies of EOCs seeded onto ePTFE coated with either collagen I or fibronectin indicated EOCs had a more robust adhesion and proliferation potential on either of these proteins than on α-elastin or collagen IV [225]. With either collagen I or fibronectin coatings, EOCs formed a confluent monolayer and were able to remain adherent at supraphysiological shear stresses [225].

The mechanical properties, particularly the elasticity, of polyurethanes have stimulated investigation into their utility as vascular graft materials. The harmful degradation products of polyurethanes have eliminated their use in long-term implants. Yet, they are still used as arteriovenous grafts to permit vascular access for dialysis patients due to polyurethane's ability to reseal following puncture. Segmented polyurethane coated with photo-cured gelatin was seeded with EOCs and subjected to a 12-hour shear stress of 30 dyn/cm^2 [200]. The EOCs remained adhered to the graft and elongated in the direction of flow. Segmented polyurethane films coated with

collagen I, resulting in grafts with internal diameters of ~4.5 mm and 6 cm in length, were also seeded with autologous canine EOCs and evaluated as an interpositional carotid artery graft [233]. After 3 months, all six grafts were patent and showed a smooth luminal surface lacking thrombi. Smooth muscle cells were identified in the graft media, though it is unclear whether the smooth muscle cells had migrated into the graft from adjacent tissue, or if the EOCs had transdifferentiated into a smooth muscle cell phenotype.

Several groups use electrospinning to create polymeric micro- to nano-sized fibers in a matrix that mimics the native extracellular matrix architecture. In comparison to thin films of the same composition, EOCs grown on an electrospun fibrous scaffold composed of hexylmethacrylate, methylmethacrylate and methacrylic acid had increased proliferation [209]. Whether proliferation is enhanced by aligned fibers rather than by random fiber orientation is controversial, and there may be a necessary degree of fiber alignment needed to increase proliferation compared to random fibers [209,236]. These studies that highlight variable EOC behavior on different substrates demonstrate the potential to modulate EOC function through scaffold design.

Synthetic scaffolds possess many advantages for vascular tissue engineering including easy transportation and storage, inter-graft consistency, and well-defined physical and chemical properties. Seeding the luminal surface of synthetic grafts with ECs has been shown to improve long-term synthetic graft patency for a number of materials [148,177–180]. However, compared to the body of research studying EC behavior on synthetic scaffolds, very little work has investigated EOCs' function on these materials. Adhesion to synthetic materials under fluid shear is often used as the

major metric of synthetic scaffold performance; however, a more thorough characterization of the scaffolds' influence on EOCs' biological regulatory function is needed.

Naturally-derived and biodegradable scaffolding

Although synthetic materials possess consistent physical and chemical properties and are often less expensive, they lack instructional biological cues of the native extracellular matrix. Examples of these cues include the fibrous topography of the typical vascular extracellular matrix which aids in cell alignment and adhesion, as well as biochemical signals, such as growth factors, that aid in healing and tissue integration [237]. Naturally-derived materials, or biodegradable materials designed to be replaced by cell-deposited matrix proteins, have therefore been utilized in an attempt to construct vascular grafts that possess these native signals.

A current technique for generating natural scaffolding for vascular tissue engineering is decellularizing preexisting blood vessels and repopulating the vessels with cells cultured *in vitro*. Decellularized blood vessels provide a scaffold with the complex structure of the native tissue and are highly-supportive of EC adhesion [238–241]. Ovine EOCs seeded onto decellularized porcine iliac arteries were pre-conditioned with fluid shear stress of 25 dyn/cm^2 and produced NO upon stimulation with a thromboxane analog [191]. When implanted into sheep, the EOC-seeded grafts remained patent for up to 130 days. Following explant at 130 days, smooth muscle cells were present in the media of the grafts which conferred vasomotor activity in response to the neurotransmitters norepinephrine, serotonin and acetylcholine. In another study, tissue engineered grafts were constructed by selectively-seeding bone marrow-derived

EOCs onto the lumen and vascular smooth muscle cells onto the exterior of decellularized vessels [235]. These constructs were cultured in a bioreactor with pulsatile flow for 7 days, then implanted as interpositional carotid grafts in canines. At 14 weeks, 9 of 10 seeded grafts were patent. No characterization of intimal hyperplasia was performed, though the authors note the number of smooth muscle cells in the graft matrix increased during the implant period. Decellularized arteries have also been modified by covalently binding heparin to the surface prior to EOC seeding [227]. These grafts were cultured for 7 days under a fluid shear stress of 30 dyn/cm^2 prior to implantation. In a canine interpositional carotid implant model, the heparin-modified grafts seeded with EOCs demonstrated a higher 3-month patency and reduced intimal thickness throughout the length of the graft compared to unseeded heparin-modified grafts.

Rather than decellularizing an explanted vessel, smooth muscle cells or fibroblasts cultured on a biodegradable scaffold can be used to generate *de novo* a vascular matrix scaffold. In this case, the degradable scaffold serves as a temporary support or pattern to facilitate extracellular matrix protein production by the smooth muscle cells. In one example, smooth muscle cells were cultured on a biodegradable polyglycolic acid rod for 10 weeks in a bioreactor, allowing the smooth muscle cells to generate a tubular extracellular matrix [207]. After decellularizing the scaffold, the mechanical properties were comparable to a human saphenous vein. The decellularized scaffolds were then seeded with autologous EOCs, preconditioned with 15 dyn/cm^2 shear stress for 24 hours, and implanted in porcine carotid arteries as end-to-side grafts to mimic clinical bypass grafts. All three EOC-seeded grafts remained patent at 30 days

and had an average increased luminal area (though not significantly) and decreased intimal area compared to autologous venous grafts, some of which occluded by intimal thickening and thrombosis. In another study, smooth muscle cells were seeded on porous, biodegradable poly(glycerol sebacate) scaffolding and cultured for 1 week in a pulsatile flow bioreactor to stimulate smooth muscle cell proliferation and the production of elastin and collagen [242]. EOCs were then seeded onto the graft where they formed a confluent monolayer on the luminal surface. Co-culture of EOCs and smooth muscle cells in the grafts increased the ultimate tensile stress and the strain at failure compared EOC-only seeded grafts; these results were attributed to the matrix proteins deposited by the smooth muscle cells.

A vascular graft composed entirely of autologous tissue is advantageous as it eliminates the potential for immune rejection. However, such autologous constructs traditionally require blood vessel harvesting to generate a scaffold and isolate vascular cells. In contrast, Aper, et al. [243] were able to construct a vascular graft using cells and proteins contained within 100 mL of peripheral porcine blood. EOCs and fibrinogen were combined and polymerized by the addition of thrombin to generate a cell-seeded, tubular fibrin graft. The graft was subsequently cultured in a perfusion bioreactor for 5 days. Although the mechanical properties remained insufficient for grafting (burst strength of only 90 mmHg), the incorporation of vascular smooth muscle cells in future designs may improve these shortcomings.

From a biological perspective, natural materials have many potential benefits including preserving native extracellular matrix architecture, presentation of physical and biochemical cues to support cell seeding and post-implantation integration, and

reduced concern of toxic degradation byproducts. However, from a translational perspective, natural materials are often much more expensive and challenging to source (typically including extensive processing to eliminate potential allergens), and have inferior mechanical properties that make them more difficult to surgically manipulate. New methods that shorten *in vitro* graft preparation time, improve mechanical robustness and the ability to withstand surgical handling and suturing would improve the clinical utility of natural scaffolds for EOC-seeded grafts.

2.9.6 Future Research Topics

Research utilizing EOCs in vascular tissue engineering has rapidly grown as investigators employ EOCs to perform endothelial functions. Still, much work needs to be done to translate this research to clinical devices. In concert with the applied research using EOCs in devices, basic research that identifies an EPC-specific marker from which EOCs are derived would enable more efficient EOC quantification and isolation from patients. The dogma that the progenitors of EOCs originate in bone marrow has recently been challenged [195], and presents another topic for investigation. Although statins [244] and erythropoietin [245] increase the quantity of circulating EPCs, determining the specific factors that induce EPCs in culture to differentiate into EOCs would further enhance protocols for efficient EOC isolation and expansion.

Many vascular graft materials are being developed with the sole performance criterion of supporting the proliferation and adhesion of EOCs under flow. When developing EOC-seeded vascular grafts, a more thorough characterization of how the underlying material impacts the function of EOCs with regards to thrombosis, intimal

hyperplasia and inflammation should be performed. Novel modifications to existing scaffold materials may improve EOCs' functionality in these processes.

In vivo, ECs reside in a complex environment of mechanical cues (fluid shear stress, vascular tone) and biochemical cues (cytokines, growth factors) which ECs integrate to regulate local vascular environment. Therefore, characterizing how the interplay between biomechanical and biochemical cues cooperatively affect EOC regulation of thrombosis, intimal hyperplasia and inflammation may more fully define *in vivo* EOC behavior. A mechanistic understanding of the signaling pathways activated by these complex environments may also identify future targets for preconditioning EOCs for improved function. Genetically engineering EOCs to have improved thromboprotection or pro-healing qualities may further improve graft function. Although the increased culture time detracts from the clinical applicability of genetically engineering EOCs, this method would be beneficial for patients with genetic vascular disorders or poor intrinsic EOC function.

2.9.7 Conclusion

EOCs derived from circulating EPCs are an attractive source for engineering a functional, autologous endothelium in vascular grafts. Work characterizing EOCs' role in the processes of thrombosis, intimal hyperplasia and inflammation has demonstrated EOCs' capacity to function as an autologous endothelium on vascular grafts. Current tissue engineered constructs that utilize EOCs have exhibited significant improvements in patency compared to non-seeded devices. Basic scientific studies that determine how biomechanical and biochemical cues interact to affect EOC behavior may identify methods to precondition or engineer EOCs for specific performance enhancements.

With continued research, EOCs show great potential to advance the field of vascular tissue engineering and improve the long-term function of vascular grafts.

CHAPTER III: Endothelial outgrowth cells regulate coagulation, platelet accumulation, and respond to tumor necrosis factor similar to carotid endothelial cells.[3]

3.1 Abstract

Endothelial cells (ECs) are central regulators of hemostasis, inflammation, and other vascular processes. ECs have been used to cover vascular graft materials in an attempt to improve the biologic integration of the grafts with the surrounding tissue. Although EC-seeded grafts demonstrated improved patency, the invasive nature of EC harvest has limited the clinical translation of this technique. Endothelial outgrowth cells (EOCs) can be derived from circulating endothelial progenitor cells, which are non-invasively isolated from a peripheral blood draw. Although EOCs have been presumed to regulate hemostasis and inflammation similarly to arterial ECs, there has been limited research that directly compares EOCs to arterial ECs, particularly using pairs of donor-matched cells. This study provides a multifaceted characterization of hemostasis regulation by baboon EOCs and carotid ECs, both in the presence and absence of inflammatory stimulus, tumor necrosis factor α (TNFα). The expression of genes involved in thrombosis and inflammation was highly similar between ECs and EOCs at a basal state and following TNFα stimulation. ECs and EOCs activated similar levels of protein C and Factor X (FX) at a basal state. Following TNFα treatment, EOCs had less of an increase in tissue factor activity than ECs. Cell-seeded ePTFE vascular grafts demonstrated no significant differences between ECs and EOCs in platelet accumulation or fibrinogen incorporation in a baboon femoral arteriovenous shunt loop.

[3] This research was originally published in *Tissue Engineering Part A*. Glynn JJ, Hinds MT. Endothelial outgrowth cells regulate coagulation, platelet accumulation, and respond to tumor necrosis factor similar to carotid endothelial cells. Tissue Eng Part A. 2015;21:174–82. © 2015 Mary Ann Liebert, Inc.

This work demonstrates that EOCs regulate thrombus formation and respond to an inflammatory stimulus similar to ECs, and supports utilizing EOCs as a source for an autologous endothelium in tissue engineering applications.

3.2 Introduction

Blood coagulation is a highly regulated process designed to enable rapid blood clot formation at the sites of vascular injury (hemostasis) while limiting excessive blood clot formation, which can result in vessel occlusion (thrombosis) or the release of a clot into circulation (embolism), where the clot may occlude distant vessels. Endothelial cells line the vasculature and inhibit thrombus formation through the expression of both surface-bound molecules such as thrombomodulin and cluster of differentiation 39 (CD39), as well as secreted factors such as nitric oxide (NO) and tissue factor pathway inhibitor (TFPI). Conversely, at sites of vascular injury, ECs initiate thrombus formation to prevent vascular leakage and hemorrhage. The process of hemostasis is promoted by endothelial expression of tissue factor, platelet endothelial cell adhesion molecule (PECAM) and downregulation of normal anti-thrombotic activity. In healthy vasculature, ECs are responsible for clot dissolution (fibrinolysis) to prevent excessive thrombus formation and to permit re-endothelialization of the injured vessel wall. In addition to regulating thrombus formation, ECs regulate inflammation by controlling leukocyte adhesion and transmigration, as well as vascular smooth muscle cell proliferation and vascular tone [19,216,217,229,246]. Leukocyte adhesion and transmigration are facilitated by endothelial expression of adhesion molecules, predominantly intercellular adhesion molecule 1 (ICAM-1), vascular cell adhesion molecule 1 (VCAM-1) and E-selectin, while smooth muscle cell contractility is regulated by NO generated by endothelial nitric oxide synthase (eNOS). Thus, ECs serve as an active interface between the blood and surrounding tissue to regulate many vascular physiological processes.

Unlike the native vascular endothelium, synthetic vascular grafts developed thus far have sought to remain inert to avoid activation of coagulation. One example of such a clinically-utilized inert material is expanded polytetrafluoroethylene (ePTFE). However, at small diameters (<6 mm) these grafts frequently become occluded due to thrombus formation and intimal hyperplasia, both of which a healthy endothelium inhibits [55]. Tissue engineering strategies to develop biological vascular replacements or cover synthetic graft materials have used ECs to improve the bioactivity of the engineered vessels [148,177–179,247]. Despite the promising results of endothelialized vascular grafts in clinical trials, the limited availability of autologous ECs and the donor site morbidity resulting from EC harvest have limited the clinical potential of these grafts [177,181]. ECs have also been incorporated into tissue engineering strategies seeking to engineer thick or metabolically active tissues[248–250]. In these applications, the ECs are incorporated to form a capillary-like network to transport nutrients through the construct.

In contrast to ECs, endothelial progenitor cells can be isolated non-invasively from peripheral blood [103]. Although a variety of cell types can be derived from endothelial progenitor cells, a population termed endothelial outgrowth cells (“EOCs”; also known as late outgrowth, blood outgrowth endothelial, or endothelial colony-forming cells) most closely resemble ECs in their expression of EC surface antigens, activation of pro- and anticoagulant factors, and influence on smooth muscle cell proliferation and vascular tone [190,200,201,212,233]. Thus, EOCs are an attractive cell source for engineering an autologous endothelium that can properly recapitulate EC interactions with the blood and surrounding vascular tissue.

Although prior work has demonstrated that EOCs modulate their expression of pro- and anti-coagulant factors in response to stimuli including fluid shear [196,212,232] and calcium [184], a direct comparison of the ability of ECs and EOCs to regulate thrombus formation in a model using flowing blood has not been performed. Thrombus formation is a dynamic process with the continuous deposition and removal of circulating cells and coagulation factors as well as the continuous activation of zymogens to both pro- and anticoagulant proteases. Characterizing thrombus formation with flowing blood is necessary to incorporate the transport dynamics of circulating coagulation factors and shear-dependent cell adhesion [204,205]. To characterize the ability of EOCs to regulate vascular physiological processes, we have compared donor-matched EOCs and carotid ECs in their expression of thrombosis-regulating surface antigens and gene expression, activation of coagulation factors, and regulation of thrombus formation in an *ex vivo* shunt model of graft thrombosis. In addition, we performed these analyses before and after stimulation with the inflammatory cytokine TNFα to identify differences in the cells' inflammatory response. Although ECs and EOCs exhibited distinct profiles of gene expression and coagulation factor activation, ECs and EOCs were similar in their ability to regulate thrombus formation on a synthetic vascular graft. This work supports the use of EOCs as an autologous endothelium for various tissue engineering applications.

3.3 Materials and Methods

3.3.1 EC Isolation

ECs were isolated from explanted baboon carotid arteries as previously described [251]. Briefly, explanted arteries were clamped shut at one end of the vessel and collagenase type II (Worthington Biochemical, 600 U/mL) was dripped into the lumen. Blood vessels were treated with collagenase for 5 minutes and manually compressed to detach ECs from the vessel wall. The cells were then deposited into well plates coated with 50 µg/mL collagen I. ECs were purified by positive selection at the first passage using CD31 Dynabeads® (Life Technologies) according to the manufacturer's protocol.

3.3.2 EOC Isolation

EOCs were isolated from the peripheral blood of baboons as previously described [190]. Briefly, peripheral blood was diluted 1:1 in Hank's Balanced Salt Solution (HBSS) and gently layered over Histopaque-1077 (Sigma-Aldrich). The mononuclear cell layer was collected and diluted 1:1 with HBSS. After washing the cells three times with HBSS, the cells were plated into a 12-well plate coated with 50 µg/mL fibronectin at a density of 10-20 M cells/well. Individual colonies were isolated and expanded in culture flasks coated with 50 µg/mL collagen I. All isolated colonies were sorted using CD31 Dynabeads® (Life Technologies) according to the manufacturer's protocol to positively select for EOCs.

3.3.3 Cell Culture and TNFα Treatment

Following isolation, cells were cultured in EGM-2 (Lonza) supplemented with 10% fetal bovine serum (FBS, HyClone). Media was exchanged every 2-3 days.

Analyses were performed on cells at passages 4-5. For all experiments, ECs and EOCs from multiple donors were used, with both ECs and EOCs being derived from the same donor. To establish a dose-response effect of TNFα treatment, 1-100 U/mL of TNFα (R&D Systems) in EGM-2 was applied for 4 hours prior to analysis and ICAM-1 expression was measured by flow cytometry (below). For all other experiments, ECs and EOCs were treated with 100 U/mL TNFα for 4 hours.

3.3.4 Flow Cytometry

ECs and EOCs were dissociated from culture flasks with TrypLE (Life Technologies) and resuspended in phosphate buffered saline (PBS) with 1% FBS at a concentration of 10 M cells/mL. Non-specific antibody binding was blocked using 5% mouse serum for 20 minutes on ice. A master mixture of fluorescent antibodies was prepared with each antibody being used at the concentration recommended by the manufacturer. The antibodies used were Brilliant Violet 421–anti-CD34 (Biolegend), FITC–anti-ICAM-1, PE–anti-CD141 (thrombomodulin, BD Pharmingen), PE/Cy7–anti-CD146 (BD Pharmingen), AlexaFluor647–anti-CD309 (VEGFR2, BD Pharmingen), APC/Cy7–anti-CD31 (PECAM, Biolegend), PerCP–anti-CD45 (BD Pharmingen). The multicolor antibody mixture was added to each sample tube and incubated for 30 minutes on ice in the dark. The cells were then washed twice in PBS with 1% FBS and transferred into wells of a 96 well plate. Fluorescent measurements were acquired using a MACSQuant analyzer (Miltenyi Biotec). FlowJo v.X was used to perform automated compensation and plot histograms of fluorescence intensity. Fluorescently-labeled cells were compared to unstained controls or fluorescent minus one (FMO) controls for

channels in which accessory fluorophores caused the background to be evidently higher than unstained samples after compensation.

3.3.5 Reverse Transcription and Quantitative Polymerase Chain Reaction (qPCR)

Cells from 3 different donors were grown in culture flasks, dissociated with TrypLE and pelleted. Cell pellets were resuspended in Buffer RLT (Qiagen) with 1% β-mercaptoethanol. RNA isolation was performed using the RNeasy Mini kit (Qiagen) according to the manufacturer's protocol. Samples were treated with DNAse I (Fermentas) and RNA was reverse transcribed using SuperScript III Reverse Transcriptase (Life Technologies) with random primers according to the manufacturer's instructions. Gene expression was quantified with Platinum® SYBR® Green qPCR SuperMix-UDG using custom primers (Supplementary Table S3.1) with ROX reference dye and the Applied Biosystems 7500 Fast Real-Time PCR system. Glyceraldehyde 3-phosphate dehydrogenase (GAPDH) served as a housekeeping gene for calculating dCT values with dCT equal to the threshold cycle of GAPDH subtracted from the threshold cycle of the gene of interest. Each sample was performed in duplicate, and the mean Ct was used to calculate dCt values. Data are presented as the mean $2^{(-dCt)}$ plus standard deviation.

3.3.6 Coagulation Factor Activation

Cells which were either cultured in well plates or seeded on ePTFE graft sections were used to characterize coagulation factor activation. When cultured in well plates, cells were seeded at a density of 100,000 cells/cm^2 and cultured overnight, producing a confluent monolayer of cells. To measure tissue factor pathway-dependent FX activation, a solution of FVIIa (20 nM, Enzyme Research Laboratories) and FX (200 nM,

Enzyme Research Laboratories) in HBSS with Ca^{2+} and Mg^{2+} supplemented with 0.1% bovine serum albumin (BSA) was added to each sample and incubated for 1 hour at 37°C. Ethylenediaminetetraacetic acid (EDTA, 15 mM) was used to quench the reaction, Spectrozyme FXa (American Diagnostica) was added for a final concentration of 1 mM, and the absorbance at 405 nm was measured every 20 seconds for 20 minutes. To measure protein C activation, thrombin (5 nM, Haemotologic Technologies) and protein C (100 nM, Haemotologic Technologies) in PBS with Ca^{2+} and Mg^{2+} were added to sample wells and incubated for 1 hour at 37°C. Hirudin (500 nM) was used to inhibit thrombin protease activity, the chromogenic substrate S-2366 (Chromogenix, 1 mM) was added to each sample and the absorbance at 405 nm was measured every 20 seconds for 20 minutes. For both FX and protein C activation assays, and the maximum slope of absorbance increase over 10 points was used to calculate the concentration by comparing to a standard curve of FXa or activated protein C (APC). Each biologic sample group had three replicates, and each of these sample replicates was split into duplicates for FXa and APC quantification.

3.3.7 Animal Care

Male baboons (*Papio anubis*) used in this study were cared for and housed at the Oregon National Primate Research Center at Oregon Health & Science University. Experiments (IS00002496) were approved by the Oregon Health & Science University West Campus Institutional Animal Care and Use Committee according to the guidelines of the NIH “Guide for the Care and Use of Laboratory Animals” prepared by the Committee on Care & Use of Laboratory Animals of the Institute of Laboratory Animal

Resources, National Research Council (International Standard Book, Number 0-309-05377-3, 1996). All baboons were juvenile males with no known co-morbidities.

3.3.8 Ex Vivo *Arteriovenous Shunt*

Four millimeter internal diameter ePTFE grafts were seeded with cells as previously described [225]. Briefly, ePTFE grafts 5 cm in length were adjoined to silicone tubing and wetted with 95% ethanol, washed with water, and perfused with 0.02 N acetic acid. Collagen I (MP Biomedicals) in 0.02 N acetic acid (4 mg/mL) was then perfused through the graft material from the distal side to coat the graft lumen and permit cell adhesion, and the distal silicone tubing was washed with 0.02 N acetic acid to remove residual collagen. The grafts were seeded with cells by perfusing the grafts with a cell suspension of 3×10^5 cells/mL. Three cell perfusions were performed 40 minutes apart, and the grafts were rotated 120° between perfusions to produce a uniform cell monolayer. The seeded grafts were cultured overnight in a custom biochamber to enable cell adhesion and spreading on the graft material. Following overnight incubation, the cell-seeded grafts were connected to a baboon arteriovenous femoral shunt (Supplementary Figure S3.1) in the absence of anti-platelet or anticoagulant therapies [205]. Autologous platelets and allogenic fibrinogen were radiolabeled with ^{111}In and ^{125}I respectively and infused into the baboon prior to the shunt study. Blood flow through the graft was held constant at 100 mL/min using a clamp downstream of the graft. The shunt loop was located above a gamma camera to enable the real-time measurement of platelet accumulation using 5 minute exposure times over the course of the 60 minute shunt study. Following the shunt study, the grafts were fixed in 3.7% paraformaldehyde and placed at 4°C until the ^{111}In had decayed >10

half-lives, at which point the grafts were sectioned and fibrinogen incorporation was measured using a WIZARD automatic gamma camera (PerkinElmer). Platelet accumulation and fibrinogen incorporation were measured on the central 2 cm of the graft to eliminate the potentially confounding effect of increased platelet accumulation at the ePTFE-silicone junctions. Three grafts for each condition were tested in the arteriovenous shunt loop.

3.3.9 Statistical Analyses

Statistical analyses were performed using SPSS 12.0 or JMP 11.1.1. To determine significant differences between experimental groups for all studies except ICAM-1 flow cytometry, a two-way ANOVA was performed with the treatment factor containing four levels (ECs, EOCs, TNFα-treated ECs and TNFα-treated EOCs) and donor as a blocking factor. For analyzing ICAM-1 flow cytometry, a two-way ANOVA was performed with the treatment factor consisting of the TNFα concentrations (no TNFα, 1 U/mL, 10 U/mL, 100 U/mL) for each of the two cell types for a total of 8 levels and with donor as a blocking factor. A Tukey's *post hoc* analysis was used to determine homogenous subsets of experimental groups, and differences between groups were considered significant if $p<0.05$. All data are presented as the mean +/- standard deviation.

3.4 Results

3.4.1 Morphology and Surface Marker Expression

As previously reported, ECs and EOCs share a similar cobblestone morphology and form a confluent monolayer in culture (Figure 3.1). Flow cytometry characterization of ECs and EOCs with and without TNFα stimulation demonstrated a similar expression

of endothelial surface markers, and the absence of leukocyte marker CD45 (Figure 3.2, data not shown in the absence of TNFα). Our results are consistent with previous work demonstrating ECs treated with 100 U/mL TNFα for 4 hours exhibit a significant upregulation of ICAM-1. The magnitude of the response to TNFα varied considerably between donors; as a result, EOCs treated with 100 U/mL TNFα did not show statistically significant increase in ICAM-1 expression compared to untreated EOCs ($p=0.190$ by two-way ANOVA). Within each individual donor, populations of cells stained for ICAM-1 and treated with TNFα had increased median fluorescence values with increasing TNFα concentrations (Supplementary Figure S3.2).

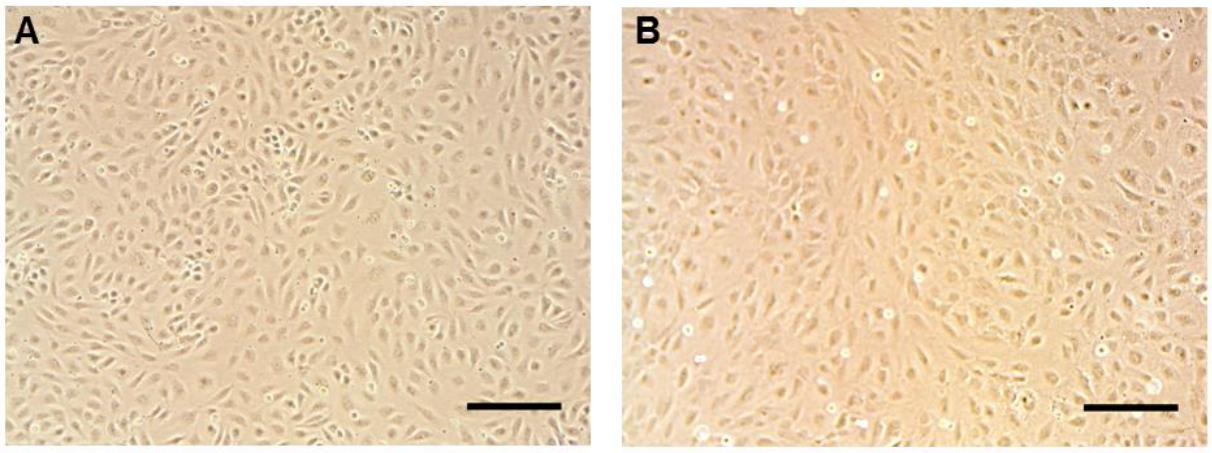

Figure 3.1: Morphology of endothelial and endothelial outgrowth cells.
Representative brightfield images of baboon carotid endothelial cells (A) and endothelial outgrowth cells (B), both of which exhibit similar cobblestone morphology. Scale bar = 200 µm.

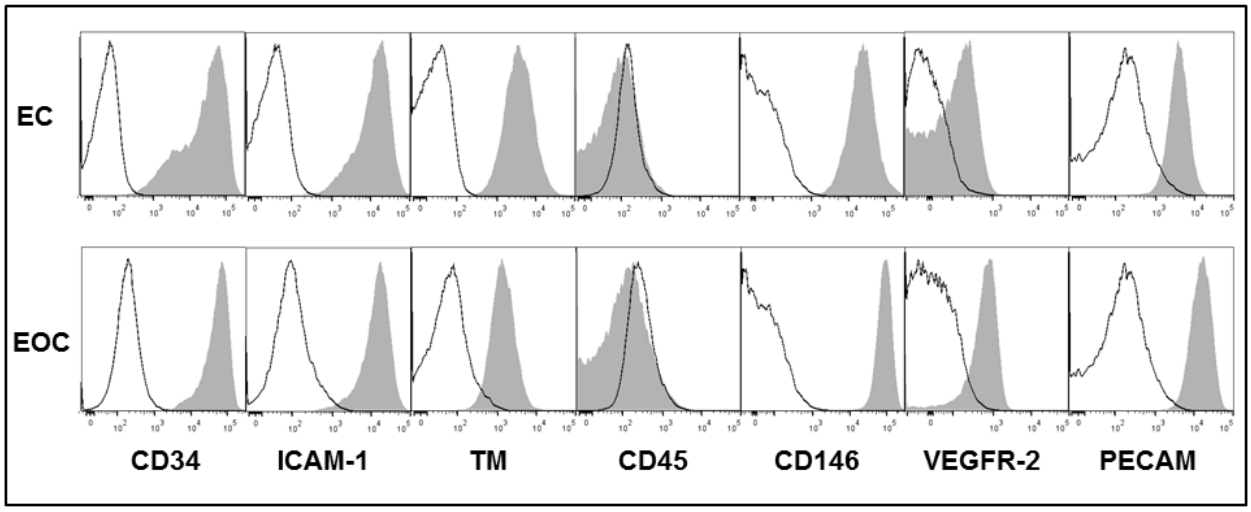

Figure 3.2: Representative flow cytometry histograms of ECs and EOCs treated with TNFα. Shaded histograms indicate samples stained with the multicolor antibody mixture, while the open histograms are the corresponding unstained or fluorescent-minus-one controls. EOCs exhibit the typical EC surface markers and are negative for the leukocyte marker CD45. TM, thrombomodulin.

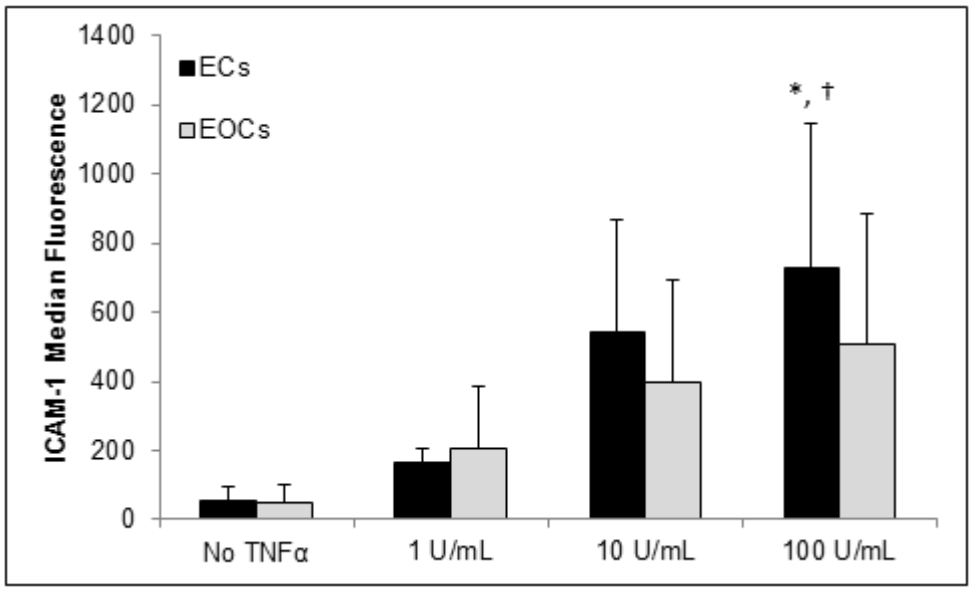

Figure 3.3: Median fluorescence of ICAM-1 by ECs and EOCs measured via flow cytometry. Both ECs and EOCs showed a dose-dependent upregulation of ICAM-1 expression induced by TNFα treatment. Data are charted as the mean + standard deviation. * $p<0.05$ vs. untreated ECs; † $p<0.05$ vs. untreated EOCs based on the *post hoc* analysis, n=3.

3.4.2 Thrombus Formation and Inflammation: Gene Expression

Quantitative PCR was performed to identify differences in gene expression between cell types and in response to TNFα (Figure 3.4 and Supplementary Table S3.2). Expression of the gene targets varied considerably between donors, though the responses of ECs and EOCs to TNFα treatment were similar for many genes. For all three donors, TNFα treatment resulted in the upregulation of the pro-thrombotic gene for TF, as well as pro-inflammatory genes for PECAM, ICAM-1, VCAM-1 and E-selectin for both ECs and EOCs. Similarly, in both ECs and EOCs, TNFα treatment downregulated the genes encoding for TFPI, TM and eNOS in all three donors. For genes encoding for TF, TFPI, PECAM and ICAM-1, the gene expression of individual donors at both the basal state and following TNFα treatment were closely matched between EC and EOCs. However, greater variability between ECs and their donor-matched EOCs were seen in genes encoding for CD39 and eNOS at a basal state, as well as for VCAM-1 and E-selectin following TNFα treatment. In summary, despite the variability between individual donors, within individual donors the expected modulation of gene expression following TNFα treatment was generally observed by both ECs and EOCs.

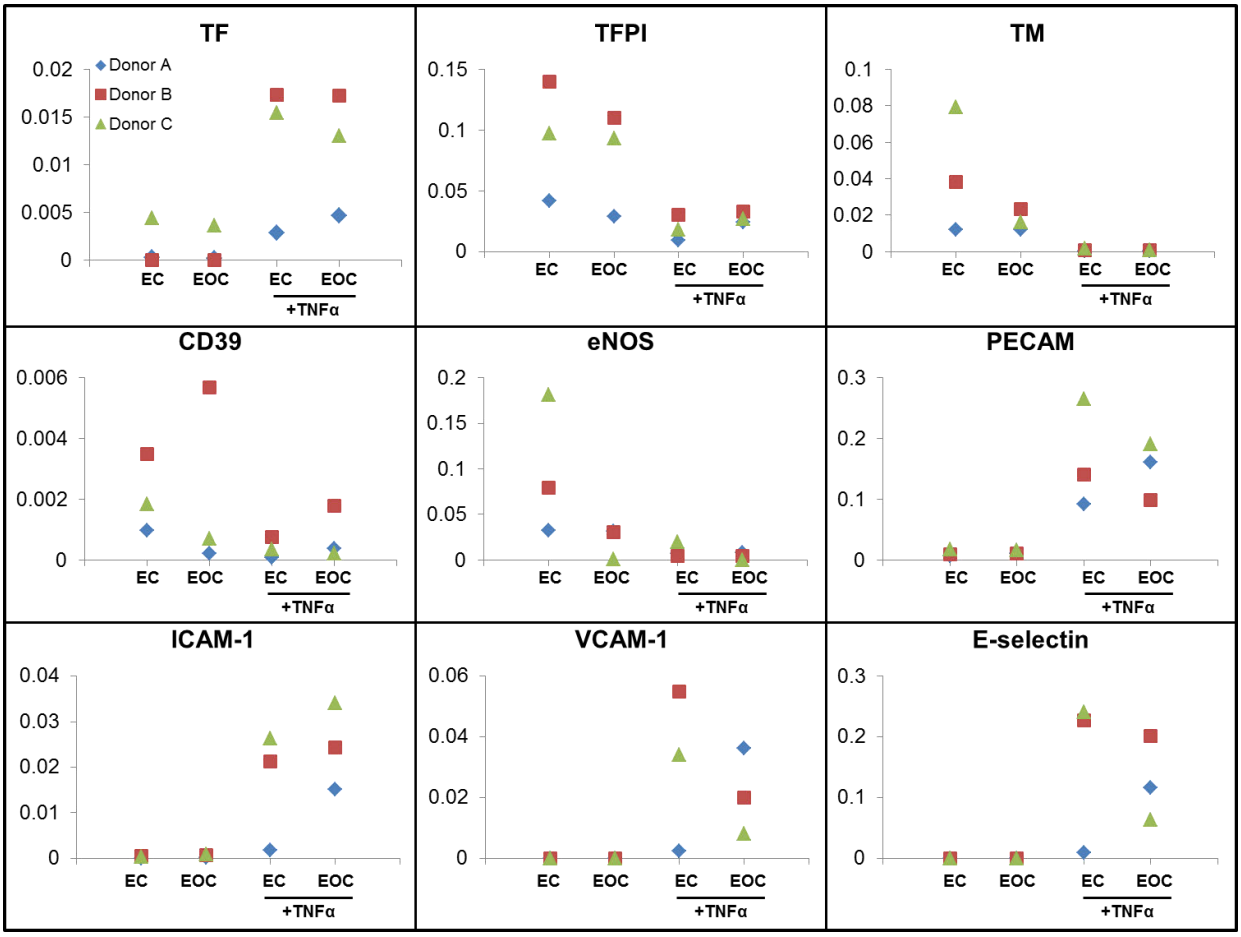

Figure 3.4: Gene expression of ECs and EOCs in the presence and absence of TNFα treatment. Gene expression of ECs and EOCs was measured with qPCR. Data are expressed as the $2^{-(dCt)}$ value using GAPDH as the housekeeping gene.

3.4.3 Coagulation Factor Activation

Protein C activation and FX activation by ECs and EOCs were quantified to determine how EOCs regulate specific anti- and pro-thrombotic pathways in response to TNFα. In the absence of TNFα, ECs and EOCs exhibited very low levels of FX activation (Figure 3.5A). Following TNFα stimulation, both ECs and EOCs significantly increased FX activation, indicating an increase in tissue factor activity. Furthermore, TNFα-treated ECs had a significantly greater increase in FX activation than EOCs (two-way ANOVA, $p<0.01$), indicating that EOCs may have a dampened pro-thrombotic response following inflammatory cytokine stimulation. There was no significant

difference in the average protein C activation between ECs and EOCs cultured in well plates (Figure 3.5B) though there was considerable inter-donor variability (Supplementary Figure S3.3). TNFα treatment did not significantly change the average protein C activation by either cell type. ECs and EOCs demonstrated similar activation of FX and protein C when seeded on vascular grafts (Figure 3.6) as when seeded in 96-well plates, with the exception that on the vascular grafts ECs had heightened FX activation in the absence of TNFα.

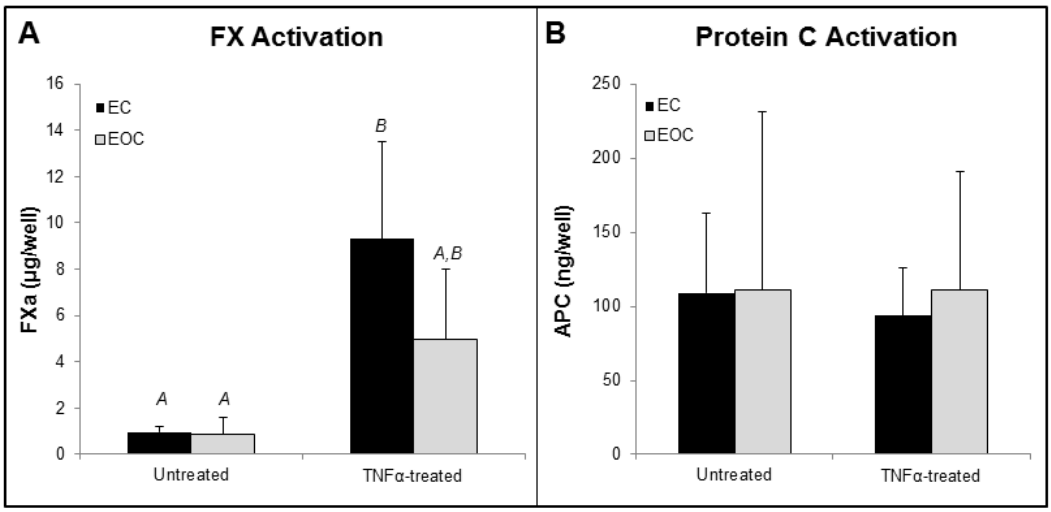

Figure 3.5: Coagulation factor activation by untreated and TNFα-treated ECs and EOCs. ECs and EOCs were assessed for FX activation (A) and protein C activation (B) at a basal state and following TNFα treatment. Letters denote groups belonging to homogenous subsets, while groups not sharing a letter are considered significantly different based on the *post hoc* analysis, n=8.

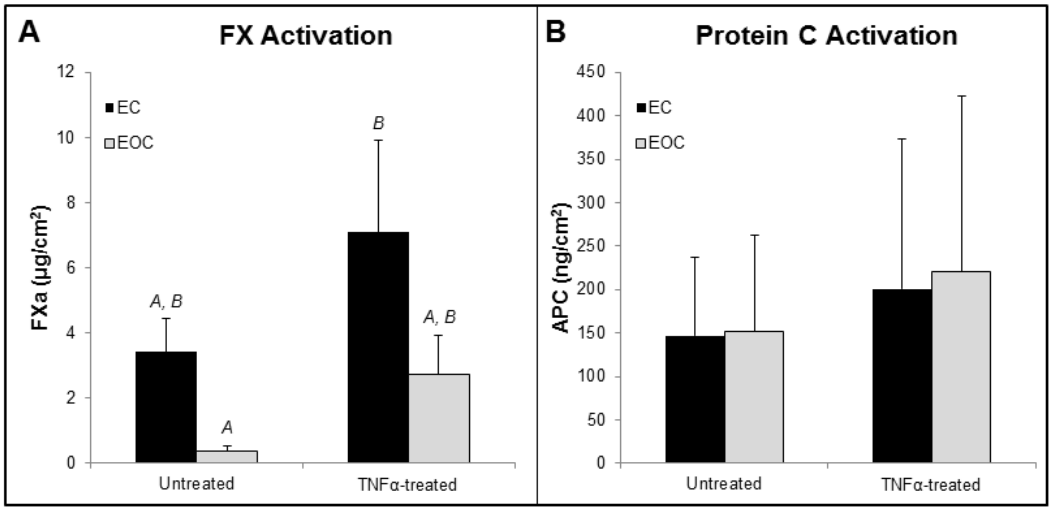

Figure 3.6: Coagulation factor activation on cell-seeded vascular grafts in the presence and absence of TNFα treatment. Sections of EC- and EOC-seeded ePTFE vascular grafts were assessed for FX activation (A) and protein C activation (B) at a basal state and following TNFα treatment. Letters denote groups belonging to homogenous subsets based on the *post hoc* analysis, while groups not sharing a letter are considered significantly different based on the *post hoc* analysis, n=3.

3.4.4 Platelet Accumulation on Cell-seeded Vascular Grafts

Following TNFα treatment, EC-seeded vascular grafts had similar platelet accumulation over the course of 1 hour as EOC-seeded grafts in the arteriovenous shunt model (Figure 3.7a). Interestingly, TNFα treatment did not significantly increase platelet accumulation on cell-seeded vascular grafts compared to untreated donor matched cell-seeded grafts (Figure 3.7a). This indicates that platelet accumulation in this model is not significantly altered by changes in cell phenotype induced by TNFα treatment. Similarly, there was no significant difference in fibrinogen incorporation between ECs and EOCs treated with TNFα or untreated (Figure 3.7b).

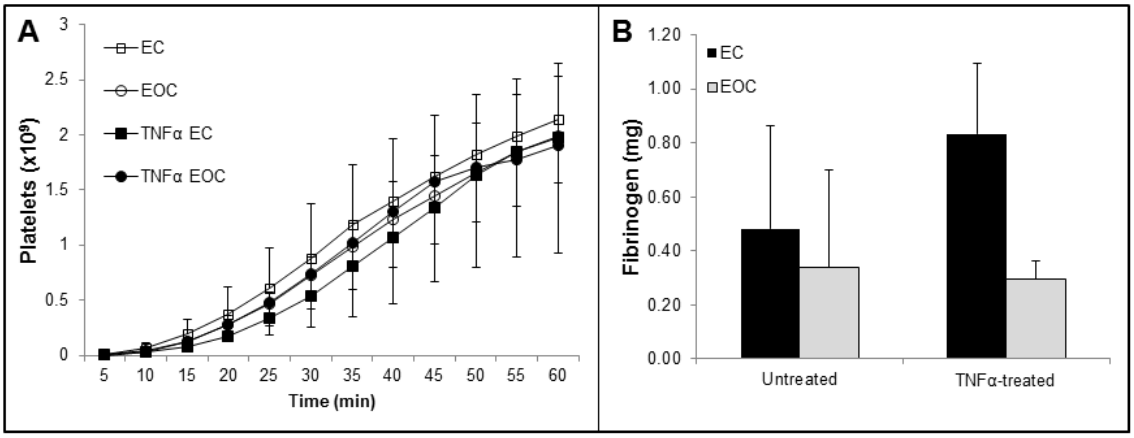

Figure 3.7: Thrombus formation on cell-seeded vascular grafts in a baboon arteriovenous shunt. Platelet accumulation (A) and fibrinogen incorporation (B) were measured on cell-seeded vascular grafts with or without TNFα treatment connected to a baboon arteriovenous shunt loop. Both platelet accumulation and fibrinogen incorporation were measured on the central 2 cm of the graft to eliminate the potentially confounding effect of increased platelet accumulation at the ePTFE-silicone junction. Data are presented as the mean ± standard deviation, n=3.

3.5 Discussion

The vascular endothelium serves as an active interface between the blood and surrounding vascular tissue. Although harvesting ECs to serve as an autologous endothelium in vascular tissue engineering applications has reduced graft complications, the process of harvesting vascular ECs is invasive. EOCs may provide an alternative source for engineering an autologous endothelium; however, there has been limited work in characterizing the capacity of EOCs to regulate thrombus formation and respond to inflammatory stimuli. This work contrasted EOCs with donor-matched, carotid ECs to characterize the capacity of EOCs to functionally regulate vascular physiological processes. Considering that the inability of acellular, synthetic vascular grafts to regulate processes such as intimal proliferation and thrombus formation has precluded the success of small diameter synthetic grafts, characterizing the

performance of EOCs in these processes has great implications for novel strategies to reduce graft thrombosis and enable vascular tissue engineering applications.

This study compared ECs and EOCs from the same animal donor, and utilized multiple donors in each analysis. As expected, there was considerable inter-donor variability in cellular function. Inter-donor differences are particularly apparent in the gene expression and flow cytometry analysis (see Supplementary Figure S3.2 for flow cytometry data of individual donors). This variability may have hindered the identification of statistically significant differences between cell types considering the low number of donors (n=3 for qPCR and flow cytometry analyses). Increasing the number of animals would likely cause the results to become statistically significant; however, a power analysis of the data indicated that due to the large variability between baboons, 24 donors would be required for sufficient statistical power to distinguish between treatment groups, and obtaining that quantity of baboon donors is not technically feasible. Tissue engineering applications using EOCs as an autologous endothelium would likely also exhibit this inter-donor variability. Therefore, rather than using cells from only one donor, we used multiple donors to identify general population responses and characterize how EOCs typically compare to ECs. More research on inter-donor EOC variability may identify relationships between EOC function and individual variances in blood composition or other health metrics.

In both ECs and EOCs, the inflammatory cytokine TNFα caused a pro-thrombotic shift in cell phenotype. Genes encoding anti-thrombotic agents such as TFPI, thrombomodulin and eNOS were lower in the TNFα stimulated cells of all three donors than in unstimulated cells, while pro-thrombotic tissue factor expression was increased.

The functional impact of lower eNOS gene expression is uncertain, though it is suggested that nitric oxide production is not significantly lower in EOCs than in ECs [184,220]. Prior work on ECs response to TNFα demonstrated that TNFα causes a modest reduction in thrombomodulin cofactor activity [252]. Although thrombomodulin activity averaged across individuals was not reduced by TNFα treatment, individual donors exhibited consistent decreases in thrombomodulin activity (Supplementary Figure S3.3). The average individual reduction in thrombomodulin activity was 9.4% in ECs and 10.2% in EOCs, which closely resembles prior findings [252]. A major limitation of this study is that all *in vitro* analyses utilized ECs and EOCs that had been cultured in static conditions. Future work could investigate differences between donor-matched EOCs and arterial ECs following fluid shear stress, as pre-conditioning EOCs and umbilical vein ECs with fluid shear stress has been shown to attenuate the cells' inflammatory response to TNFα [212].

Increased tissue factor activity, resulting from both increased tissue factor expression and reduced TFPI secretion, by the vascular endothelium and the resulting increase in local FX activation is generally considered to be a major contributor to platelet accumulation and hemostasis *in vivo* [253]. Perhaps the most surprising result in this work was that increased tissue factor activity resulting from TNFα treatment did not significantly alter platelet accumulation. This finding was demonstrated by the lack of difference in platelet accumulation between TNFα-treated and untreated grafts, as well as a lack of difference between EC- and EOC-seeded grafts treated with TNFα. In the latter case, ECs were shown to have increased tissue factor-mediated FX activation following TNFα treatment but did not have a corresponding increase in platelet

accumulation. Though unexpected, this result demonstrates how the complex interaction of pro- and anti-thrombotic pathways, as well as fibrinolytic activity, can dominate single pro-coagulant factors such as endothelial tissue factor expression. In this shunt model, tissue factor from other cell types, such as activated leukocytes or platelets, may be greater than EC- or EOC-expressed tissue factor, thereby overpowering any differences between these cell types. Alternatively, the contact activation pathway initiating with Factor XII activation could drive the initial generation of FXa. The initiation of fluid flow through the grafts may have caused the cells to release NO, a process which occurs in <2 min after the onset of flow [254], and may have overpowered differences in cell phenotype due to cell type and treatment. Regardless of the mechanism, once a small amount of thrombin has been generated, FXa generation *in vivo* is predominantly accom plished via the tissue factor-independent intrinsic pathway due to thrombin's positive feedback on intrinsic coagulation factors [25].

The baboon arteriovenous shunt model used in this work allows for a characterization of thrombus formation on cell-seeded vascular grafts with flowing whole blood in the absence of anticoagulants. This system enables flow conditions that are hemodynamically similar to the *in vivo* arterial environment and does not limit the activity of key coagulation factors in the highly-regulated process of hemostasis. As blood coagulation and platelet accumulation are regulated by multiple interdependent pathways, the absence of anticoagulants is notable as it maintains the function of all regulatory pathways and feedback mechanisms. This work demonstrates how the complex regulation of coagulation, and the flow-dependent transport dynamics of coagulation factors, which are not accounted for in many *in vitro* analyses of

thrombogenicity, can have a significant impact on cell thrombogenicity. Specifically, even though TNFα treatment altered the cellular thrombotic phenotype, including increased FX activation, platelet accumulation on cell-seeded vascular grafts was not affected. This result should be cautionary to drawing conclusions regarding cell thrombogenicity based on the activity of individual pro-coagulant pathways or the expression of thrombosis-related genes.

3.6 Conclusion

This work highlights the utility of characterizing thrombus formation in models that include flowing whole blood to properly simulate the *in vivo* regulatory pathways and transport dynamics. The similarity of EOCs and ECs in gene expression, coagulation factor activation, and regulation of platelet accumulation, at both a basal state and following TNFα treatment, supports the use of EOCs as an autologous endothelium in cardiovascular applications.

Gene Target	Forward	Reverse	Amplicon Size (bp)
E-selectin	GAAGGATGGACGCTCAATGG	AGTGGGAGCTTCACAGGTAG	90
ICAM	GCAGTCAACAGCTAAAACCTTCCT	GCAGCGTAGGGTAAGGTTCTTG	109
VCAM	GGGAAGATGGTCGTGATCCTT	TGAGACGGAGTCACCAATCTG	126
Thrombomodulin	GGTGGACGGCGAGTGTGTGG	GGTGTTGGGGTCGCAGTCGG	193
Tissue factor	CACCGACGAGATTGTGAAGGAT	TTCCCTGCCGGGTAGGAG	69
TFPI	GACTCCGCAATCAACCAAGGT	TGCTGGAGTGAGACACCATGA	70
PECAM	CAGCCTTCAACAGAGCCAACC	CACTCCGATGATAACCACTGC	116
CD39	AGTGATTCCAAGGTCCCAGCACC	TCCTGAGCAACCGCATGCCT	74
eNOS	TGGTACATGAGCACTGAGATCG	CCACGTTGATTTCCACTGCTG	148
GAPDH	CCTCAACGACCACTTTGTCA	TTACTCCTTGGAGGCCATGT	104

Supplementary Table S3.1. Primer sequences used for qPCR gene expression analysis and the size of the amplified cDNA in base pairs (bp).

	EC	EOC	TNF EC	TNF EOC
TF				
Animal A	0.000274	0.000241	0.002835	0.004697
Animal B	5.12E-05	4.92E-05	0.01736	0.017233
Animal C	0.00442	0.003681	0.015464	0.013021
TFPI				
Animal A	0.042003	0.028763	0.00941	0.024109
Animal B	0.140189	0.110376	0.0303	0.032925
Animal C	0.09711	0.093087	0.017896	0.026687
TM				
Animal A	0.012156	0.012257	0.000501	0.000399
Animal B	0.038407	0.023521	0.000658	0.000723
Animal C	0.079211	0.016185	0.001843	0.000598
CD39				
Animal A	0.000958	0.000209	8.27E-05	0.000379
Animal B	0.003488	0.005676	0.000756	0.00177
Animal C	0.001828	0.000698	0.000353	0.000216
eNOS				
Animal A	0.032437	0.03159	0.007027	0.00747
Animal B	0.078919	0.030145	0.003896	0.004661
Animal C	0.180795	0.000464	0.019686	5.95E-05
ICAM				
Animal A	4.02E-05	4.81E-05	0.001685	0.015156
Animal B	0.000516	0.00061	0.021281	0.024408
Animal C	0.000302	0.000781	0.026294	0.03406
VCAM				
Animal A	1.53E-05	2.38E-06	0.00245	0.036314
Animal B	7.09E-06	5.94E-05	0.054993	0.020033
Animal C	2.63E-05	1.33E-06	0.034084	0.008077
E-selectin				
Animal A	2.63E-06	1.94E-06	0.008374	0.116215
Animal B	9.88E-06	1.6E-05	0.227377	0.201006
Animal C	1.32E-05	1.12E-05	0.241054	0.063103
PECAM				
Animal A	0.005757	0.009751	0.09092	0.160591
Animal B	0.009137	0.009915	0.140066	0.098624
Animal C	0.017557	0.015621	0.26453	0.190259

Supplementary Table S3.2. Gene expression of ECs and EOCs in the presence and absence of TNFα treatment. Gene expression of ECs and EOCs was measured with qPCR. Data are expressed as $2^{-(dCt)}$ value using GAPDH as the housekeeping gene.

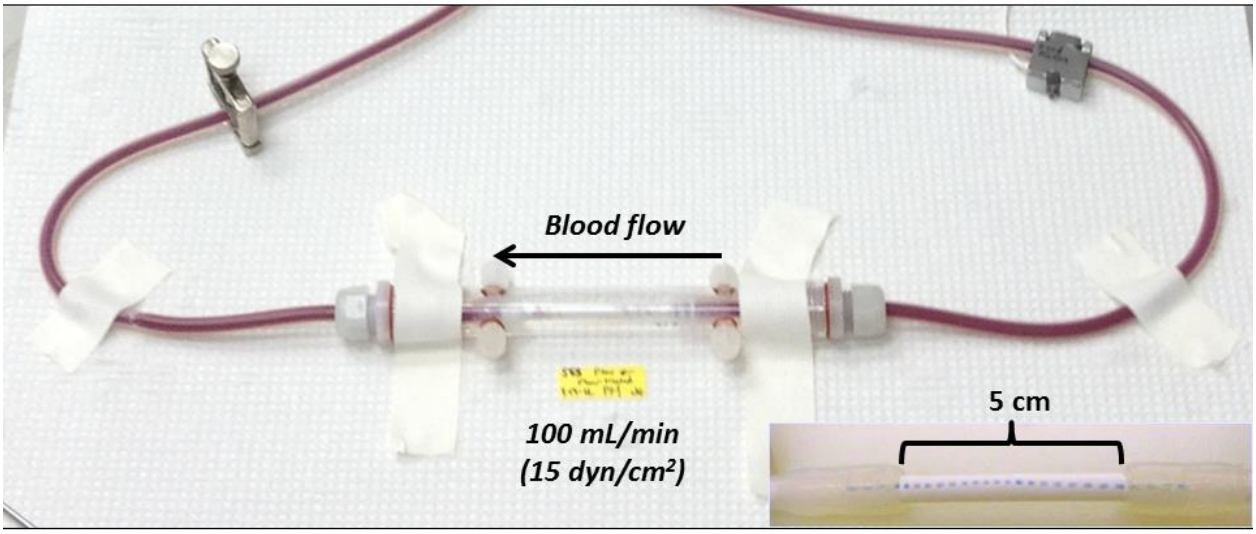

Supplementary Figure S3.1: A cell-seeded ePTFE vascular graft connected to the baboon arteriovenous shunt loop. Vascular grafts 5 cm in length are connected to silicone tubing (inset) for connection to the shunt loop. Blood flows from the femoral artery of the baboon, through the graft, and back into the femoral vein. The blood flow rate is monitored with a transonic flow probe and held constant at 100 mL/min by a clamp downstream of the graft.

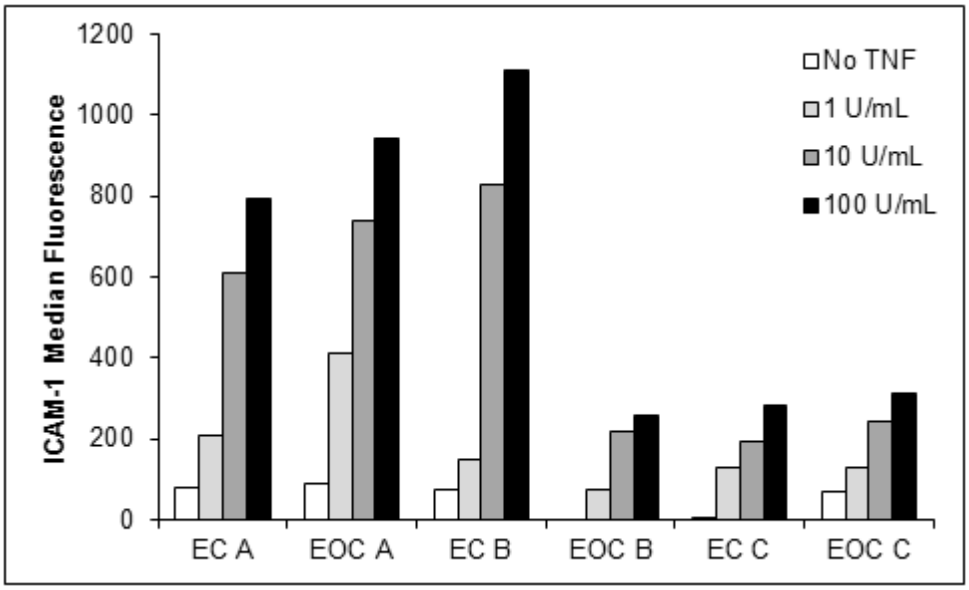

Supplementary Figure S3.2: ICAM-1 expression of TNFα-treated ECs and EOCs measured by flow cytometry. Each individual donor showed the expected dose-dependent upregulation of ICAM-1 induced by TNFα treatment. Large differences between donors was observed, with some cells being much more responsive to TNFα treatment.

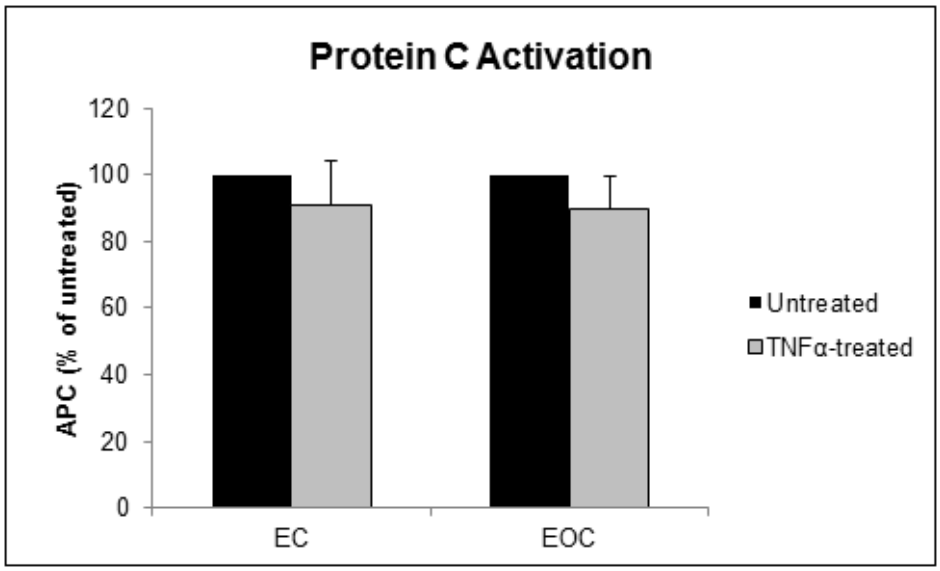

Supplementary Figure S3.3: APC generation of TNFα-treated ECs and EOCs normalized to untreated cells. Both ECs and EOCs consistently reduced protein C activation following TNFα treatment, though the degree of TNF α-induced reduction varied between donors. Decreases in protein C activation were not significant between untreated and treated (paired t-test, $p = 0.094$ for ECs, $p = 0.10$ for EOCs, $n=8$, analysis performed prior to normalization).

CHAPTER IV: *In vivo* assessment of two endothelialization approaches on bioprosthetic valves for the treatment of chronic deep venous insufficiency[4]

4.1 Abstract

Chronic deep venous insufficiency is a debilitating disease with limited therapeutic interventions. A bioprosthetic venous valve could not only replace a diseased valve, but has the potential to fully integrate into the patient with a minimally invasive procedure. Previous work with valves constructed from small intestinal submucosa (SIS) showed improvements in patients' symptoms in clinical studies; however, substantial thickening of the implanted valve leaflets also occurred. As endothelial cells are key regulators of vascular homeostasis, their presence on the SIS valves may reduce the observed thickening. This work tested an off-the-shelf approach to capture circulating endothelial cells *in vivo* using biotinylated anti-KDR antibodies in a suspended leaflet ovine model. The antibodies on SIS were oriented to promote cell capture and showed positive binding to endothelial cells *in vitro*; however, no differences were observed in leaflet thickness *in vivo* between antibody-modified and unmodified SIS. In an alternative approach, valves were pre-seeded with autologous endothelial cells and tested *in vivo*. Nearly all the implanted pre-seeded valves were patent and functioning; however, no statistical difference was observed in valve thickness with cell pre-seeding. Additional cell capture schemes or surface modifications should be examined to find an optimal

[4] This research was originally published in *Journal of biomedical materials research. Part B, Applied biomaterials*. Glynn JJ, Jones CM, Anderson DEJ, Pavčnik D, Hinds MT. In vivo assessment of two endothelialization approaches on bioprosthetic valves for the treatment of chronic deep venous insufficiency. *J Biomed Mater Res B Appl Biomater*. 2015; published online ahead of print.

method for encouraging SIS valve endothelialization to improve long-term valve function *in vivo*.

4.2 Introduction

In a healthy venous system, one-way blood flow from the extremities to the heart is maintained by a series of bi-leaflet venous valves that prevent blood backflow. Chronic deep venous insufficiency (CDVI) is a disease characterized by venous valves in the deep veins that are unable to close and prevent the backflow of blood [166,167]. Compression therapy, the current standard of care for venous insufficiency, aids in the healing of ulcers; however, approximately 20% of patients have ulcer recurrence despite ongoing compression therapy [168,169]. Open surgical treatment options that involve transplanting or ligating functional veins to diseased veins have not demonstrated significant improvements in ulcer healing over compression therapy; furthermore, many CDVI patients are not good surgical candidates due to pre-existing conditions including diabetes mellitus [169,255]. The inability of current therapies to treat the cause of chronic venous insufficiency has motivated the development of novel treatment methods to restore the function of venous valves.

Transcatheter bioprosthetic venous valves were suggested by Dotter in 1981 as a curative and minimally-invasive therapy for deep venous insufficiency [256]. Work by Pavčnik et al. constructed an artificial valve amenable to percutaneous delivery using decellularized, porcine small intestinal submucosa (SIS) sutured onto a metal frame that could be collapsed into a catheter [257]. After initial studies in sheep, the valve was redesigned to resist migration and to form a better seal with the vein wall [258]. In a clinical trial, 15 patients whose symptoms did not improve with prior standard surgical treatment received these advanced SIS valves. At 3 months post-implantation, 12 patients (80%) showed reduction of symptoms, including the healing of ulcers [258,259].

Despite these improvements, 13 of the 15 implanted valves were unable to prevent blood backflow after 3 months, and no valves were able to close after 12 months. Characterization of SIS valves implanted in sheep identified that SIS valve leaflets thicken with neotissue due to thrombus formation and intimal hyperplasia; this thickening resulted in reduced leaflet mobility and incomplete valve closure [258,259]. Therefore, strategies to sustain SIS leaflet mobility and prolong artificial valve function should actively limit thrombus formation and intimal hyperplasia.

Endothelialization of vascular devices is thought to be crucial to long-term resistance of thrombosis and intimal thickening [260–262]. Rather than mature endothelial cells, which require invasive procedures and donor site morbidity to obtain, endothelial outgrowth cells (EOCs) are a promising source for autologous endothelialization of vascular devices [263]. EOCs are isolated from a whole blood draw, expanded rapidly *in vitro*, and express mature endothelial cell markers [190]. *In vitro* seeding of biomedical devices with EOCs has been investigated with metal and polymer devices, as well as seeding on a select number of biomaterials [197,225,263–266]. Prior to our studies published in 2012, the seeding of EOCs on SIS biomaterial had not yet been reported [267]. This work optimized the endothelialization of SIS valves and confirmed the retention of an endothelial layer through the manipulations necessary for transcatheter implantation and the application of *in vitro* or *ex vivo* flow in the ovine model.

Pre-seeding of vascular devices is one method of establishing device endothelialization; however, *in situ* endothelialization enabled by surface modification of acellular biomaterials could offer greatly improved clinical translatability [268]. Studies

using suspended SIS valves to isolate endothelialization by circulating progenitors from migration from the vessel wall demonstrated that unmodified SIS valves had only partial endothelialization at 8 and 18 week time points [269], motivating the use of an endothelial cell capture technique. Kinase insert domain receptor (KDR), also known as vascular endothelial growth factor receptor 2, is a surface protein unique to endothelial cells and therefore a suitable target for endothelial cell capture [270]. Previous work demonstrated the ability of anti-KDR antibodies to capture human umbilical cord vascular endothelial cells *in vitro* under low flow conditions [158]. In this work, cell capture more than doubled when the antibody was oriented using a G-protein strategy. However, the G-protein linker would not be suitable for implantation due to its immunogenicity; thus, alternative antibody orientation strategies must be explored. For this work, we employed a biotin-streptavidin system for antibody binding and orientation. Biotin-streptavidin binding is one of the strongest non-covalent bonds in biological systems [271]. This work evaluated the capacity of this binding scheme to orient anti-KDR antibodies for capturing endothelial cells on SIS leaflets.

The goal of this research was to promote early endothelialization of SIS, either by pre-seeding *in vitro* or capture *in vivo*, to ultimately reduce the thickening of implanted artificial venous valve leaflets. We hypothesized that early endothelialization of SIS leaflets by either of these two strategies would limit the formation of intimal hyperplasia on bioprosthetic venous valves.

4.3 Materials and Methods

4.3.1 EOC capture on antibody-modified SIS

Antibody biotinylation

Biotin was covalently attached to the heavy chain of the anti-human KDR antibody (Clone 89106, R&D Systems) using a two-step procedure: oxidation followed by biotinylation. To oxidize the antibody heavy chain, anti-KDR was diluted in 20mM sodium meta-periodate in 0.1M sodium acetate buffer (pH=5.5) for 30 minutes on ice in the dark to convert the vicinal diol groups on the sugars from hydroxyls to aldehydes. After quenching the reaction with glycerol, the antibody was concentrated and excess reagents were excluded using Amicon Ultra-0.5 spin columns with a 10 kDa molecular weight cutoff (Millipore) according to the manufacturer's protocol. To conjugate biotin to the antibody, the antibody was re-diluted in PBS and 1/10th volume EZ-Link^{TM} hydrazide-biotin solution (50mM in DMSO, Thermo Scientific) was added to covalently conjugate biotin to the antibody via a hydrazone bond. Biotinylated antibody solutions were concentrated and excess reagents removed using the Amicon spin columns, and final concentrations were determined using a FluoroProfile™ kit (Sigma Aldrich) according to the manufacturer's protocol. A mouse IgG1 standard antibody (Dako) was used to generate a standard curve.

The specificity of the biotinylation for the heavy chain of anti-KDR was confirmed via western blot. Biotinylated anti-KDR was denatured by heating for 5 min at 95 °C, run on a Novex 4-12% bis-tris gel (Invitrogen) using standard western blotting techniques. Denaturation of the antibody was validated by identifying distinct bands for the light and heavy chains with ponceau-S staining. The antibody biotinylation reaction was then

confirmed using streptavidin-HRP and measurement of the chemiluminescent SuperSignal West Pico Substrate (Pierce). Unmodified antibody was used as a negative control.

Immunofluorescent staining was used to confirm that the biotinylated antibody retained reactivity to EOCs using methods described previously [267]. EOCs were grown to confluence on 8-well chamber slides and fixed with 3.7% paraformaldehyde. EOCs were incubated with either biotinylated anti-KDR or unmodified anti-KDR, followed by Alexa Fluor 568-conjugated streptavidin (Invitrogen) and counterstained with DAPI.

Antibody orientation on SIS

Vacuum pressed SIS sheets were provided by Cook Biotech, Inc. SIS was biotinylated by treating with a 0.5 mg/mL solution of EZ-Link^{TM} Sulfo NHS-LC-biotin (Thermo Scientific) in PBS for 24 hrs at room temperature. Biotinylated SIS was rinsed with water and incubated for 2 hr at room temperature with 0.1 mg/mL streptavidin solution in PBS (Thermo Scientific). SIS samples were then rinsed with PBS-Tween (0.05% Tween 20 in PBS) and incubated with biotinylated anti-KDR solutions overnight at room temperature. Samples were thoroughly rinsed with PBS-Tween prior to experiments.

To quantify the binding of the antibody to the biotinylated-SIS surface, anti-KDR was radiolabeled with the isotope ^{125}I using Pierce Iodination Beads (Thermo Fisher). Iodination beads (2 beads per 5-500ug protein) were rinsed with PBS and combined with Na^{125}I. Antibody was added to the reaction for 15 min at room temperature with agitation. Radiolabeling efficiency was determined with a trichloroacetic acid

precipitation. A constant amount of ^{125}I labeled antibody was combined with a varied amount of non-radiolabeled antibody to yield the desired concentrations of antibody solution. These solutions were incubated for 2 hrs at room temperature on biotin and streptavidin-bound SIS surfaces. Radioactivity of the samples was quantified using a WIZARD automated gamma camera (PerkinElmer).

To confirm the activity of anti-KDR following attachment to SIS, the amount of ^{125}I-labeled recombinant human KDR (rhKDR) bound to the antibody-modified SIS was quantified. Anti-KDR coated SIS samples were made as previously described using concentrations of 10, 20, 40, and 80 µg/mL biotinylated antibody. The rhKDR (R&D Systems) was labeled with ^{125}I using Pierce Iodination Beads using the same technique as KDR antibody. The rhKDR solution (0.1 µg/mL) was added to the antibody-modified SIS samples (n=5) and incubated overnight at room temperature. Samples were rinsed with PBS-Tween until rinse solutions were at background levels of radioactivity. The radioactivity of the rhKDR was measured on a WIZARD automated gamma camera.

Suspended SIS leaflet devices

To explicitly test circulating cell capture *in vivo* and eliminate any potential cell migration from the vessel wall, suspended, non-functioning leaflet devices previously designed by our group [272] were deployed via catheter in sheep. All suspended leaflet devices used in this experiment were constructed to fit within the ovine inferior vena cava (IVC), which ranged from 18 to 26 mm in diameter. The device consisted of 2 parts (**Figure 4.1a-c**): (1) a rehydrated SIS leaflet was sewn onto a stainless steel frame (14-mm edge lengths) with 7-0 Prolene monofilament sutures (Ethicon; Johnson & Johnson); these SIS leaflets were suspended from (2) a flexible, 25 mm or 32 mm

diameter stent frame, with 5-0 Prolene sutures (Ethicon). The mid-line of the SIS leaflet was cut open to create a valve-like opening. As the biologically-derived SIS material has an intrinsic sidedness with different properties for its serosal and mucosal sides [273,274], the SIS was mounted on the frame such that the serosal side of the SIS was always the distal face of the valve for consistency. The suspended SIS leaflets were air dried, coated with anti-KDR capture antibodies (80 µg/mL, measured post-biotinylation with the FluoroProfile™ kit), manually folded along the horizontal axis of the larger frame, and sterilized with ethylene oxide prior to implantation. Control implants followed an identical set of steps excluding the antibody coating.

Devices were constructed to enable implantation of two leaflet devices proximal to the renal veins and two distal. The diameter of the IVC proximal to the renal veins is generally larger than distal to the renal veins; therefore, the outer frames of the leaflet devices were 32 mm and 28 mm for the proximal and distal devices, respectively, to prevent device migration to the heart. The inner leaflets were identical in dimension above and below the renal veins.

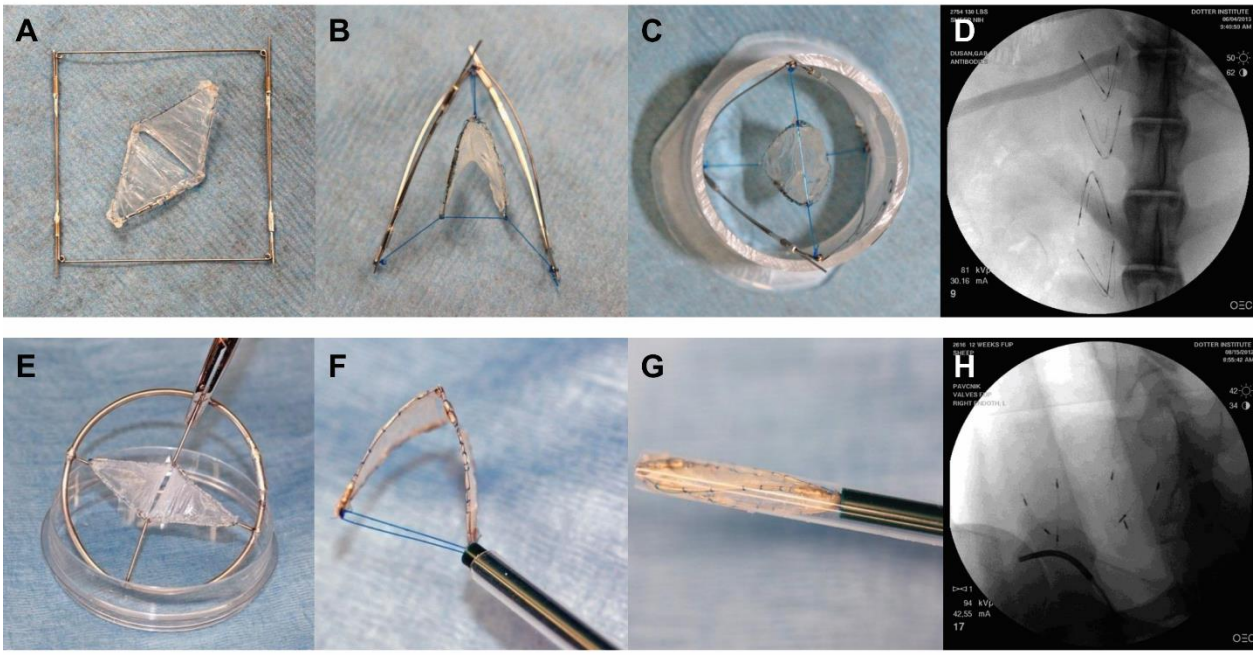

Figure 4.1: SIS Device Construction and Deployment. (a-d) Suspended SIS leaflet devices were modified with anti-KDR and implanted in the inferior vena cava of a sheep to capture circulating EOCs in vivo. (a and b) The non-functioning valve-like devices were suspended from a steel frame designed to suspend the valve in the sheep inferior vena cava to test cell capture in the absence of cell migration onto the devices. (d) Angiography was used to confirm the placement of the suspended devices. (e-h) SIS venous valves were pre-seeded with EOCs and implanted in sheep jugular veins. (e) SIS valves were mounted onto a circular frame for uniform seeding of EOCs. (f and g)The valves could then be pulled into a catheter using a suture loop. (h) Valves were placed in the jugular veins of sheep and the position was confirmed using angiography.

Animal studies

All animal experiments were performed in female domestic sheep (*Ovis aries*; Western crossbreed) and were approved by the OHSU Institutional Animal Care and Use Committee according to the “Guide for the Care and Use of Laboratory Animals” prepared by the Committee on Care & Use of Laboratory Animals of the Institute of Laboratory Animal Resources, National Research Council (International Standard Book, Number 0-309-05377-3, 1996). Prior to surgery, each sheep was given preoperative antibiotics, Ancef (cefazolin) 1 gm/day intramuscular. Animals were transported to the

Dotter lab in appropriate cages on the morning of the surgery and anesthetized with intravenous midazolam (0.025 mg/kg) + ketamine (0.9 mg/kg). The animals were then intubated and placed on a mechanical ventilator with isoflurane anesthetic (2.0% - 2.5%) in oxygen while being monitored for respiration, corneal and papillary reflex, and muscle tone and placed supine on an angiographic table. The needle puncture area was scrubbed with betadine solution and draped in the sterile fashion. During the surgical procedure, each animal's vital signs (heart rate, respiratory rate, and arterial blood pressure) were continuously monitored. Veins were punctured with a 21 gauge needle and appropriately size catheters were placed. An initial heparin loading dose of 3000 - 5000 units was delivered and additional heparin administered as needed to maintain an activated clotting time > 300 sec. Digital imaging was performed with a mobile cardiac fluoroscopic unit (OEC9800, GE/OEC) at 15 frames per sec and Omnipaque contrast dye (Amersham Health). Vein internal diameter measurements were calibrated with a graduated guidewire (Cook Medical). Proper placement of the implanted devices was confirmed with venograms of the jugular vein or IVC as appropriate.

IVC implant procedure

Four suspended SIS leaflet devices were implanted into each of three domestic sheep (51-65 kg). Each animal had 2 control SIS devices and 2 SIS devices coated with oriented anti-KDR. In each animal, one of the leaflet devices proximal to the renal veins was anti-KDR coated and the other an unmodified control. The order of devices in the IVC was evenly distributed between treatment groups to mitigate possible differences in cell capture due to placement location within the IVC. The IVC was accessed via a

femoral puncture and angiography was used to measure the vein width and determine implant location [275]. The suspended leaflet device was front-loaded inside a 5 cm-long chamber of a 12 Fr delivery catheter. After deployment, the suspended SIS leaflet device self-expanded across the width of the vein. Angiography was used to confirm placement at implant (Figure 4.1d). The three sheep were sacrificed at 2 weeks to determine the effects of antibody modification on the early endothelial cell capture and remodeling of the suspended SIS devices. At explant, angiography was used to identify any positional shifting and confirm proper flow through the vein. After exsanguination, the IVC was flushed with 1-2 L heparinized saline. The IVC was accessed and the suspended leaflet devices were removed and immediately placed in 3.7% paraformaldehyde.

Histology

After 24 hrs fixation in 3.7% paraformaldehyde, the two leaflets of each explanted device were separated, one half placed in a new solution of 3.7% paraformaldehyde and the other half placed in 10% formalin for histology. The leaflet stored in formalin was cut in half perpendicular to the wire frame and mounted in paraffin with the cut face of each half of the leaflet parallel to the histology cut surface. Sections were stained according to standard procedures with hemotoxylin and eosin and Masson's trichrome. The leaflets that remained stored in paraformaldehyde were measured using digital calipers (Fisher Scientific) for the thickness at both the original cut surface of the valve and at the opposite end. These thickness measurements were averaged for each leaflet. A one-way analysis of variance (ANOVA) with Tukey's post hoc was used to determine differences between treatment groups, with $p<0.05$ considered significant.

4.3.2 EOC pre-seeded SIS valves

EOC isolation and characterization

Ovine EOCs were collected, isolated, and purified as described previously.[267] Briefly, outgrowth colonies were isolated from a culture of the mononuclear cell layer of a whole blood draw. EOCs were expanded in endothelial growth media (EGM-2, Lonza) with a final fetal bovine serum (FBS, Hyclone, Thermo Scientific) concentration of 10%. Cells were used at passage 5 for all studies.

Flow cytometry was used to confirm the presence of typical endothelial cell surface markers. After dissociation from culture flasks with TrypLE (Life Technologies), EOCs were resuspended at a concentration of $1x10^6$ cells/mL and blocked using 5% mouse serum for 20 min on ice. A master mixture of the antibodies PE/Cy7–anti-CD146 (MCAM, BD Pharmingen), AlexaFluor647–anti-KDR (VEGFR2, BD Pharmingen), and FITC–anti-CD31 (PECAM, Biolegend) was prepared with each antibody being used at the concentration recommended by the manufacturer. Samples were incubated in the multicolor antibody master mixture for 30 min on ice in the dark, washed twice in PBS with 1% FBS and transferred into a 96 well plate. Fluorescent intensity measurements were acquired using a MACSQuant analyzer (Miltenyi Biotec). Samples stained with a single antibody were used to perform automated compensation in FlowJo v.X. Fluorescent minus one (FMO) controls were used in channels where emission overlap caused the background fluorescence to be evidently higher than unstained samples after compensation.

SIS device construction

SIS bioprosthetic valves were constructed with custom dimensions to match each sheep's unique anatomy. Angiography was used to identify the maximum diameter of the left and right jugular vein in each of six sheep (9.8-12.3 mm). Valves were constructed by suturing SIS to a custom made stainless steel frame with 7-0 Prolene monofilament sutures. The frame was constrained prior to suturing on the SIS with a Prolene loop to customize the dimensions of expansion upon delivery. After the constraining Prolene loop was removed, a slit was cut across the SIS mid-line to create the valve opening.

SIS seeding

SIS valves were pre-seeded with autologous EOCs as previously described with minor modifications [267]. Briefly, a 10 cm petri dish was agarose coated, and a sterile customized metal frame was used to raise the SIS off of the bottom surface and to allow for easy device turning (Figure 4.1e). Devices were soaked overnight in cell culture media, and the serosal side was seeded first with 10^6 cells/valve (100 µL/leaflet, $0.5x10^6$ cells/leaflet). After a 1hr incubation at 37 °C, the device was flipped and 10^6 cells/valve were seeded on the mucosal side. Additional media was added after 1hr. Devices were implanted 48 hrs after seeding the serosal side.

Jugular vein implant procedure

Six sheep were each implanted with two valves – one into each jugular vein. One valve in each animal was EOC-seeded and the other was an unmodified control. Valves were delivered via catheter as described and tested previously *ex vivo* with slight modification [267]. To collapse and load the valve into a 12 Fr catheter, a 7-0 Prolene

loop was created by feeding the suture through opposing corners of the frame distal to the valve orifice (**Figure 4.1f**). Drawing the loop into the catheter resulted in gentle valve collapse and proper loading for delivery (**Figure 4.1g**). Valve placement was confirmed with angiography at the time of implantation (**Figure 4.1h**). After 3 months, valves were evaluated for function (i.e., patency and competency) via angiography, as well as thickness and cellular remodeling using histology. At explantation, contrast was injected distal to the valve to confirm the valve remained patent. Injecting contrast proximal to the valve allowed for the assessment of competency, defined as the ability of the valve to block retrograde flow. After sacrifice and exsanguination, the vein was cut above and below the valve, rinsed with PBS, and placed immediately into 10% formalin. The distal end of the valve was marked with a suture to preserve orientation for embedding.

Histology

Samples were fixed in 10% neutral buffered formalin for 48 hrs and then transferred to 70% ethanol until all samples were collected. Explants were embedded whole in methacrylate and then sectioned along the axial axis of each leaflet with a diamond blade (Alizee, Inc.). Sections were stained according to standard procedures with hematoxylin and eosin, as well as von Willebrand factor (vWF) and smooth muscle actin (SMA) via immunohistochemistry.

4.4 Results

4.4.1 Sheep EOC Characterization

Multicolor flow cytometry was used to characterize sheep EOC surface marker expression (Figure 4.2). The sheep EOCs expressed the typical endothelial markers CD31, CD146 (MCAM), and KDR. There was a strong positive staining for CD146 and a

weak positive staining for CD31 and KDR, which was likely due to limited cross-reactivity of the anti-human antibodies against sheep cells.

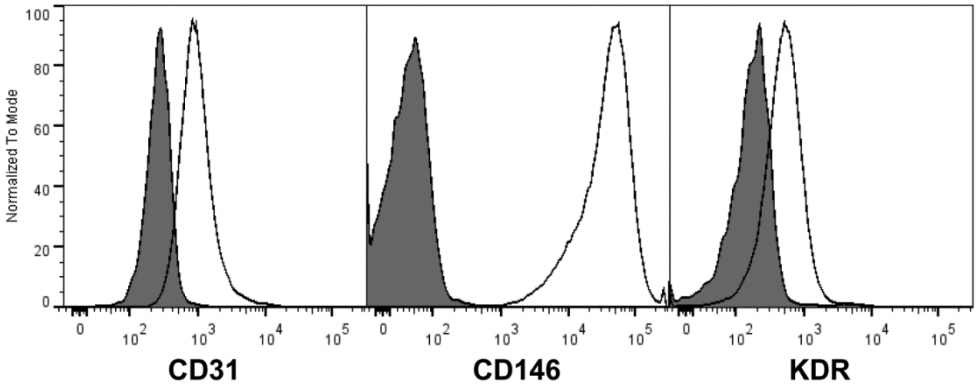

Figure 4.2: Flow cytometry characterization of sheep EOCs. Compared to controls (filled histograms), multicolor stained sheep EOCs (unfilled) demonstrated strong positive staining for CD146, and weak positive staining for CD31 and KDR.

4.4.2 Antibody Orientation

The anti-KDR antibody was successfully biotinylated selectively on the heavy chain and remained reactive after modification. The western blot analysis determined that 1) streptavidin was non-reactive towards the unmodified antibody, and 2) streptavidin predominantly bound the biotinylated antibody on the heavy chain (Figure 4.3b). The biotinylated anti-KDR also remained reactive to the ovine EOCs (Figure 4.3c). The attachment of biotinylated anti-KDR to SIS was quantified using radiolabelled antibody. The amount of biotinylated antibody bound to the SIS increased linearly with increasing concentrations of biotinylated antibody (Figure 4.4a). Using radiolabeled rhKDR also showed that rhKDR binding to antibody-modified SIS increased with increasing concentrations of biotinylated antibody with a plateau occurring at an anti-KDR concentration of 40µg/mL (Figure 4.4b).

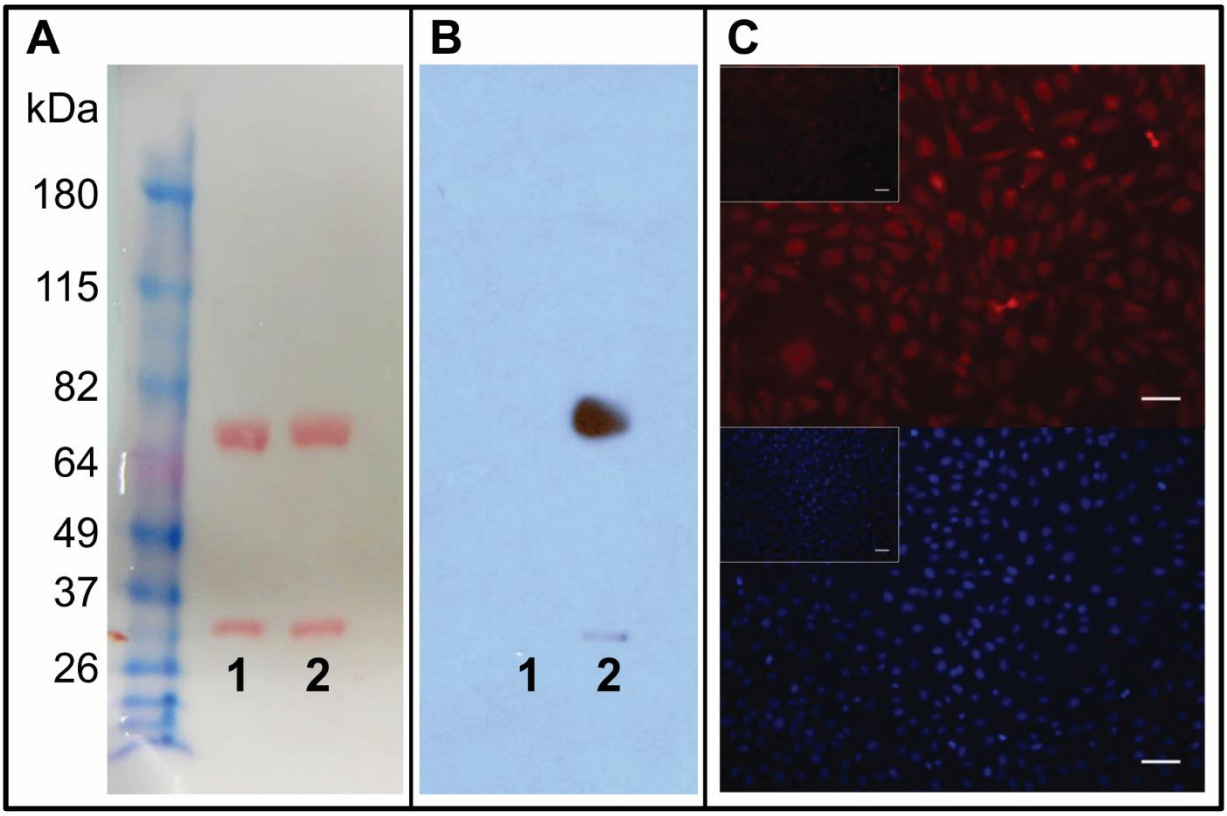

Figure 4.3: Biotinylation of anti-KDR antibody. (a) Ponceau stain indicates the total protein of the heavy and light chains for both the unmodified anti-KDR antibody (column 1) and the biotinylated anti-KDR antibody (column 2). (b) Streptavidin HRP preferentially bound to the heavy chain of the biotinylated anti-KDR antibody. Activity of the biotinylated antibodies was confirmed with staining of EOCs. (c) The biotinylated anti-KDR antibody adhered to fixed EOCs as detected by AlexaFluor 568-conjugated streptavidin (top) with DAPI indicating total cells (bottom). Inset contains negative control of unmodified anti-KDR stained EOCs. Scale bars = 100 μm.

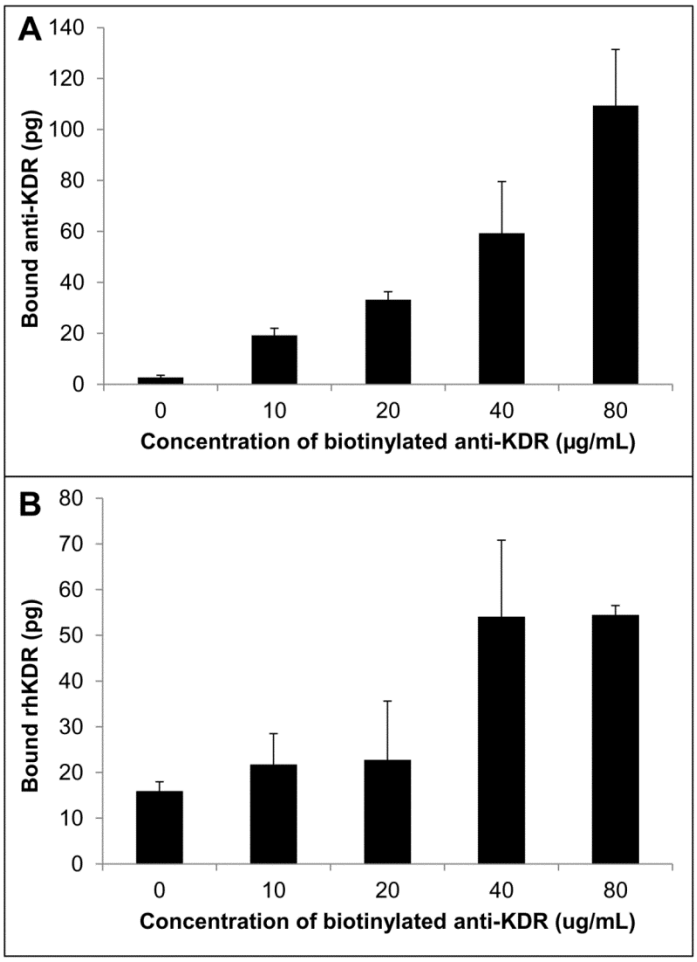

Figure 4.4: Confirmation of SIS modification. (a) SIS punches modified with biotin and streptavidin were exposed to I125 radiolabeled biotinylated KDR. Radioactivity of the punches was measured to give a quantification of bound biotinylated anti-KDR. (b) Modified SIS punches were incubated with increasing concentrations of biotinylated anti-KDR and then exposed to I125 radiolabeled recombinant human KDR. Radioactivity of the punches was measured to give a quantification of bound KDR protein. All data is presented as the mean ± standard deviation, n=4.

4.4.3 In vivo *EOC Capture Using Anti-KDR Antibody*

All suspended SIS leaflet devices remained in place in the IVC as shown in Figure 1d for the duration of the study. One minor migration occurred during implantation, which caused two suspended leaflets to fuse together over the two-week implantation. One unmodified leaflet and one antibody-coated leaflet each developed a blood clot that blocked flow thorough the leaflets. There was no statistical difference in

the thickness of SIS leaflets modified with anti-KDR compared to unmodified SIS leaflets (**Figure 4.5**). The remodeling response varied greatly between animals with some leaflets demonstrating extensive thickening, while others maintained thin leaflet dimensions. Minimal endothelialization was observed in both unmodified and anti-KDR modified valves, indicating a lack of rapid endothelialization regardless of anti-KDR modification.

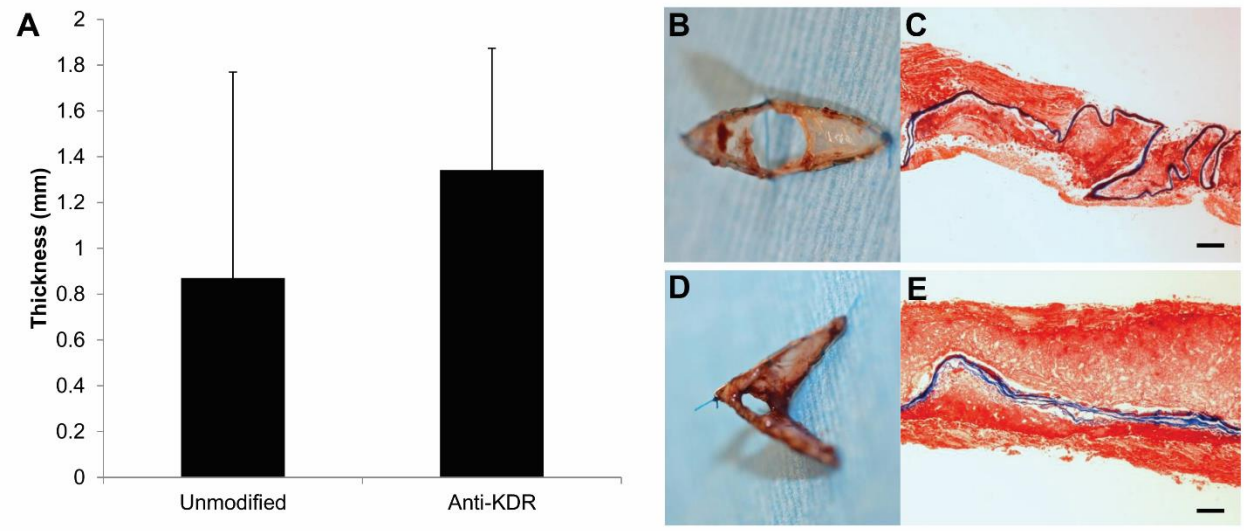

Figure 4.5: Thickness of suspended SIS devices post-implantation. (a) Suspended devices that were constructed with leaflets of either unmodified SIS or SIS modified with anti-KDR were implanted into sheep inferior vena cava for 2 weeks, and the leaflet thickness was measured at explantation. Data is presented as the mean + standard deviation, n=3. Panels b and c show a representative device constructed with unmodified SIS, while d and e show an anti-KDR modified SIS device. (c and e) Mason's trichrome staining was used to highlight the collagenous SIS material (blue) surrounded by a cellular remodeling response. Scale bar = 100 µm.

4.4.4 In vivo A*ssessment of EOC-pre-seeded SIS Valves*

At sacrifice after 3 months, angiography indicated that all valves remained in their original position in the jugular vein as seen in Figure 4.1h with no migration. Angiography also revealed that all valves remained patent (Figure 4.6a), which was

confirmed by observing the explanted valves (Figure 4.6d). Valve competency could not be measured in some cases where the implanted valve obstructed the side branch of the jugular vein immediately proximal to the valve that was required to inject contrast. Of valves that allowed for proximal contrast injection, all valves appeared competent (Figure 4.6b and c), though the injection of contrast dye may have influenced valve closure.

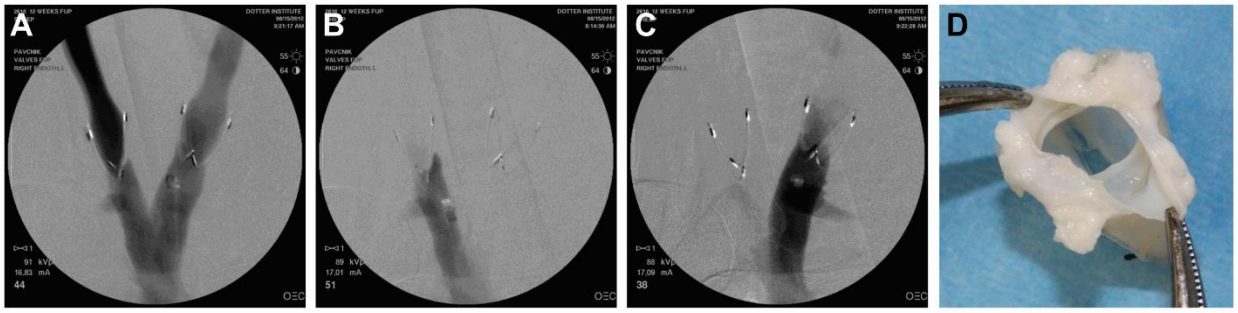

Figure 4.6: Representative angiography of EOC-seeded SIS devices in sheep jugular veins and of a valve post-explantation. (a) Contrast dye injected distally to the valve demonstrated that both valves were patent. (b and c) Contrast dye injected proximally to the valves did not regurgitate through the valve, suggesting competent valves were able to prevent retrograde blood flow. (d) Representative photograph of an SIS valve explanted after 3 months.

Thickness measurements of explanted valve leaflets revealed no difference between valves pre-seeded with EOCs and unmodified SIS control valves (Figure 4.7a). The remodeling response was highly animal-dependent with thicker pre-seeded valves seen in animals with thicker control valves (Figure 4.7b). The prevalence of smooth muscle cell infiltration into EOC-pre-seeded SIS seen with histology was very broad, ranging from a uniform thin layer just under the endothelial layer (Figure 4.8a) to permeating through the entire thickness of the neotissue (Figure 4.8b). Staining the histology sections for vWF, the presence of an endothelial layer was confirmed on all implants regardless of pre-seeding. These results indicate that tissue remodeling was

prevalent in all groups, but surprisingly, the original SIS material was not degraded during the 3 month implantation in the majority (9/12) of valves.

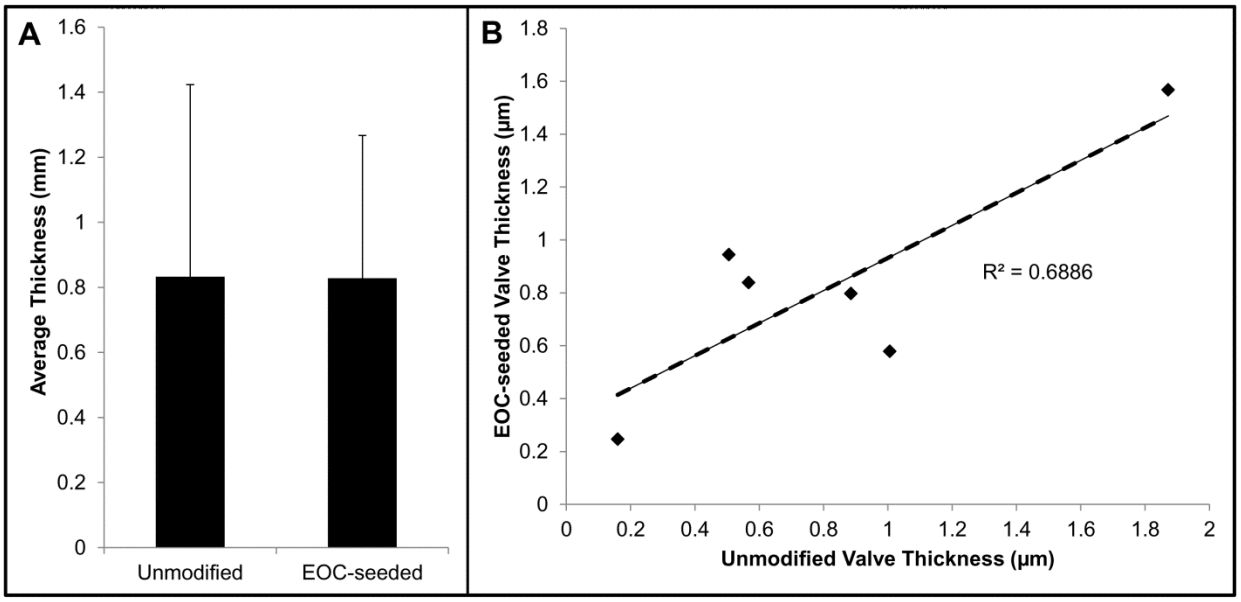

Figure 4.7: Thickness of explanted SIS valves post-implantation. (a) Bioartificial SIS venous valves that were either unmodified or pre-seeded with EOCs were implanted in sheep jugular veins for 3 months, and the thickness of the valve leaflets were measured at explantation. Data is presented as the mean + standard deviation, n=3. (b) A plot comparing the thickness of unmodified SIS valves compared with the contralaterally implanted EOC-seeded valves indicates that the degree of thickening varied greatly between animals but was similar between treatment groups.

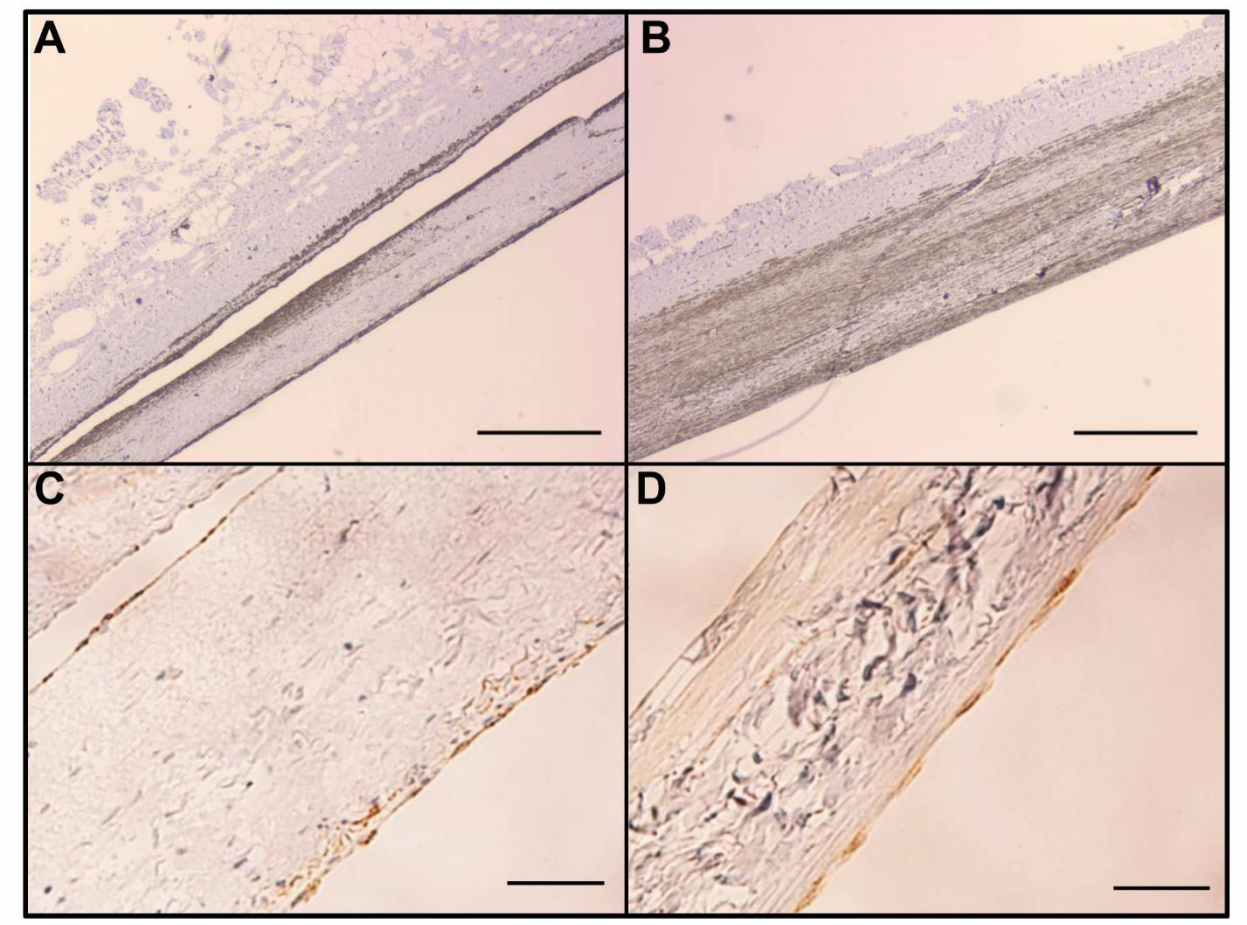

Figure 4.8: Immunohistochemical staining of SIS valves. (a and b) EOC-seeded valves were stained for smooth muscle actin; this stain showed that some valves had relatively little smooth muscle cell infiltration (a), while others had robust smooth muscle cell infiltration and proliferation on the valve leaflet (b). (c and d) Von Willebrand factor staining of unmodified SIS valves (c) and EOC-seeded valves (d) demonstrated that all valves regardless of treatment developed an endothelial cell lining on the luminal surface of the leaflet by the end of the 3 month implant period. Scale bars = 500 µm (a and b) or 50 µm (c and d).

4.5 Discussion

Venous insufficiency currently affects over 2.5 million Americans, and approximately 20% of patients develop skin ulceration [276–278]. Venous ulcers resulting from CDVI cause an estimated loss of 2 million workdays per year in the US [276,277]. The development of an artificial venous valve amenable to transcatheter

delivery would provide a novel treatment for chronic deep venous insufficiency capable of treating underlying venous valve incompetence in patients that are poor candidates for open surgery. This work builds upon prior studies using a bioprosthetic venous valve with leaflets made from SIS, and attempted to reduce leaflet remodeling and hyperplasia that hindered the long-term function of implanted valves. Venous valve replacement using allografts or autografts in animals, where the valve endothelium remained intact, did not demonstrate the intimal hyperplasia observed with the SIS venous valve [279,280]. As this type of valve replacement is a similar therapeutic strategy to SIS valve insertion, this result suggests the endothelial cell lining is a key facilitator for maintaining valve function. Furthermore, in studies using SIS for pulmonary valve reconstruction in which extensive *in situ* leaflet endothelialization existed, there was constructive remodeling with limited intimal hyperplasia and good long-term function [281,282]. Thus, we hypothesized that early endothelialization of SIS leaflets, either by capturing circulating cells or pre-seeding SIS with EOCs, would limit the development of intimal hyperplasia on bioprosthetic venous valves while also providing anti-thrombogenic activity. Previous studies have demonstrated that EOCs can regulate platelet accumulation and coagulation factor activation similar to mature endothelial cells [283], and EOCs have been seeded onto vascular grafts to improve hemocompatibility [225,263,266,284–288]. However, the utility of covering SIS with EOCs to reduce hyperplasia on SIS bioprosthetic venous valves had not been investigated.

The first part of this work sought to attach a capture antibody targeting the endothelial surface protein KDR onto the biomaterial SIS to capture EOCs from blood

and accelerate endothelialization of the SIS leaflets. Attaching capture antibodies to surfaces by methods that orient the antigen binding domains outward from the surface have been shown to significantly increase the efficacy of the bound antibodies [158,289,290]. To apply this strategy to SIS, we successfully biotinylated anti-KDR specifically on the heavy chain, enabling the oriented conjugation of the antibody to streptavidin-coated SIS surfaces. In our *in vitro* studies of adhering biotinylated anti-KDR to SIS, we were surprised to find that the quantity of bound antibody did not reach a plateau. We attribute this to the large effective surface area of SIS, which is increased by its fibrous texture and porosity. Therefore, the highest concentration of antibody tested (approximately 80 μg/mL) was used for all future studies.

With both of the *in vivo* studies, there was significant animal-to-animal variability with regard to the remodeling and thickening of implanted SIS leaflets. As such, no clear differences were seen between treatment groups and the unmodified SIS controls. Preliminary *in vivo* studies with valves constructed with unmodified SIS showed such significant remodeling that the number of valves implanted in this study was anticipated to provide adequate statistical power; however, the endothelialization strategies investigated in this work did not alter remodeling to the extent necessary to overcome the inter-animal variability in remodeling response. In cases such as stent deployment or vascular grafting, intimal thickening is thought to result from endothelium disruption causing insufficient inhibition of SMC proliferation [260–262]. In our antibody-mediated capture studies, we hypothesize that a lack of inhibitory signaling from the captured cells similarly permitted intimal thickening. The animal-specific nature of intimal thickening may therefore indicate inter-animal variability in a number of factors including

circulating quantities of EOCs, resulting in differential efficacy of cell capture, or differential production of inhibitors of SMC proliferation such as NO. Previous studies have indicated that certain disease states can result in measureable differences in circulating EOCs between human subjects [291–293] as well as altered eNOS activity [294], indicating that variability in these attributes may exist, though the underlying mechanism is unclear.

In the study using anti-KDR to facilitate EOC capture and accelerate endothelialization, it is possible that the inclusion of streptavidin in our conjugation chemistry led to an immune response that resulted in increased cellular adhesion and remodeling of the SIS. Additionally, variable immune responses between animals may have contributed to the animal-to-animal variability seen in these experiments. This result motivates a need for alternate site-specific binding strategies with reduced immunogenicity, such as copper-free click chemistry [295]. Interestingly, other groups using antibody-coated stents to accelerate EOC capture have shown results similar to ours, where *in vitro* data demonstrates increased EOC capture on antibody-modified surfaces [296,297], but clinical trials evaluating stent restenosis did not demonstrated significant improvements in clinical outcomes [298–300]. Factors including sub-optimal antibody selection and the inhibitory effect of thrombus formation on cell capture may have reduced the efficacy of antibody-mediated endothelialization in these cases. Therefore, using antibody-coated surfaces to accelerate endothelialization may have limited clinical utility, and alternate mechanisms of enhancing endothelialization, including EOC-specific capture aptamers or EOC-promoting growth factors, should continue to be explored [268].

As an alternate approach to antibody-mediated EOC capture, we investigated if pre-seeding SIS valves with EOCs would reduce valve remodeling and hyperplasia. However, our data suggest that pre-seeding the valves with EOCs did not appreciably reduce the thickening of implanted valve leaflets. The increased variability observed with the addition of a cellular component to the EOC-seeded valves was greater than expected and hindered the ability to identify differences between groups. Numerous groups have previously demonstrated that EOCs have a lower gene expression of endothelial nitric oxide synthase (eNOS) compared to aortic ECs [301–303] or umbilical vein ECs [304]. Therefore, it is possible that endothelialization with EOCs might have provided insufficient expression of eNOS to suppress SMC proliferation and minimize the formation of intimal hyperplasia. Pre-seeding the valve leaflets with alternatively-sourced endothelial cells that exhibit higher eNOS expression may result in sufficient NO to reduce SMC proliferation. Additionally, pre-conditioning EOCs with fluid shear stress has been shown to cause cellular alignment and increase NO production and therefore is another promising method to enhance NO release from EOC-seeded SIS valves [303,305,306]. Genetic engineering of EOCs to overexpress either eNOS [307] or thrombomodulin [308] may also increase EOC-mediated inhibition of intimal hyperplasia. Alternatively, different EOC seeding conditions may need to be established. In this study both pre-seeded valves and unmodified SIS controls were soaked in endothelial growth media including 10% fetal bovine serum. Despite thorough washing with saline prior to implantation, it is possible that one of the growth factors contained within the media or serum could have been retained in the SIS and contributed to the lack of difference between pre-seeded valves and bare SIS controls.

An additional difference between this work and previous studies using SIS in a bioprosthetic venous valve was the use of vacuum-pressed SIS. Overall, this version of SIS appeared to have a more uniform texture and reduced starting thickness. We attribute these physical characteristics to alterations in the SIS manufacturing process, most notably the inclusion of a vacuum press process as opposed to lyophilization. Interestingly, this vacuum-pressed SIS seemed to have slower degradation, as evidenced by the uncharacteristic presence of non-degraded SIS in the histology of valves explanted after 3 months. The amount of SIS remaining was not associated with the thickness of the explanted leaflets. To assess the kinetics of endothelialization and remodeling of vacuum-pressed SIS, future studies with multiple time points are needed. Although constructive remodeling of SIS has been demonstrated when SIS is utilized in pulmonary valve reconstruction [281,282,309], differences in blood flow dynamics and adjacent cellular populations between the pulmonary valve and the jugular vein may have contributed to the detrimental thickening seen in our studies.

In conclusion, this work utilized two different strategies to enhance early endothelialization of bioartificial SIS venous valves. The first strategy utilized an oriented capture antibody targeting KDR to accelerate endothelialization *in situ*, while the second strategy utilized pre-endothelialized SIS valve leaflets. In both strategies, the remodeling response and thickening of the implanted SIS devices varied greatly between animal subjects. Furthermore, no significant differences were seen between unmodified control SIS devices and those that had been coated with either anti-KDR or EOCs to promote endothelialization. The effects of the endothelialization achieved in this study were not sufficient to alter remodeling of the SIS leaflets such that any

significant reduction of thickening was observed. The lack of improvement from these strategies may be due to immune responses to the anti-KDR attachment strategy that may have limited the efficacy of the capture antibody, and the pre-seeded EOCs may not have produced sufficient nitric oxide to limit intimal ingrowth. Future studies will look at alternate strategies to orient capture antibodies to SIS, as well as methods to increase nitric oxide production by EOCs, possibly by flow pre-conditioning.

4.6 Conclusion

Rapid endothelialization of SIS, either through pre-seeding with EOCs or by using immobilized antibodies to capture circulating prognenitor cells, did not have the expected result of reducing thickening of SIS. The lack of improvement with the capture strategy is similar to other studies that attempted to accelerate endothelialization of stents but did not show significant improvement compared to bare metal stents. Alternate capture strategies, including aptamers and small peptides, may offer advantages of antibody-based capture. Previous research has demonstrated that an intact endothelial monolayer can be maintained on SIS through the manipulations required for transcethater delivery of a bioprosthetic venous valve. However, the special considerations that needed to be followed to ensure endothelial retention may preclude widespread usage and also provide additional opportunities for error in the implant procedure. Future work may investigate alternative cell-free strategies to reduce thrombus formation and intimal hyperplasia on SIS valves.

CHAPTER V: Crosslinking decreases the hemocompatibility of decellularized, porcine small intestinal submucosa [5]

5.1 Abstract

Decellularized tissues have been widely used as scaffolds for biomedical applications due to their presentation of adhesion peptide sequences and growth factors, which facilitate integration with surrounding tissue. One of the most commonly used decellularized tissue is derived from porcine small intestinal submucosa (SIS). In some applications, SIS is crosslinked to modulate the mechanical properties or degradation rate of the scaffold. Despite the widespread use of SIS, there has been no mechanistic characterization of blood reactions with SIS, nor how crosslinking affects these reactions. Therefore, we characterized the effect of SIS and carbodiimide-crosslinked SIS (cSIS) on plasma coagulation, including targeted assessments of the intrinsic and extrinsic coagulation pathways, and thrombus formation using flowing whole blood. SIS inhibited plasma coagulation initiated by recalcification, as well as low concentrations of thrombin or tissue factor. SIS prolonged the activated partial thromboplastin time by 14.3±1.54 sec, indicating inhibition of the intrinsic coagulation pathway. Carbodiimide crosslinking abrogated all anticoagulant effects of SIS, as did heparinase I and III treatment, suggesting heparin and heparan sulfate are predominantly responsible for SIS anticoagulant effects. Inhibiting contact activation of the intrinsic pathway prevented cSIS-mediated coagulation. When tubular SIS devices were connected to a nonhuman primate arteriovenous shunt loop, which enables whole

[5] This research was originally published in *Acta Biomaterialia.* Glynn JJ, Polsin EG, Hinds MT. Crosslinking decreases the hemocompatibility of decellularized, porcine small intestinal submucosa. *Acta Biomater*. 2015;14:96–103. © 2015 Elsevier BV.

blood to flow across devices without the use of anticoagulants, SIS demonstrated remarkably limited platelet accumulation and fibrinogen incorporation, while cSIS initiated significantly higher platelet and fibrinogen accumulation. These results demonstrate that SIS is a thromboresistant material and crosslinking markedly reduces the hemocompatibility of SIS.

5.2 Introduction

The extracellular matrix presents cells with a variety of topographical and biochemical cues that help coordinate proper cellular function [310,311]. To recapitulate these signals, researchers have utilized decellularized extracellular matrices as a scaffold for a variety of biomedical and tissue engineering applications [312,313]. In cardiovascular applications, decellularized blood vessels [314,315], heart valves [316,317], and even full hearts [318] have been shown to support robust cell proliferation both *in vitro* and *in vivo* and similar cellular organization to the native tissue. In all applications of decellularized matrices, the processing of the tissue can significantly alter the mechanical and biological properties of the final decellularized product [319–321]. Crosslinking is often performed on decellularized tissues to reduce immunogenicity as well as to increase mechanical stiffness and reduce degradation [322]. However, the techniques used to accomplish this crosslinking have significant effects on the biological response following implantation [323,324].

SIS is primarily composed of a network of collagens, glycosaminoglycans (GAGs), and growth factors including FGF-2 and VEGF [325–327]. The bioactive nature of the SIS material generally confers a favorable host response, characterized by cellular infiltration, tissue ingrowth, and limited pro-inflammatory M1-polarized macrophages [328]. Despite being derived from porcine intestine, SIS does not generally elicit any substantial adverse adaptive immune response [329]. Due to these advantageous characteristics, SIS has been successfully used clinically for numerous surgical procedures including dural grafts [330], hernia repair [331] and abdominal wall reconstruction [332]. In some applications, SIS is crosslinked to increase the

mechanical robustness or reduce the degradation rate of the material [333,334]. However, crosslinking SIS can result in a chronic inflammatory response and fibrosis when implanted into an abdominal wall defect [328]. Thus, the inflammatory response and remodeling of SIS implanted in soft tissues can be fundamentally altered by crosslinking the material.

A number of groups have sought to use SIS for cardiovascular applications including vascular grafting [335,336], stent coverings [337,338] and venous valve replacement [259]. In these applications, SIS interacts predominantly with blood rather than soft tissues alone, and must serve as a non-thrombogenic surface with minimal activation of platelets or coagulation factors. Studies using SIS for cardiovascular applications have generally demonstrated low rates of thrombosis that were similar to autologous saphenous vein [336] and ePTFE [339]. However, unlike the thorough characterization of the inflammatory and immune responses to SIS, the thrombotic response has not been well-studied. Furthermore, the effect of crosslinking on the hemocompatibility of SIS has not been addressed.

The thrombogenicity of a biomaterial can be characterized using experimental procedures that vary greatly in complexity and similarity to *in vivo* conditions [32,204]. Purified systems that measure the activity of a defined subset of coagulation factors provide straightforward information on biomaterial thrombogenicity and are useful for providing mechanistic insight into biomaterial-associated thrombosis. However, these results may not translate to *in vivo* performance due to the highly-interconnected regulatory pathways of coagulation pathways as well as the blood flow-dependent transport of coagulation factors to and from the material. Methods that study biomaterial

hemocompatibility using whole blood, particularly at physiological flow rates, provide the best indication of *in vivo* thrombogenicity, though these systems can confound the roles of individual blood components. To characterize SIS hemocompatibility, we utilized an array of *in vitro* coagulation assays using either purified solutions of coagulation factors or platelet-poor plasma to determine the effect of SIS on the intrinsic and extrinsic coagulation pathways. Additionally, an *ex vivo* arteriovenous shunt loop was used to characterize thrombus formation using flowing whole blood. These studies provide a multi-faceted characterization of coagulation factor activation, plasma coagulation, and thrombus formation on SIS, and also determine how crosslinking SIS affects these thrombotic processes.

5.3 Materials and Methods

5.3.1 SIS Preparation

Sheets of sterile, vacuum-pressed SIS were generously provided by Cook Biotech. Unless otherwise specified, SIS was cut into discs to fit into standard 96-well plates using 5 mm biopsy punches for all studies. Crosslinking SIS was performed according to the general crosslinking instructions provided by the carbodiimide manufacturer (Pierce), and similarly to other crosslinking procedures for SIS [340][340][327][323][322] and collagen-based biomaterials [341][328][324][323].

Briefly, SIS was soaked in a solution of 0.4 mg/mL 1-Ethyl-3-(3-dimethylaminopropyl) carbodiimide (Pierce) and 0.6 mg/mL *N*-hydroxysuccinimide (Pierce) in Activation Buffer (0.1 M 2-[N-morpholino]ethane sulfonic acid, 0.5 M NaCl, pH 5.0) for 15 minutes, followed by 2 hours incubation in Coupling Buffer (100 mM

sodium phosphate, 150 mM NaCl, pH 7.2). Prior to *in vitro* and *ex vivo* experiments, crosslinked SIS (cSIS) was thoroughly washed with Tris-buffered saline (TBS).

To construct tubular devices suitable for use in the arteriovenous shunt, SIS was rolled around a 4 mm polytetrafluoroethylene dowel with heat shrink connectors at each end. Larger diameter heat shrink tubing was placed on the outside of the SIS and briefly heated to form a tight sheath. Silicone tubing was then stretched over the internal connectors and the outer sheath to create a smooth luminal connection, and the junction was wrapped with Parafilm® (Curwood) to provide a leak-proof seal (Supplementary Figure S5.1A).

5.3.2 Extrinsic Pathway Activity

The extrinsic coagulation pathway is initiated by tissue factor. Tissue factor activity of SIS was quantified by measuring the ability of SIS to catalyze the conversion of Factor X (FX) to activated Factor X (FXa) in a solution containing activated Factor VII (FVIIa). SIS was incubated with 20nM FVIIa and 200nM FX (Enzyme Research Laboratories) in Hank's Balanced Salt Solution (HBSS) with Ca^{2+} and Mg^{2+} for 1 hour at 37°C. The reaction was quenched with ethylenediaminetetraacetic acid (EDTA, 15 mM), and the concentration of FXa was quantified using the chromogenic substrate Spectrozyme® FXa (American Diagnostica) by measuring absorbance at 405 nm for 20 minutes and comparing to known concentrations of FXa.

5.3.3 Platelet-poor Plasma Coagulation

Citrated, platelet-poor plasma was collected from 5 juvenile nonhuman primates (*Papio anubis*) and pooled. The diagnostic assays most-commonly used for assessing biomaterial hemocompatibility are the prothrombin time (PT) and the activated partial

thromboplastin time (APTT), which measure extrinsic and intrinsic pathway-dependent coagulation, respectively (graphical summary in Supplementary Figure S5.2). These assays typically measure coagulation mechanically by monitoring a stainless steel ball bearing in a rotating cuvette containing platelet-poor plasma and the pro-coagulant reagent. The time of coagulation is determined when the ball bearing is displaced due to fibrin polymerization entrapping the bearing. To utilize this testing system, SIS was cut into rings using 2 biopsy punches (outer = 8 mm, inner = 4 mm) and placed at the bottom of the testing cuvettes. The ball bearing, plasma, and pro-coagulant reagent, either Innovin® (Dade®) for the PT or HemosIL® (Instrumentation Laboratories) for the APTT, were then added on top of the SIS and the time to coagulation was automatically measured using a KC1 Delta™ (Tcoag).

The concentration of pro-coagulant stimuli in the PT and APTT reagents are much higher than physiological concentrations. For instance, the PT assay requires >50% inhibition or depletion of extrinsic pathway factors to result in an abnormal clotting time [342]. Therefore, to permit the use of lower concentrations of pro-coagulant stimuli and correspondingly longer clotting times, coagulation was measured optically using a plate reader [343]. Pooled plasma was placed into wells containing SIS, cSIS or no SIS for 15 minutes at 37°C prior to the initiation of coagulation by the addition of an equal volume of 25 mM $CaCl_2$. The absorbance at 405 nm was measured every 30 seconds, and the clotting time was determined as the time at which the absorbance increased 20% from the initial baseline. Absorbance measurements were stopped at 45 minutes. Clinically, the seminal test to discern whether prolonged clotting is due to an inhibitor or coagulation factor deficiency is to mix the sample plasma with reference plasma 1:1 and

perform the APTT. Complete correction of prolonged clotting times is diagnostic of a factor deficiency [344]. Therefore, to determine whether SIS-mediated anticoagulant effects were caused by the presence of an anticoagulant or by coagulation factor depletion via adsorption, SIS-conditioned plasma was mixed 1:1 with native plasma and both the APTT as well as the clotting times following recalcification were measured. In addition to measuring coagulation following recalcification, coagulation was actively stimulated with Innovin that had been diluted in 25 mM Ca^{2+} yielding an estimated final tissue factor concentration of 0.1 pM [345–347], mixed in a ratio of 2:1 reagent to plasma. Coagulation was also stimulated with the addition of 1 nM α-thrombin (Haematologic Technologies, Inc.) to the 25 mM calcium chloride solution. To determine the contribution of contact activation of the intrinsic pathway to SIS-mediated clotting, clotting times were also measured after plasma had been treated with 50 µg/mL corn trypsin inhibitor, which specifically inhibits contact activation [348]. Fibrin polymerization independent of thrombin activation was measured by adding recombinant batroxobin (ProSpec Bio, final concentration 100 ng/mL) to the $CaCl_2$ solution used to recalcify the plasma.

5.3.4 Glycosaminoglycan Digestion

A number of glycosaminoglycans (GAGs) with anticoagulant properties are known to be present in SIS [325]; however, the relative contribution of these GAGs to the anticoagulant quality of SIS is unknown. To determine the roles of the various GAGs in SIS-mediated anticoagulation, enzymes were used to selectively remove GAGs and characterize the effect on the plasma clotting time. SIS was treated with enzymes that act on hyaluronic acid (hyaluronidase, Sigma), dermatan sulfate (chondroitinase ABC,

Sigma), heparin (heparinase I from *Flavobacterium heparinum*, Sigma), and heparan sulfate (heparinase III from *Flavobacterium heparinum*, Sigma) according to the conditions listed in Supplementary Table S5.1. Following enzymatic removal of the GAGs, the treated SIS was incubated in plasma for 15 min, and conditioned plasma was recalcified with an equal volume of 25 mM $CaCl_2$ to initiate coagulation. Clotting times of plasma samples lacking SIS were used as normalization controls for enzymatic treatments.

5.3.5 Thrombus Formation in a Whole Blood Arteriovenous Shunt

Male baboons (*Papio anubis*) used in this study were cared for at the Oregon National Primate Research Center (ONPRC). Experiments were approved by the ONPRC Institutional Animal Care and Use Committee according to the guidelines of the NIH “Guide for the Care and Use of Laboratory Animals” prepared by the Committee on Care & Use of Laboratory Animals of the Institute of Laboratory Animal Resources, National Research Council (International Standard Book, Number 0-309-05377-3, 1996).

Tubular SIS devices (4 per condition) 4 mm in diameter and 7 cm in length were connected to a baboon arteriovenous femoral shunt (Supplementary Figure S5.1B) in the absence of anti-platelet or anticoagulant therapies [46]. Autologous platelets and allogenic fibrinogen were radiolabeled with ^{111}In and ^{125}I, respectively, and infused into the baboon prior to the shunt study. Blood flow through the SIS device was held constant at 100 mL/min using a clamp downstream of the device. The shunt loop was located above a gamma camera (GE 400T gamma scintillation camera with Nuquest® software) to enable the real-time measurement of platelet accumulation using 5 minute

exposure times over the course of the 60 minute shunt study. Following the shunt study, the grafts were fixed in 10% formalin (Fisher Scientific) and stored at 4°C until the ^{111}In had decayed >10 half-lives, at which point the fibrinogen deposition on the SIS devices was measured using a WIZARD automatic gamma camera (PerkinElmer). Platelet accumulation and fibrinogen deposition were measured on the central 2 cm of the graft to eliminate the potentially confounding effect of increased platelet thrombus formation at the SIS/tubing junctions.

5.3.6 Statistics

All data are reported as the mean ± standard deviation. A one-way ANOVA with Tukey's *post hoc* was used to determine significant differences between groups in the *in vitro* plasma coagulation experiments. A student's t-test was used to determine significant differences between SIS and cSIS in the *ex vivo* whole blood shunt studies. Differences between groups were considered statistically significant if $p<0.05$.

5.4. Theory

The biomaterial small intestinal submucosa has been used for vascular applications with very minimal reports of thrombotic complications. The molecular mechanisms responsible for the observed hemocompatibility are currently not well-defined. SIS contains multiple glycosaminoglycans that are known to exert anticoagulant effects by accelerating serpin-mediated inhibition of coagulation factors in the intrinsic and common coagulation pathways. This study uses multiple coagulation assays, spanning from purified systems to a whole blood ex vivo shunt loop, to determine the predominant coagulation pathways specifically inhibited by SIS. By using a variety of model systems, this work provides a thorough characterization of the

thrombotic response to SIS, which complements the existing work describing the inflammatory and immunologic responses to the material when used for soft tissue applications [10,11]. Furthermore, this work defines the negative effects of carbodiimide-mediated crosslinking, a treatment commonly applied to SIS, on the hemocompatibility of this biomaterial. Knowing the mechanisms by which SIS biomaterials inhibit thrombus formation, as well as identifying the detrimental effect of crosslinking SIS on hemocompatibility, enables the future development of material modifications, including cell capture strategies and protein linkages which alter local cellular responses and coagulation factor activation.

5.5. Results

5.5.1 SIS Tissue Factor Activity

Innovin®, a source of recombinant tissue factor, activated FX in a concentration-dependent manner as expected (Figure 5.1A). In contrast, SIS generated no measurable amount of FXa and was not significantly different from the samples lacking Innovin® ($p>0.05$, one-way ANOVA). Plasma treated with corn trypsin inhibitor to block contact activation of the intrinsic pathway had a clotting time that was similar whether in the presence or absence of cSIS (Figure 5.1B), further demonstrating a lack of tissue factor activity in SIS.

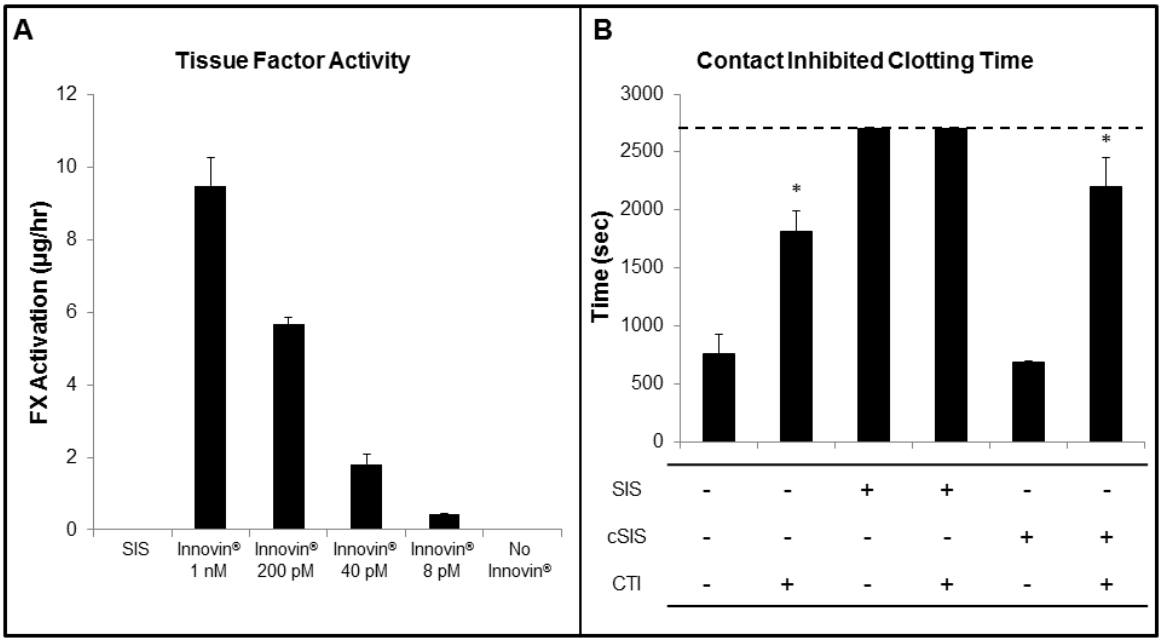

Figure 5.1: Tissue factor activity of SIS and clotting times of plasma treated with corn trypsin inhibitor. (A) Tissue factor activity was measured by quantifying the ability of SIS to activate FX in a solution of FVIIa and FX. FX activation was compared to known concentrations of Innovin® – a recombinant, lipidated tissue factor. SIS demonstrated no measurable tissue factor activity ($p>0.05$, one-way ANOVA with Tukey's *post hoc*, n=3). (B) Corn trypsin inhibitor (50 µg/mL) was added to plasma to inhibit the contact activation of the intrinsic coagulation pathway. Regardless of whether corn trypsin inhibitor was present or absent, plasma clotted at a similar time with and without cSIS. "*" indicates significantly different than plasma only, ($p<0.05$, one-way ANOVA with Tukey's *post hoc*, n=3). Bars reaching the dotted line indicate the samples did not coagulate by the end of the 45 minute (2700 sec) measurement.

5.5.2 Platelet-poor Plasma Coagulation

The PT and APTT are clinical diagnostic assays used to monitor the extrinsic and intrinsic coagulation pathways, respectively. Prolongation of either time indicates a deficiency or inhibition of the respective pathway. Using the standard diagnostic dose of Innovin® for the prothrombin assay, there were no significant differences between native plasma only and plasma with either SIS or cSIS rings in the cuvettes (Figure 5.2A). In contrast, the APTT was significantly prolonged by SIS compared to plasma

only, with a difference between the mean times of 14.3±1.54 seconds (Figure 5.2B). Crosslinking the SIS abrogated APTT prolongation.

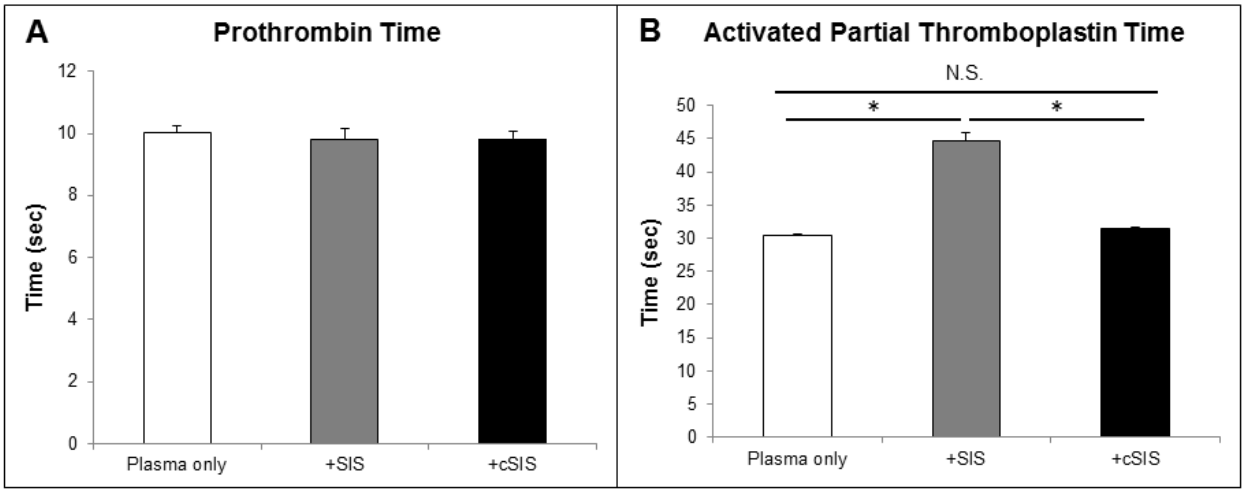

Figure 5.2: Prothrombin time (PT) and activated partial thromboplastin time (APTT) of plasma and plasma with SIS or cSIS. Rings of SIS or cSIS were placed at the bottom of testing cuvettes, and plasma was placed on top of the material. Coagulation was initiated with Innovin® (A), or HemosIL (B). "N.S." indicates no significant difference, while "*" indicates a significant difference between groups (one-way ANOVA with Tukey's *post hoc*, $p<0.05$, $n=4$).

Because of the high concentration of procoagulant stimuli in the APTT and PT reagents, blood clotting times were measured optically to permit lower coagulation stimuli and longer coagulation times. After incubation with SIS for 15 minutes at 37°C, pooled plasma would not coagulate when recalcified (Figure 5.3A). Crosslinking the SIS abrogated this anticoagulant effect. When plasma was stimulated to coagulate with the addition of 1 nM thrombin, plasma incubated with SIS would not coagulate; in contrast, plasma incubated with cSIS coagulated normally (Figure 5.3B). Recombinant batroxobin, a thrombin-like serine protease derived from the venom of *Bothrops atrox*, causes fibrin polymerization similar to thrombin, but unlike thrombin, it is not prone to inactivation by antithrombin or heparin cofactor II [8]. Plasma with either SIS or cSIS did

not alter the time to coagulation when batroxobin was used to stimulate coagulation (Figure 5.3C). Prolonged clotting times can be due to coagulation factor deficiencies, due to adsorption on the biomaterial, or an anticoagulant effector. Mixing factor-deficient plasma 1:1 with normal plasma restores coagulation times to normal levels. Conversely, if an anticoagulant is present in plasma, mixing with normal plasma will not restore coagulation times. Mixing SIS-conditioned plasma 50:50 with native plasma did not restore coagulation times to normal when plasma was recalcified or stimulated with APTT reagent (Figure 5.4), indicating the anticoagulant effect is mediated by a factor released from the SIS rather than coagulation factor depletion resulting from adsorption to the SIS.

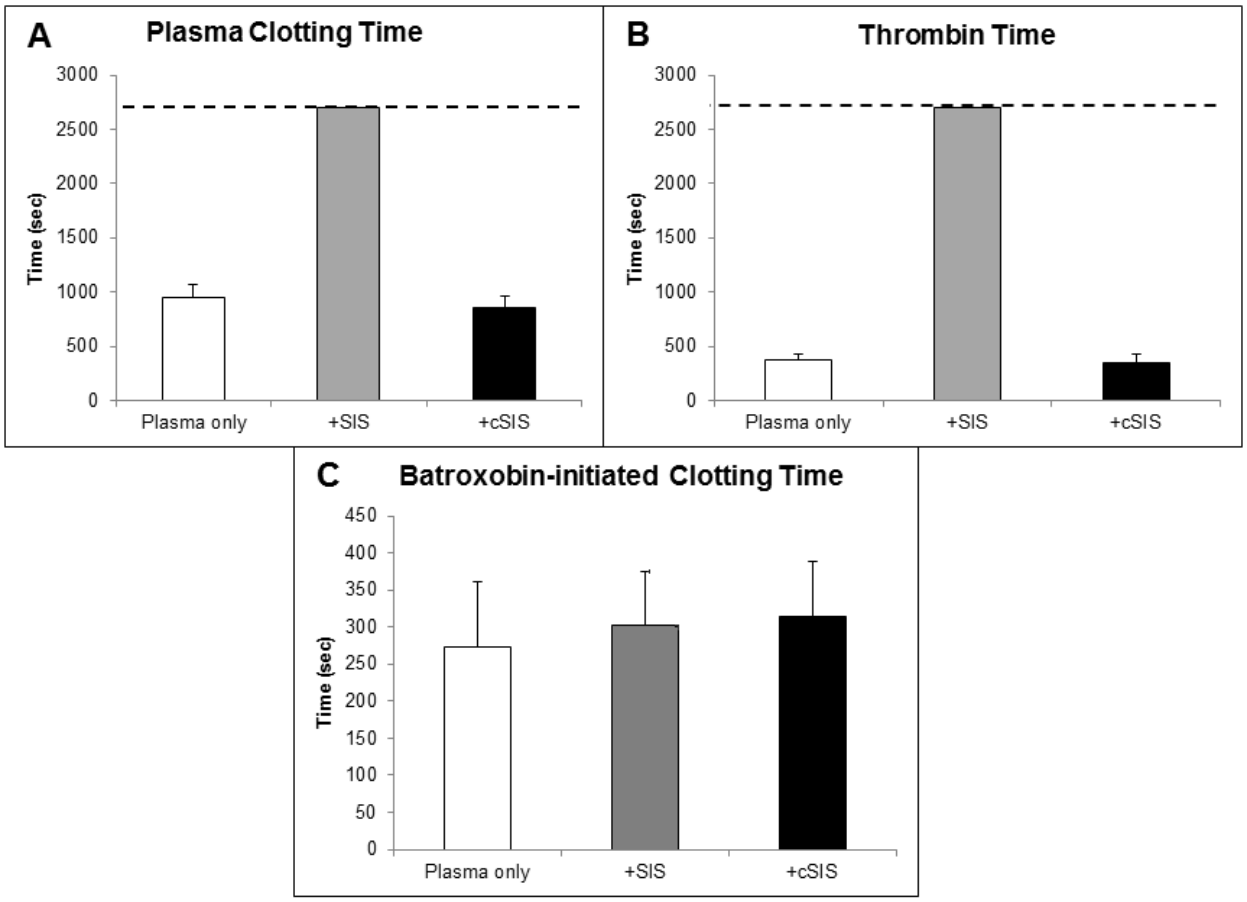

Figure 5.3: Coagulation times of plasma with SIS and cSIS. Plasma was added to well containing SIS, cSIS, or no SIS for 15 minutes at 37°C, and coagulation was initiated either by recalcification with 25 nM $CaCl_2$ (A), 5 pM thrombin and 25 nM $CaCl_2$ (B), or recombinant batroxobin (C). cSIS was not significantly different than plasma lacking SIS for any assay ($p>0.05$, one-way ANOVA with Tukey's *post hoc*, n=3). Bars reaching the dotted line indicate the samples did not coagulate by the end of the 45 minute (2700 sec) measurement.

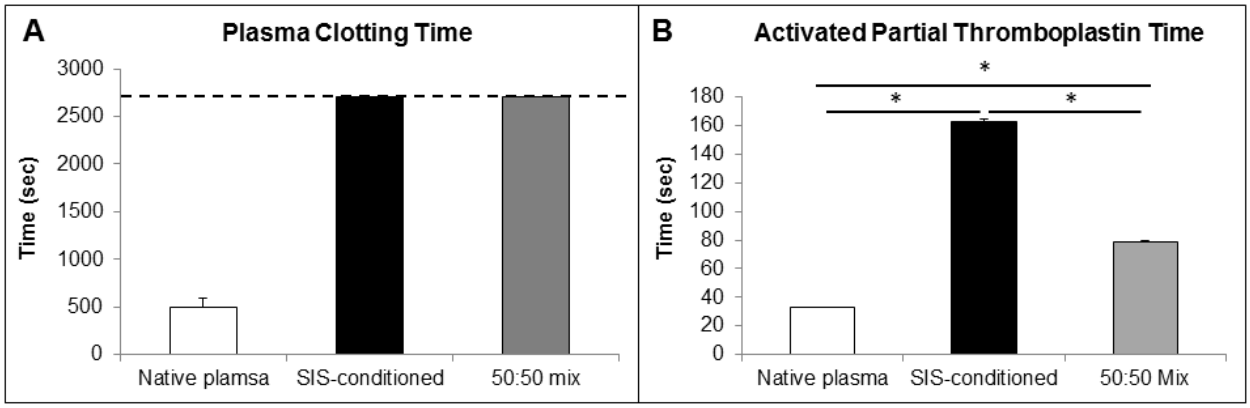

Figure 5.4: Mixed plasma clotting times. Plasma was diluted 1:1 in TBS and stimulated to coagulate by recalcification with an equal volume of 25 mM $CaCl_2$ (A), or APTT reagent (B). The time to coagulation for native plasma, plasma that had been preconditioned with SIS, and a 50:50 mixture of the two were recorded. Bars reaching the dotted line indicate the samples did not coagulate by the end of the 45 minute (2700 sec) measurement. "*" indicates a significant difference between groups (one-way ANOVA with Tukey's *post hoc*, $p<0.05$, n=3.

5.5.3 Platelet Accumulation and Fibrinogen Deposition

To examine thrombus formation on SIS using flowing whole blood, tubular SIS devices were constructed and connected to an *ex vivo* baboon arteriovenous shunt loop. The number of platelets that accumulated on the central 2 cm of the SIS devices peaked at 35 minutes at $4.16\pm1.36 \times 10^8$ platelets per cm^2 (Figure 5.5A), and reduced to $2.49\pm0.52 \times 10^8$ platelets per cm^2 at 60 minutes. In contrast, platelet accumulation continued to increase on cSIS devices for duration of the study, concluding with $9.43\pm1.35 \times 10^8$ platelets per cm^2 at 60 minutes. The average amount of fibrinogen deposited onto the central 2 cm of the SIS devices was 105 µg, which was significantly lower than the cSIS devices that had an average of 628 µg of fibrinogen (Figure 5.5B).

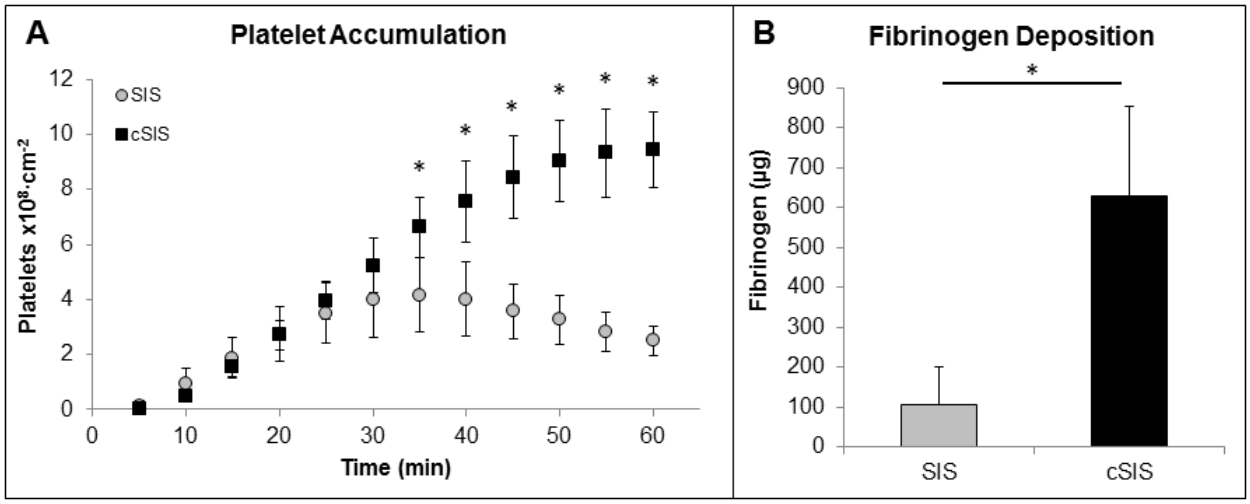

Figure 5.5: Platelet accumulation and fibrin deposition on SIS and cSIS devices. Autologous platelets and allogenic fibrinogen were radiolabeled with ^{111}In and ^{125}I respectively and infused into the baboon prior to the shunt study. Tubular SIS devices were connected to an *ex vivo* baboon arteriovenous shunt loop absent of anticoagulant or anti-platelet therapies. Real-time platelet accumulation was measured using a gamma camera (A), and end-point fibrinogen deposition was measured after the ^{111}In had decayed > 10 half-lives (B). "*" indicates significantly different from SIS devices, $p < 0.5$ using a Student's T-test, n = 3-4.

5.5.4 Glycosaminoglycan Digestion

SIS contains a variety of glycosaminoglycans; notably, a number of these confer anticoagulant activity by increasing serpin-mediated inhibition of FXa and/or thrombin [90,349]. To identify the molecular constituents of SIS responsible for anticoagulant activity, SIS was digested with various enzymes to selectively remove various glycosaminoglycans. Following digestion with the enzymes heparinase I and heparinase III, SIS no longer prolonged plasma coagulation on SIS (Figure 5.6), resulting in clotting times similar to native plasma and cSIS-treated plasma. However, treatment with chondroitinase ABC (capable of digesting dermatan sulfate) or hyaluronidase did not inhibit SIS anticoagulant activity.

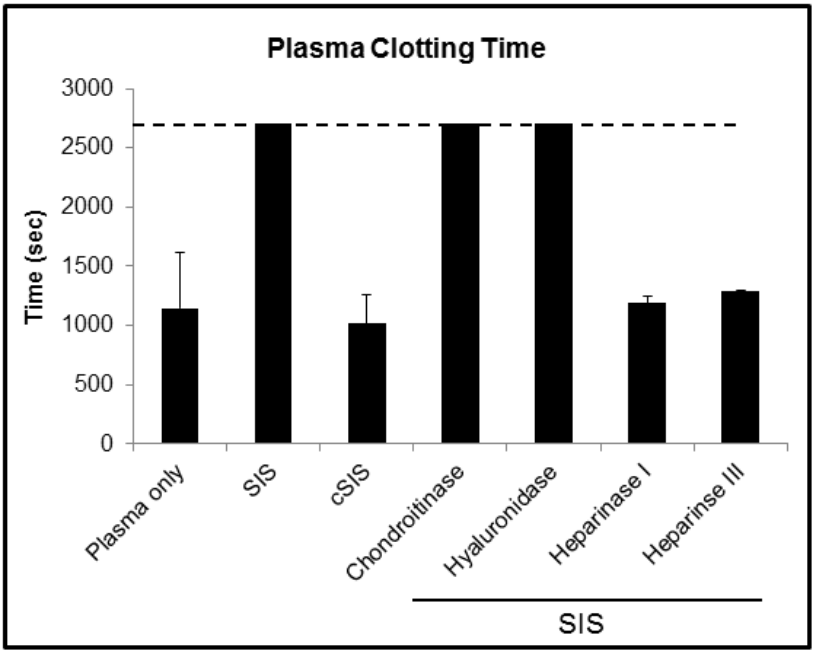

Figure 5.6: Plasma clotting time following enzymatic removal of GAGs. After treating SIS with various enzymes to remove glycosaminoglycans, coagulation of SIS-conditioned plasma was initiated with an equal volume of 25 mM $CaCl_2$. Bars reaching the dotted line indicate the samples did not coagulate by the end of the 45 minute (2700 sec) measurement. Plasma only, as well as plasma incubated with cSIS, heparinase I-treated SIS, and heparinase III-treated SIS were not significantly different ($p>0.05$, one-way ANOVA with Tukey's *post hoc*, n=3).

5.6 Discussion

The decellularized matrix SIS has been utilized as a biomaterial scaffold for many different applications. The prevalent use of SIS in soft tissue reconstruction has resulted in the extensive study of the inflammatory and immune responses to SIS. Carbodiimide-mediated crosslinking of SIS has also been performed to alter the mechanical properties of the material, augment the degradation rate, and functionalize the material with biological molecules [333,340,350]. Recently, SIS has been incorporated into cardiovascular tissue engineering and devices, and in at least one of these cases SIS was carbodiimide-crosslinked [337]. Gross analyses of SIS-based vascular grafts have indicated a lack of thrombus formation [335,336]. To determine the mechanisms of these observations, this work provides a comprehensive characterization of SIS

interactions with blood and blood components that utilizes multiple pro-coagulants to stimulate plasma coagulation, including flowing whole blood absent of anticoagulants, and additionally identifies heparin and heparan sulfate as the predominant anticoagulant effectors. This work agrees well with the existing literature on SIS-based cardiovascular devices and provides a more mechanistic understanding of the ability of SIS to inhibit thrombus formation and the effect of carbodiimide-mediated crosslinking on hemocompatibility.

In native vessel hemostasis and thrombosis, it is generally considered that the extrinsic pathway is the initiator of thrombus formation via tissue factor expression on disturbed vascular endothelium [351]. The extrinsic pathway is responsible for the initial generation of a small amount thrombin, which subsequently triggers local platelet activation. SIS demonstrated a lack of tissue factor activity (Figure 5.1), defined as the ability to activate FX in a solution of FVIIa and FX. Additionally, cSIS failed to accelerate coagulation when the contact activation was inhibited, further supporting a lack of tissue factor activity. This agrees with past work, showing that tissue factor is generally associated with cells rather than the extracellular matrix [352], and indicates that tissue factor was not released into the SIS during the decellularization process. *In vivo*, once a small amount of thrombin is generated, the intrinsic pathway then becomes the dominant means of FXa and thrombin generation [25]. However, because biomaterials, such as SIS, lack tissue factor and have surface properties different from that of the native vascular endothelium, the intrinsic contact activation pathway may play a more dominant role in biomaterial-mediated thrombosis, though this is controversial [30,32]. The PT and the APTT are two widely-used assays used to identify deficiencies of the

extrinsic and intrinsic coagulation pathways, respectively. Using the standard diagnostic concentration of Innovin® (recombinant, lipidated tissue factor), the PT was not affected by the inclusion of SIS or cSIS (Figure 5.2). In contrast to the PT, inclusion of SIS significantly prolonged the APTT by 14.3±1.54 seconds, indicating inhibition of the intrinsic coagulation pathway. Conversely, cSIS did not significantly alter the APTT. Digestion of the SIS with enzymes that target various GAGs demonstrated that removal of heparin, but not dermatan sulfate or hyaluronic acid, eliminated the anticoagulant effect of SIS. This result is consistent with a prolongation of the APTT, as this assay is known to be particularly sensitive to heparin anticoagulation [342].

The supra-physiological concentrations of pro-coagulant stimuli in the PT and APTT assays enable rapid testing for the clinical setting; however, it also greatly reduces the sensitivity to anticoagulants and factor deficiencies, as evidenced by the need for extrinsic and common pathway coagulation factors (VII, X, V, prothrombin) to be below 50% of normal to result in a prolonged PT [342]. Therefore, fibrin polymerization was measured optically using low concentrations of pro-coagulant stimuli to initiate coagulation of plasma in SIS-containing wells [343]. When plasma coagulation was initiated by recalcification, as well as when stimulated by the pro-coagulant effectors thrombin (1 nM) or diluted Innovin® (~0.1 pM final tissue factor concentration), plasma with SIS had significantly prolonged coagulation times compared to native plasma (Figure 5.3). Thus, optical measurement of coagulation revealed that SIS can inhibit tissue factor-initiated coagulation at low tissue factor concentrations but not at the higher concentrations used in the clinical hemostasis assays (i.e. Figure 5.2). This result is consistent with heparin anticoagulant activity which acts on common pathway

coagulation factors (FXa and thrombin) to inhibit coagulation, and also indicates a threshold where high concentrations of tissue factor can overcome this anticoagulant activity. The clinical definition of a coagulation factor deficiency is when a prolonged APTT can be corrected by mixing the patient's plasma 1:1 with a standard reference plasma [344]. Conversely, failure to restore the APTT to normal indicates the presence of an inhibitor. Because a 1:1 mixture may not be sensitive to detect weak or low concentrations of inhibitors, a 4:1 ratio of patient to standard plasma may be used and the mixed plasma may be incubated for up to 120 minutes to permit inhibitor activity [353]. In this work, SIS conditioned plasma was mixed 1:1 with normal plasma and used immediately, thus using the least sensitive diagnostic conditions to detect coagulation inhibitors. This procedure resulted in a significantly prolonged APTT (Figure 5.4), indicating the presence of a potent anticoagulant.

Thrombus formation is a dynamic process in whole blood that depends on the transport of cells and factors to the developing thrombus. Flowing blood is therefore necessary to account for the transport dynamics of thrombogenesis as well as shear-dependent platelet accumulation [22]. The *ex vivo* baboon arteriovenous shunt allows whole blood absent of anticoagulant or anti-platelet agents to flow across devices in a controlled manner. After 1 hour of blood flow, SIS devices demonstrated significantly lower platelet accumulation and fibrinogen deposition than cSIS devices. This result corresponds well with the *in vitro* coagulation assays performed in this study, as well as the existing literature that describe minimal thrombus formation on SIS vascular grafts [335,336]. Additionally, the SIS grafts averaged a peak platelet accumulation at 35 minutes, with decreasing numbers of adhered platelets from 40-60 minutes. This result

suggests fibrinolysis and loss of fibrin-bound platelets occurring during this time, and suggests minimal thrombus buildup on the devices at longer time periods. In contrast, platelet accumulation on cSIS devices continued to rise throughout the duration of the study, though the rate of accumulation had slowed by 60 minutes (Supplemental figure S5.3). Similar to the platelet accumulation results, fibrinogen deposition at 60 minutes was also significantly higher on cSIS grafts than on SIS grafts. Platelet accumulation on cSIS per unit surface area is similar to previous results with expanded polytetrafluoroethylene (ePTFE) vascular grafts with 4 mm internal diameter (0.943 platelets x $10^9/cm^2$ in this study vs. ~0.87 platelets x $10^9/cm^2$ historically) [354,355]. Although no cSIS devices occluded by 60 minutes, the continual increase in platelet accumulation indicates a risk of eventual occlusion.

Ex vivo arteriovenous shunt experiments were performed to characterize thrombus formation on SIS-based devices in flowing whole blood absent of anticoagulant and anti-platelet therapies to simulate the conditions of vascular devices, such as stents and grafts, in which SIS is being employed. Although this model does not directly measure platelet activation, prior work with this model has determined that reduced platelet accumulation in this shunt model is associated with reduced platelet activation. Specifically, clopidogrel at low-dose (0.2 $mg \cdot kg^{-1}$ for 6 days) significantly reduced platelet and fibrinogen accumulation on vascular grafts and stents, and the addition of aspirin therapy (10 $mg \cdot kg^{-1} \cdot day^{-1}$) further decreased platelet accumulation and fibrinogen deposition [356]. These studies demonstrate that platelet and fibrinogen accumulation in this shunt system is sensitive to inhibition of platelet activation by both ADP and thromboxane A_2. In addition to activation, platelet accumulation in the shunt

model is also dependent on platelet adhesion molecule expression [48] and activated protein C levels [49]. Therefore, platelet accumulation in this arteriovenous shunt model provides a metric that is dependent on multiple pathways of thrombus formation, thus providing a metric of overall thrombogenicity but lacking direct insight on the mechanism or extent of platelet activation. Future studies may investigate the mechanisms of platelet activation and adhesion on SIS and cSIS.

In all experiments in which SIS exerted an anticoagulant effect, crosslinking the SIS with a carbodiimide consistently eliminated the anticoagulant activity. Coagulation times for plasma with cSIS were similar to plasma alone in both clotting time following recalcification as well as recalcification with inhibition of contact inhibition; furthermore, cSIS demonstrated similar platelet accumulation as previous work with the inert material ePTFE. Thus, crosslinking essentially abolished all biological activity of the SIS with regard to blood-material interaction. Carbodiimides react with free carboxyl groups to enable a reaction with hydroxyl groups and form an amide bond. The GAGs have many free carboxyls, and the collagens have both carboxyl and primary amine groups in their molecular structure and thus could participate in the crosslinking. GAGs known to be in SIS, including heparin, heparan sulfate and dermatan sulfate, are all known to exert anticoagulant effects by enhancing serpin-mediated inhibition of thrombin and FXa [90,325,349]. However, only heparinase I and heparinase III treatment of SIS resulted in a reduction in anticoagulant activity, suggesting that heparin and/or heparan sulfate are the dominant anticoagulant GAGs in SIS, and that glycosaminoglycan crosslinking, which may result in entrapment or chemical alteration of the glycosaminoglycan molecules, is the predominant mechanism by which carbodiimide treatment abrogated

the intrinsic anticoagulant activity of SIS. The loss of heparin due to washing away of heparin during the crosslinking process is unlikely, as SIS washed overnight in buffer retained anticoagulant activity, though incubation in plasma eliminated anticoagulant activity (Supplementary Figure S5.4). Plasma is known to have heparinase enzymes [357,358], giving addition support to the hypothesis that heparin/heparin sulfate are responsible for the anticoagulant effects. Whereas heparinase I cleaves heparin and heparan sulfate at a 3:1 relative activity, heparinase III is generally considered to have a high specificity for heparan sulfate[52]; therefore, the reduction in anticoagulant activity following heparinase III treatment suggests heparan sulfate is the dominant anticoagulant GAG.

Prior work has demonstrated crosslinked SIS to have slower cellular infiltration and an increased inflammatory response [333]. Although crosslinking may be advantageous for increasing the mechanical robustness of SIS, the additional effects on hemocompatibility and inflammatory response may ultimately reduce the clinical utility of the modification in cardiovascular applications such as a vascular graft. The detriment of crosslinking to anticoagulant activity may be overcome by the addition of exogenous heparin during the crosslinking procedure.[334] The addition of exogenous heparin or other anticoagulants, as well as other molecules to enable capture of specific circulating cells or enhance endothelialization, are potential modifications to the crosslinking procedure that may overcome the detriments to hemocompatibility. Novel modifications to SIS and cSIS to have more favorable hemocompatibility or re-endothelialization are areas that could be explored for designing SIS-based cardiovascular devices.

5.7 Conclusion

This study investigated the hemocompatibility of SIS and carbodiimide crosslinked SIS using an array of assays from individual coagulation factor activation, plasma coagulation, and an *ex vivo* shunt with flowing whole blood. These analyses provide a more in-depth characterization of thrombus formation on SIS and cSIS that agrees with and builds upon existing literature describing histological observations of SIS-based cardiovascular devices. Our results indicate that SIS possesses intrinsic anticoagulant activity due to the presence of heparin/heparan sulfate that confers excellent hemocompatibility; however, crosslinking SIS eliminates this anticoagulant activity and facilitates significant thrombus formation on the material.

GAG Enzyme	**Solution (50 µL)**	**Incubation time**
Hyaluronidase	48 µL 0.1 M acetate buffer (pH 5.5) 2 µL Hyaluronidase (1U/µL)	2 hours
Chondroitinase ABC	48 µL of 50 mM Tris, 60 mM acetate, 1 mM EDTA and 0.02% BSA (pH 8.0) 2 µL Chondroitinase ABC (0.5 U/µL)	2 hours
Heparinase I	49 µL TBS containing 4mM $CaCl_2$ and 0.1 mg/mL BSA in TBS 1 µL Heparinase I (1 U/µL)	2 hours
Heparinase III	49 µL buffer containing 4mM $CaCl_2$ and 0.1 mg/mL BSA in TBS 1 µL Heparinase III (1 U/µL)	2 hours

Supplementary Table S5.1: Reaction conditions for enzymatic digestion of glycosaminoglycans (GAGs). SIS was treated with various enzymes according to the chart above to remove GAGs known to exert anticoagulant effects. All reactions were performed at 37°C.

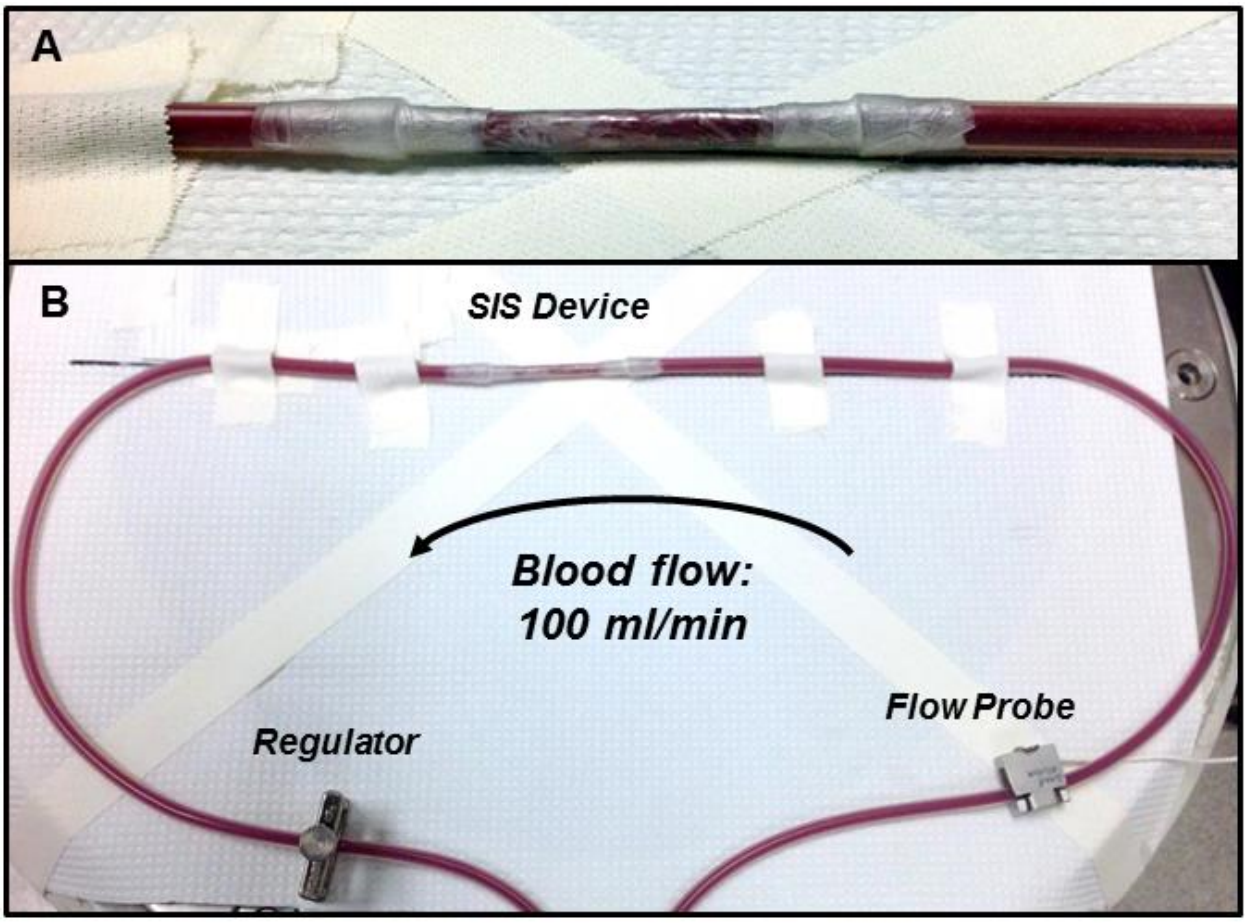

Supplementary Figure S5.1: *Ex vivo* baboon arteriovenous shunt loop. Tubular SIS devices with 4 mm internal diameter (A) were constructed and connected to an *ex vivo* baboon arteriovenous shunt loop (B). Blood flow rate was measured using an ultrasonic flow probe, and maintained at 100 mL/min using a clamp downstream of the device.

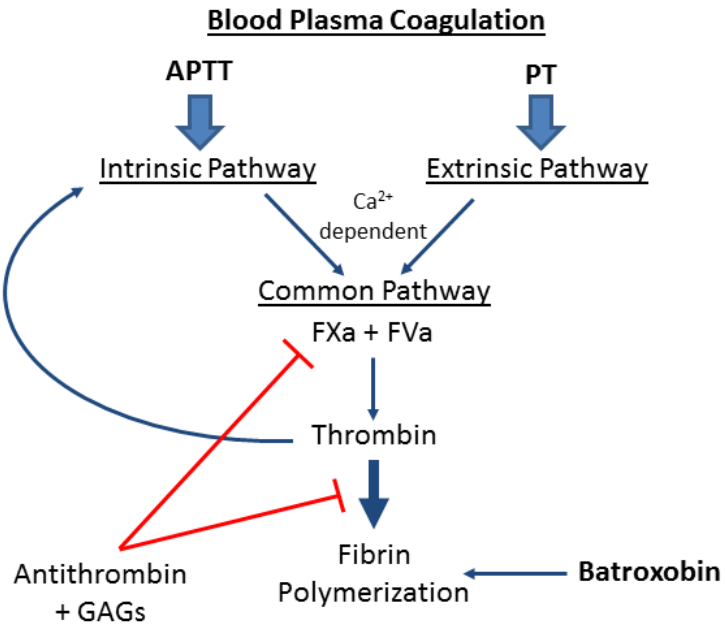

Supplementary Figure S5.2: Simplified diagram of plasma coagulation and coagulation assay reagents. The activated partial thromboplastin time (APTT) reagent contains pro-coagulant surfaces to stimulate coagulation via the intrinsic (contact) pathway. The prothrombin time (PT) reagent contains a high concentration of tissue factor to stimulate the extrinsic (tissue factor) pathway. The common pathway activates thrombin via Factor Xa (FXa) and FVa. Calcium is required for the intrinsic and extrinsic pathways to activate FX in the common pathway. Batroxobin polymerizes fibrin independent of thrombin activity. Glycosaminoglycans (GAGs) significantly increase the antithrombin-mediated inhibition of FXa and thrombin.

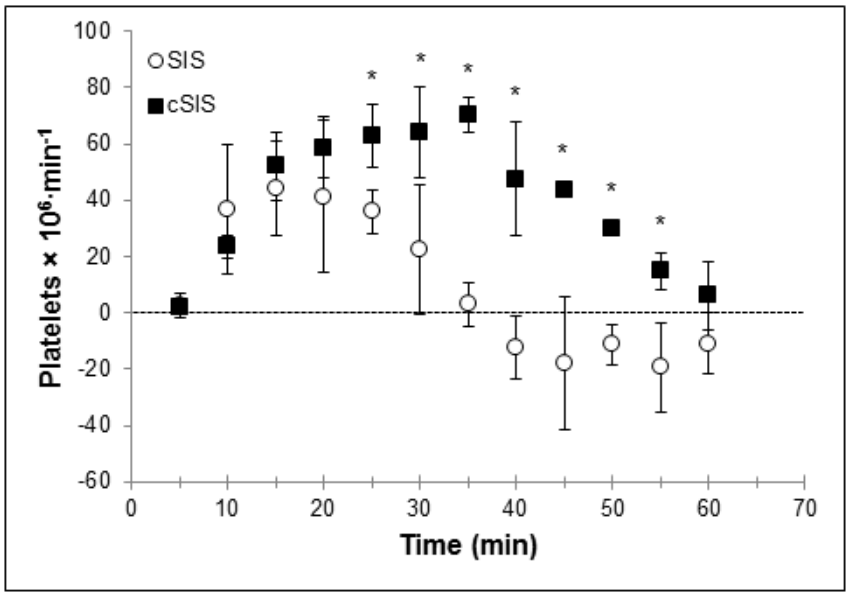

Supplementary Figure S5.3: Rate of platelet accumulation on SIS and cSIS. The number of platelets adhered on tubular SIS and cSIS devices was measured every five minutes. The difference in the number of platelets between 5 minute measurements was calculated and divided by 5 to yield the change in platelets per minute. "*" = $p < 0.5$ vs. unmodified SIS using a Student's T-test, n = 3-4.

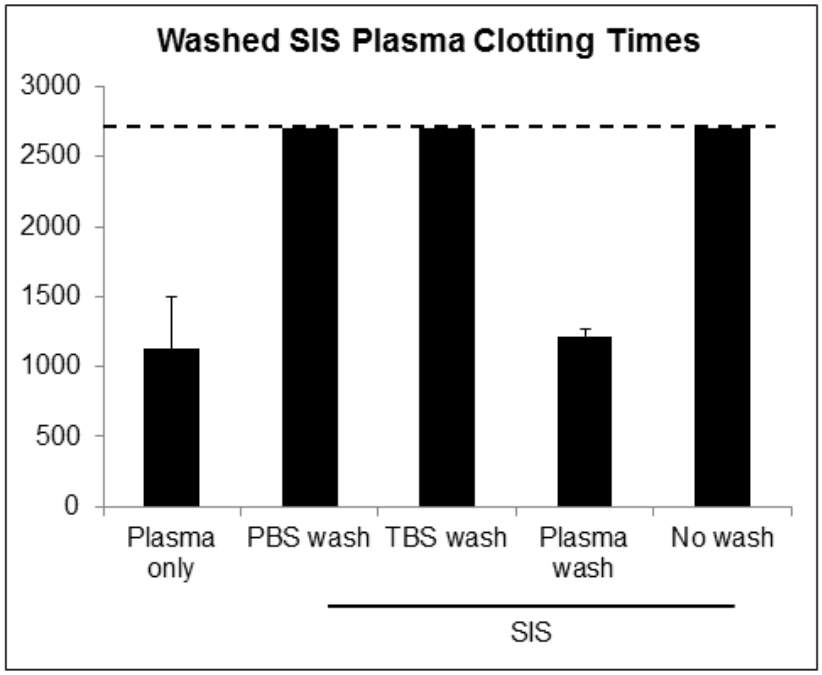

Supplementary Figure S5.4: Residual anticoagulant activity of SIS. SIS was incubated overnight at room temperature in either plasma or buffer solutions (PBS or TBS). After washing, SIS that had been in plasma did not prolong blood coagulation. However, SIS that had been stored in buffer maintained anticoagulant activity.

CHAPTER VI: Thrombomodulin-modified decellularized small intestinal submucosa

6.1 Abstract

Current materials used in vascular applications are selected to be non-reactive towards blood. In contrast, bioactive modifications can be applied to vascular materials to interact with blood proteins and modulate both the local cellular and thrombotic responses. Decellularized matrix derived from porcine small intestinal submucosa (SIS) is a biomaterial being investigated for novel vascular applications including a small diameter vascular graft and an artificial venous valve. This work incorporates the endothelial cell membrane protein thrombomodulin to determine the effects on blood plasma coagulation, platelet adhesion and the generation of activated protein C (APC). Modifying SIS with thrombomodulin enabled APC generation and significantly prolonged plasma coagulation initiated from the material surface, indicating anticoagulant activity. Thrombomodulin activity was still present on modified SIS following 12 hours of flow, overnight drying, or 90 minutes of incubation in blood plasma. When SIS devices were inserted into an *ex vivo* baboon arteriovenous shunt, TM modification did not reduce thrombus formation. The anti-thrombotic activity of APC generated by TM-SIS may be more potent under venous flow conditions.

6.2 Introduction

Decellularized extracellular matrices have been widely used as biomaterial scaffolds for reconstructing tissues due to their topographical and biochemical cues that help coordinate proper cellular function. One decellularized matrix widely used for soft tissue repair is derived from porcine small intestinal submucosa (SIS) [237]. In addition to soft tissue repair, SIS has been utilized in cardiovascular applications including vascular grafting [335,336,360,361], stent coverings [338], pulmonary valve reconstruction [362,363], and venous valve replacement [257,259]. In these blood-contacting applications, the primary function of the SIS is to serve as a non-thrombogenic surface while also facilitating endothelialization, as the development of a confluent endothelium is a key facilitator of long-term thromboprotection [207]. In some of these applications, for example a large diameter vascular graft implanted in the infrarenal aorta of dogs, SIS facilitated endothelialization and remodeling while remaining patent [335,360]. However, in applications more prone to thrombosis, such as a venous valve prosthesis, thrombus formation and neointimal ingrowth on SIS resulted in thickened and immobile leaflets. Strategies to rapidly endothelialize SIS leaflets, either through seeding prior to implantation or by using immobilized capture antibodies to bind circulating endothelial progenitor cells, did not show significant reduction in detrimental remodeling [364]. Thus, strategies that do not require rapid endothelialization to reduce thrombus formation and intimal hyperplasia on SIS should be explored as alternative approaches.

To advance the development of SIS as a cardiovascular biomaterial, this work employs a novel modification to SIS in an attempt to limit thrombus formation on SIS

(Figure 6.1). Thrombus formation on blood-contacting materials is caused by the activation of the intrinsic and extrinsic coagulation cascades which results in conversion of the circulating zymogen prothrombin to the active enzyme thrombin at the blood-material interface. Thrombin is the central enzyme in coagulation and promotes thrombus formation by activating platelets and cleaving fibrinogen to generate a fibrin thrombus. To counteract these processes, the vascular endothelial cell surface protein thrombomodulin binds circulating thrombin and blocks the binding of fibrinogen while simultaneously acting as a cofactor to enhance APC generation by thrombin [365,366]. APC functions as an anticoagulant by proteolytically degrading coagulation factors necessary for the prothrombin to thrombin conversion, as well as inhibiting the intrinsic coagulation pathway, which is necessary for accelerating thrombin generation to a concentration needed for thrombosis [25,367]. In addition to anticoagulant effects, APC attenuates inflammation-induced endothelial apoptosis to maintain endothelium-dependent regulation of thrombosis and vascular smooth muscle proliferation [60,65]. Thus, thrombomodulin and APC act through multiple pathways to limit the processes central to SIS-mediated thrombosis.

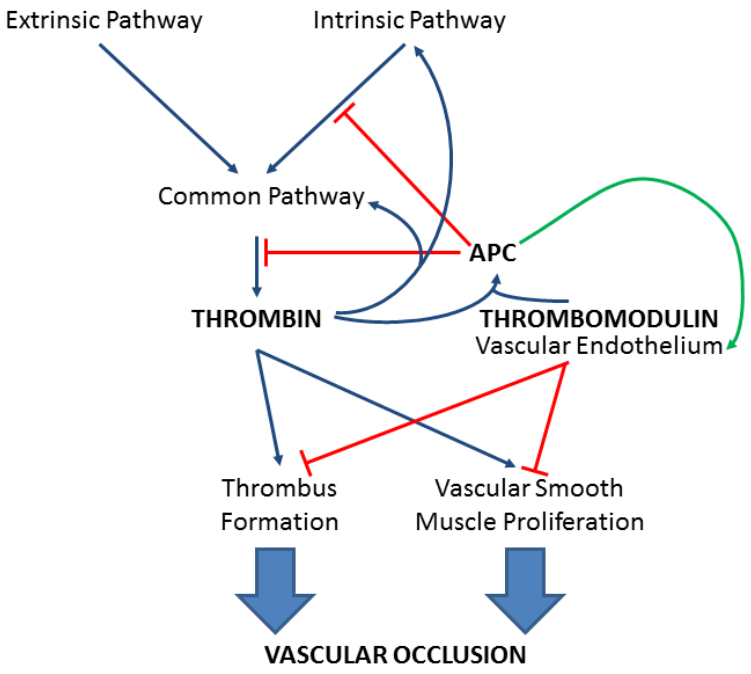

Figure 6.1: Role of thrombin, thrombomodulin and APC thrombosis. Blue arrows represent an activating role, red arrows represent an inhibitory role, and the green arrow represents a protective role, specifically against inflammation-induced apoptosis. APC inhibits processes contributing to thrombosis by inhibiting thrombin activation and the downstream effects, as well as by protecting proper vascular endothelial function. Thrombomodulin, expressed on the vascular endothelium, is the key catalyst for APC generation.

6.3 Materials and Methods

6.3.1 Reagents

Vacuum-pressed SIS was generously provided by Cook Biotech. Thrombomodulin, protein C, α-thrombin, and APC were from Haematologic Technologies. Heparin sodium solution was from Sigma Aldrich. Baboon platelet poor plasma from at least 5 animals was pooled using previously collected aliquots that had been stored at -80°C. The prothrombin time (PT) reagent Innovin® was purchased from Dade®, and the activated partial thromboplastin time (APTT) reagent HemosIL® was from Instrumentation Laboratories. The chromogenic substrate S-2366 used for APC quantification was from Chromogenix. Baboon carotid endothelial cells (ECs) were

isolated as described previously [283,301]. Baboon ECs were cultured in endothelial growth medium-2 (EGM-2) from Lonza, supplemented with the MV BulletKit and 10% fetal bovine serum (FBS, HyClone). Phosphate buffered saline (PBS) with Ca^{2+} and Mg^{2+} was from Corning.

6.3.2 Thrombomodulin Modification

Thrombomodulin was diluted in tris-buffered saline (TBS; 50 mM Tris-Cl, 150 mM NaCl, pH 7.5) at a concentration of 4 µg/mL unless otherwise noted. For all assays except mechanical coagulation assays and the baboon arteriovenous shunt, SIS was cut into 5 mm discs using a biopsy punch and placed into wells of a 96-well plate. Discs were soaked in thrombomodulin solution or TBS for 2 hrs. Adsorption was chosen as the surface modification strategy because prior work demonstrated that carbodiimide-mediated crosslinking of SIS reduced the hemocompatibility [368].

6.3.3 APC Generation

Following modification of SIS, punches were washed 3 times in PBS with Ca^{2+} and Mg^{2+}, followed by a 1 hr reaction in a solution of protein C (100 nM) and thrombin (5 nM) at 37°C. After the reaction, two replicates per sample were removed and placed into wells containing the direct thrombin inhibitor hirudin (final conc. 1 µM) to quench the reaction. The APC concentration was determined by adding the chromogenic substrate S-2366 and using a plate reader (Tecan Infinite m200) to measure the maximal rate of change in absorbance at 405 nm over 20 minutes. A well containing protein C and thrombin only (i.e. no thrombomodulin) was used to determine the background APC concentration, and this was subtracted from all measurements. To quantify APC

generated by TM-SIS, samples were compared to a standard curve of known APC concentrations.

6.3.4 In Vitro *Stability*

Preliminary measures of the stability of TM activity on modified SIS were assessed using *in vitro* methods. To determine the stability of TM activity under flow, a square of modified SIS (10 mm x 10 mm) was placed into a GlycoTech flow chamber with flow chamber dimensions of 0.254 mm height x 5 mm wide. A syringe pump was used to drive PBS over the SIS for 12 hours with a wall shear rate of 50 sec^{-1}. The APC generation of TM-SIS post-flow was compared to SIS that had been kept in PBS under static conditions for the duration of flow. To determine if TM-SIS could be dried and maintain activity, the stability of thrombomodulin activity following a 24 hour drying was determined by comparing APC generation of the dried SIS to samples of freshly-modified SIS. The stability of SIS in plasma was determined by incubating 5 mm diameter discs of TM-SIS in baboon pooled plasma for times ranging from 5-90 minutes at 37°C. After incubation in plasma, discs of SIS were washed with PBS and the APC generation was compared to freshly-modified SIS.

6.3.5 Coagulation Assays

Mechanical

Two assays used clinically to monitor anticoagulant dosing or to identify coagulation factor deficiencies are the activated partial thromboplastin time (APTT) and the prothrombin time (PT), which identify inhibition or deficiency of the contact and tissue factor pathways, respectively. In this study, these assays were performed with normal plasma in cuvettes with SIS in an attempt to measure the anticoagulant activity

of the TM modification. SIS was cut into rings with an 8 mm outer diameter and a 4 mm inner diameter using biopsy punches. Rings of SIS were placed into cuvettes for use in the KC1 Delta (Tcoag). The APTT and PT assays were then performed as would be done diagnostically, but with the addition of a SIS ring placed in the bottom of the cuvette. 100 µl platelet poor plasma (as well as 100 µL HemosIL® for the APTT only) was placed into rotating cuvettes containing a steel bearing over a ring of SIS and incubated for 3 minutes. Then, either 100 µl of 25 mM $CaCl_2$ for the APTT or 200 µl of Innovin® for the PT was added to the cuvette and the time to coagulation was automatically measured by the KC1 when fibrin polymerization disrupted the motion of the steel bearing.

Optical

The PT and APTT reagents utilize high concentrations of pro-coagulants to enable rapid coagulation times for clinical diagnostics; however, these assays are not sensitive to subtle anticoagulant activity. For instance, the PT assay requires >50% inhibition or depletion of extrinsic pathway factors to result in a significantly prolonged clotting time [342]. Furthermore, the assays are more sensitive to anticoagulant activity in the bulk of the plasma (i.e. from systemic anticoagulation in a patient) rather than surface-mediated anticoagulant effects [369]. Therefore, to permit the use of lower concentrations of pro-coagulant stimuli, coagulation was measured optically using a plate reader [343]. Two different methods of initiating coagulation were used. In the first strategy, 5 mm diameter discs of modified SIS were placed into 96 well plates, followed by 50 µl of plasma and 100 µL of either PT or APTT reagent diluted in 25 mM $CaCl_2$ (1:2000 for the PT and1:20 for the APTT). Plates were immediately transferred to a

plate reader pre-warmed to 37 °C and coagulation was monitored optically by measuring the absorbance at 405 nm every 20 sec. The time at which the absorbance increased 20% from baseline value was considered to be the time of coagulation. Absorbance measurements were stopped at 45 min. Alternatively, coagulation was initiated at the SIS surface by soaking discs of modified SIS for 1 hr with pro-coagulant reagents used for the APTT or the PT diluted in TBS for 1 hr (1:100 for the PT and 1:1 for the APTT). The SIS discs were then washed 3 times with TBS, and 50 µl of plasma was added. Immediately after addition of the plasma, 100 µl of 25 mM $CaCl_2$ was added, and the plasma coagulation was monitored optically. To verify that altered coagulation times following modification of SIS was due to TM activity and not due to pre-adsorption of protein resulting in reduced pro-coagulant adsorption, non-specific proteins IgG or bovine serum albumin (BSA) were used to modify SIS instead of thrombomodulin at concentrations 5 times greater than thrombomodulin (i.e. 20 µg/ml). These non-specific proteins did not prolong coagulation compared to unmodified SIS (Supplemental Figure S6.1).

6.3.6 Baboon Ex Vivo Arteriovenous Shunt

Thrombus formation *in vivo* is governed by the transport of blood cells and proteins to and away from the developing thrombus[43]. To incorporate blood flow-dependent reactions into our hemocompatibility evaluation, we utilized a baboon femoral arteriovenous shunt that allows whole blood to flow across devices in the absence of anticoagulant or anti-platelet therapies [46,205,266]. Prior to each study, autologous ^{111}In-labeled platelets and allogenic ^{125}I-labeled fibrinogen were infused into the baboon. Tubular SIS devices (4 mm dia, 5 cm long) were connected to the shunt

loop and placed over a gamma camera (GE 400T gamma scintillation camera with Nuquest® software) for real-time measurement of platelet accumulation on the SIS devices. Following the 60 minute study, SIS devices were placed in 10% formalin and stored at 4°C until the ^{111}In had decayed >10 half-lives, at which point ^{125}I-labeled fibrinogen deposition was measured using a WIZARD automatic gamma counter (PerkinElmer). Platelet accumulation and fibrinogen deposition were measured on the central 2 cm of the graft to eliminate the potentially confounding effect of increased platelet accumulation at the connectors used to join the SIS device and shunt tubing. For each condition, 4 tubular SIS devices were tested.

6.3.7 Statistics

All data are reported as the mean ± standard deviation. Significant differences between groups were determined using a one-way ANOVA with Tukey's *post hoc* analysis. Differences between groups were considered statistically significant if $p<0.05$.

6.4 Results

6.4.1 Thrombomodulin-modified SIS Generates APC

Modifying SIS with thrombomodulin catalyzed APC generation in a solution of protein C and thrombin (**Figure 6.2**). APC generation increased with greater concentrations of thrombomodulin, though no further increase in catalytic activity was seen at concentrations over 2 µg/ml. All future experiments with TM-SIS were done with a thrombomodulin concentration of 4 µg/ml. To compare the quantity of APC generated by TM-SIS to endothelial cells, baboon carotid ECs were cultured to confluence in a 96 well plate, and the APC generation assay was performed in parallel on these cells and with 5 mm diameter discs of SIS also in wells of a 96 well plate. Normalizing the APC

generated to that of the endothelial cells, TM-SIS generated 5.46 ± 1.00-fold greater APC than the cells.

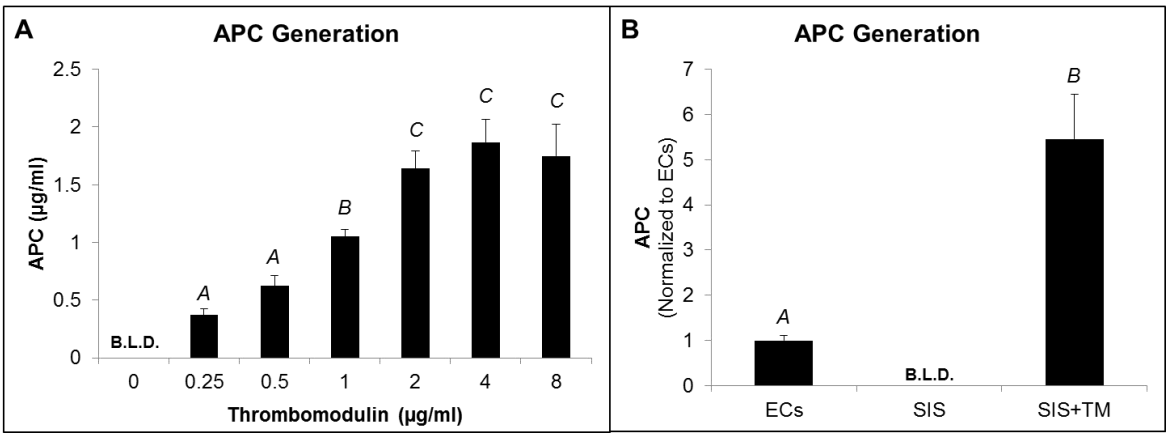

Figure 6.2: APC Generation of TM-SIS. (A) The quantity of APC generated by TM-SIS increased with increasing concentrations of thrombomodulin solution up to 2 µg/mL. (B) The APC generated by a 5 mm disc of SIS in a 96-well plate was approximately 5.5-fold greater than a confluent layer of baboon carotid ECs in a 96 well plate. "B.L.D.", below limit of detection. Letters indicate homogenous subsets based on a one-way ANOVA and Tukey's *post hoc,* n=4 (A) and n=3 (B).

6.4.2 In Vitro *Stability*

Following 12 hours of flow with a shear rate of 50 sec^{-1}, the APC generated by TM-SIS activity decreased from 260.2 ± 23.8 ng/cm^2 to 103.0 ± 79.0 ng/cm^2. Dried TM-SIS retained TM activity, though APC generation decreased from 263.5 ± 40.2 ng/cm^2 to 131.1 ± 24.4 ng/cm^2. After incubation in plasma, TM-SIS decreased in activity by approximately 48%; however, no further loss in TM activity was observed over 90 minutes (Figure 6.3). Based on these results, future studies with TM-SIS used freshly-modified SIS that was kept hydrated until the time of the experiment.

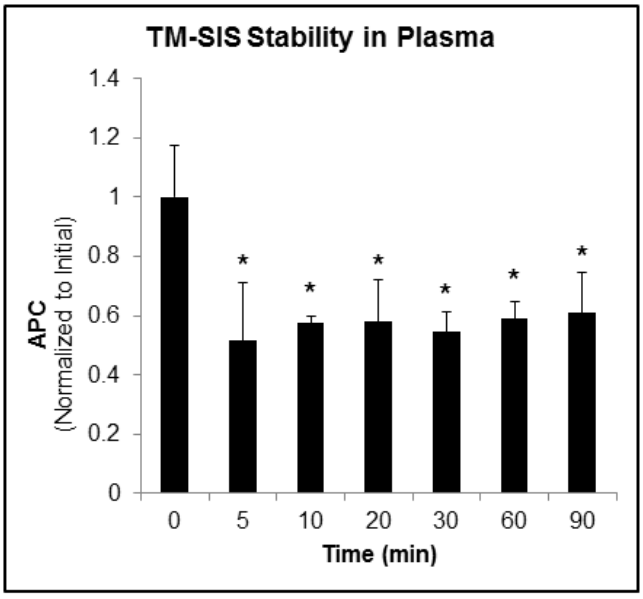

Figure 6.3: Activity of TM-SIS following incubation in plasma. TM-SIS was incubated in plasma at 37°C for the specified time. APC generation was quantified post-incubation. After 5 minutes, a reduction in activity of approximately 48% was observed; however, no further loss in TM activity occurred over the 90 minute treatment. "*" indicates significantly different than time 0, $p<0.05$ by one-way ANOVA and Tukey's post hoc, n=3.

6.4.3 Coagulation Assays

Mechanical

Rings of SIS were modified with thrombomodulin and the APTT and PT coagulation assays were performed as normal. Similar to prior results [368], unmodified SIS slightly prolonged the APTT, whereas modifying SIS with thrombomodulin did not significantly prolong the coagulation times for with the APTT (Figure 6.4). In fact, TM-SIS did not prolong coagulation to the extent that unmodified SIS did. Neither SIS nor TM-SIS altered the PT.

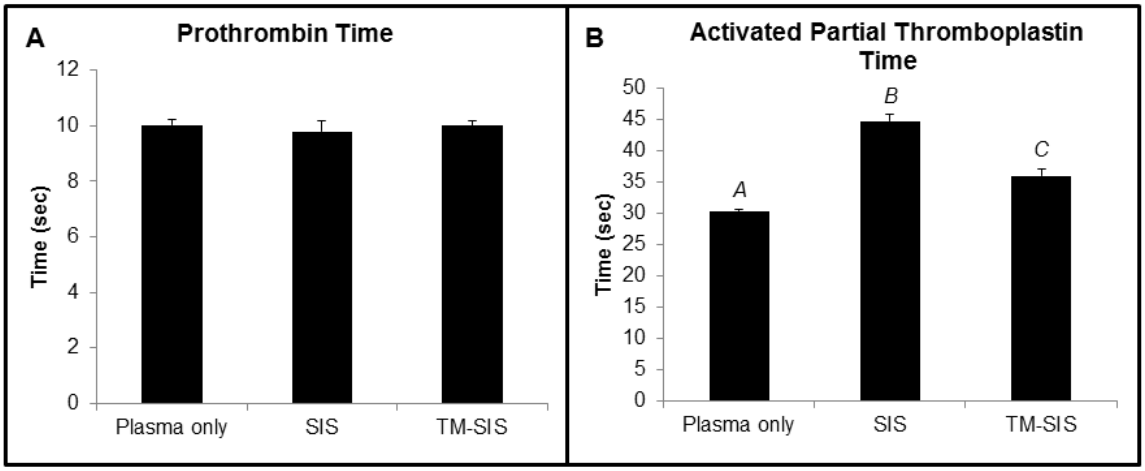

Figure 6.4: Prothrombin Time (PT) and Activated Partial Thromboplastin Time (APTT) of SIS and TM-SIS. Neither SIS nor TM-SIS had any significant effect of the prothrombin time. Both SIS and TM-SIS prolonged the APTT, with SIS resulting in greater prolongation than TM-SIS (14.34 ± 1.18 sec vs. 5.62 ± 1.73 sec). Letters indicate homogenous subsets based on a one-way ANOVA and Tukey's *post hoc,* n=4.

Optical

Optical measurement of coagulation utilized more dilute pro-coagulant stimuli for more physiologically relevant coagulation times. When plasma was stimulated to coagulate with diluted PT and APTT reagents delivered in solution, modifying SIS with thrombomodulin did not prolong coagulation, even at thrombomodulin concentrations considerably higher than the standard 4 µg/ml (Supplemental Figure S6.2). However, when SIS was soaked in dilute PT and APTT reagents to localize the pro-coagulant stimuli to the material surface, thrombomodulin modification significantly prolonged coagulation at the standard concentration of 4 µg/ml (Figure 6.5). The discrepancy in these assays highlights the importance of designing coagulation experiments that appropriately test for surface-initiated anti-thrombotic activity (i.e. TM-SIS) vs. bulk plasma coagulation (i.e. from systemic anticoagulation therapy).

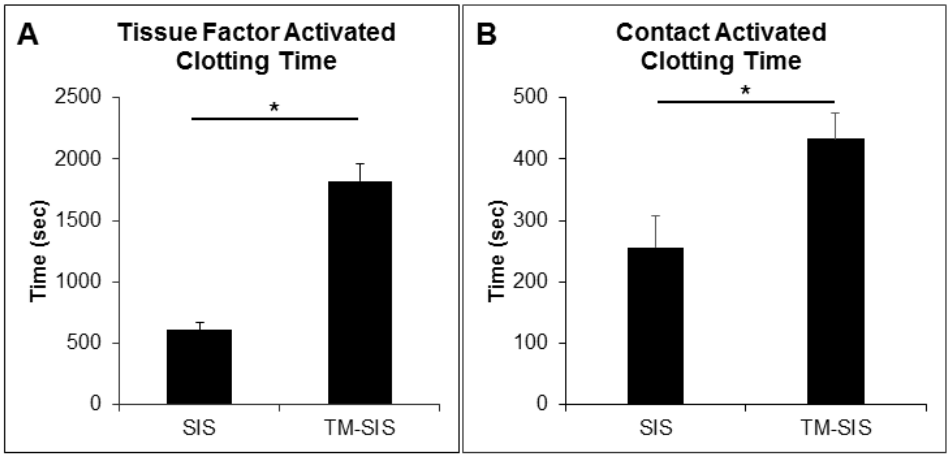

Figure 6.5: Surface-initiated, tissue factor and contact activated coagulation times. SIS and TM-SIS were soaked in TF and contact activation solutions to initiate coagulation from the material surface. TM-SIS prolonged plasma coagulation initiated by (A) tissue factor or (B) contact activation. "*" indicates significantly different groups, $p<0.05$ by one-way ANOVA and Tukey's post hoc, n=3.

6.4.4 Baboon Arteriovenous Shunt

Tubular SIS devices with 4 mm inner diameter were connected to a baboon *ex vivo* arteriovenous shunt, and whole blood flowed through the devices at a flow rate of 100 ml/min for 1 hr. Platelet accumulation during the 1 hour was low for both SIS and TM-SIS devices with no significant differences at any time point (Figure 6.6A). Interestingly, TM-SIS had a significantly greater deposition of fibrinogen (Figure 6.6B).

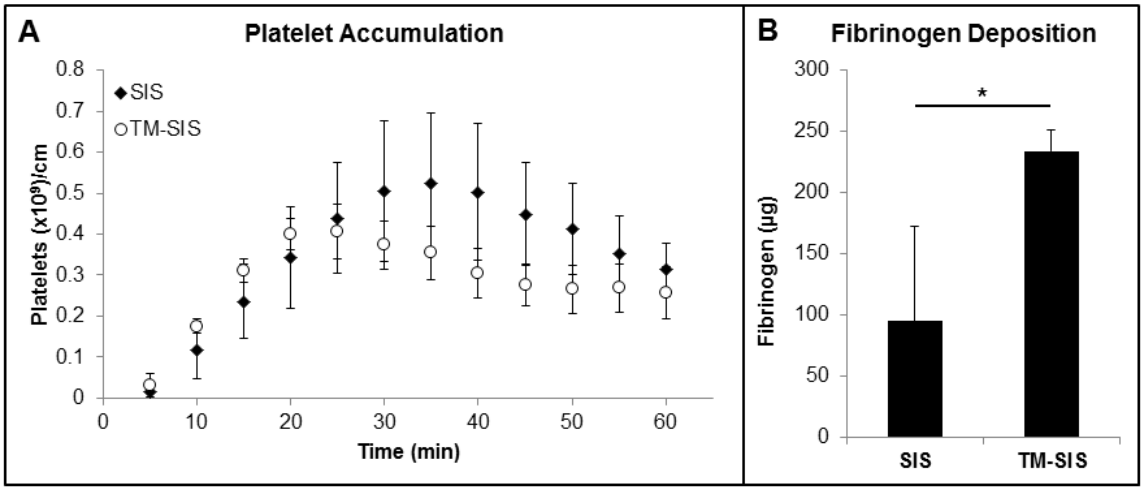

Figure 6.6: Platelet accumulation and fibrinogen deposition on SIS and TM-SIS. Tubular SIS devices were connected to a baboon arteriovenous shunt. The accumulation of ^{111}In-labeled platelets was measure in real time, as well as the total ^{125}I-labeled fibrinogen deposition. Both SIS and TM-SIS demonstrated low platelet accumulation over the 60 minute study with no significant difference seen at any time point. However, TM-SIS had significantly greater fibrinogen deposition on devices.

6.5 Discussion

In fact, the amount of APC generated by a 5 mm disc of TM-SIS was approximately 5.5-fold greater than a confluent layer of baboon carotid ECs (6.4 mm well diameter). Due to the fibrous structure of SIS, the total surface area of an SIS disc is difficult to determine; however, this result indicates that any application using a piece of TM-SIS in a vascular device would generate a similar, if not greater, quantity of APC than an equivalent planar surface area of endothelium.

Clinical coagulation assays such as the PT and APTT are useful for identifying significant coagulation factor deficiencies; thus, this work utilized these assays to characterize the anticoagulant activity of TM-SIS (Figure 6.4). Neither SIS nor TM-SIS prolonged the PT, which is attributed to the high concentration of TF in the PT reagent, as well as the initiation of coagulation in the plasma volume rather than at the material surface. Consistent with previous results, SIS prolonged the APTT; however, TM-SIS

did not prolong the APTT. The APTT is known to be highly-sensitive to heparin anticoagulation, and SIS is known to be partially composed of heparin. Therefore, the TM modification may interfere with heparin anticoagulant activity intrinsic to SIS.

The PT and APTT provide some information on the anticoagulant activity of materials. However, due to their lack of sensitivity to material properties, these assays are often not recommended to demonstrate hemocompatibility of biomaterials [369]. Optical measurement of coagulation allows for much longer coagulation times (on the order of minutes) that are closer to physiological clotting times. Initial optical coagulation measurements that added pro-coagulant stimuli to the bulk plasma solution did not reflect any anticoagulant activity of the thrombomodulin modification. However, unlike heparin which is readily released from SIS in plasma [368], thrombomodulin is stable on SIS in plasma (Figure 6.3) and the anticoagulant activity is catalyzed at the surface of the material. Because thrombus formation *in vivo* initiates at the material or vessel surface rather than in the bulk blood flow, the assay was refined to localize the pro-coagulant stimuli to the material surface. Using these methods, TM-SIS significantly prolonged coagulation initiated by TF or contact pathway activation compared to unmodified SIS (Figure 6.5). Importantly, this prolongation was due to TM activity rather than reduced pro-coagulant adsorption due to previous TM adsorption on SIS (Supplemental Figure S6.1). This result highlights that studies measuring anticoagulant activity of biomaterials should be designed to appropriately measure the anticoagulant mechanism.

A baboon arteriovenous shunt was used to measure thrombus formation on SIS using flowing whole blood. The physical shunt configuration and lack of anticoagulant or

anti-platelet drugs results in rapid platelet deposition such that even clinically-approved materials and devices have substantial platelet accumulation over a 60 minute study, which allows for rapid comparative assessments of biomaterial thrombogenicity [205,370]. Consistent with previous results, overall thrombus formation on SIS was low, and modifying SIS with TM did not significantly alter platelet accumulation on SIS, and unexpectedly resulted in increased fibrin deposition. Although the best-known activity of the thrombin-thrombomodulin complex is APC generation, thrombin activatable fibrinolysis inhibitor (TAFI) is also efficiently activated by this complex [371,372]. The thrombomodulin modification may therefore have resulted in an increased quantity of activated TAFI, the resulting anti-fibrinolytic activity facilitated increased fibrin deposition. Prior work has demonstrated that low concentrations of thrombomodulin in plasma have been shown to favor anti-fibrinolytic activity via TAFI over anticoagulant activity of APC [373]. Future work should investigate TAFI activation on TM-SIS compared to unmodified SIS.

In conclusion, modifying SIS with TM enabled APC generation and prolonged plasma coagulation as measured by a number of *in vitro* assessments, indicating an anti-coagulant effect. TM modification resulted in increased fibrin deposition on tubular SIS devices in a baboon arteriovenous shunt model. Future work may also investigate the stability of TM-SIS *in vivo*, strategies to increase thrombomodulin concentration on the SIS, as well as determining the effects of APC generated by TM-SIS on EC phenotype.

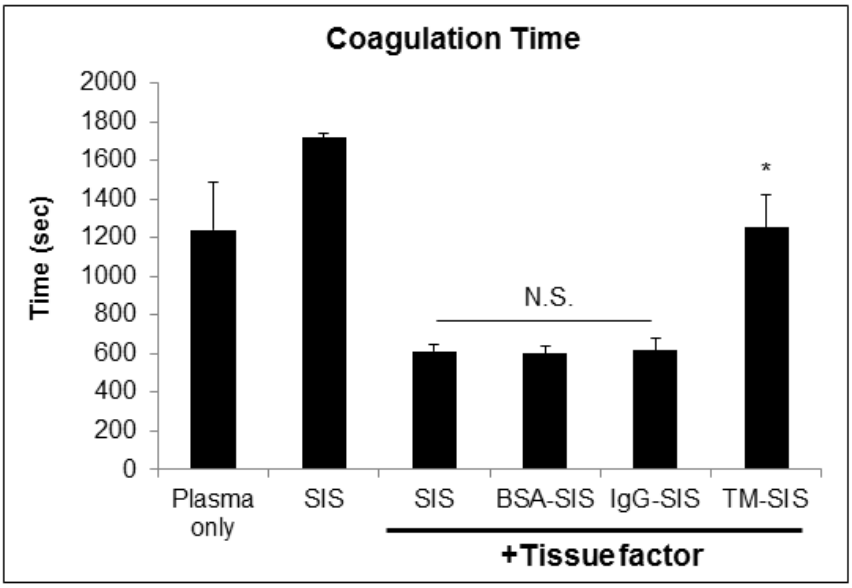

Supplemental Figure S6.1: Surface-initiated coagulation times of SIS modified with non-specific proteins. Modifying SIS with the proteins bovine serum albumin (BSA) or immunoglobulin G (IgG) did not prolong plasma coagulation compared to unmodified SIS. However, TM-SIS significantly prolonged plasma coagulation, indicating anticoagulant activity specifically attributable to TM. "N.S.", not significant; "*" indicates significantly different that SIS + tissue factor, $p < 0.05$ by one-way ANOVA and Tukey's post hoc, n=3.

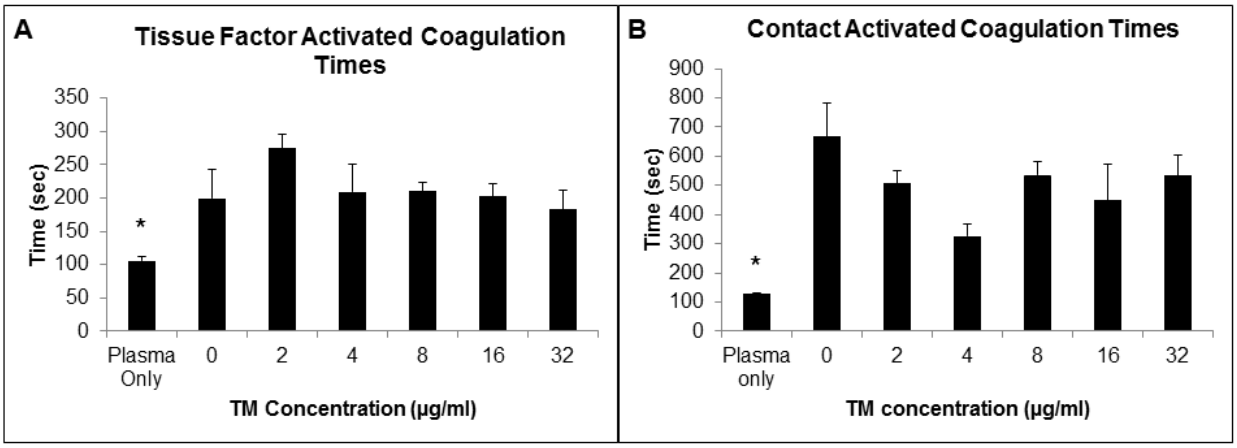

Supplemental Figure S6.2: Plasma coagulation times initiated in solution. Plasma coagulation was initiated by tissue factor or contact pathway activation by adding a solution of the pro-coagulant reagent to plasma containing SIS. Unmodified SIS (i.e. TM concentration = 0 µg/ml) slightly prolonged plasma coagulation. However, no TM-modified SIS groups significantly prolonged plasma coagulation compared to unmodified SIS, $p > 0.05$ by one-way ANOVA and Tukey's post hoc, n=3.

CHAPTER VII: Summary

Cardiovascular disease is the leading cause of death in most developed countries and imparts a massive clinical burden. As a result, numerous cardiovascular devices have been developed to treat these conditions. However, there are still significant complications in cardiovascular medicine that result from device-associated thrombosis. In contrast to typical materials used in cardiovascular device construction, a healthy vascular endothelium produces a number of factors that interact with blood cells and proteins to regulate hemostasis and thrombosis. The hypothesis of this work was that recapitulating endothelial function by applying biologically-active coatings to biomaterials would reduce thrombus formation on biomaterials. Therefore, this thesis explored multiple biologically-active, anti-thrombotic coatings that were applied to biomaterials and the resulting anti-thrombotic effects were characterized.

The importance of the endothelium in regulating hemostasis and thrombosis has been well-documented. Therefore, there has been considerable research into endothelializing devices, such as vascular grafts, with a patient's endothelial cells to improve graft patency. However, limitations of this technique, including vein excision and limited proliferation of mature venous endothelial cells, has limited this technique from widespread clinical use. In contrast to using mature endothelial cells, endothelial outgrowth cells (EOCs) can be isolated and expanded from a peripheral blood draw. Using EOCs to cover vascular graft materials is an exciting alternative to using venous endothelial cells, and a thorough review of this research was presented in Section 2.9. In particular, the effects of stimulating EOCs with fluid shear were highlighted due to the

well-known role that fluid shear plays in maintaining an atheroprotective phenotype in mature endothelial cells.

Although the existing literature documented that EOCs expressed molecules to regulate inflammation and thrombosis, there were no studies that compared donor-matched EC and EOCs with regard to these functions. Furthermore, a direct comparison of thrombus formation on EC- and EOC-seeded vascular grafts in a model using flowing blood had not been performed. Therefore, in Chapter III baboon EOCs were compared to donor-matched ECs with regard to their expression of thrombosis-regulating surface antigens, gene expression, activation of coagulation factors, and regulation of thrombus formation in an *ex vivo* shunt model. We found that there was considerable inter-donor variability in cellular function, and this variability was particularly apparent in the gene expression. Treatment of ECs and EOCs with the inflammatory cytokine TNFα caused a pro-thrombotic shift in cell phenotype. Tissue factor gene expression and activity increased following TNFα, and the response was similar between ECs and EOCs. Platelet accumulation and fibrinogen deposition on EC- and EOC-seeded ePTFE vascular grafts was studied using a baboon arteriovenous shunt. In this system, ECs and EOCs demonstrated similar quantities of adhered platelets and fibrinogen. We conclude from this work that the similarity of ECs and EOCs supports the use of EOCs as an autologous endothelium for cardiovascular applications.

Similarly to a small diameter vascular graft, there is no commercially-available artificial venous valve, as all valves that have been investigated have had unacceptably high rates of thrombosis. One of the few valves that progressed to clinical trials is a

bioprosthetic venous valve developed by Pavčnik, et al., which has leaflets constructed of decellularized porcine small intestinal submucosa (SIS). In a clinical trial, patients displayed improvement in the healing of venous ulcers; however, the function of the SIS valve was limited by leaflet thickening attributed to thrombus formation and neointimal hyperplasia. As endothelial cells are key regulators of vascular homeostasis, their presence on the SIS valves may reduce the observed thickening. Therefore, in Chapter IV we examined two strategies to endothelialize an SIS bioprosthetic valve. One technique utilized biotinylated anti-KDR antibodies to capture circulating endothelial progenitor cells to accelerate *in situ* endothelialization. Alternatively, valves were pre-seeded with autologous EOCs prior to implantation. Endothelialization of SIS, either through pre-seeding with EOCs or by using immobilized antibodies to capture circulating prognenitor cells, did not have the expected result of reducing thickening of SIS. The lack of improvement with the capture strategy is similar to other studies that attempted to accelerate endothelialization of stents using anti-CD34 antibodies but did not show significant improvement compared to bare metal stents. Potential immunogenicity of the biotin-streptavidin linkage system may have contributed to detrimental modeling seen with antibody-modified SIS. Alternate capture strategies, including aptamers and small peptides, may offer advantages over antibody-based capture. Regarding pre-seeded SIS valves, previous research has demonstrated that an intact endothelial monolayer can be maintained on SIS throughout the manipulations required for transcethater delivery of a bioprosthetic venous valve. However, the special considerations that needed to be followed to ensure endothelial retention may preclude widespread usage and also provide additional opportunities for error in the implant

procedure. The lack of benefit from pre-implant endothelialization supports investigating alternative cell-free strategies to reduce thrombus formation and intimal hyperplasia on SIS valves.

In addition to being used for constructing a bioprosthetic venous valve, SIS is used in other cardiovascular applications including as a vascular graft and in a stent graft. Crosslinking decellularized matrices is a common procedure used to increase the mechanical properties, slow degradation and reduce immunogenicity. However, the consequences of crosslinking SIS with regard to hemocompatibility had not been investigated. Therefore, in Chapter V we crosslinked SIS using 1-ethyl-3-(3-dimethylaminopropyl)carbodiimide (EDC) and *N*-hydroxysuccinimide (NHS), common crosslinking reagents used for protein conjugation, and performed multiple coagulation assays to determine that crosslinking significantly reduced the hemocompatibility of SIS. Unmodified SIS demonstrated modest anticoagulant activity, evidenced by prolonging the coagulation of plasma in the activated partial thromboplastin time assay as well as prolonged recalcification and thrombin times. However, the prothrombin time was not prolonged by SIS, indicating that the anticoagulant activity is not sufficient to prolong coagulation initiated by high concentrations of tissue factor. Carbodiimide crosslinking abrogated all anticoagulant activity of SIS, as did enzymatic treatment with heparinase I and III, suggesting heparin and heparan sulfate are predominantly responsible for the anticoagulant activity. This finding is consistent with previous studies on the composition of SIS. A baboon arteriovenous shunt loop was used to measure platelet accumulation and fibrinogen deposition on tubular SIS devices. Although SIS demonstrated relatively limited platelet accumulation and fibrinogen incorporation, crosslinked SIS initiated

significantly higher platelet and fibrinogen accumulation. These results demonstrate that SIS has limited anticoagulant activity and that crosslinking markedly reduces the hemocompatibility of SIS.

Integrating the results of Chapters IV-V, a cell-free modification to SIS that provides anti-thrombotic activity and does not involve carbodiimide-mediated crosslinking is a potential approach for reducing thrombus formation on SIS. As highlighted in Section 2.3.4, activated protein C (APC) catalyzed by thrombomodulin is an anticoagulant and anti-inflammatory enzyme; therefore, thrombomodulin-modified SIS (TM-SIS) may act through multiple pathways to reduce thrombus formation on SIS. In Chapter VI we determined that TM-SIS catalyzes the production of APC that is similar to, if not greater than, an equivalent area of ECs. In addition, TM-SIS prolongs blood plasma coagulation, indicating an anticoagulant effect. Although flow, drying and incubation in plasma all reduce the activity of TM-SIS, APC generation was still present following all stability tests. When connected to a baboon arteriovenous shunt, TM-SIS did not demonstrate significantly lower platelet accumulation of fibrinogen deposition compared to unmodified SIS; however, the anti-thrombotic effect of APC generated at the surface may be more pronounced at venous flow rates than the arterial flow used here. Future studies that perform these shunt studies under venous conditions, as well as investigating the effects of APC on ECs and characterizing the stability of TM-SIS *in vivo*, are recommended for future research.

CHAPTER VIII: Future Directions

The studies conducted in this thesis have characterized the utility of endothelial outgrowth cells for autologous endothelialization of vascular grafts (Chapter III), performed *in vivo* analyses of two methods for rapid endothelialization of SIS (Chapter IV), determined the detrimental effect of crosslinking on the hemocompatibility of SIS (Chapter V), and the anti-thrombotic effects of an endothelial-inspired, acellular coating of SIS using thrombomodulin (Chapter VI). This thesis work provides the foundation for future studies, particularly with regard to the endothelial-inspired coating of SIS. Future directions proposed for this research would investigate 1) additional modifications to enhance anticoagulant activity, 2) the effects of APC generated by modified SIS on endothelial cells, and 3) retaining function of biologically-active coatings *in vivo*. Preliminary studies performed in these areas will be discussed.

8.1 Heparin and Thrombomodulin-modified SIS

Heparin is a glycosaminoglycan that markedly increases the anticoagulant activity of antithrombin III (ATIII). ATIII is a serpin that irreversibly binds to and inactivates FXIIa, FXIa, FXa, FIXa and thrombin. Inhibition of FXa is the primary action that results in anticoagulant activity. Unfractionated heparin enhances ATIII activity through two mechanisms. A pentasaccharide sequence binds to ATIII, changing its conformation to accelerate inhibition primarily of FXa. Long heparin molecules also act as a template mechanism by which both ATIII and activated coagulation factors bind the same negatively-charged heparin molecule to increase their rate of interaction [90].

Modifying materials with heparin has been applied to metal stents and vascular graft materials to reduce thrombosis [374,375]. However, these modifications have not

been applied to SIS, and the interaction of SIS modified with both thrombomodulin and heparin is unknown. Therefore, preliminary work has characterized plasma coagulation and thrombus formation on SIS modified with thrombomodulin and heparin to evaluate its utility as a novel vascular biomaterial.

8.1.1 Heparin-modified SIS Prolongs Plasma Coagulation

Modifying SIS with increasing concentrations of heparin resulted in significant prolongation of blood plasma coagulation initiated by a solution of either tissue factor (Innovin diluted 1:2000) or contact activation (HemosIL diluted 1:20), with concentrations of 125 µg/mL prolonging plasma coagulation to times over 45 minutes (Figure 8.1). All future experiments using heparin-modified SIS used 100 µg/mL.

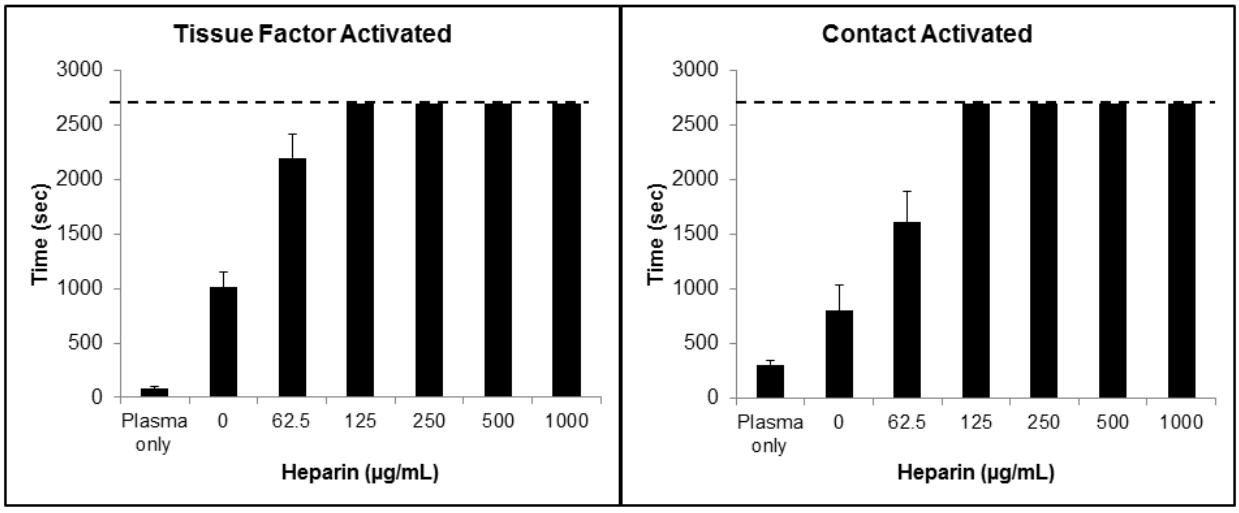

Figure 8.1: Coagulation times of plasma incubated with Hep-SIS. Tissue factor or contact activation were used to stimulate plasma coagulation. Increasing heparin concentrations led to more prolonged blood plasma coagulation initiated by either pathway. Dotted lines indicate the end of absorption measurements at 45 min (2700 sec).

8.1.2 Dual-modified SIS Retains Full Thrombomodulin and Heparin Activities

To enable both APC generation and heparin anticoagulant activity on SIS, SIS was modified with both thrombomodulin and heparin. To determine if the order of the modification affects the activities of thrombomodulin or heparin modifications, SIS was modified with either thrombomodulin or heparin first, followed sequentially with the second modification. SIS modified first with thrombomodulin then with heparin (Hep-TM-SIS) demonstrated APC generation similar to TM-SIS, and also prolonged plasma coagulation to a similar extent as Hep-SIS (Figure 8.2). Interestingly, SIS modified first with heparin and then with thrombomodulin (TM-Hep-SIS) demonstrated a reduction in both APC generation and heparin anticoagulant activity; thus, all future studies utilizing a dual modification performed the modifications sequentially with thrombomodulin first followed by heparin.

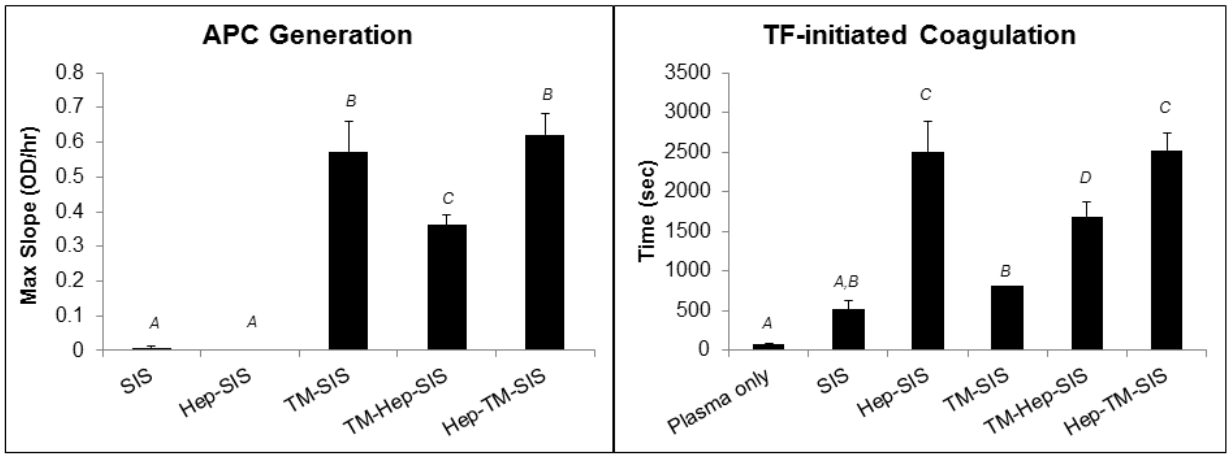

Figure 8.2: APC generation and plasma coagulation times for dual-modified SIS. SIS modified with thrombomodulin then heparin (Hep-TM-SIS) demonstrated APC generation similarly to TM-SIS, and also prolonged plasma coagulation to a similar extent as Hep-SIS. Conversely, SIS modified heparin followed by thrombomodulin (TM-Hep-SIS) had lower APC generation and anticoagulant activity. Letters indicate homogenous subsets, $p<0.05$ via one-way ANOVA and Tukey's post-hoc, n =4.

8.1.3 Dual-modified SIS Reduces Platelet Accumulation

Prior work investigating TM-SIS did not demonstrate a significant reduction in platelet accumulation on tubular devices that were connected to a baboon arteriovenous shunt loop. Considering the potent anticoagulant effect of the dual modification *in vitro*, devices made of Hep-TM-SIS were constructed for use in the shunt loop. In contrast to TM-SIS, Hep-TM-SIS devices demonstrated a significantly reduction in platelet accumulation compared to unmodified SIS devices (Figure 8.3).

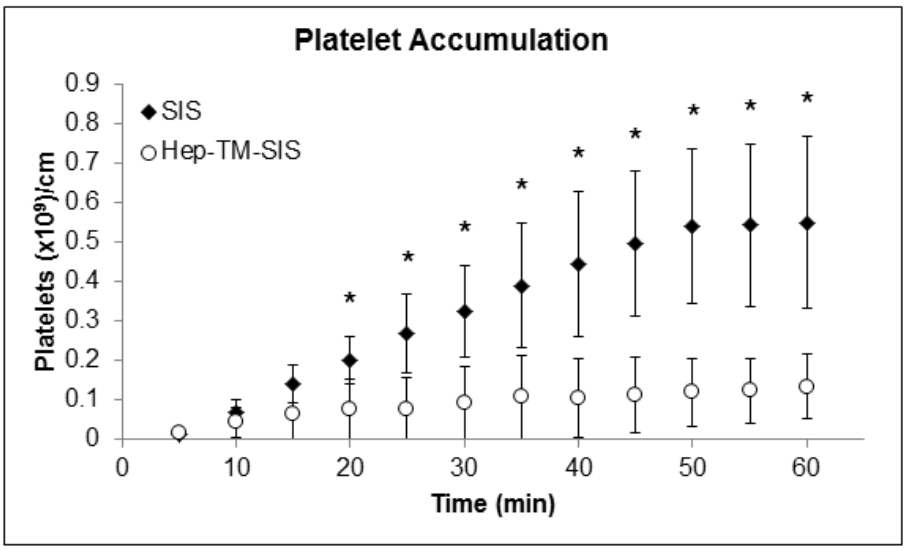

Figure 8.3: Platelet accumulation on SIS and Hep-TM-SIS devices. Tubular SIS devices were connected to a baboon arteriovenous shunt. The accumulation of ^{111}In-labeled platelets was measured in real time. Hep-TM-SIS had significantly less platelet accumulation from 20 minutes through the 60 minute study. "*" indicates time points of significantly different platelet accumulation based on a two-tailed student's t-test, $p<0.05$, n=4.

8.1.4 Summary: Heparin and Thrombomodulin-modified SIS

Heparin exerts potent anticoagulant activity by binding to ATIII and markedly accelerating the ATIII-dependent inhibition of FXIIa, FXIa, FXa, FIXa and thrombin. This preliminary work determined that modifying SIS with exogenous heparin results in potent anticoagulant activity. A dual modification of SIS with both thrombomodulin and

heparin, performed sequentially in that order, confers both robust APC generation as well as anticoagulant activity on SIS. This dual-modified SIS demonstrated reduced platelet accumulation compared to unmodified SIS and TM-SIS. SIS dual-modified with heparin and thrombomodulin is thus another novel biologically-active coating that demonstrates improved hemocompatibility for vascular applications. Future work can investigate the anti-thrombotic function of this material *in vivo*.

8.2 APC Signaling on ECs

This dissertation characterized the anticoagulant activity of APC generated by TM-SIS; however, APC also signals on endothelial membrane protease activated receptors (PARs) to reduce inflammation-induced apoptosis and permeability. Prior work by Feistritzer and Riewald [376] has demonstrated that treating ECs with 5 nM APC reduces the permeability of a monolayer of ECs cultured on a porous membrane (Figure 8.4).

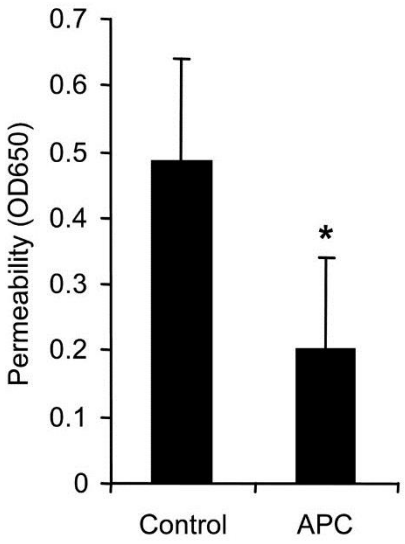

Figure 8.4: APC enhances barrier integrity of ECs. ECs pre-treated with APC maintained barrier function compared to untreated ECs treated with thrombin to induce permeability. Reprinted from Feistritzer and Riewald, 2005 [376].

My preliminary studies demonstrated that APC also reduces TNFα-induced permeability (**Figure 8.5**). In this experiment, ECs were cultured to confluence on collagen-coated Millipore well inserts with 3 µm pores. Cells were then treated with TNFα (100 U/mL) and 200 nM or 20 nM APC in endothelial basal media (EBM) with 4% BSA for 4 hours. To assess permeability post-treatment, a solution of 4% BSA in PBS with Ca^{2+} and Mg^{2+} and 0.67 mg/ml Evan's Blue dye was placed in the top chamber of the well insert , and 4% BSA in PBS placed into the bottom well. After 20 min to allow diffusion across the membrane, the well inserts were removed and the absorbance at 650 nm of the solution in the bottom chamber was measured using a plate reader.

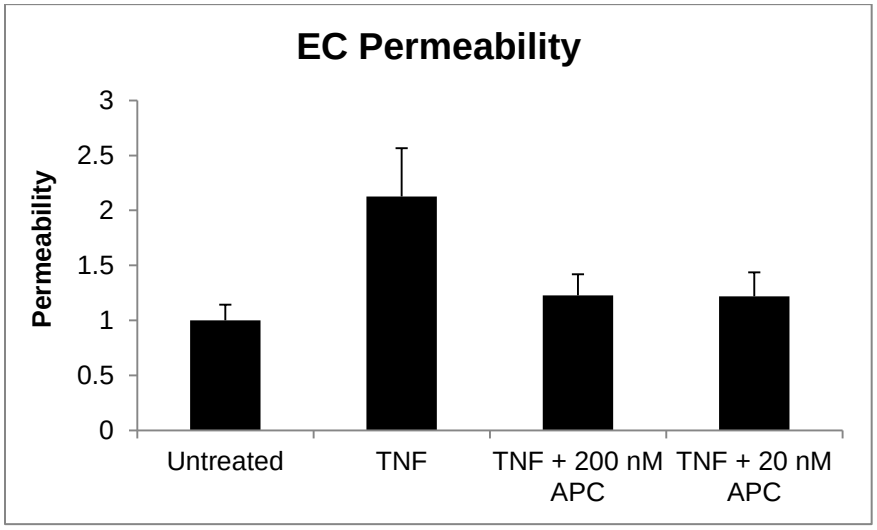

Figure 8.5: Barrier function of ECs treated with APC and TNFα. ECs treated with TNFα had increased permeability; co-treatment with APC prevented this increase in permeability.

The capacity of APC generated by TM-SIS to similarly enhance endothelial barrier integrity has not been established. Other effects of APC and TM-SIS on ECs, such as tissue factor activity, are also potential topics for future study.

8.3 Stability of Biologically-active Coatings *In Vivo*

One limitation of the research characterizing thrombomodulin-modified SIS is the lack of a long-term implant model that could be used to determine the stability *in vivo* of the biologically-active coatings, as well as characterize the long-term remodeling. A sheep model, such as that used in Chapter IV, would be a suitable system to study TM-SIS, particularly with regard to prolonging bioprosthetic valve function. Prior work has demonstrated that the catalytic activity of thrombomodulin may be inactivated over time *in vivo* by oxidation. However, engineered thrombomodulin mutants have been developed that possess improved anti-thrombotic activity through enhanced APC generation and reduced inactivation by oxidation [79,102]. The minimum fragment of thrombomodulin that can catalyze APC generation is composed of epidermal growth factor-like domains 4-6 [73]. This fragment is unable to catalyze thrombin-activatable fibrinolysis inhibitor (TAFI) activation, and is therefore unable to exert anti-fibrinolytic (clot stabilizing) activity. Importantly, mutating the amino acid methionine-388 to leucine (M388L) in this thrombomodulin fragment prevents oxidation at this site. In addition, the M388L mutant acts as a more effective cofactor than wild-type thrombomodulin for APC generation [77]. This particular mutant could be used in future studies as a bioactive modification of SIS that generates APC to improve long-term anti-thrombotic activity.

References

[1] R. Busse, I. Fleming, Vascular endothelium and blood flow, Handb. Exp. Pharmacol. (2006) 43–78.

[2] K.B. Vartanian, S.J. Kirkpatrick, O.J.T. McCarty, T.Q. Vu, S.R. Hanson, M.T. Hinds, Distinct extracellular matrix microenvironments of progenitor and carotid endothelial cells, J. Biomed. Mater. Res. A. 91A (2009) 528–539. doi:10.1002/jbm.a.32225.

[3] K.B. Vartanian, M.A. Berny, O.J.T. McCarty, S.R. Hanson, M.T. Hinds, Cytoskeletal structure regulates endothelial cell immunogenicity independent of fluid shear stress, Am. J. Physiol. - Cell Physiol. 298 (2010) C333–C341. doi:10.1152/ajpcell.00340.2009.

[4] D.B. Cines, E.S. Pollak, C.A. Buck, J. Loscalzo, G.A. Zimmerman, R.P. McEver, et al., Endothelial Cells in Physiology and in the Pathophysiology of Vascular Disorders, Blood. 91 (1998) 3527–3561.

[5] D.E.J. Anderson, M.T. Hinds, Extracellular matrix production and regulation in micropatterned endothelial cells, Biochem. Biophys. Res. Commun. 427 (2012) 159–164. doi:10.1016/j.bbrc.2012.09.034.

[6] D.B. Zilversmit, Atherogenesis: a postprandial phenomenon, Circulation. 60 (1979) 473–485.

[7] W.J. Hayes Jr., Control of Norway rats with residual rodenticide warfarin., Public Health Rep. 65 (1950) 1537–1555.

[8] S. Braud, C. Bon, A. Wisner, Snake venom proteins acting on hemostasis, Biochimie. 82 (2000) 851–859. doi:10.1016/S0300-9084(00)01178-0.

[9] P.H. Reitsma, H.H. Versteeg, S. Middeldorp, Mechanistic view of risk factors for venous thromboembolism, Arterioscler. Thromb. Vasc. Biol. 32 (2012) 563–568. doi:10.1161/ATVBAHA.111.242818.

[10] J.W. Blom, C.J.M. Doggen, S. Osanto, F.R. Rosendaal, Malignancies, prothrombotic mutations, and the risk of venous thrombosis, J. Am. Med. Assoc. 293 (2005) 715–722. doi:10.1001/jama.293.6.715.

[11] R.M. Bertina, B.P.C. Koeleman, T. Koster, F.R. Rosendaal, R.J. Dirven, H. De Ronde, et al., Mutation in blood coagulation factor V associated with resistance to activated protein C, Nature. 369 (1994) 64–67. doi:10.1038/369064a0.

[12] H. Jick, S.S. Jick, M.W. Myers, C. Vasilakis, V. Gurewich, Risk of idiopathic cardiovascular death and rionfatal venous thromboembolism in women using oral contraceptives with differing progestagen components, The Lancet. 346 (1995) 1589–1593. doi:10.1016/S0140-6736(95)91928-7.

[13] G.H. Lyman, A.A. Khorana, A. Falanga, D. Clarke-Pearson, C. Flowers, M. Jahanzeb, et al., American Society of Clinical Oncology Guideline: Recommendations for venous thromboembolism prophylaxis and treatment in patients with cancer, J. Clin. Oncol. 25 (2007) 5490–5505. doi:10.1200/JCO.2007.14.1283.

[14] R.P. Dellinger, M.M. Levy, A. Rhodes, D. Annane, H. Gerlach, S.M. Opal, et al., Surviving sepsis campaign: International guidelines for management of severe sepsis and septic shock: 2012, Crit. Care Med. 41 (2013) 580–637. doi:10.1097/CCM.0b013e31827e83af.

[15] A.P. Yoganathan, K.B. Chandran, F. Sotiropoulos, Flow in prosthetic heart valves: State-of-the-art and future directions, Ann. Biomed. Eng. 33 (2005) 1689–1694. doi:10.1007/s10439-005-8759-z.

[16] M. Verso, G. Agnelli, Venous thromboembolism associated with long-term use of central venous catheters in cancer patients, J. Clin. Oncol. 21 (2003) 3665–3675. doi:10.1200/JCO.2003.08.008.

[17] T. Watson, E. Shantsila, G.Y. Lip, Mechanisms of thrombogenesis in atrial fibrillation: Virchow's triad revisited, The Lancet. 373 (2009) 155–166. doi:10.1016/S0140-6736(09)60040-4.

[18] K. van Langevelde, A. Šrámek, F.R. Rosendaal, The Effect of Aging on Venous Valves, Arterioscler. Thromb. Vasc. Biol. 30 (2010) 2075–2080. doi:10.1161/ATVBAHA.110.209049.

[19] P.F. Davies, Hemodynamic shear stress and the endothelium in cardiovascular pathophysiology, Nat. Clin. Pract. Cardiovasc. Med. 6 (2009) 16–26. doi:10.1038/ncpcardio1397.

[20] A.D. Blann, G.Y.H. Lip, The endothelium in atherothrombotic disease: Assessment of function, mechanisms and clinical implications, Blood Coagul. Fibrinolysis. 9 (1998) 297–306.

[21] K. Broos, H.B. Feys, S.F. De Meyer, K. Vanhoorelbeke, H. Deckmyn, Platelets at work in primary hemostasis, Blood Rev. 25 (2011) 155–167. doi:10.1016/j.blre.2011.03.002.

[22] Z.M. Ruggeri, G.L. Mendolicchio, Adhesion mechanisms in platelet function, Circ. Res. 100 (2007) 1673–1685. doi:10.1161/01.RES.0000267878.97021.ab.

[23] E.W. Davie, O.D. Ratnoff, WATERFALL SEQUENCE FOR INTRINSIC BLOOD CLOTTING, Science. 145 (1964) 1310–1312.

[24] R.G. Macfarlane, An Enzyme Cascade in the Blood Clotting Mechanism, and its Function as a Biochemical Amplifier, Nature. 202 (1964) 498–499. doi:10.1038/202498a0.

[25] K.G. Mann, T. Orfeo, S. Butenas, A. Undas, K. Brummel-Ziedins, Blood coagulation dynamics in haemostasis, Hamostaseologie. 29 (2009) 7–16.

[26] T.H. Bugge, Q. Xiao, K.W. Kombrinck, M.J. Flick, K. Holmbäck, M.J. Danton, et al., Fatal embryonic bleeding events in mice lacking tissue factor, the cell-associated initiator of blood coagulation, Proc. Natl. Acad. Sci. U. S. A. 93 (1996) 6258–6263.

[27] E. Camerer, A.-B. Kolstø, H. Prydz, Cell biology of tissue factor, the principal initiator of blood coagulation, Thromb. Res. 81 (1996) 1–41. doi:10.1016/0049-3848(95)00209-X.

[28] J. Sánchez, P.B. Lundquist, G. Elgue, R. Larsson, P. Olsson, Measuring the degree of plasma contact activation induced by artificial materials, Thromb. Res. 105 (2002) 407–412. doi:10.1016/S0049-3848(02)00051-8.

[29] S.A. Smith, N.J. Mutch, D. Baskar, P. Rohloff, R. Docampo, J.H. Morrissey, Polyphosphate modulates blood coagulation and fibrinolysis, Proc. Natl. Acad. Sci. U. S. A. 103 (2006) 903–908. doi:10.1073/pnas.0507195103.

[30] E.A. Vogler, C.A. Siedlecki, Contact activation of blood-plasma coagulation, Biomaterials. 30 (2009) 1857–1869. doi:10.1016/j.biomaterials.2008.12.041.

[31] D. Gailani, G.J. Broze, Factor XI activation in a revised model of blood coagulation, Science. 253 (1991) 909–912. doi:10.1126/science.1652157.

[32] M.B. Gorbet, M.V. Sefton, Biomaterial-associated thrombosis: Roles of coagulation factors, complement, platelets and leukocytes, Biomaterials. 25 (2004) 5681–5703. doi:10.1016/j.biomaterials.2004.01.023.

[33] M.J. Manco-Johnson, T.C. Abshire, A.D. Shapiro, B. Riske, M.R. Hacker, R. Kilcoyne, et al., Prophylaxis versus episodic treatment to prevent joint disease in boys with severe hemophilia, N. Engl. J. Med. 357 (2007) 535–544. doi:10.1056/NEJMoa067659.

[34] O. Salomon, D.M. Steinberg, U. Seligshon, Variable bleeding manifestations characterize different types of surgery in patients with severe factor XI deficiency enabling parsimonious use of replacement therapy, Haemophilia. 12 (2006) 490–493. doi:10.1111/j.1365-2516.2006.01304.x.

[35] T. Renné, M. Pozgajová, S. Grüner, K. Schuh, H.-U. Pauer, P. Burfeind, et al., Defective thrombus formation in mice lacking coagulation factor XII, J. Exp. Med. 202 (2005) 271–281. doi:10.1084/jem.20050664.

[36] C. Kleinschnitz, G. Stoll, M. Bendszus, K. Schuh, H.-U. Pauer, P. Burfeind, et al., Targeting coagulation factor XII provides protection from pathological thrombosis in cerebral ischemia without interfering with hemostasis, J. Exp. Med. 203 (2006) 513–518. doi:10.1084/jem.20052458.

[37] E.D. Rosen, J.C. Chan, E. Idusogie, F. Clotman, G. Vlasuk, T. Luther, et al., Mice lacking factor VII develop normally but suffer fatal perinatal bleeding, Nature. 390 (1997) 290–294. doi:10.1038/36862.

[38] M. Dewerchin, Z. Liang, L. Moons, P. Carmeliet, F.J. Castellino, D. Collen, et al., Blood coagulation factor X deficiency causes partial embryonic lethality and fatal neonatal bleeding in mice, Thromb. Haemost. 83 (2000) 185–190.

[39] T.L. Yang, J. Cui, J.M. Taylor, A. Yang, S.B. Gruber, D. Ginsburg, Rescue of fatal neonatal hemorrhage in factor V deficient mice by low level transgene expression, Thromb. Haemost. 83 (2000) 70–77.

[40] H.J. Weiss, V.T. Turitto, H.R. Baumgartner, Effect of shear rate on platelet interaction with subendothelium in citrated and native blood. I. Shear rate--dependent decrease of adhesion in von Willebrand's disease and the Bernard-Soulier syndrome, J. Lab. Clin. Med. 92 (1978) 750–764.

[41] T.W. Chow, J.D. Hellums, J.L. Moake, M.H. Kroll, Shear stress-induced von Willebrand factor binding to platelet glycoprotein Ib initiates calcium influx associated with aggregation, Blood. 80 (1992) 113–120.

[42] J.J. Hathcock, Flow effects on coagulation and thrombosis, Arterioscler. Thromb. Vasc. Biol. 26 (2006) 1729–1737. doi:10.1161/01.ATV.0000229658.76797.30.

[43] S.R. Hanson, K.S. Sakariassen, Blood flow and antithrombotic drug effects, Am. Heart J. 135 (1998) S132–S145.

[44] G.D.O. Lowe, Virchow's triad revisited: Abnormal flow, Pathophysiol. Haemost. Thromb. 33 (2003) 455–457. doi:10.1159/000083845.

[45] W. van Oeveren, I.F. Tielliu, J. de Hart, Comparison of Modified Chandler, Roller Pump, and Ball Valve Circulation Models for In Vitro Testing in High Blood Flow Conditions: Application in Thrombogenicity Testing of Different Materials for Vascular Applications, Int. J. Biomater. 2012 (2012). doi:10.1155/2012/673163.

[46] S.R. Hanson, L.A. Harker, B.D. Ratner, A.S. Hoffman, In vivo evaluation of artificial surfaces with a nonhuman primate model of arterial thrombosis, J. Lab. Clin. Med. 95 (1980) 289–304.

[47] S.R. Hanson, J.H. Griffin, L.A. Harker, A.B. Kelly, C.T. Esmon, A. Gruber, Antithrombotic effects of thrombin-induced activation of endogenous protein C in primates, J. Clin. Invest. 92 (1993) 2003–2012. doi:10.1172/JCI116795.

[48] Y. Cadroy, S.R. Hanson, A.B. Kelly, U.M. Marzec, B.L. Evatt, T.J. Kunicki, et al., Relative antithrombotic effects of monoclonal antibodies targeting different platelet glycoprotein-adhesive molecule interactions in nonhuman primates, Blood. 83 (1994) 3218–3224.

[49] A. Gruber, S.R. Hanson, A.B. Kelly, B.S. Yan, N. Bang, J.H. Griffin, et al., Inhibition of thrombus formation by activated recombinant protein C in a primate model of arterial thrombosis, Circulation. 82 (1990) 578–585.

[50] E.I. Tucker, U.M. Marzec, T.C. White, S. Hurst, S. Rugonyi, O.J.T. McCarty, et al., Prevention of vascular graft occlusion and thrombus-associated thrombin generation by inhibition of factor XI, Blood. 113 (2009) 936–944. doi:10.1182/blood-2008-06-163675.

[51] Q. Cheng, E.I. Tucker, M.S. Pine, I. Sisler, A. Matafonov, M.-F. Sun, et al., A role for factor XIIa-mediated factor XI activation in thrombus formation in vivo, Blood. 116 (2010) 3981–3989. doi:10.1182/blood-2010-02-270918.

[52] M.W.C. Hatton, S.L. Moar, M. Richardson, Deendothelialization in vivo initiates a thrombogenic reaction at the rabbit aorta surface. Correlation of uptake of fibrinogen and antithrombin III with thrombin generation by the exposed subendothelium, Am. J. Pathol. 135 (1989) 499–508.

[53] M. Richardson, M.W.C. Hatton, M.R. Buchanan, S. Moore, Wound healing in the media of the normolipemic rabbit carotid artery injured by air drying or by balloon catheter de-endothelialization, Am. J. Pathol. 137 (1990) 1453–1465.

[54] A.C. Thomas, J.H. Campbell, Differences in response of rat and rabbit arteries to injury, Biomed. Res. India. 11 (2000) 189–196.

[55] S. Li, J.J.D. Henry, Nonthrombogenic Approaches to Cardiovascular Bioengineering, Annu. Rev. Biomed. Eng. 13 (2011) 451–475. doi:10.1146/annurev-bioeng-071910-124733.

[56] M.W. Radomski, R.M.J. Palmer, S. Moncada, ENDOGENOUS NITRIC OXIDE INHIBITS HUMAN PLATELET ADHESION TO VASCULAR ENDOTHELIUM, The Lancet. 330 (1987) 1057–1058. doi:10.1016/S0140-6736(87)91481-4.

[57] Z.M. Ruggeri, Platelets in atherothrombosis, Nat. Med. 8 (2002) 1227–1234. doi:10.1038/nm1102-1227.

[58] B.F. Becker, D. Chappell, D. Bruegger, T. Annecke, M. Jacob, Therapeutic strategies targeting the endothelial glycocalyx: acute deficits, but great potential, Cardiovasc. Res. 87 (2010) 300–310. doi:10.1093/cvr/cvq137.

[59] J.A. Florian, J.R. Kosky, K. Ainslie, Z. Pang, R.O. Dull, J.M. Tarbell, Heparan Sulfate Proteoglycan Is a Mechanosensor on Endothelial Cells, Circ. Res. 93 (2003) e136–e142. doi:10.1161/01.RES.0000101744.47866.D5.

[60] J.H. Griffin, J.A. Fernández, A.J. Gale, L.O. Mosnier, Activated protein C, J. Thromb. Haemost. 5 (2007) 73–80. doi:10.1111/j.1538-7836.2007.02491.x.

[61] C.T. Esmon, W.G. Owen, The discovery of thrombomodulin, J. Thromb. Haemost. 2 (2004) 209–213. doi:10.1046/j.1538-7933.2003.00537.x.

[62] I. Martinelli, V. De Stefano, P.M. Mannucci, Inherited risk factors for venous thromboembolism, Nat. Rev. Cardiol. 11 (2014) 140–156. doi:10.1038/nrcardio.2013.211.

[63] D.J. Stearns-Kurosawa, S. Kurosawa, J.S. Mollica, G.L. Ferrell, C.T. Esmon, The endothelial cell protein C receptor augments protein C activation by the thrombin-thrombomodulin complex, Proc. Natl. Acad. Sci. 93 (1996) 10212–10216.

[64] Z. Laszik, A. Mitro, F.B. Taylor Jr., G. Ferrell, C.T. Esmon, Human protein C receptor is present primarily on endothelium of large blood vessels: Implications for the control of the protein C pathway, Circulation. 96 (1997) 3633–3640.

[65] L.O. Mosnier, B.V. Zlokovic, J.H. Griffin, The cytoprotective protein C pathway, Blood. 109 (2007) 3161–3172. doi:10.1182/blood-2006-09-003004.

[66] M. Riewald, R.J. Petrovan, A. Donner, W. Ruf, Activated protein C signals through the thrombin receptor PAR1 in endothelial cells, J. Endotoxin Res. 9 (2003) 317–321. doi:10.1179/096805103225002584.

[67] M.V. de Wouwer, Thrombomodulin-Protein C-EPCR System: Integrated to Regulate Coagulation and Inflammation, Arterioscler. Thromb. Vasc. Biol. 24 (2004) 1374–1383. doi:10.1161/01.ATV.0000134298.25489.92.

[68] F.B. Taylor Jr., D.J. Stearns-Kurosawa, S. Kurosawa, G. Ferrell, A.C.K. Chang, Z. Laszik, et al., The endothelial cell proten C receptor aids in host defense against Escherichia coli sepsis, Blood. 95 (2000) 1680–1686.

[69] W.A. Dittman, P.W. Majerus, Structure and function of thrombomodulin: a natural anticoagulant, Blood. 75 (1990) 329–336.

[70] E.M. Conway, Thrombomodulin and its role in inflammation, Semin. Immunopathol. 34 (2012) 107–125. doi:10.1007/s00281-011-0282-8.

[71] E.M. Conway, M. Van de Wouwer, S. Pollefeyt, K. Jurk, H. Van Aken, A. De Vriese, et al., The Lectin-like Domain of Thrombomodulin Confers Protection from Neutrophil-mediated Tissue Damage by Suppressing Adhesion Molecule Expression via Nuclear Factor κB and Mitogen-activated Protein Kinase Pathways, J. Exp. Med. 196 (2002) 565–577. doi:10.1084/jem.20020077.

[72] C.-S. Shi, G.-Y. Shi, S.-M. Hsiao, Y.-C. Kao, K.-L. Kuo, M. Chih-Yuan, et al., Lectin-like domain of thrombomodulin binds to its specific ligand Lewis y antigen and neutralizes lipopolysaccharide-induced inflammatory response, Blood. 112 (2008) 3661–3670. doi:10.1182/blood-2008-03-142760.

[73] M. Zushi, K. Gomi, S. Yamamoto, I. Maruyama, T. Hayashi, K. Suzuki, The last three consecutive epidermal growth factor-like structures of human thrombomodulin comprise the minimum functional domain for protein C-activating cofactor activity and anticoagulant activity, J. Biol. Chem. 264 (1989) 10351–10353.

[74] M. Tsiang, S.R. Lentz, J.E. Sadler, Functional domains of membrane-bound human thrombomodulin. EGF-like domains four to six and the serine/threonine-rich domain are required for cofactor activity, J. Biol. Chem. 267 (1992) 6164–6170.

[75] P. Fuentes-Prior, Y. Iwanaga, R. Huber, R. Pagila, G. Rumennik, M. Seto, et al., Structural basis for the anticoagulant activity of the thrombin–thrombomodulin complex, Nature. 404 (2000) 518–525. doi:10.1038/35006683.

[76] C.B. Glaser, J. Morser, J.H. Clarke, E. Blasko, K. McLean, I. Kuhn, et al., Oxidation of a specific methionine in thrombomodulin by activated neutrophil products blocks cofactor activity. A potential rapid mechanism for modulation of coagulation, J. Clin. Invest. 90 (1992) 2565–2573.

[77] J.H. Clarke, D.R. Light, E. Blasko, J.F. Parkinson, M. Nagashima, K. McLean, et al., The short loop between epidermal growth factor-like domains 4 and 5 is critical for human thrombomodulin function, J. Biol. Chem. 268 (1993) 6309–6315.

[78] M. Nagashima, E. Lundh, J.C. Leonard, J. Morser, J.F. Parkinson, Alanine-scanning mutagenesis of the epidermal growth factor-like domains of human thrombomodulin identifies critical residues for its cofactor activity, J. Biol. Chem. 268 (1993) 2888–2892.

[79] J.R. Koeppe, M.A. Beach, A. Baerga-Ortiz, S.J. Kerns, E.A. Komives, Mutations in the fourth EGF-like domain affect thrombomodulin-induced changes in the active site of thrombin, Biochemistry (Mosc.). 47 (2008) 10933–10939. doi:10.1021/bi8008278.

[80] M.C. Bourin, E. Lundgren-Akerlund, U. Lindahl, Isolation and characterization of the glycosaminoglycan component of rabbit thrombomodulin proteoglycan, J. Biol. Chem. 265 (1990) 15424–15431.

[81] A. Slungaard, G.M. Vercellotti, T. Tran, G.J. Gleich, N.S. Key, Eosinophil cationic granule proteins impair thrombomodulin function. A potential mechanism for thromboembolism in hypereosinophilic heart disease, J. Clin. Invest. 91 (1993) 1721–1730. doi:10.1172/JCI116382.

[82] A.R. Rezaie, S.T. Cooper, F.C. Church, C.T. Esmon, Protein C Inhibitor Is a Potent Inhibitor of the Thrombin-Thrombomodulin Complex, J. Biol. Chem. 270 (1995) 25336–25339. doi:10.1074/jbc.270.43.25336.

[83] C.T. Esmon, The Protein C Pathway, CHEST J. 124 (2003) 26S–32S. doi:10.1378/chest.124.3_suppl.26S.

[84] Y. Dargaud, J.Y. Scoazec, S.J.H. Wielders, C. Trzeciak, T.M. Hackeng, C. Négrier, et al., Characterization of an autosomal dominant bleeding disorder caused by a thrombomodulin mutation, Blood. 125 (2015) 1497–1501. doi:10.1182/blood-2014-10-604553.

[85] W.A. Dittman, T. Kumada, J.E. Sadler, P.W. Majerus, The structure and function of mouse thrombomodulin. Phorbol myristate acetate stimulates degradation and synthesis of thrombomodulin without affecting mRNA levels in hemangioma cells, J. Biol. Chem. 263 (1988) 15815–15822.

[86] K.L. Moore, C.T. Esmon, N.L. Esmon, Tumor necrosis factor leads to the internalization and degradation of thrombomodulin from the surface of bovine aortic endothelial cells in culture, Blood. 73 (1989) 159–165.

[87] S.R. Coughlin, Thrombin signalling and protease-activated receptors, Nature. 407 (2000) 258–264. doi:10.1038/35025229.

[88] B. Dahlbäck, M. Carlsson, P.J. Svensson, Familial thrombophilia due to a previously unrecognized mechanism characterized by poor anticoagulant response to activated protein C: prediction of a cofactor to activated protein C., Proc. Natl. Acad. Sci. U. S. A. 90 (1993) 1004–1008.

[89] J.S. Greengard, X. Sun, X. Xu, J.A. Fernandez, J.H. Griffin, B. Evatt, Activated protein C resistance caused by Arg506Gln mutation in factor Va, Lancet Lond. Engl. 343 (1994) 1361–1362.

[90] J.C. Rau, L.M. Beaulieu, J.A. Huntington, F.C. Church, Serpins in thrombosis, hemostasis and fibrinolysis, J. Thromb. Haemost. 5 (2007) 102–115. doi:10.1111/j.1538-7836.2007.02516.x.

[91] J.-S. Bae, L. Yang, A.R. Rezaie, Receptors of the protein C activation and activated protein C signaling pathways are colocalized in lipid rafts of endothelial cells, Proc. Natl. Acad. Sci. 104 (2007) 2867–2872. doi:10.1073/pnas.0611493104.

[92] L. Wang, R. Jiang, X.-L. Sun, Recombinant Thrombomodulin of Different Domains for Pharmaceutical, Biomedical, and Cell Transplantation Applications, Med. Res. Rev. 34 (2014) 479–502. doi:10.1002/med.21294.

[93] J.H. Griffin, B.V. Zlokovic, L.O. Mosnier, Activated protein C: biased for translation, Blood. (2015) blood–2015–02–355974. doi:10.1182/blood-2015-02-355974.

[94] F.B. Taylor, A. Chang, C.T. Esmon, A. D'Angelo, S. Vigano-D'Angelo, K.E. Blick, Protein C prevents the coagulopathic and lethal effects of Escherichia coli infusion in the baboon., J. Clin. Invest. 79 (1987) 918–925.

[95] G.R. Bernard, J.-L. Vincent, P.-F. Laterre, S.P. LaRosa, J.-F. Dhainaut, A. Lopez-Rodriguez, et al., Efficacy and safety of recombinant human activated protein C for severe sepsis, N. Engl. J. Med. 344 (2001) 699–709. doi:10.1056/NEJM200103083441001.

[96] S. Ridley, D. Wyncoll, The withdrawal of Xigris, J. Intensive Care Soc. 13 (2012) 7–9.

[97] L.M. Quinn, C. Drakeford, J.S. O'Donnell, R.J.S. Preston, Engineering activated protein C to maximize therapeutic efficacy, Biochem. Soc. Trans. 43 (2015) 691–695. doi:10.1042/BST20140312.

[98] L.O. Mosnier, A.J. Gale, S. Yegneswaran, J.H. Griffin, Activated protein C variants with normal cytoprotective but reduced anticoagulant activity, Blood. 104 (2004) 1740–1744. doi:10.1182/blood-2004-01-0110.

[99] H. Saito, I. Maruyama, S. Shimazaki, Y. Yamamoto, N. Aikawa, R. Ohno, et al., Efficacy and safety of recombinant human soluble thrombomodulin (ART-123) in disseminated intravascular coagulation: Results of a phase III, randomized, double-blind clinical trial, J. Thromb. Haemost. 5 (2007) 31–41. doi:10.1111/j.1538-7836.2006.02267.x.

[100] J.-L. Vincent, M.K. Ramesh, D. Ernest, S.P. Larosa, J. Pachl, N. Aikawa, et al., A randomized, double-blind, placebo-controlled, phase 2b Study to evaluate the safety and efficacy of recombinant human soluble thrombomodulin, ART-123, in patients with sepsis and suspected disseminated intravascular coagulation, Crit. Care Med. 41 (2013) 2069–2079. doi:10.1097/CCM.0b013e31828e9b03.

[101] E.J. Su, M. Geyer, M. Wahl, K. Mann, D. Ginsburg, H. Brohmann, et al., The thrombomodulin analog Solulin promotes reperfusion and reduces infarct volume in a thrombotic stroke model, J. Thromb. Haemost. 9 (2011) 1174–1182. doi:10.1111/j.1538-7836.2011.04269.x.

[102] T. Van Iersel, H. Stroissnig, P. Giesen, J. Wemer, K. Wilhelm-Ogunbiyi, Phase I study of Solulin, a novel recombinant soluble human thrombomodulin analogue, Thromb. Haemost. 105 (2011) 302–312. doi:10.1160/TH10-05-0287.

[103] T. Asahara, T. Murohara, A. Sullivan, M. Silver, R. Van Der Zee, T. Li, et al., Isolation of putative progenitor endothelial cells for angiogenesis, Science. 275 (1997) 964–967. doi:10.1126/science.275.5302.964.

[104] M. Vasa, S. Fichtlscherer, A. Aicher, K. Adler, C. Urbich, H. Martin, et al., Number and Migratory Activity of Circulating Endothelial Progenitor Cells Inversely

Correlate With Risk Factors for Coronary Artery Disease, Circ. Res. 89 (2001) e1–e7. doi:10.1161/hh1301.093953.

[105] U. Laufs, N. Werner, A. Link, M. Endres, S. Wassmann, K. Jürgens, et al., Physical training increases endothelial progenitor cells, inhibits neointima formation, and enhances angiogenesis, Circulation. 109 (2004) 220–226. doi:10.1161/01.CIR.0000109141.48980.37.

[106] R. Du, K.V. Lu, C. Petritsch, P. Liu, R. Ganss, E. Passegué, et al., HIF1α Induces the Recruitment of Bone Marrow-Derived Vascular Modulatory Cells to Regulate Tumor Angiogenesis and Invasion, Cancer Cell. 13 (2008) 206–220. doi:10.1016/j.ccr.2008.01.034.

[107] T. Takahashi, C. Kalka, H. Masuda, D. Chen, M. Silver, M. Kearney, et al., Ischemia- and cytokine-induced mobilization of bone marrow-derived endothelial progenitor cells for neovascularization, Nat. Med. 5 (1999) 434–438. doi:10.1038/7434.

[108] D.P. Griese, A. Ehsan, L.G. Melo, D. Kong, L. Zhang, M.J. Mann, et al., Isolation and Transplantation of Autologous Circulating Endothelial Cells into Denuded Vessels and Prosthetic Grafts: Implications for Cell-Based Vascular Therapy, Circulation. 108 (2003) 2710–2715. doi:10.1161/01.CIR.0000096490.16596.A6.

[109] T. Asahara, A. Kawamoto, H. Masuda, Concise review: Circulating endothelial progenitor cells for vascular medicine, Stem Cells. 29 (2011) 1650–1655. doi:10.1002/stem.745.

[110] A.Y. Chong, A.D. Blann, J. Patel, B. Freestone, E. Hughes, G.Y.H. Lip, Endothelial dysfunction and damage in congestive heart failure: Relation of flow-mediated dilation to circulating endothelial cells, plasma indexes of endothelial damage, and brain natriuretic peptide, Circulation. 110 (2004) 1794–1798. doi:10.1161/01.CIR.0000143073.60937.50.

[111] K.W. Lee, G.Y.H. Lip, M. Tayebjee, W. Foster, A.D. Blann, Circulating endothelial cells, von Willebrand factor, interleukin-6, and prognosis in patients with acute coronary syndromes, Blood. 105 (2005) 526–532. doi:10.1182/blood-2004-03-1106.

[112] P.K.Y. Goon, G.Y.H. Lip, C.J. Boos, P.S. Stonelake, A.D. Blann, Circulating Endothelial Cells, Endothelial Progenitor Cells, and Endothelial Microparticles in Cancer, Neoplasia N. Y. N. 8 (2006) 79–88.

[113] D.E. Schmidt, M. Manca, I.E. Hoefer, Circulating endothelial cells in coronary artery disease and acute coronary syndrome, Trends Cardiovasc. Med. 25 (2015) 578–587. doi:10.1016/j.tcm.2015.01.013.

[114] M. Mutunga, B. Fulton, R. Bullock, A. Batchelor, A. Gascoigne, J.I. Gillespie, et al., Circulating endothelial cells in patients with septic shock, Am. J. Respir. Crit. Care Med. 163 (2001) 195–200.

[115] R. Clancy, G. Marder, V. Martin, H.M. Belmont, S.B. Abramson, J. Buyon, Circulating activated endothelial cells in systemic lupus erythematosus: Further evidence for diffuse vasculopathy, Arthritis Rheum. 44 (2001) 1203–1208. doi:10.1002/1529-0131(200105)44:5<1203::AID-ANR204>3.0.CO;2-C.

[116] G. Fürstenberger, R. Von Moos, R. Lucas, B. Thürlimann, H.-J. Senn, J. Hamacher, et al., Circulating endothelial cells and angiogenic serum factors during neoadjuvant chemotherapy of primary breast cancer, Br. J. Cancer. 94 (2006) 524–531. doi:10.1038/sj.bjc.6602952.

[117] L.V. Beerepoot, N. Mehra, J.S.P. Vermaat, B.A. Zonnenberg, M.F.G.B. Gebbink, E.E. Voest, Increased levels of viable circulating endothelial cells are an indicator of progressive disease in cancer patients, Ann. Oncol. 15 (2004) 139–145. doi:10.1093/annonc/mdh017.

[118] P. Mancuso, A. Burlini, G. Pruneri, A. Goldhirsch, G. Martinelli, F. Bertolini, Resting and activated endothelial cells are increased in the peripheral blood of cancer patients, Blood. 97 (2001) 3658–3661. doi:10.1182/blood.V97.11.3658.

[119] F. Bertolini, Y. Shaked, P. Mancuso, R.S. Kerbel, The multifaceted circulating endothelial cell in cancer: Towards marker and target identification, Nat. Rev. Cancer. 6 (2006) 835–845. doi:10.1038/nrc1971.

[120] J.A. Mund, M.L. Estes, M.C. Yoder, D.A. Ingram, J. Case, Flow cytometric identification and functional characterization of immature and mature circulating endothelial cells, Arterioscler. Thromb. Vasc. Biol. 32 (2012) 1045–1053. doi:10.1161/ATVBAHA.111.244210.

[121] M. Hristov, S. Schmitz, F. Nauwelaers, C. Weber, A flow cytometric protocol for enumeration of endothelial progenitor cells and monocyte subsets in human blood, J. Immunol. Methods. 381 (2012) 9–13. doi:10.1016/j.jim.2012.04.003.

[122] M.C. Yoder, L.E. Mead, D. Prater, T.R. Krier, K.N. Mroueh, F. Li, et al., Redefining endothelial progenitor cells via clonal analysis and hematopoietic stem/progenitor cell principals, Blood. 109 (2007) 1801–1809. doi:10.1182/blood-2006-08-043471.

[123] D.G. Duda, K.S. Cohen, D.T. Scadden, R.K. Jain, A protocol for phenotypic detection and enumeration of circulating endothelial cells and circulating progenitor cells in human blood, Nat. Protoc. 2 (2007) 805–810. doi:10.1038/nprot.2007.111.

[124] C.G. Willett, Y. Boucher, E. di Tomaso, D.G. Duda, L.L. Munn, R.T. Tong, et al., Direct evidence that the VEGF-specific antibody bevacizumab has antivascular effects in human rectal cancer, Nat. Med. 10 (2004) 145–147. doi:10.1038/nm988.

[125] D.A. Ingram, N.M. Caplice, M.C. Yoder, Unresolved questions, changing definitions, and novel paradigms for defining endothelial progenitor cells, Blood. 106 (2005) 1525–1531. doi:10.1182/blood-2005-04-1509.

[126] Y. Lin, D.J. Weisdorf, A. Solovey, R.P. Hebbel, Origins of circulating endothelial cells and endothelial outgrowth from blood, J. Clin. Invest. 105 (2000) 71–77.

[127] Biomaterials Science:: An Introduction to Materials in Medicine, 1st edition, Academic Press, 1997.

[128] D.F. Williams, Definitions in biomaterials., Elsevier Amst. 26 (1987) 414–414. doi:10.1002/pol.1988.140260910.

[129] J.D. Bryers, C.M. Giachelli, B.D. Ratner, Engineering biomaterials to integrate and heal: The biocompatibility paradigm shifts, Biotechnol. Bioeng. 109 (2012) 1898–1911. doi:10.1002/bit.24559.

[130] M. Gaddh, A. Antun, K. Yamada, P. Gupta, H. Tran, F.E. Rassi, et al., Venous access catheter-related thrombosis in patients with cancer, Leuk. Lymphoma. 55 (2014) 501–508. doi:10.3109/10428194.2013.813503.

[131] R.D. Lopes, R.H. Mehta, G.E. Hafley, J.B. Williams, M.J. Mack, E.D. Peterson, et al., Relationship Between Vein Graft Failure and Subsequent Clinical Outcomes After Coronary Artery Bypass Surgery, Circulation. 125 (2012) 749–756. doi:10.1161/CIRCULATIONAHA.111.040311.

[132] S. Garg, P.W. Serruys, Coronary StentsCurrent Status, J. Am. Coll. Cardiol. 56 (2010) S1–S42. doi:10.1016/j.jacc.2010.06.007.

[133] C.F. Wertz, M.M. Santore, Adsorption and relaxation kinetics of albumin and fibrinogen on hydrophobic surfaces: Single-species and competitive behavior, Langmuir. 15 (1999) 8884–8894. doi:10.1021/la990089q.

[134] S. Nagaoka, A. Nakao, Clinical application of antithrombogenic hydrogel with long poly (ethylene oxide) chains, Biomaterials. 11 (1990) 119–121. doi:10.1016/0142-9612(90)90126-B.

[135] N.A. Alcantar, E.S. Aydil, J.N. Israelachvili, Polyethylene glycol–coated biocompatible surfaces, J. Biomed. Mater. Res. 51 (2000) 343–351. doi:10.1002/1097-4636(20000905)51:3<343::AID-JBM7>3.0.CO;2-D.

[136] M. Amiji, K. Park, Prevention of protein adsorption and platelet adhesion on surfaces by PEO/PPO/PEO triblock copolymers, Biomaterials. 13 (1992) 682–692. doi:10.1016/0142-9612(92)90128-B.

[137] L. Li, S. Chen, J. Zheng, B.D. Ratner, S. Jiang, Protein adsorption on oligo(ethylene glycol)-terminated alkanethiolate self-assembled monolayers: The

molecular basis for nonfouling behavior, J. Phys. Chem. B. 109 (2005) 2934–2941. doi:10.1021/jp0473321.

[138] M. Fischer, C. Sperling, P. Tengvall, C. Werner, The ability of surface characteristics of materials to trigger leukocyte tissue factor expression, Biomaterials. 31 (2010) 2498–2507. doi:10.1016/j.biomaterials.2009.12.016.

[139] B.D. Ratner, The Catastrophe Revisited, Biomaterials. 28 (2007) 5144–5147. doi:10.1016/j.biomaterials.2007.07.035.

[140] R.Y. Kannan, H.J. Salacinski, P.E. Butler, G. Hamilton, A.M. Seifalian, Current status of prosthetic bypass grafts: A review, J. Biomed. Mater. Res. - Part B Appl. Biomater. 74 (2005) 570–581. doi:10.1002/jbm.b.30247.

[141] D.J. Farrar, Development of a prosthetic coronary artery bypass graft, Heart Surg. Forum. 3 (2000) 36–40.

[142] F.W. Hehrlein, M. Schlepper, F. Loskot, H.H. Scheld, P. Walter, J. Mulch, The use of expanded polytetrafluoroethylene (PTFE) grafts for myocardial revascularization, J. Cardiovasc. Surg. (Torino). 25 (1984) 549–553.

[143] K. Berger, L.R. Sauvage, A.M. Rao, S.J. Wood, Healing of arterial prostheses in man: its incompleteness., Ann. Surg. 175 (1972) 118–127.

[144] P. Zilla, D. Bezuidenhout, P. Human, Prosthetic vascular grafts: Wrong models, wrong questions and no healing, Biomaterials. 28 (2007) 5009–5027. doi:10.1016/j.biomaterials.2007.07.017.

[145] P. Zilla, R. Fasol, U. Dudeck, S. Siedler, P. Preiss, T. Fischlein, et al., In situ cannulation, microgrid follow-up and low-density plating provide first passage endothelial cell masscultures for in vitro lining, J. Vasc. Surg. 12 (1990) 180–189. doi:10.1016/0741-5214(90)90106-K.

[146] J. Meinhart, M. Halbmayer, P. Zilla, M. Deutsch, Reversible growth impairment of autologous endothelial cell cultures due to hyperlipidemia, Cardiovasc Pathol. 7 (1988) 275.

[147] J. Kaehler, P. Zilla, R. Fasol, M. Deutsch, M. Kadletz, Precoating substrate and surface configuration determine adherence and spreading of seeded endothelial cells on polytetrafluoroethylene grafts, J. Vasc. Surg. 9 (1989) 535–541. doi:10.1016/0741-5214(89)90469-2.

[148] M. Deutsch, J. Meinhart, T. Fischlein, P. Preiss, P. Zilla, Clinical autologous in vitro endothelialization of infrainguinal ePTFE grafts in 100 patients: A 9-year experience, Surgery. 126 (1999) 847–855. doi:10.1016/S0039-6060(99)70025-5.

[149] J.G. Meinhart, M. Deutsch, T. Fischlein, N. Howanietz, A. Fröschl, P. Zilla, Clinical autologous in vitro endothelialization of 153 infrainguinal ePTFE grafts, Ann. Thorac. Surg. 71 (2001) S327–S331. doi:10.1016/S0003-4975(01)02555-3.

[150] F.J. Veith, S.K. Gupta, E. Ascer, S. White-Flores, R.H. Samson, L.A. Scher, et al., Six-year prospective multicenter randomized comparison of autologous saphenous vein and expanded polytetrafluoroethylene grafts in infrainguinal arterial reconstructions, J. Vasc. Surg. 3 (1986) 104–114.

[151] M.R. Jackson, T.P. Belott, T. Dickason, W.J. Kaiser, J.G. Modrall, R.J. Valentine, et al., The consequences of a failed femoropopliteal bypass grafting: Comparison of saphenous vein and PTFE grafts, J. Vasc. Surg. 32 (2000) 498–505. doi:10.1067/mva.2000.108634.

[152] L. Norgren, W.R. Hiatt, J.A. Dormandy, M.R. Nehler, K.A. Harris, F.G.R. Fowkes, et al., Inter-Society Consensus for the Management of Peripheral Arterial Disease (TASC II), J. Vasc. Surg. 45 Suppl S (2007) S5–67. doi:10.1016/j.jvs.2006.12.037.

[153] A.J. Melchiorri, N. Hibino, J.P. Fisher, Strategies and techniques to enhance the in situ endothelialization of small-diameter biodegradable polymeric vascular grafts, Tissue Eng. - Part B Rev. 19 (2013) 292–307. doi:10.1089/ten.teb.2012.0577.

[154] M. Zhou, Z. Liu, K. Li, W. Qiao, X. Jiang, F. Ran, et al., Beneficial effects of granulocyte-colony stimulating factor on small-diameter heparin immobilized decellularized vascular graft, J. Biomed. Mater. Res. A. 95 (2010) 600–610. doi:10.1002/jbm.a.32864.

[155] U. Edlund, T. Sauter, A.-C. Albertsson, Covalent VEGF protein immobilization on resorbable polymeric surfaces, Polym. Adv. Technol. 22 (2011) 166–171. doi:10.1002/pat.1811.

[156] G. De Visscher, L. Mesure, B. Meuris, A. Ivanova, W. Flameng, Improved endothelialization and reduced thrombosis by coating a synthetic vascular graft with fibronectin and stem cell homing factor SDF-1α, Acta Biomater. 8 (2012) 1330–1338. doi:10.1016/j.actbio.2011.09.016.

[157] J. Aoki, P.W. Serruys, H. Van Beusekom, A.T.L. Ong, E.P. McFadden, G. Sianos, et al., Endothelial progenitor cell capture by stents coated with antibody against CD34: The HEALING-FIM (Healthy Endothelial Accelerated Lining Inhibits Neointimal Growth-First in Man) registry, J. Am. Coll. Cardiol. 45 (2005) 1574–1579. doi:10.1016/j.jacc.2005.01.048.

[158] B.D. Markway, O.J.T. McCarty, U.M. Marzec, D.W. Courtman, S.R. Hanson, M.T. Hinds, Capture of flowing endothelial cells using surface-immobilized anti-kinase insert domain receptor antibody., Tissue Eng. Part C Methods. 14 (2008) 97–105. doi:10.1089/ten.tec.2007.0300.

[159] E.T.H. Yeh, S. Zhang, H.D. Wu, M. Körbling, J.T. Willerson, Z. Estrov, Transdifferentiation of human peripheral blood CD34+-enriched cell population into cardiomyocytes, endothelial cells, and smooth muscle cells in vivo, Circulation. 108 (2003) 2070–2073. doi:10.1161/01.CIR.0000099501.52718.70.

[160] C. Tuerk, L. Gold, Systematic evolution of ligands by exponential enrichment: RNA ligands to bacteriophage T4 DNA polymerase, Science. 249 (1990) 505–510.

[161] J. Hoffmann, A. Paul, M. Harwardt, J. Groll, T. Reeswinkel, D. Klee, et al., Immobilized DNA aptamers used as potent attractors for porcine endothelial precursor cells, J. Biomed. Mater. Res. A. 84 (2008) 614–621. doi:10.1002/jbm.a.31309.

[162] E. Uhlmann, A. Ryte, A. Peyman, Studies on the mechanism of stabilization of partially phosphorothioated oligonucleotides against nucleolytic degradation, Antisense Nucleic Acid Drug Dev. 7 (1997) 345–350.

[163] U. Hersel, C. Dahmen, H. Kessler, RGD modified polymers: biomaterials for stimulated cell adhesion and beyond, Biomaterials. 24 (2003) 4385–4415. doi:10.1016/S0142-9612(03)00343-0.

[164] P.H. Blit, W.G. McClung, J.L. Brash, K.A. Woodhouse, J.P. Santerre, Platelet inhibition and endothelial cell adhesion on elastin-like polypeptide surface modified materials, Biomaterials. 32 (2011) 5790–5800. doi:10.1016/j.biomaterials.2011.04.067.

[165] M.R. Cesarone, G. Belcaro, A.N. Nicolaides, G. Geroulakos, M. Griffin, L. Incandela, et al., “Real” epidemiology of varicose veins and chronic venous diseases: The San Valentino Vascular Screening Project, Angiology. 53 (2002) 119–130.

[166] R.T. Eberhardt, J.D. Raffetto, Chronic venous insufficiency, Circulation. 111 (2005) 2398–2409. doi:10.1161/01.CIR.0000164199.72440.08.

[167] R.M. Kaplan, M.H. Criqui, J.O. Denenberg, J. Bergan, A. Fronek, Quality of life in patients with chronic venous disease: San Diego population study, J. Vasc. Surg. 37 (2003) 1047–1053. doi:10.1067/mva.2003.168.

[168] M.S. Gohel, J.R. Barwell, M. Taylor, T. Chant, C. Foy, J.J. Earnshaw, et al., Long term results of compression therapy alone versus compression plus surgery in chronic venous ulceration (ESCHAR): Randomised controlled trial, Br. Med. J. 335 (2007) 83–87. doi:10.1136/bmj.39216.542442.BE.

[169] P. Gloviczki, A.J. Comerota, M.C. Dalsing, B.G. Eklof, D.L. Gillespie, M.L. Gloviczki, et al., The care of patients with varicose veins and associated chronic venous diseases: Clinical practice guidelines of the Society for Vascular Surgery

and the American Venous Forum, J. Vasc. Surg. 53 (2011) 2S–48S. doi:10.1016/j.jvs.2011.01.079.

[170] O. Maleti, M. Perrin, Reconstructive surgery for deep vein reflux in the lower limbs: techniques, results and indications, Eur. J. Vasc. Endovasc. Surg. Off. J. Eur. Soc. Vasc. Surg. 41 (2011) 837–848. doi:10.1016/j.ejvs.2011.02.013.

[171] A.N. Nicolaides, C. Allegra, J. Bergan, A. Bradbury, M. Cairols, P. Carpentier, et al., Management of chronic venous disorders of the lower limbs guidelines according to scientific evidence, Int. Angiol. 27 (2008) 1–59.

[172] C. Zervides, A.D. Giannoukas, Historical overview of venous valve prostheses for the treatment of deep venous valve insufficiency, J. Endovasc. Ther. 19 (2012) 281–290.

[173] A.S. Go, D. Mozaffarian, V.L. Roger, E.J. Benjamin, J.D. Berry, W.B. Borden, et al., Heart disease and stroke statistics-2013 update: A Report from the American Heart Association, Circulation. 127 (2013) e6–e245. doi:10.1161/CIR.0b013e31828124ad.

[174] R.B. Chard, D.C. Johnson, G.R. Nunn, T.B. Cartmill, Aorta-coronary bypass grafting with polytetrafluoroethylene conduits. Early and late outcome in eight patients, J. Thorac. Cardiovasc. Surg. 94 (1987) 132–134.

[175] P. Klinkert, P.N. Post, P.J. Breslau, J.H. van Bockel, Saphenous vein versus PTFE for above-knee femoropopliteal bypass. A review of the literature, Eur. J. Vasc. Endovasc. Surg. Off. J. Eur. Soc. Vasc. Surg. 27 (2004) 357–362. doi:10.1016/j.ejvs.2003.12.027.

[176] J. Chlupác, E. Filová, L. Bacáková, Blood vessel replacement: 50 years of development and tissue engineering paradigms in vascular surgery, Physiol. Res. Acad. Sci. Bohemoslov. 58 Suppl 2 (2009) S119–139.

[177] M. Deutsch, J. Meinhart, P. Zilla, N. Howanietz, M. Gorlitzer, A. Froeschl, et al., Long-term experience in autologous in vitro endothelialization of infrainguinal ePTFE grafts, J. Vasc. Surg. 49 (2009) 352–362. doi:10.1016/j.jvs.2008.08.101.

[178] H. Kobayashi, M. Kabuto, H. Ide, K. Hosotani, T. Kubota, An artificial blood vessel with an endothelial-cell monolayer, J. Neurosurg. 77 (1992) 397–402.

[179] M. Pasic, W. Muller-Glauser, L.K. Von Segesser, M. Lachat, T. Mihaljevic, M.I. Turina, Superior late patency of small-diameter dacron grafts seeded with omental microvascular cells: An experimental study, Ann. Thorac. Surg. 58 (1994) 677–684.

[180] S.K. Williams, D.G. Rose, B.E. Jarrell, Microvascular endothelial cell sodding of ePTFE vascular grafts: Improved patency and stability of the cellular lining, J. Biomed. Mater. Res. 28 (1994) 203–212.

[181] A. Tiwari, H.J. Salacinski, G. Hamilton, A.M. Seifalian, Tissue Engineering of Vascular Bypass Grafts: Role of Endothelial Cell Extraction, Eur. J. Vasc. Endovasc. Surg. 21 (2001) 193–201. doi:10.1053/ejvs.2001.1316.

[182] P.J. Critser, M.C. Yoder, Endothelial colony-forming cell role in neoangiogenesis and tissue repair, Curr. Opin. Organ Transplant. 15 (2010) 68–72. doi:10.1097/MOT.0b013e32833454b5.

[183] F. Timmermans, J. Plum, M.C. Yöder, D.A. Ingram, B. Vandekerckhove, J. Case, Endothelial progenitor cells: Identity defined?, J. Cell. Mol. Med. 13 (2009) 87–102. doi:10.1111/j.1582-4934.2008.00598.x.

[184] R. Gulati, D. Jevremovic, T.E. Peterson, S. Chatterjee, V. Shah, R.G. Vile, et al., Diverse Origin and Function of Cells with Endothelial Phenotype Obtained from Adult Human Blood, Circ. Res. 93 (2003) 1023–1025. doi:10.1161/01.RES.0000105569.77539.21.

[185] D.A. Ingram, L.E. Mead, H. Tanaka, V. Meade, A. Fenoglio, K. Mortell, et al., Identification of a novel hierarchy of endothelial progenitor cells using human peripheral and umbilical cord blood, Blood. 104 (2004) 2752–2760. doi:10.1182/blood-2004-04-1396.

[186] S. Mariucci, B. Rovati, K. Bencardino, M. Manzoni, M. Danova, Flow cytometric detection of circulating endothelial cells and endothelial progenitor cells in healthy subjects, Int. J. Lab. Hematol. 32 (2010) e40–e48. doi:10.1111/j.1751-553X.2008.01105.x.

[187] J. Kraan, M.H. Strijbos, A.M. Sieuwerts, J.A. Foekens, M.A. Den Bakker, C. Verhoef, et al., A new approach for rapid and reliable enumeration of circulating endothelial cells in patients, J. Thromb. Haemost. 10 (2012) 931–939. doi:10.1111/j.1538-7836.2012.04681.x.

[188] J.M. Hill, G. Zalos, J.P.J. Halcox, W.H. Schenke, M.A. Waclawiw, A.A. Quyyumi, et al., Circulating endothelial progenitor cells, vascular function, and cardiovascular risk, N. Engl. J. Med. 348 (2003) 593–600. doi:10.1056/NEJMoa022287.

[189] M. Vasa, S. Fichtlscherer, A. Aicher, K. Adler, C. Urbich, H. Martin, et al., Number and migratory activity of circulating endothelial progenitor cells inversely correlate with risk factors for coronary artery disease., Circ. Res. 89 (2001) E1–7.

[190] M.T. Hinds, M. Ma, N. Tran, A.E. Ensley, S.M. Kladakis, K.B. Vartanian, et al., Potential of baboon endothelial progenitor cells for tissue engineered vascular grafts, J. Biomed. Mater. Res. A. 86A (2008) 804–812. doi:10.1002/jbm.a.31672.

[191] S. Kaushal, G.E. Amiel, K.J. Guleserian, O.M. Shapira, T. Perry, F.W. Sutherland, et al., Functional small-diameter neovessels created using endothelial progenitor

cells expanded ex vivo, Nat. Med. 7 (2001) 1035–1040. doi:10.1038/nm0901-1035.

[192] K.K. Hirschi, D.A. Ingram, M.C. Yoder, Assessing Identity, Phenotype, and Fate of Endothelial Progenitor Cells, Arterioscler. Thromb. Vasc. Biol. 28 (2008) 1584–1595. doi:10.1161/ATVBAHA.107.155960.

[193] J. Case, L.E. Mead, W.K. Bessler, D. Prater, H.A. White, M.R. Saadatzadeh, et al., Human CD34+AC133+VEGFR-2+ cells are not endothelial progenitor cells but distinct, primitive hematopoietic progenitors, Exp. Hematol. 35 (2007) 1109–1118. doi:10.1016/j.exphem.2007.04.002.

[194] F. Timmermans, F. Van Hauwermeiren, M. De Smedt, R. Raedt, F. Plasschaert, M.L. De Buyzere, et al., Endothelial outgrowth cells are not derived from CD133+ Cells or CD45+ hematopoietic precursors, Arterioscler. Thromb. Vasc. Biol. 27 (2007) 1572–1579. doi:10.1161/ATVBAHA.107.144972.

[195] O. Tura, E.M. Skinner, R. Barclay, K. Samuel, R.C.J. Gallagher, M. Brittan, et al., Late outgrowth endothelial cells resemble mature endothelial cells and are not derived from bone marrow, Stem Cells. 31 (2013) 338–348. doi:10.1002/stem.1280.

[196] A.E. Ensley, R.M. Nerem, D.E.J. Anderson, S.R. Hanson, M.T. Hinds, Fluid shear stress alters the hemostatic properties of endothelial outgrowth cells, Tissue Eng. - Part A. 18 (2012) 127–136. doi:10.1089/ten.tea.2010.0290.

[197] H.E. Achneck, R.M. Jamiolkowski, A.E. Jantzen, J.M. Haseltine, W.O. Lane, J.K. Huang, et al., The biocompatibility of titanium cardiovascular devices seeded with autologous blood-derived endothelial progenitor cells. EPC-seeded antithrombotic Ti Implants, Biomaterials. 32 (2011) 10–18. doi:10.1016/j.biomaterials.2010.08.073.

[198] R.F. Ankeny, M.T. Hinds, R.M. Nerem, Dynamic Shear Stress Regulation of Inflammatory and Thrombotic Pathways in Baboon Endothelial Outgrowth Cells, Tissue Eng. Part A. (2013). doi:10.1089/ten.TEA.2012.0300.

[199] L. Mazzolai, K. Bouzourene, D. Hayoz, F. Dignat-George, J.W. Liu, H. Bounameaux, et al., Characterization of human late outgrowth endothelial progenitor-derived cells under various flow conditions, J. Vasc. Res. 48 (2011) 443–451. doi:10.1159/000324844.

[200] T. Shirota, H. He, H. Yasui, T. Matsuda, Human endothelial progenitor cell-seeded hybrid graft: Proliferative and antithrombogenic potentials in vitro and fabrication processing, Tissue Eng. 9 (2003) 127–136. doi:10.1089/107632703762687609.

[201] J.B. Allen, S. Khan, K.A. Lapidos, G.A. Ameer, Toward engineering a human neoendothelium with circulating progenitor cells, Stem Cells. 28 (2010) 318–328. doi:10.1002/stem.275.

[202] J.D. Stroncek, B.S. Grant, M.A. Brown, T.J. Povsic, G.A. Truskey, W.M. Reichert, Comparison of endothelial cell phenotypic markers of late-outgrowth endothelial progenitor cells isolated from patients with coronary artery disease and healthy volunteers, Tissue Eng. Part A. 15 (2009) 3473–3486. doi:10.1089/ten.TEA.2008.0673.

[203] V.W.M. Van Hinsbergh, The endothelium: vascular control of haemostasis, Eur. J. Obstet. Gynecol. Reprod. Biol. 95 (2001) 198–201. doi:10.1016/S0301-2115(00)00490-5.

[204] A.P. McGuigan, M.V. Sefton, The influence of biomaterials on endothelial cell thrombogenicity, Biomaterials. 28 (2007) 2547–2571. doi:10.1016/j.biomaterials.2007.01.039.

[205] S.R. Hanson, H.F. Kotze, B. Savage, L.A. Harker, Platelet interactions with dacron vascular grafts. A model of acute thrombosis in baboons, Arteriosclerosis. 5 (1985) 595–603.

[206] A. Gruber, S.R. Hanson, Factor XI-dependence of surface- and tissue factor-initiated thrombus propagation in primates, Blood. 102 (2003) 953–955. doi:10.1182/blood-2003-01-0324.

[207] C. Quint, Y. Kondo, R.J. Manson, J.H. Lawson, A. Dardik, L.E. Niklason, Decellularized tissue-engineered blood vessel as an arterial conduit, Proc. Natl. Acad. Sci. U. S. A. 108 (2011) 9214–9219. doi:10.1073/pnas.1019506108.

[208] C. Zhu, D. Ying, J. Mi, L. Li, W. Zeng, C. Hou, et al., Development of anti-atherosclerotic tissue-engineered blood vessel by A20-regulated endothelial progenitor cells seeding decellularized vascular matrix, Biomaterials. 29 (2008) 2628–2636. doi:10.1016/j.biomaterials.2008.03.005.

[209] A.N. Veleva, D.E. Heath, J.K. Johnson, J. Nam, C. Patterson, J.J. Lannutti, et al., Interactions between endothelial cells and electrospun methacrylic terpolymer fibers for engineered vascular replacements, J. Biomed. Mater. Res. - Part A. 91 (2009) 1131–1139. doi:10.1002/jbm.a.32276.

[210] X. Zhang, Y. Xu, V. Thomas, S.L. Bellis, Y.K. Vohra, Engineering an antiplatelet adhesion layer on an electrospun scaffold using porcine endothelial progenitor cells, J. Biomed. Mater. Res. - Part A. 97 A (2011) 145–151. doi:10.1002/jbm.a.33040.

[211] J.D. Stroncek, Y. Xue, N. Haque, J.H. Lawson, W.M. Reichert, In vitro functional testing of endothelial progenitor cells that overexpress thrombomodulin, Tissue Eng. - Part A. 17 (2011) 2091–2100. doi:10.1089/ten.tea.2010.0631.

[212] K.A. Ahmann, S.L. Johnson, R.P. Hebbel, R.T. Tranquillo, Shear Stress Responses of Adult Blood Outgrowth Endothelial Cells Seeded on Bioartificial Tissue, Tissue Eng. Part A. 17 (2011) 2511–2521. doi:10.1089/ten.tea.2011.0055.

[213] D. Kong, L.G. Melo, A.A. Mangi, L. Zhang, M. Lopez-Ilasaca, M.A. Perrella, et al., Enhanced Inhibition of Neointimal Hyperplasia by Genetically Engineered Endothelial Progenitor Cells, Circulation. 109 (2004) 1769–1775. doi:10.1161/01.CIR.0000121732.85572.6F.

[214] Q. Liu, Y. Xi, T. Terry, S.-P. So, A. Mohite, J. Zhang, et al., Engineered endothelial progenitor cells that overexpress prostacyclin protect vascular cells, J. Cell. Physiol. 227 (2012) 2907–2916. doi:10.1002/jcp.23035.

[215] J.M. Anderson, Biological Responses to Materials, Annu. Rev. Mater. Res. 31 (2001) 81–110. doi:10.1146/annurev.matsci.31.1.81.

[216] A. Zarbock, K. Ley, Neutrophil adhesion and activation under flow., Microcirc. N. Y. N 1994. 16 (2009) 31–42. doi:10.1080/10739680802350104.

[217] W.A. Muller, Mechanisms of transendothelial migration of leukocytes, Circ. Res. 105 (2009) 223–230. doi:10.1161/CIRCRESAHA.109.200717.

[218] E. Galkina, K. Ley, Immune and inflammatory mechanisms of atherosclerosis, 2009.

[219] T.M. Carlos, J.M. Harlan, Leukocyte-endothelial adhesion molecules, Blood. 84 (1994) 2068–2101.

[220] M.A. Brown, C.S. Wallace, M. Angelos, G.A. Truskey, Characterization of Umbilical Cord Blood–Derived Late Outgrowth Endothelial Progenitor Cells Exposed to Laminar Shear Stress, Tissue Eng. Part A. 15 (2009) 3575–3587. doi:10.1089/ten.tea.2008.0444.

[221] W. Cuccuini, S. Poitevin, G. Poitevin, F. Dignat-George, P. Cornillet-Lefebvre, F. Sabatier, et al., Tissue factor up-regulation in proinflammatory conditions confers thrombin generation capacity to endothelial colony-forming cells without influencing non-coagulant properties in vitro, J. Thromb. Haemost. 8 (2010) 2042–2052. doi:10.1111/j.1538-7836.2010.03936.x.

[222] P.R. Sreerekha, L.K. Krishnan, Cultivation of endothelial progenitor cells on fibrin matrix and layering on dacron/polytetrafluoroethylene vascular grafts, Artif. Organs. 30 (2006) 242–249. doi:10.1111/j.1525-1594.2006.00211.x.

[223] J.M. Waugh, J. Li-Hawkins, E. Yuksel, M.D. Kuo, P.N. Cifra, P.R. Hilfiker, et al., Thrombomodulin overexpression to limit neointima formation, Circulation. 102 (2000) 332–337.

[224] G. Wong, J. -m. Li, G. Hendricks, M.H. Eslami, M.J. Rohrer, B.S. Cutler, Inhibition of experimental neointimal hyperplasia by recombinant human thrombomodulin coated ePTFE stent grafts, J. Vasc. Surg. 47 (2008) 608–615. doi:10.1016/j.jvs.2007.11.025.

[225] D.E.J. Anderson, K.A. McKenna, J.J. Glynn, U. Marzec, S.R. Hanson, M.T. Hinds, Thrombotic responses of endothelial outgrowth cells to protein-coated surfaces, Cells Tissues Organs. 199 (2014) 238–248. doi:10.1159/000368223.

[226] J.D. Stroncek, L.C. Ren, B. Klitzman, W.M. Reichert, Patient-derived endothelial progenitor cells improve vascular graft patency in a rodent model, Acta Biomater. 8 (2012) 201–208. doi:10.1016/j.actbio.2011.09.002.

[227] M. Zhou, Z. Liu, C. Liu, X. Jiang, Z. Wei, W. Qiao, et al., Tissue engineering of small-diameter vascular grafts by endothelial progenitor cells seeding heparin-coated decellularized scaffolds, J. Biomed. Mater. Res. - Part B Appl. Biomater. 100 B (2012) 111–120. doi:10.1002/jbm.b.31928.

[228] D. Hughes, A.A. Fu, A. Puggioni, J.F. Glockner, B. Anwer, A.M. McGuire, et al., Adventitial transplantation of blood outgrowth endothelial cells in porcine haemodialysis grafts alleviates hypoxia and decreases neointimal proliferation through a matrix metalloproteinase-9-mediated pathway - A pilot study, Nephrol. Dial. Transplant. 24 (2009) 85–96. doi:10.1093/ndt/gfn433.

[229] J.-J. Chiu, S. Chien, Effects of disturbed flow on vascular endothelium: Pathophysiological basis and clinical perspectives, Physiol. Rev. 91 (2011) 327–387. doi:10.1152/physrev.00047.2009.

[230] P.F. Davies, Flow-mediated endothelial mechanotransduction, Physiol. Rev. 75 (1995) 519–560.

[231] A.D. Egorova, M.C. DeRuiter, H.C. De Boer, S. Van De Pas, A.C. Gittenberger-De Groot, A.J. Van Zonneveld, et al., Endothelial colony-forming cells show a mature transcriptional response to shear stress, Vitro Cell. Dev. Biol. - Anim. 48 (2012) 21–29. doi:10.1007/s11626-011-9470-z.

[232] T. Lund, S.E. Hermansen, T.V. Andreasen, J.O. Olsen, B. Østerud, T. Myrmel, et al., Shear stress regulates inflammatory and thrombogenic gene transcripts in cultured human endothelial progenitor cells, Thromb. Haemost. 104 (2010) 582–591. doi:10.1160/TH09-12-0854.

[233] H. He, T. Shirota, H. Yasui, T. Matsuda, Canine endothelial progenitor cell-lined hybrid vascular graft with nonthrombogenic potential, J. Thorac. Cardiovasc. Surg. 126 (2003) 455–464. doi:10.1016/S0022-5223(02)73264-9.

[234] B.W. Tillman, S.K. Yazdani, L.P. Neff, M.A. Corriere, G.J. Christ, S. Soker, et al., Bioengineered vascular access maintains structural integrity in response to

arteriovenous flow and repeated needle puncture, J. Vasc. Surg. 56 (2012) 783–793. doi:10.1016/j.jvs.2012.02.030.

[235] T.A. Sagban, E. Schiegel, K. Grabitz, W. Sandmann, K.M. Balzer, Bioengineering of a semiautologous arterial vessels with reconstructed media and intima, longtime tested in vivo, Adv. Eng. Mater. 13 (2011) B518–B528. doi:10.1002/adem.201080143.

[236] H. Lu, Z. Feng, Z. Gu, C. Liu, Growth of outgrowth endothelial cells on aligned PLLA nanofibrous scaffolds, J. Mater. Sci. Mater. Med. 20 (2009) 1937–1944. doi:10.1007/s10856-009-3744-y.

[237] S.F. Badylak, The extracellular matrix as a biologic scaffold material, Biomaterials. 28 (2007) 3587–3593. doi:10.1016/j.biomaterials.2007.04.043.

[238] G.E. Amiel, M. Komura, O. Shapira, J.J. Yoo, S. Yazdani, J. Berry, et al., Engineering of blood vessels from acellular collagen matrices coated with human endothelial cells, Tissue Eng. 12 (2006) 2355–2365. doi:10.1089/ten.2006.12.2355.

[239] A. Bader, G. Steinhoff, A. Haverich, Tissue engineering of vascular grafts: Human cell seeding of decellularised porcine matrix, Eur. J. Vasc. Endovasc. Surg. 19 (2000) 381–386. doi:10.1053/ejvs.1999.1004.

[240] S.-W. Cho, H.J. Park, J.H. Ryu, S.H. Kim, Y.H. Kim, C.Y. Choi, et al., Vascular patches tissue-engineered with autologous bone marrow-derived cells and decellularized tissue matrices, Biomaterials. 26 (2005) 1915–1924. doi:10.1016/j.biomaterials.2004.06.018.

[241] Y. Narita, H. Kagami, H. Matsunuma, Y. Murase, M. Ueda, Y. Ueda, Decellularized ureter for tissue-engineered small-caliber vascular graft, J. Artif. Organs. 11 (2008) 91–99. doi:10.1007/s10047-008-0407-6.

[242] J. Gao, P. Crapo, R. Nerem, Y. Wang, Co-expression of elastin and collagen leads to highly compliant engineered blood vessels, J. Biomed. Mater. Res. A. 85A (2008) 1120–1128. doi:10.1002/jbm.a.32028.

[243] T. Aper, A. Schmidt, M. Duchrow, H.-P. Bruch, Autologous Blood Vessels Engineered from Peripheral Blood Sample, Eur. J. Vasc. Endovasc. Surg. 33 (2007) 33–39. doi:10.1016/j.ejvs.2006.08.008.

[244] J.F. Gómez-Cerezo, B. Pagán-Muñoz, M. López-Rodríguez, M. Estébanez-Muñoz, F.J. Barbado-Hernández, The role of endothelial progenitor cells and statins in endothelial function: A review, Cardiovasc. Hematol. Agents Med. Chem. 5 (2007) 265–272. doi:10.2174/187152507782109836.

[245] C. Heeschen, A. Aicher, R. Lehmann, S. Fichtlscherer, M. Vasa, C. Urbich, et al., Erythropoietin is a potent physiologic stimulus for endothelial progenitor cell mobilization, Blood. 102 (2003) 1340–1346. doi:10.1182/blood-2003-01-0223.

[246] W.C. Aird, Spatial and temporal dynamics of the endothelium, J. Thromb. Haemost. 3 (2005) 1392–1406. doi:10.1111/j.1538-7836.2005.01328.x.

[247] P. Zilla, M. Deutsch, J. Meinhart, R. Puschmann, T. Eberl, E. Minar, et al., Clinical in vitro endothelialization of femoropopliteal bypass grafts: An actuarial follow-up over three years, J. Vasc. Surg. 19 (1994) 540–548.

[248] S. Levenberg, J. Rouwkema, M. Macdonald, E.S. Garfein, D.S. Kohane, D.C. Darland, et al., Engineering vascularized skeletal muscle tissue, Nat. Biotechnol. 23 (2005) 879–884. doi:10.1038/nbt1109.

[249] P.M. Baptista, M.M. Siddiqui, G. Lozier, S.R. Rodriguez, A. Atala, S. Soker, The use of whole organ decellularization for the generation of a vascularized liver organoid, Hepatology. 53 (2011) 604–617. doi:10.1002/hep.24067.

[250] K.R. Stevens, K.L. Kreutziger, S.K. Dupras, F.S. Korte, M. Regnier, V. Muskheli, et al., Physiological function and transplantation of scaffold-free and vascularized human cardiac muscle tissue, Proc. Natl. Acad. Sci. U. S. A. 106 (2009) 16568–16573. doi:10.1073/pnas.0908381106.

[251] K.B. Vartanian, S.J. Kirkpatrick, S.R. Hanson, M.T. Hinds, Endothelial cell cytoskeletal alignment independent of fluid shear stress on micropatterned surfaces, Biochem. Biophys. Res. Commun. 371 (2008) 787–792. doi:10.1016/j.bbrc.2008.04.167.

[252] B. Nan, P. Lin, A.B. Lumsden, Q. Yao, C. Chen, Effects of TNF-α and curcumin on the expression of thrombomodulin and endothelial protein C receptor in human endothelial cells, Thromb. Res. 115 (2005) 417–426. doi:10.1016/j.thromres.2004.10.010.

[253] J. Steffel, T.F. Lüscher, F.C. Tanner, Tissue factor in cardiovascular diseases: Molecular mechanisms and clinical implications, Circulation. 113 (2006) 722–731. doi:10.1161/CIRCULATIONAHA.105.567297.

[254] A.M. Andrews, D. Jaron, D.G. Buerk, P.L. Kirby, K.A. Barbee, Direct, real-time measurement of shear stress-induced nitric oxide produced from endothelial cells in vitro, Nitric Oxide. 23 (2010) 335–342. doi:10.1016/j.niox.2010.08.003.

[255] W.H. Geerts, D. Bergqvist, G.F. Pineo, J.A. Heit, C.M. Samama, M.R. Lassen, et al., Prevention of venous thromboembolism*: American college of chest physicians evidence-based clinical practice guidelines (8th edition), CHEST J. 133 (2008) 381S–453S. doi:10.1378/chest.08-0656.

[256] C.T. Dotter, Interventional radiology—Review of an emerging field, Semin. Roentgenol. 16 (1981) 7–12. doi:10.1016/0037-198X(81)90015-8.

[257] D. Pavcnik, B.T. Uchida, H.A. Timmermans, C.L. Corless, M. O'Hara, N. Toyota, et al., Percutaneous bioprosthetic venous valve: A long-term study in sheep, J. Vasc. Surg. 35 (2002) 598–602. doi:10.1067/mva.2002.118825.

[258] D. Pavcnik, J. Kaufman, L. Machan, B. Uchida, F.S. Keller, J. Rösch, Percutaneous therapy for deep vein reflux, Semin. Interv. Radiol. 22 (2005) 225–232. doi:10.1055/s-2005-921956.

[259] D. Pavcnik, B. Uchida, J. Kaufman, M. Hinds, F.S. Keller, J. Rösch, Percutaneous management of chronic deep venous reflux: Review of experimental work and early clinical experience with bioprosthetic valve, Vasc. Med. 13 (2008) 75–84. doi:10.1177/1358863X07083474.

[260] R.D. Rudic, E.G. Shesely, N. Maeda, O. Smithies, S.S. Segal, W.C. Sessa, Direct evidence for the importance of endothelium-derived nitric oxide in vascular remodeling, J. Clin. Invest. 101 (1998) 731–736.

[261] J. Kotani, M. Awata, S. Nanto, M. Uematsu, F. Oshima, H. Minamiguchi, et al., Incomplete neointimal coverage of sirolimus-eluting stents: angioscopic findings., J. Am. Coll. Cardiol. 47 (2006) 2108–11. doi:10.1016/j.jacc.2005.11.092.

[262] S.D. Patel, M. Waltham, A. Wadoodi, K.G. Burnand, A. Smith, The role of endothelial cells and their progenitors in intimal hyperplasia., Ther. Adv. Cardiovasc. Dis. 4 (2010) 129–41. doi:10.1177/1753944710362903.

[263] J.J. Glynn, M.T. Hinds, Endothelial outgrowth cells: function and performance in vascular grafts., Tissue Eng. Part B Rev. 20 (2014) 294–303. doi:10.1089/ten.TEB.2013.0285.

[264] T. Shirota, H. Yasui, H. Shimokawa, T. Matsuda, Fabrication of endothelial progenitor cell (EPC)-seeded intravascular stent devices and in vitro endothelialization on hybrid vascular tissue., Biomaterials. 24 (2003) 2295–302.

[265] J.E. Jordan, J.K. Williams, S.-J. Lee, D. Raghavan, A. Atala, J.J. Yoo, Bioengineered self-seeding heart valves., J. Thorac. Cardiovasc. Surg. 143 (2012) 201–8. doi:10.1016/j.jtcvs.2011.10.005.

[266] D.E.J. Anderson, J.J. Glynn, H.K. Song, M.T. Hinds, Engineering an endothelialized vascular graft: A rational approach to study design in a non-human primate model, PLoS ONE. 9 (2014). doi:10.1371/journal.pone.0115163.

[267] C.M. Jones, M.T. Hinds, D. Pavcnik, Retention of an autologous endothelial layer on a bioprosthetic valve for the treatment of chronic deep venous insufficiency., J. Vasc. Interv. Radiol. JVIR. 23 (2012) 697–703. doi:10.1016/j.jvir.2012.01.062.

[268] A.J. Melchiorri, N. Hibino, J.P. Fisher, Strategies and techniques to enhance the in situ endothelialization of small-diameter biodegradable polymeric vascular grafts., Tissue Eng. Part B Rev. 19 (2013) 292–307. doi:10.1089/ten.TEB.2012.0577.

[269] K. Yavuz, S. Geyik, D. Pavcnik, B.T. Uchida, C.L. Corless, D.E. Hartley, et al., Comparison of the endothelialization of small intestinal submucosa, dacron, and expanded polytetrafluoroethylene suspended in the thoracoabdominal aorta in sheep, J. Vasc. Interv. Radiol. JVIR. 17 (2006) 873–882. doi:10.1097/01.RVI.0000217938.20787.BB.

[270] K. Holmes, O.L. Roberts, A.M. Thomas, M.J. Cross, Vascular endothelial growth factor receptor-2: Structure, function, intracellular signalling and therapeutic inhibition, Cell. Signal. 19 (2007) 2003–2012.

[271] E. Diamandis, T. Christopoulos, The biotin-(strept)avidin system: principles and applications in biotechnology, Clin Chem. 37 (1991) 625–636.

[272] E. Brountzos, D. Pavcnik, H.A. Timmermans, C. Corless, B.T. Uchida, E.S. Nihsen, et al., Remodeling of Suspended Small Intestinal Submucosa Venous Valve: An Experimental Study in Sheep to Assess the Host Cells' Origin, J. Vasc. Interv. Radiol. 14 (2003) 349–356. doi:10.1097/01.RVI.0000058410.01661.62.

[273] B.K. Ferrand, K. Kokini, S.F. Badylak, L.A. Geddes, M.C. Hiles, R.J. Morff, Directional porosity of porcine small-intestinal submucosa, in: J. Biomed. Mater. Res., 1993: pp. 1235–1241.

[274] D. Raghavan, B.P. Kropp, H.-K. Lin, Y. Zhang, R. Cowan, S. V Madihally, Physical characteristics of small intestinal submucosa scaffolds are location-dependent., J. Biomed. Mater. Res. A. 73 (2005) 90–6. doi:10.1002/jbm.a.30268.

[275] C.M. Jones, S.M. Baker-Groberg, F.A. Cianchetti, J.J. Glynn, L.D. Healy, W.Y. Lam, et al., Measurement science in the circulatory system., Cell. Mol. Bioeng. 7 (2014) 1–14. doi:10.1007/s12195-013-0317-4.

[276] R.M. Kaplan, M.H. Criqui, J.O. Denenberg, J. Bergan, A. Fronek, Quality of life in patients with chronic venous disease: San Diego population study, J. Vasc. Surg. 37 (2003) 1047–1053. doi:10.1067/mva.2003.168.

[277] R.T. Eberhardt, J.D. Raffetto, Chronic venous insufficiency, Circulation. 111 (2005) 2398–2409. doi:10.1161/01.CIR.0000164199.72440.08.

[278] M.R. Cesarone, G. Belcaro, A.N. Nicolaides, G. Geroulakos, M. Griffin, L. Incandela, et al., "Real" Epidemiology of Varicose Veins and Chronic Venous Diseases: The San Valentino Vascular Screening Project, Angiology. 53 (2002) 119–130. doi:10.1177/000331970205300201.

[279] D. Pavcnik, Q. Yin, B. Uchida, W.K. Park, H. Hoppe, M.D. Kim, et al., Percutaneous autologous venous valve transplantation: short-term feasibility study in an ovine model., J. Vasc. Surg. 46 (2007) 338–45. doi:10.1016/j.jvs.2007.04.060.

[280] O.E. Teebken, C. Puschmann, T. Aper, A. Haverich, H. Mertsching, Tissue-engineered bioprosthetic venous valve: a long-term study in sheep., Eur. J. Vasc. Endovasc. Surg. Off. J. Eur. Soc. Vasc. Surg. 25 (2003) 305–12. doi:10.1053/ejvs.2002.1873.

[281] R.G. Matheny, M.L. Hutchison, P.E. Dryden, M.D. Hiles, C.J. Shaar, Porcine small intestine submucosa as a pulmonary valve leaflet substitute, J. Heart Valve Dis. 9 (2000) 769–775.

[282] A.M. Fallon, T.T. Goodchild, J.L. Cox, R.G. Matheny, In vivo remodeling potential of a novel bioprosthetic tricuspid valve in an ovine model., J. Thorac. Cardiovasc. Surg. 148 (2014) 333–340.e1. doi:10.1016/j.jtcvs.2013.10.048.

[283] J.J. Glynn, M.T. Hinds, Endothelial Outgrowth Cells Regulate Coagulation, Platelet Accumulation, and Respond to Tumor Necrosis Factor Similar to Carotid Endothelial Cells., Tissue Eng. Part A. (2014). doi:10.1089/ten.TEA.2014.0032.

[284] H. He, T. Shirota, H. Yasui, T. Matsuda, Canine endothelial progenitor cell-lined hybrid vascular graft with nonthrombogenic potential, J. Thorac. Cardiovasc. Surg. 126 (2003) 455–464. doi:10.1016/S0022-5223(02)73264-9.

[285] S. Kaushal, G.E. Amiel, K.J. Guleserian, O.M. Shapira, T. Perry, F.W. Sutherland, et al., Functional small-diameter neovessels created using endothelial progenitor cells expanded ex vivo, Nat. Med. 7 (2001) 1035–1040. doi:10.1038/nm0901-1035.

[286] T.A. Sagban, E. Schiegel, K. Grabitz, W. Sandmann, K.M. Balzer, Bioengineering of a semiautologous arterial vessels with reconstructed media and intima, longtime tested in vivo, Adv. Eng. Mater. 13 (2011) B518–B528. doi:10.1002/adem.201080143.

[287] C. Quint, Y. Kondo, R.J. Manson, J.H. Lawson, A. Dardik, L.E. Niklason, Decellularized tissue-engineered blood vessel as an arterial conduit, Proc. Natl. Acad. Sci. U. S. A. 108 (2011) 9214–9219. doi:10.1073/pnas.1019506108.

[288] J. Gao, P. Crapo, R. Nerem, Y. Wang, Co-expression of elastin and collagen leads to highly compliant engineered blood vessels, J. Biomed. Mater. Res. A. 85A (2008) 1120–1128. doi:10.1002/jbm.a.32028.

[289] J.E. Butler, L. Ni, R. Nessler, K.S. Joshi, M. Suter, B. Rosenberg, et al., The physical and functional behavior of capture antibodies adsorbed on polystyrene, J. Immunol. Methods. 150 (1992) 77–90. doi:10.1016/0022-1759(92)90066-3.

[290] P. Peluso, D.S. Wilson, D. Do, H. Tran, M. Venkatasubbaiah, D. Quincy, et al., Optimizing antibody immobilization strategies for the construction of protein microarrays, Anal. Biochem. 312 (2003) 113–124. doi:10.1016/S0003-2697(02)00442-6.

[291] G.P. Fadini, M. Schiavon, M. Cantini, I. Baesso, M. Facco, M. Miorin, et al., Circulating progenitor cells are reduced in patients with severe lung disease., Stem Cells Dayt. Ohio. 24 (2006) 1806–13. doi:10.1634/stemcells.2005-0440.

[292] M. Toshner, R. Voswinckel, M. Southwood, R. Al-Lamki, L.S.G. Howard, D. Marchesan, et al., Evidence of dysfunction of endothelial progenitors in pulmonary arterial hypertension., Am. J. Respir. Crit. Care Med. 180 (2009) 780–7. doi:10.1164/rccm.200810-1662OC.

[293] Y. Matsumoto, V. Adams, C. Walther, C. Kleinecke, P. Brugger, A. Linke, et al., Reduced number and function of endothelial progenitor cells in patients with aortic valve stenosis: a novel concept for valvular endothelial cell repair., Eur. Heart J. 30 (2009) 346–55. doi:10.1093/eurheartj/ehn501.

[294] T. Thum, S. Hoeber, S. Froese, I. Klink, D.O. Stichtenoth, P. Galuppo, et al., Age-dependent impairment of endothelial progenitor cells is corrected by growth-hormone-mediated increase of insulin-like growth-factor-1., Circ. Res. 100 (2007) 434–43. doi:10.1161/01.RES.0000257912.78915.af.

[295] M.D. Best, Click chemistry and bioorthogonal reactions: unprecedented selectivity in the labeling of biological molecules., Biochemistry (Mosc.). 48 (2009) 6571–84. doi:10.1021/bi9007726.

[296] W.-H. Lim, W.-W. Seo, W. Choe, C.-K. Kang, J. Park, H.-J. Cho, et al., Stent coated with antibody against vascular endothelial-cadherin captures endothelial progenitor cells, accelerates re-endothelialization, and reduces neointimal formation., Arterioscler. Thromb. Vasc. Biol. 31 (2011) 2798–805. doi:10.1161/ATVBAHA.111.226134.

[297] M. Avci-Adali, G. Ziemer, H.P. Wendel, Induction of EPC homing on biofunctionalized vascular grafts for rapid in vivo self-endothelialization — A review of current strategies, Biotechnol. Adv. 28 (2010) 119–129.

[298] W.K. den Dekker, J.H. Houtgraaf, Y. Onuma, E. Benit, R.J. de Winter, W. Wijns, et al., Final results of the HEALING IIB trial to evaluate a bio-engineered CD34 antibody coated stent (Genous^{TM}Stent) designed to promote vascular healing by capture of circulating endothelial progenitor cells in CAD patients, Atherosclerosis. 219 (2011) 245–252. doi:10.1016/j.atherosclerosis.2011.06.032.

[299] M. Klomp, M.A. Beijk, C. Varma, J.J. Koolen, E. Teiger, G. Richardt, et al., 1-year outcome of TRIAS HR (TRI-stent adjudication study-high risk of restenosis) a multicenter, randomized trial comparing genous endothelial progenitor cell

capturing stents with drug-eluting stents., JACC Cardiovasc. Interv. 4 (2011) 896–904. doi:10.1016/j.jcin.2011.05.011.

[300] M.A.M. Beijk, M. Klomp, N.J.W. Verouden, N. van Geloven, K.T. Koch, J.P.S. Henriques, et al., Genous endothelial progenitor cell capturing stent vs. the Taxus Liberte stent in patients with de novo coronary lesions with a high-risk of coronary restenosis: a randomized, single-centre, pilot study., Eur. Heart J. 31 (2010) 1055–64. doi:10.1093/eurheartj/ehp476.

[301] M.T. Hinds, M. Ma, N. Tran, A.E. Ensley, S.M. Kladakis, K.B. Vartanian, et al., Potential of baboon endothelial progenitor cells for tissue engineered vascular grafts, J. Biomed. Mater. Res. A. 86A (2008) 804–812. doi:10.1002/jbm.a.31672.

[302] R. Gulati, D. Jevremovic, T.E. Peterson, S. Chatterjee, V. Shah, R.G. Vile, et al., Diverse Origin and Function of Cells with Endothelial Phenotype Obtained from Adult Human Blood, Circ. Res. 93 (2003) 1023–1025. doi:10.1161/01.RES.0000105569.77539.21.

[303] M.A. Brown, C.S. Wallace, M. Angelos, G.A. Truskey, Characterization of umbilical cord blood-derived late outgrowth endothelial progenitor cells exposed to laminar shear stress., Tissue Eng. Part A. 15 (2009) 3575–87. doi:10.1089/ten.TEA.2008.0444.

[304] T. Shirota, H. He, H. Yasui, T. Matsuda, Human endothelial progenitor cell-seeded hybrid graft: Proliferative and antithrombogenic potentials in vitro and fabrication processing, Tissue Eng. 9 (2003) 127–136. doi:10.1089/107632703762687609.

[305] A.E. Ensley, R.M. Nerem, D.E.J. Anderson, S.R. Hanson, M.T. Hinds, Fluid Shear Stress Alters the Hemostatic Properties of Endothelial Outgrowth Cells, Tissue Eng. Part A. 18 (2012) 127–136. doi:10.1089/ten.tea.2010.0290.

[306] J.D. Stroncek, B.S. Grant, M.A. Brown, T.J. Povsic, G.A. Truskey, W.M. Reichert, Comparison of endothelial cell phenotypic markers of late-outgrowth endothelial progenitor cells isolated from patients with coronary artery disease and healthy volunteers, Tissue Eng. Part A. 15 (2009) 3473–3486. doi:10.1089/ten.TEA.2008.0673.

[307] D. Kong, L.G. Melo, A.A. Mangi, L. Zhang, M. Lopez-Ilasaca, M.A. Perrella, et al., Enhanced Inhibition of Neointimal Hyperplasia by Genetically Engineered Endothelial Progenitor Cells, Circulation. 109 (2004) 1769–1775. doi:10.1161/01.CIR.0000121732.85572.6F.

[308] J.D. Stroncek, Y. Xue, N. Haque, J.H. Lawson, W.M. Reichert, In vitro functional testing of endothelial progenitor cells that overexpress thrombomodulin, Tissue Eng. - Part A. 17 (2011) 2091–2100. doi:10.1089/ten.tea.2010.0631.

[309] M.W. Gerdisch, A.O. Akinwande, R.G. Matheny, Use of a novel acellular xenograft as a patch for aortic annular enlargement during aortic valve replacement., Innov. Phila. Pa. 5 (2010) 60–2. doi:10.1097/IMI.0b013e3181cbb421.

[310] C.M. Nelson, M.J. Bissell, Of extracellular matrix, scaffolds, and signaling: Tissue architecture regulates development, homeostasis, and cancer, 2006.

[311] F. Guilak, D.M. Cohen, B.T. Estes, J.M. Gimble, W. Liedtke, C.S. Chen, Control of Stem Cell Fate by Physical Interactions with the Extracellular Matrix, Cell Stem Cell. 5 (2009) 17–26. doi:10.1016/j.stem.2009.06.016.

[312] S.F. Badylak, D.O. Freytes, T.W. Gilbert, Extracellular matrix as a biological scaffold material: Structure and function, Acta Biomater. 5 (2009) 1–13. doi:10.1016/j.actbio.2008.09.013.

[313] A.V. Piterina, A.J. Cloonan, C.L. Meaney, L.M. Davis, A. Callanan, M.T. Walsh, et al., ECM-Based Materials in Cardiovascular Applications: Inherent Healing Potential and Augmentation of Native Regenerative Processes, Int. J. Mol. Sci. 10 (2009) 4375–4417. doi:10.3390/ijms10104375.

[314] C.E. Schmidt, J.M. Baier, Acellular vascular tissues: Natural biomaterials for tissue repair and tissue engineering, Biomaterials. 21 (2000) 2215–2231. doi:10.1016/S0142-9612(00)00148-4.

[315] P.J. Schaner, N.D. Martin, T.N. Tulenko, I.M. Shapiro, N.A. Tarola, R.F. Leichter, et al., Decellularized vein as a potential scaffold for vascular tissue engineering, J. Vasc. Surg. 40 (2004) 146–153. doi:10.1016/j.jvs.2004.03.033.

[316] C. Booth, S.A. Korossis, H.E. Wilcox, K.G. Watterson, J.N. Kearney, J. Fisher, et al., Tissue engineering of cardiac valve protheses I: Development and histological characterization of an acellular porcine scaffold, J. Heart Valve Dis. 11 (2002) 457–462.

[317] K. Mendelson, F.J. Schoen, Heart valve tissue engineering: Concepts, approaches, progress, and challenges, Ann. Biomed. Eng. 34 (2006) 1799–1819. doi:10.1007/s10439-006-9163-z.

[318] H.C. Ott, T.S. Matthiesen, S.-K. Goh, L.D. Black, S.M. Kren, T.I. Netoff, et al., Perfusion-decellularized matrix: Using nature’s platform to engineer a bioartificial heart, Nat. Med. 14 (2008) 213–221. doi:10.1038/nm1684.

[319] E. Rieder, M.-T. Kasimir, G. Silberhumer, G. Seebacher, E. Wolner, P. Simon, et al., Decellularization protocols of porcine heart valves differ importantly in efficiency of cell removal and susceptibility of the matrix to recellularization with human vascular cells, J. Thorac. Cardiovasc. Surg. 127 (2004) 399–405. doi:10.1016/j.jtcvs.2003.06.017.

[320] P.M. Crapo, T.W. Gilbert, S.F. Badylak, An overview of tissue and whole organ decellularization processes, Biomaterials. 32 (2011) 3233–3243. doi:10.1016/j.biomaterials.2011.01.057.

[321] T.J. Keane, I.T. Swinehart, S.F. Badylak, Methods of tissue decellularization used for preparation of biologic scaffolds and in vivo relevance, Methods. 84 (2015) 25–34. doi:10.1016/j.ymeth.2015.03.005.

[322] M.E. Tedder, J. Liao, B. Weed, C. Stabler, H. Zhang, A. Simionescu, et al., Stabilized collagen scaffolds for heart valve tissue engineering, Tissue Eng. - Part A. 15 (2009) 1257–1268. doi:10.1089/ten.tea.2008.0263.

[323] A.B. Van de Walle, J.S. Uzarski, P.S. McFetridge, The Consequence of Biologic Graft Processing on Blood Interface Biocompatibility and Mechanics, Cardiovasc. Eng. Technol. 6 (2015) 303–313. doi:10.1007/s13239-015-0221-2.

[324] H. Tam, W. Zhang, K.R. Feaver, N. Parchment, M.S. Sacks, N. Vyavahare, A novel crosslinking method for improved tear resistance and biocompatibility of tissue based biomaterials, Biomaterials. 66 (2015) 83–91. doi:10.1016/j.biomaterials.2015.07.011.

[325] J.P. Hodde, S.F. Badylak, A.O. Brightman, S.L. Voytik-Harbin, Glycosaminoglycan content of small intestinal submucosa: A bioscaffold for tissue replacement, Tissue Eng. 2 (1996) 209–217.

[326] J.P. Hodde, M.C. Hiles, Bioactive FGF-2 in Sterilized Extracellular Matrix, Wounds. 13 (2001) 195–201.

[327] J.P. Hodde, R.D. Record, H.A. Liang, S.F. Badylak, Vascular endothelial growth factor in porcine-derived extracellular matrix, Endothel. J. Endothel. Cell Res. 8 (2001) 11–24.

[328] S.F. Badylak, J.E. Valentin, A.K. Ravindra, G.P. McCabe, A.M. Stewart-Akers, Macrophage phenotype as a determinant of biologic scaffold remodeling, Tissue Eng. - Part A. 14 (2008) 1835–1842. doi:10.1089/ten.tea.2007.0264.

[329] L. Ansaloni, P. Cambrini, F. Catena, S. Di Saverio, S. Gagliardi, F. Gazzotti, et al., Immune response to small intestinal submucosa (Surgisis) implant in humans: Preliminary observations, J. Invest. Surg. 20 (2007) 237–241. doi:10.1080/08941930701481296.

[330] G.K. Bejjani, J. Zabramski, Safety and efficacy of the porcine small intestinal submucosa dural substitute: Results of a prospective multicenter study and literature review, J. Neurosurg. 106 (2007) 1028–1033. doi:10.3171/jns.2007.106.6.1028.

[331] M.E. Franklin Jr., J.J. Gonzalez Jr., J.L. Glass, Use of porcine small intestinal submucosa as a prosthetic device for laparoscopic repair of hernias in contaminated fields: 2-year follow-up, Hernia. 8 (2004) 186–189.

[332] H. Naji, J. Foley, H. Ehren, Use of surgisis for abdominal wall reconstruction in children with abdominal wall defects, Eur. J. Pediatr. Surg. 24 (2014) 94–96. doi:10.1055/s-0033-1354587.

[333] J.E. Valentin, A.M. Stewart-Akers, T.W. Gilbert, S.F. Badylak, Macrophage participation in the degradation and remodeling of extracellular matrix scaffolds, Tissue Eng. - Part A. 15 (2009) 1687–1694. doi:10.1089/ten.tea.2008.0419.

[334] T. Jiang, G. Wang, J. Qiu, L. Luo, G. Zhang, Preparation and biocompatibility of polyvinyl alcohol-small intestinal submucosa hydrogel membranes, J. Med. Biol. Eng. 29 (2009) 102–107.

[335] G.C. Lantz, S.F. Badylak, M.C. Hiles, A.C. Coffey, L.A. Geddes, K. Kokini, et al., Small intestinal submucosa as a vascular graft: A review, J. Invest. Surg. 6 (1993) 297–310.

[336] G.E. Sandusky Jr., S.F. Badylak, R.J. Morff, W.D. Johnson, G. Lantz, Histologic findings after in vivo placement of small intestine submucosal vascular grafts and saphenous vein grafts in the carotid artery in dogs, Am. J. Pathol. 140 (1992) 317–324.

[337] T. Jiang, G. Wang, J. Qiu, L. Luo, G. Zhang, Heparinized poly(vinyl alcohol)-small intestinal submucosa composite membrane for coronary covered stents, Biomed. Mater. 4 (2009). doi:10.1088/1748-6041/4/2/025012.

[338] N. Toyota, D. Pavcnik, W. VanAlstine, B.T. Uchida, H.A. Timmermans, Q. Yin, et al., Comparison of small intestinal submucosa-covered and noncovered nitinol stents in sheep iliac arteries: A pilot study, J. Vasc. Interv. Radiol. 13 (2002) 489–498.

[339] S.F. Badylak, A.C. Coffey, G.C. Lantz, W.A. Tacker, L.A. Geddes, Comparison of the resistance to infection of intestinal submucosa arterial autografts versus polytetrafluoroethylene arterial prostheses in a dog model, J. Vasc. Surg. 19 (1994) 465–472.

[340] T.-W. Yue, W.-C. Chien, S.-J. Tseng, S.-C. Tang, EDC/NHS-mediated heparinization of small intestinal submucosa for recombinant adeno-associated virus serotype 2 binding and transduction, Biomaterials. 28 (2007) 2350–2357. doi:10.1016/j.biomaterials.2007.01.035.

[341] M.J.B. Wissink, R. Beernink, J.S. Pieper, A.A. Poot, G.H.M. Engbers, T. Beugeling, et al., Immobilization of heparin to EDC/NHS-crosslinked collagen. Characterization and in vitro evaluation, Biomaterials. 22 (2001) 151–163. doi:10.1016/S0142-9612(00)00164-2.

[342] K.A. Tanaka, N.S. Key, J.H. Levy, Blood Coagulation: Hemostasis and Thrombin Regulation, Anesth. Analg. May 2009. 108 (2009) 1433–1446. doi:10.1213/ane.0b013e31819bcc9c.

[343] A.S. Wolberg, Thrombin generation and fibrin clot structure, Blood Rev. 21 (2007) 131–142. doi:10.1016/j.blre.2006.11.001.

[344] M.A. Sahud, Laboratory Diagnosis of Inhibitors, Semin. Thromb. Hemost. Volume 26 (2000) 195–204. doi:10.1055/s-2000-9823.

[345] B. Sørensen, J. Ingerslev, Whole blood clot formation phenotypes in hemophilia A and rare coagulation disorders. Patterns of response to recombinant factor VIIa, J. Thromb. Haemost. 2 (2004) 102–110. doi:10.1111/j.1538-7836.2004.00528.x.

[346] J. van Veen, A. Gatt, P. Cooper, S. Kitchen, A. Bowyer, M. Makris, Corn trypsin inhibitor in fluorogenic thrombin-generation measurements is only necessary at low tissue factor concentrations and influences the relationship between factor VIII coagulant activity and thrombogram parameters, Blood Coagul. Fibrinolysis April 2008. 19 (2008) 183–189. doi:10.1097/MBC.0b013e3282f4bb47.

[347] M. Zucker, U. Seligsohn, O. Salomon, A.S. Wolberg, Abnormal plasma clot structure and stability distinguish bleeding risk in patients with severe factor XI deficiency, J. Thromb. Haemost. (2014) n/a–n/a. doi:10.1111/jth.12600.

[348] M.D. Rand, J.B. Lock, C. Van't Veer, D.P. Gaffney, K.G. Mann, Blood clotting in minimally altered whole blood, Blood. 88 (1996) 3432–3445.

[349] J.A. Huntington, Thrombin inhibition by the serpins, J. Thromb. Haemost. 11 (2013) 254–264. doi:10.1111/jth.12252.

[350] S.K. Moon, D.H. Keum, W.S. Hye, H.K. Seon, H.K. Soon, S.L. Min, et al., Preparation of porcine small intestinal submucosa sponge and their application as a wound dressing in full-thickness skin defect of rat, Int. J. Biol. Macromol. 36 (2005) 54–60. doi:10.1016/j.ijbiomac.2005.03.013.

[351] B. Furie, B.C. Furie, In vivo thrombus formation, J. Thromb. Haemost. 5 (2007) 12–17. doi:10.1111/j.1538-7836.2007.02482.x.

[352] T.A. Drake, J.H. Morissey, T.S. Edgington, Selective cellular expression of tissue factor in human tissues. Implications for disorders of hemostasis and thrombosis, Am. J. Pathol. 134 (1989) 1087–1097.

[353] S. Chang, V. Tillema, D. Scherr, A "Percent Correction" Formula for Evaluation of Mixing Studies, Am. J. Clin. Pathol. 117 (2002) 62–73.

[354] S.W. Jordan, K.M. Faucher, J.M. Caves, R.P. Apkarian, S.S. Rele, X.-L. Sun, et al., Fabrication of a phospholipid membrane-mimetic film on the luminal surface of

an ePTFE vascular graft, Biomaterials. 27 (2006) 3473–3481. doi:10.1016/j.biomaterials.2006.01.009.

[355] S.W. Jordan, C.A. Haller, R.E. Sallach, R.P. Apkarian, S.R. Hanson, E.L. Chaikof, The effect of a recombinant elastin-mimetic coating of an ePTFE prosthesis on acute thrombogenicity in a baboon arteriovenous shunt, Biomaterials. 28 (2007) 1191–1197. doi:10.1016/j.biomaterials.2006.09.048.

[356] L.A. Harker, U.M. Marzec, A.B. Kelly, N.R.F. Chronos, I.B. Sundell, S.R. Hanson, et al., Clopidogrel Inhibition of Stent, Graft, and Vascular Thrombogenesis With Antithrombotic Enhancement by Aspirin in Nonhuman Primates, Circulation. 98 (1998) 2461–2469. doi:10.1161/01.CIR.98.22.2461.

[357] I. Shafat, A.B. Barak, S. Postovsky, R. Elhasid, N. Ilan, I. Vlodavsky, et al., Heparanase levels are elevated in the plasma of pediatric cancer patients and correlate with response to anticancer treatment, Neoplasia. 9 (2007) 909–916. doi:10.1593/neo.07673.

[358] I. Vlodavsky, M. Blich, J.-P. Li, R.D. Sanderson, N. Ilan, Involvement of heparanase in atherosclerosis and other vessel wall pathologies, Matrix Biol. 32 (2013) 241–251. doi:10.1016/j.matbio.2013.03.002.

[359] R.J. Linhardt, J.E. Turnbull, H.M. Wang, D. Loganathan, J.T. Gallagher, Examination of the substrate specificity of heparin and heparan sulfate lyases, Biochemistry (Mosc.). 29 (1990) 2611–2617. doi:10.1021/bi00462a026.

[360] S.F. Badylak, G.C. Lantz, A. Coffey, L.A. Geddes, Small intestinal submucosa as a large diameter vascular graft in the dog, J. Surg. Res. 47 (1989) 74–80.

[361] D. Pavcnik, J. Obermiller, B.T. Uchida, W.V. Alstine, J.M. Edwards, G.J. Landry, et al., Angiographic Evaluation of Carotid Artery Grafting with Prefabricated Small-Diameter, Small-Intestinal Submucosa Grafts in Sheep, Cardiovasc. Intervent. Radiol. 32 (2008) 106–113. doi:10.1007/s00270-008-9449-7.

[362] R.G. Matheny, M.L. Hutchison, P.E. Dryden, M.D. Hiles, C.J. Shaar, Porcine small intestine submucosa as a pulmonary valve leaflet substitute, J. Heart Valve Dis. 9 (2000) 769–775.

[363] A.M. Fallon, T.T. Goodchild, J.L. Cox, R.G. Matheny, In vivo remodeling potential of a novel bioprosthetic tricuspid valve in an ovine model, J. Thorac. Cardiovasc. Surg. 148 (2014) 333–340.e1. doi:10.1016/j.jtcvs.2013.10.048.

[364] J.J. Glynn, C.M. Jones, D.E.J. Anderson, D. Pavcnik, M.T. Hinds, In vivo assessment of two endothelialization approaches on bioprosthetic valves for the treatment of chronic deep venous insufficiency, J. Biomed. Mater. Res. B Appl. Biomater. (2015) n/a–n/a. doi:10.1002/jbm.b.33507.

[365] S.H. Qureshi, L. Yang, C. Manithody, A. V. Iakhiaev, A.R. Rezaie, Mutagenesis Studies toward Understanding Allostery in Thrombin, Biochemistry (Mosc.). 48 (2009) 8261–8270. doi:10.1021/bi900921t.

[366] P.M. Gasper, B. Fuglestad, E.A. Komives, P.R.L. Markwick, J.A. McCammon, Allosteric networks in thrombin distinguish procoagulant vs. anticoagulant activities, Proc. Natl. Acad. Sci. U. S. A. 109 (2012) 21216–21222. doi:10.1073/pnas.1218414109.

[367] K.G. Mann, S. Butenas, K. Brummel, The Dynamics of Thrombin Formation, Arterioscler. Thromb. Vasc. Biol. 23 (2003) 17–25. doi:10.1161/01.ATV.0000046238.23903.FC.

[368] J.J. Glynn, E.G. Polsin, M.T. Hinds, Crosslinking decreases the hemocompatibility of decellularized, porcine small intestinal submucosa, Acta Biomater. 14 (2015) 96–103. doi:10.1016/j.actbio.2014.11.038.

[369] W. Van Oeveren, J. Haan, P. Lagerman, P. Schoen, Comparison of Coagulation Activity Tests In Vitro for Selected Biomaterials, Artif. Organs. 26 (2002) 506–511. doi:10.1046/j.1525-1594.2002.06872.x.

[370] P.H. Lin, C. Chen, R.L. Bush, Q. Yao, A.B. Lumsden, S.R. Hanson, Small-caliber heparin-coated ePTFE grafts reduce platelet deposition and neointimal hyperplasia in a baboon model, J. Vasc. Surg. 39 (2004) 1322–1328. doi:10.1016/j.jvs.2004.01.046.

[371] L. Bajzar, J. Morser, M. Nesheim, TAFI, or plasma procarboxypeptidase B, couples the coagulation and fibrinolytic cascades through the thrombin-thrombomodulin complex, J. Biol. Chem. 271 (1996) 16603–16608. doi:10.1074/jbc.271.28.16603.

[372] M. Nesheim, W. Wang, M. Boffa, M. Nagashima, J. Morser, L. Bajzar, Thrombin, thrombomodulin and TAFI in the molecular link between coagulation and fibrinolysis, Thromb. Haemost. 78 (1997) 386–391.

[373] J.H. Foley, K.-U. Petersen, C.J. Rea, L. Harpell, S. Powell, D. Lillicrap, et al., Solulin increases clot stability in whole blood from humans and dogs with hemophilia, Blood. 119 (2012) 3622–3628. doi:10.1182/blood-2011-11-392308.

[374] J.F. Kocsis, G. Llanos, E. Holmer, Heparin-coated stents, J. Long. Term Eff. Med. Implants. 10 (2000) 19–45.

[375] P.C. Begovac, R.C. Thomson, J.L. Fisher, A. Hughson, A. Gällhagen, Improvements in GORE-TEX® vascular graft performance by Carmeda® BioActive Surface heparin immobilization, Eur. J. Vasc. Endovasc. Surg. 25 (2003) 432–437. doi:10.1053/ejvs.2002.1909.

[376] C. Feistritzer, M. Riewald, Endothelial barrier protection by activated protein C through PAR1-dependent sphingosine 1–phosphate receptor-1 crossactivation, Blood. 105 (2005) 3178–3184. doi:10.1182/blood-2004-10-3985.

Biographical Sketch

Jeremy Glynn was born in Milwaukee, WI on December 19, 1987 to Lloyd and Susan Glynn. Jeremy grew up in Arbor Vitae, WI and attended high school at Lakeland Union High School in Minocqua, WI.

Following high school, Jeremy enrolled at the University of Wisconsin – Madison in September 2006. There, he studied Biomedical Engineering with a focus in Biomaterials, Cellular and Tissue Engineering. During this time, he participated in a research project in the lab of Dr. Sean Palecek in the Chemical and Biological Engineering department. Additionally, Jeremy was actively involved in the local chapter of the Biomedical Engineering Society, serving as the Outreach Chair, Faculty Relations Chair, and Vice-president during his time at UW-Madison. Jeremy earned his Bachelor of Science degree in Biomedical Engineering in May 2011.

Jeremy continued his education at Oregon Health & Science University (OHSU) joining the lab of Dr. Monica Hinds in August 2011. Coming to OHSU, Jeremy had received a National Science Foundation Graduate Research Fellowship and was also an Achievement Rewards for College Scientists (ARCS) scholar for OHSU based upon his research history. During his time at OHSU, Jeremy submitted a successfully funded proposal to receive an American Heart Association Pre-doctoral fellowship. Additionally, Jeremy was awarded a Vertex Pharmaceutical Scholarship to sponsor travel to present his research at the 2015 Society for Biomaterials Annual Meeting, where he became the Student Representative for the Cardiovascular Biomaterials special interest group (SIG). To build on his interest in technology commercialization, Jeremy completed the Technology Entrepreneurship Certificate offered as a joint program between OHSU and the University of Portland. Jeremy's research has been published in a number of peer-reviewed publications, and also presented at academic conferences including the Society for Biomaterials, Tissue Engineering and Regenerative Medicine Society (TERMIS), and BioInterfaces. Current publications and presentations are listed below.

Selected Peer-reviewed Publications

1. Cheston Hsiao, Matthew Tomai, **Jeremy Glynn**, Sean P. Palecek. "Effects of 3-D microwell culture on initial fate specification in human embryonic stem cells." *AIChE Journal.* 2014, **60**(4); 1225–1235.

2. **Jeremy J. Glynn**, Monica T. Hinds. "Endothelial Outgrowth Cells: Function and Performance in Vascular Grafts." *Tissue Engineering, Part B: Reviews*. 2014, **20**(4); 294 - 303.

3. Casey M. Jones, Sandra M. Baker-Groberg, Flor A. Cianchetti, **Jeremy J. Glynn**, Laura D. Healy, Wai Yan Lam, Jonathan W. Nelson, Diana C. Parrish, Kevin G. Phillips, Devon E. Scott-Drechsel, Ian J. Tagge, Jaime E. Zelaya, Monica T. Hinds, Owen J. T. McCarty. "Measurement Science in the Circulatory System." *Cellular and Molecular Bioengineering*. 2014, **7**(10); 1-14.

4. Deirdre E. J. Anderson, Kathryn A. McKenna, **Jeremy J. Glynn**, Ulla Marzec, Stephen R. Hanson, and Monica T. Hinds. "Thrombotic responses of endothelial

outgrowth cells to protein-coated surfaces." *Cells Tissues Organs*. 2014, **199**(4); 238-48.

5. Deirdre E.J. Anderson, **Jeremy J. Glynn**, Howard K. Song, Monica T. Hinds. "Engineering an endothelialized vascular graft: A rational approach to study design in a non-human primate model." *PLOS One.* 2014, **9**(12):e115163.

6. **Jeremy J. Glynn**, Monica T. Hinds. "Endothelial Outgrowth Cells Regulate Coagulation, Platelet Accumulation and Respond to Tumor Necrosis Factor Similar to Carotid Endothelial Cells." *Tissue Engineering Part A.* 2015, **21**(1-2):174-82.

7. **Jeremy J. Glynn**, Elizabeth G. Polsin, Monica T. Hinds. "Crosslinking Decreases the Hemocompatibility of Decellularized, Porcine Small Intestinal Submucosa." *Acta Biomaterialia.* 2015*,* **14**; 96–103.

8. **Jeremy J. Glynn**, Deirdre E.J. Anderson, Casey M. Jones, Dusan Pavcnik, Monica T. Hinds. "In vivo assessment of two endothelialization approaches on bioprosthetic valves for the treatment of chronic deep venous insufficiency." *J Biomed Mater Res Part B: Appl Biomater.* 2015, published online ahead of print.

Selected Conference Abstracts

Presenting author is underlined

1. **Jeremy Glynn**, Andrew Dias, Jeremy Schaefer, Andrew Bremer, David Van Sickle. "Design and Development of a Low-cost Spirometer" *Biomedical Engineering Society Annual Meeting*. Austin, TX, October 6-9, 2010.

2. Deirdre E.J. Anderson, **Jeremy J. Glynn**, Randall F. Ankeny, Robert M. Nerem, and Monica T. Hinds. "Functional Assessment of Flow-conditioned, Endothelialized ePTFE Grafts and their Correlation to In Vitro Hemostatic Markers" *International Symposium on Biomechanics in Vascular Biology & Cardiovascular Disease*. Atlanta, GA, April 26-27, 2012.

3. **Jeremy J. Glynn**, Deirdre E.J. Anderson and Monica T. Hinds. "Characterization of the Heterogeneity in Endothelial Outgrowth Cells' Surface Marker Expression and Thromboprotective Function." *Gordon Research Conference: Signal Transduction by Engineered Extracellular Matrices*. Biddeford, ME, July 7-8, 2012.

4. Deirdre E.J. Anderson, **Jeremy J. Glynn**, Monica T. Hinds. "Steady Flow Preconditioning of Endothelial Outgrowth Cells on Ex Vivo and In Vivo ePTFE Grafts" *American Society of Mechanical Engineers: Summer Bioengineering Conference*. Sunriver, OR, June 26-29, 2013.

5. **Jeremy J. Glynn**, Monica T. Hinds. “Contrasting the Thrombotic Phenotype of Donor-matched Endothelial Outgrowth Cells and Endothelial Cells.” *American Society of Mechanical Engineers: Summer Bioengineering Conference*. Sunriver, OR, June 26-29, 2013.

6. Monica T. Hinds, **Jeremy J. Glynn**, Deirdre E.J. Anderson. “Endothelial progenitor outgrowth cells on ePTFE grafts respond to hemodynamic preconditioning” *International Society on Thrombosis and Haemostasis Congress*. Amsterdam, Netherlands, June 29-July 4, 2013.

7. Deirdre E.J. Anderson, **Jeremy J. Glynn**, Monica T. Hinds. “Ex Vivo and In Vivo Evaluation of Endothelialized Vascular Grafts after Fluid Shear Stress Stimulation” *Biomedical Engineering Society Annual Meeting*. Seattle, WA, September 25-28, 2013.

8. Elizabeth Polsin, **Jeremy J. Glynn**, Monica T. Hinds. “Bioactive modification of venous valve biomaterial to enable Protein C activation.” *Biomedical Engineering Society Annual Meeting*. Seattle, WA, September 25-28, 2013.

9. **Jeremy J. Glynn**, Elizabeth Polsin, Monica T. Hinds. “Modifying Venous Valve Biomaterial for Protein C Activation.” *Society for Biomaterials Annual Meeting.* Denver, CO, April 16-19 2014.

10. Deirdre Anderson, **Jeremy Glynn**, Dusan Pavcnik, Monica Hinds. “Generating an Off-the-Shelf In Vivo Cell Capture System on a Decellularized Biomaterial using Modified Antibodies for Venous Valve Replacement.” *Biomedical Engineering Society Annual Meeting*. San Antonio, TX, October 22-25, 2014.

11. **Jeremy J. Glynn**, Elizabeth G. Polsin, Monica T. Hinds. “The Effects of a Bioactive Modification of Decellularized Matrix on Protein C Activation, Coagulation and Platelet Accumulation.” *TERMIS Annual Meeting*. Washington, D.C., December 13-16 2014.
    ***Selected for student poster competition**

12. **Jeremy J. Glynn**, Monica T. Hinds. “Modifying Decellularized Matrix to Alter Blood Plasma Coagulation, Platelet Adhesion and Protein C Activation.” *University of Washington Biomaterials Day*. March 2, 2015.

13. **Jeremy J. Glynn**, Elizabeth G. Polsin , Monica T. Hinds. “Hemocompatibility of Crosslinked or Thrombomodulin-modified Decellularized Matrix.” *Society for Biomaterials Annual Meeting*. Charlotte, NC, April 16-19 2015.
    ***Awarded a Society for Biomaterials Student Travel Achievement Recognition (STAR) award**